

**UTRECHT
MICROPALAEONTOLOGICAL
BULLETINS**

S. THEODORIDIS

**CALCAREOUS NANNOFOSSIL BIOZONATION OF THE MIOCENE AND
REVISION OF THE HELICOLITHS AND DISCOASTERS**

32

UTRECHT MICROPALAEONTOLOGICAL BULLETINS

Editor C. W. Drooger

Department of Stratigraphy and Paleontology

State University of Utrecht

Budapestlaan 4, Postbus 80.021

3508 TA Utrecht, Netherlands

In the series have been published:

- Bull. 1. T. FREUDENTHAL – Stratigraphy of Neogene deposits in the Khania Province, Crete, with special reference to foraminifera of the family Planorbulinidae and the genus *Heterostegina*. 208 p., 15 pl., 33 figs. (1969) *f* 32,–
- Bull. 2. J. E. MEULENKAMP – Stratigraphy of Neogene deposits in the Rethymnon Province, Crete, with special reference to the phylogeny of uniserial *Uvigerina* from the Mediterranean region. 172 p., 6 pl., 53 figs. (1969) *f* 29,–
- Bull. 3. J. G. VERDENIUS – Neogene stratigraphy of the Western Guadalquivir basin, S. Spain. 109 p., 9 pl., 12 figs. (1970) *f* 28,–
- Bull. 4. R. C. TJALSMA – Stratigraphy and foraminifera of the Neogene of the Eastern Guadalquivir basin, S. Spain. 161 p., 16 pl., 28 figs. (1971) *f* 44,–
- Bull. 5. C. W. DROOGER, P. MARKS, A. PAPP et al. – Smaller radiate *Nummulites* of northwestern Europe. 137 p., 5 pl., 50 figs. (1971) *f* 37,–
- Bull. 6. W. SISSINGH – Late Cenozoic Ostracoda of the South Aegean Island arc. 187 p., 12 pl., 44 figs. (1972) *f* 57,–
- Bull. 7. author's edition. F. M. GRADSTEIN – Mediterranean Pliocene *Globorotalia*, a biometrical approach. 128 p., 8 pl., 44 figs. (1974) *f* 39,–
- Bull. 8. J. A. BROEKMAN – Sedimentation and paleoecology of Pliocene lagoonal-shallow marine deposits on the island of Rhodos (Greece). 148 p., 7 pl., 9 figs. (1974) *f* 47,–
- Bull. 9. D. S. N. RAJU – Study of Indian Miogypsinidae. 148 p., 8 pl., 39 figs. (1974) *f* 38,–
- Bull. 10. W. A. VAN WAMEL – Conodont biostratigraphy of the Upper Cambrian and Lower Ordovician of north-western Öland, south-eastern Sweden. 128 p., 8 pl., 25 figs. (1974) *f* 40,–
- Bull. 11. W. J. ZACHARIASSE – Planktonic foraminiferal biostratigraphy of the Late Neogene of Crete (Greece). 171 p., 17 pl., 23 figs. (1975) *f* 52,–
- Bull. 12. J. T. VAN GORSEL – Evolutionary trends and stratigraphic significance of the Late Cretaceous *Helicorbitoides-Lepidorbitoides* lineage. 100 p., 15 pl., 14 figs. (1975) *f* 37,–
- Bull. 13. E. F. J. DE MULDER – Microfauna and sedimentary-tectonic history of the Oligo-Miocene of the Ionian Islands and western Epirus (Greece). 140 p., 4 pl., 47 figs. (1975) *f* 45,–
- Bull. 14. R. T. E. SCHÜTTENHELM – History and modes of Miocene carbonate deposition in the interior of the Piedmont Basin, NW Italy. 208 p., 5 pl., 54 figs. (1976) *f* 56,–

(continued on back cover)

CALCAREOUS NANNOFOSSIL BIOZONATION OF THE MIOCENE AND
REVISION OF THE HELICOLITHS AND DISCOASTERS

S. THEODORIDIS

Printed in the Netherlands by Loonzetterij Abé, Hoogeveen
9 November 1984

CONTENTS

Chapter 1. Introduction	5
General	5
Methods	6
Species concept	7
Depository of samples	8
Chapter 2. Provenance of the material	9
Introduction	9
Lithostratigraphy and biostratigraphy	10
Miocene material	11
DSDP Sites	11
Land sections	18
Sicily	18
Gozo	27
Malta	29
Zakynthos	33
Crete	34
Java	36
Individual samples	37
Non Miocene material	38
Chapter 3. Biozonation	47
Introduction	47
Comparison between the two biozonal schemes	49
Biostratigraphic problems related to the Mediterranean Miocene	50
Description of the Miocene zonations: the Mediterranean Miocene Zonation and the Integrated Miocene Zonation	53
Taxonomic notes	80
Chapter 4. Helicoliths	91
Introduction	91
Terminology	91
Structure of the helicoliths	91
Optical pattern of the helicoliths	99
Generic and specific characteristics of the helicoliths	100
Origin of <i>Helicosphaera</i>	102
Specific evolution of the helicoliths	104
Taxonomy	104
<i>Helicosphaera</i> group I	106
<i>Helicosphaera</i> group II	113

Chapter 5. Discoasters.	135
Introduction	135
Emendation of the discoaster genera introduced by Tan Sin Hok	135
Structure of the discoasters.	136
<i>Helio-discoaster</i> Tan emended.	137
<i>Eu-discoaster</i> Tan emended.	138
Terminology	139
Lineages in the genera <i>Helio-discoaster</i> and <i>Eu-discoaster</i>	139
Taxonomy.	140
Genus <i>Helio-discoaster</i>	140
<i>Helio-discoaster mohleri</i> group	140
<i>Helio-discoaster binodosus</i> group	150
Genus <i>Eu-discoaster</i>	154
<i>Eu-discoaster deflandrei</i> group	155
<i>Eu-discoaster exilis</i> group	162
<i>Eu-discoaster kugleri</i> group	169
<i>Eu-discoaster coalitus</i> group	173
<i>Eu-discoaster hamatus</i> group.	174
<i>Eu-discoaster brouweri</i> group	176
Morphologic categories without status of separate species.	180
E. asymmetricus morphotypes	180
E. tamalis morphotypes.	181
E. triradiatus morphotypes	181
E. neohamatus morphotypes.	181
E. moorei morphotypes.	182
References.	183
Index.	268

Chapter 1

INTRODUCTION

GENERAL

“Calcareous nannofossils” form a heterogeneous group of minute calcareous objects that range in size from 1 to 30 microns. The majority of the fossils resemble the coccoliths of the exterior calcareous cover (coccosphere) of the Haptophyceae and therefore it is generally accepted that these fossils are remains of such unicellular algae.

Reviews of basic information about the calcareous nannofossils have been published by Hay (1977), Gartner (1977), Haq (1978), Tappan (1980) and Lord and Taylor (1982).

The recognition of the calcareous nannofossils as a worthwhile tool for biostratigraphic correlations is generally credited to Bramlette and his co-workers Riedel, Sullivan, Martini and Wilcoxon (1954–1967). Following these pioneering efforts, intensive taxonomic and biostratigraphic studies of calcareous nannofossils have been carried out, and these have formed the basis for several biozonal schemes of the Mesozoic and the Cenozoic Systems.

The Cenozoic zonations are far more refined than the Mesozoic ones, mainly owing to the great number of Cenozoic sections with well-preserved nannofossil content obtained by the coring of deep ocean sediments. The two comprehensive zonations of the Cenozoic most frequently used are the compilations of Martini (1971) and of Bukry (1971, 1975). Although both zonal schemes have so far provided a good working basis for biostratigraphic correlations, they are not applicable everywhere. The Neogene of the Mediterranean area has proved especially hard to calibrate with the standard Zonations of the open oceans.

Our biostratigraphic investigation was concentrated on Miocene Mediterranean sections, firstly because numerous land sections and cores of this interval were either available in the Utrecht collections or easily accessible, and secondly because the “standard” Miocene zonations were inadequate for biostratigraphic correlations in the Mediterranean region.

As most of the Mediterranean sections were fragmentary, a large number of sections were studied in order to cover the Miocene interval completely and to check the reproducibility of our initial biostratigraphic results. This

study led to the composition of a new "Mediterranean Miocene Zonation" (fig. 44).

The applicability of our biostratigraphic data from the Mediterranean sections was checked on some DSDP cores and land sections in extra-Mediterranean areas. The use of our new markers in combination with the conventional ones that we found in these sections resulted in a more refined general biozonal scheme: the "Integrated Miocene Zonation" (fig. 45).

A large amount of taxonomic information was gathered during the progress of our investigation. Of all the taxa encountered we chose to make a thorough revision of the taxonomy of two major groups, namely the helicoliths and the discoasters. As a basis for this revision we used our new findings concerning the ultrastructure of the nannoliths of these groups (chapters 4 and 5). Both groups were chosen because of their rich and diverse representation in our Miocene samples. In order to complete our knowledge about these nannofossil groups and to reconstruct "evolutional patterns" we expanded our study by incorporating data from several pre-Miocene and post-Miocene sections and samples (fig. 2).

METHODS

Preparation of the samples

Three types of preparation were used for our investigation.

A. Fixed mounts: For the preparation of these mounts a small quantity of fresh sediment was soaked in distilled water to let it disintegrate. Care was taken not to shake the wet samples because shaking might cause sorting of the nannoliths through suspension and subsequent settling of the sediment particles. A fraction of the treated sediment was smeared on a cover slide, dried and embedded on an objective slide with Canada balsam.

B. Mobile mounts: A small quantity of sediment was allowed to disintegrate in water, was smeared on a slide, dried and finally scratched off the surface of the slide. The powdered sediment was mixed with castor-oil.

C. S.E.M. preparations: Scanning Electron Microscope mounts were usually prepared by drying a droplet of sediment suspension in water directly on the surface of a S.E.M. stub and afterwards coating it with gold. The methods described by Moshkovitz (1974) and Hansen et al. (1975) were useful for making observations of the same object both in the L.M. and the S.E.M., but this procedure was not a standard routine.

Observations and documentation

Light microscopic observations were carried out with a Leitz Orthoplan microscope, with polarization equipment, a gypsum plate and a revolving object stage. During a later stage of our investigation we stopped using the gypsum plate as the information gained with this device did not seem any better than that gained by the ordinary microscopic examination. The specimens were observed at a magnification of 1250 \times .

The distribution charts which are presented in the following chapter are based on light microscopic examination of five traverses (32 mm each) along each slide; an additional examination of five more traverses was used in order to establish the position of datum levels.

For the S.E.M. observation we used a Cambridge Stereoscan 600 M for magnifications up to 20,000 \times , whereas a Cambridge Stereoscan 150 and a Jeol STEM were used in order to obtain magnifications as high as 100,000 \times .

Our original intention was to present micrographs of all the species discussed in this paper but we had to abandon this plan. Although containing sufficient morphological information, most electron micrographs did not meet the quality standards necessary for their reproduction through printing. If we had chosen to present the few reproducible pictures this would have resulted in an unbalanced presentation.

To avoid this problem, nearly all species are depicted by light micrographs. The helicoliths have been documented additionally by drawings. All drawings have been made by the author on the basis of the information gained through series of unpublishable electron micrographs and direct electron microscopic observations.

SPECIES CONCEPT

Species of calcareous nannofossils are obviously no more than species founded on the morphological characteristics of fragments – isolated coccoliths – of individual organisms. Such species are clearly artificial categories as there is no biological argument favouring the view that two morphologically distinct coccoliths belonged to two different biological species. On the contrary, observations on recent Haptophyceae have demonstrated that individual algal cells may bear polymorphic coccospheres, or may be covered by two layers of coccoliths without morphological similarity (dithecatism). Furthermore, it has been observed that the morphology of the coccoliths may change during successive phases of the life cycle of an individual and morphological changes in certain Haptophyceae may even be induced by differences in temperature.

Our nannofossil "species" must be regarded as convenient units for the practice of biostratigraphic correlations. The same remark is valid for all other taxa of a higher or of a lower taxonomic rank.

DEPOSITORY OF SAMPLES

All samples, as well as the holotypes and isotypes of new species are stored in the micropaleontological collections of the Department of Stratigraphy and Paleontology of the State University of Utrecht.

Acknowledgements

I am indebted to: C. W. Drooger and A. J. T. Romein for their critical reading of the manuscript, R. R. Schmidt for introducing me to the study of calcareous nannofossils, B. W. M. Driever for his helpful discussions, T. van Hinte and P. Hoonhout for their skilful drawing of the figures, W. den Hartog for his photographic work and G. J. van 't Veld, G. C. Ittmann and C. W. van den Dood for the preparation of the samples.

J. Pieters is thanked for introducing me to electron microscopy.

Thanks is expressed to K. Perch-Nielsen for her useful remarks.

I am grateful to W. Geeraets for his kind technical assistance during the printing of the manuscript.

The financial support from the Rotary Foundation, the Dutch Ministry of Education and Science and the Netherlands Organization for the advancement of Pure Research (Z.W.O.) is gratefully acknowledged.

The D.S.D.P. Board kindly put the material of sites 369A, 372, 231 and 219 at our disposal.

S. M. McNab is thanked for making linguistic improvements in the text.

Special thanks are extended to my parents for their encouragement during the preparation of this thesis.

I greatly appreciate the help and moral support given to me by Petra J. van der Schaar who painstakingly typed several versions of the manuscript. This thesis is dedicated to her and to my parents.

Chapter 2

PROVENANCE OF THE MATERIAL

INTRODUCTION

This study is based on closely spaced samples from D.S.D.P. cores and land sections – 27 in total – and on individual samples from various localities in the Mediterranean region and in the adjacent oceanic areas (figs. 1 and 2).

The bulk of the investigated sequences is of Miocene Age. Although fragmentary, most of them overlap and together they span the entire Miocene interval. These Miocene sections were studied in detail and form the basis of the new zonal schemes (chapter 3, figs. 44 and 45) and the Miocene part of the lineages (chapter 4, fig. 61 and chapter 5, figs. 64 and 65).

The study of non-Miocene material was necessary in order to complete our knowledge of the taxonomy and the evolution of the genera *Helico-*

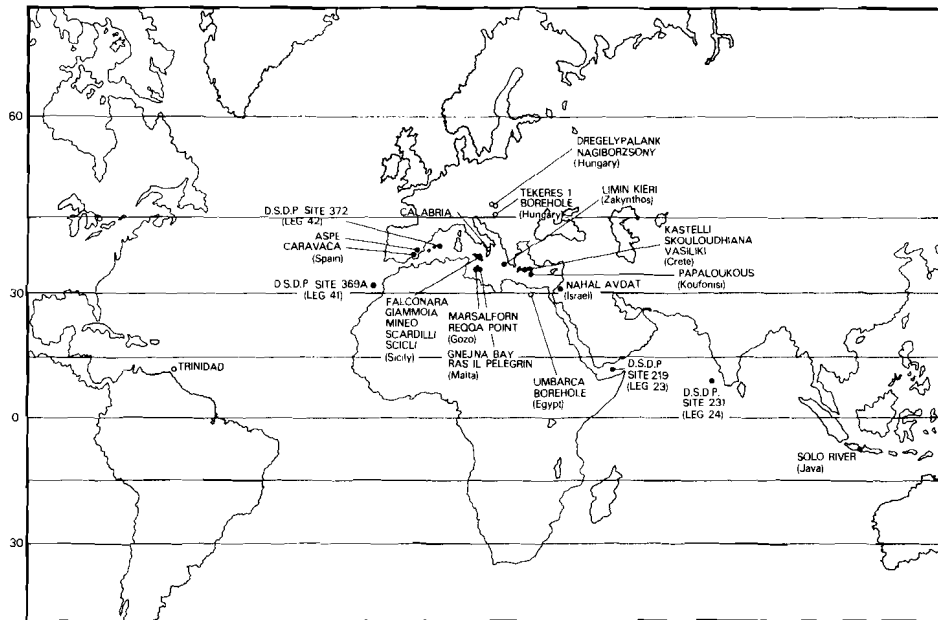
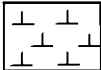
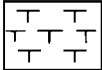
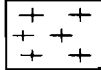

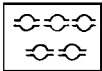
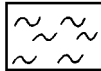
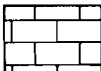
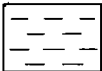
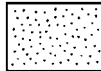
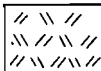
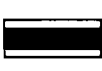
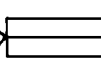
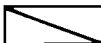
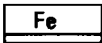



Fig. 1. Location of the sample-sites. Dots represent closely sampled land sections and D.S.D.P. cores. Circles represent localities from which individual samples were studied.

sphaera, *Helio-discoaster* and *Eu-discoaster*. The range-charts compiled from the non-Miocene sections do not contain the ranges of the species of other genera and the biostratigraphic position has been inferred from the data of other authors who studied the same samples.

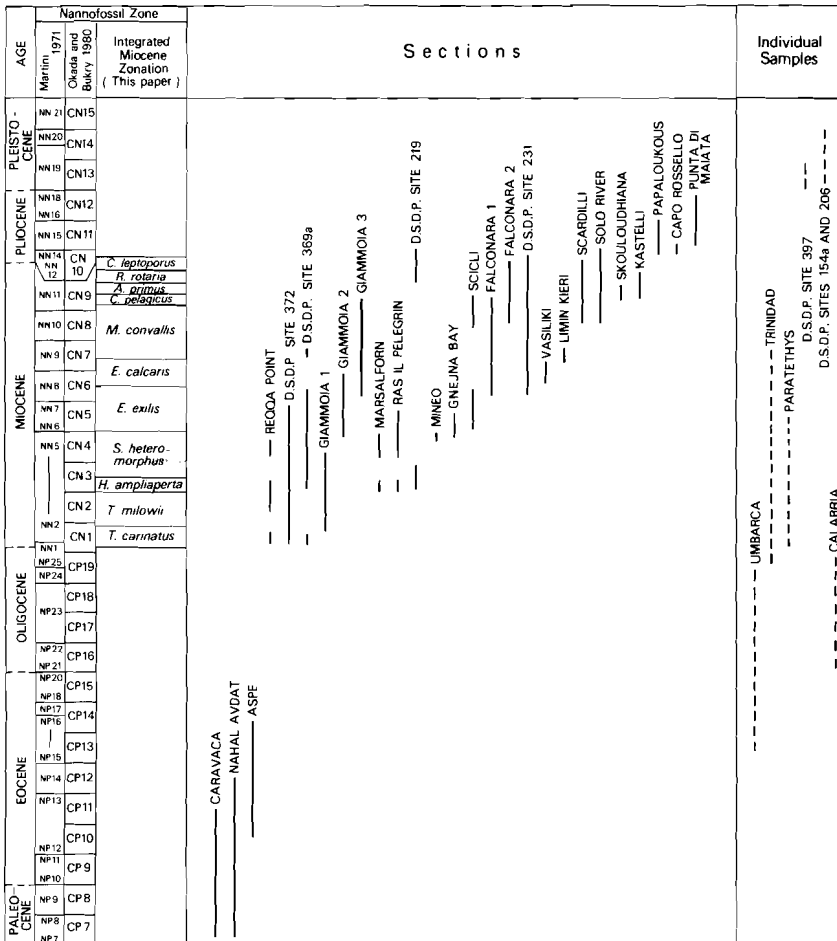
Legend of lithologic symbols

	nano-fossil ooze		foraminiferal ooze		nanno-foram ooze
	nano-fossil marl		diatomite		marl
	limestone		clay		sand
	volcanic ash		laminated bed		fault
	covered interval		ferruginous horizon		hiatus

LITHOSTRATIGRAPHY AND BIOSTRATIGRAPHY

The lithostratigraphic and biostratigraphic descriptions of our sequences have been grouped under the headings "Miocene material" and "non-Miocene material". The order followed for the presentation within each group is: D.S.D.P. Sites, land sections, individual samples. A legend of lithological symbols is given above.

Most of the land sections have been sampled along several traverses. These traverses have been given a number and they are described as different sections when no apparent lithological correlation was possible in the field (e.g. Falconara and Giammoia sections).



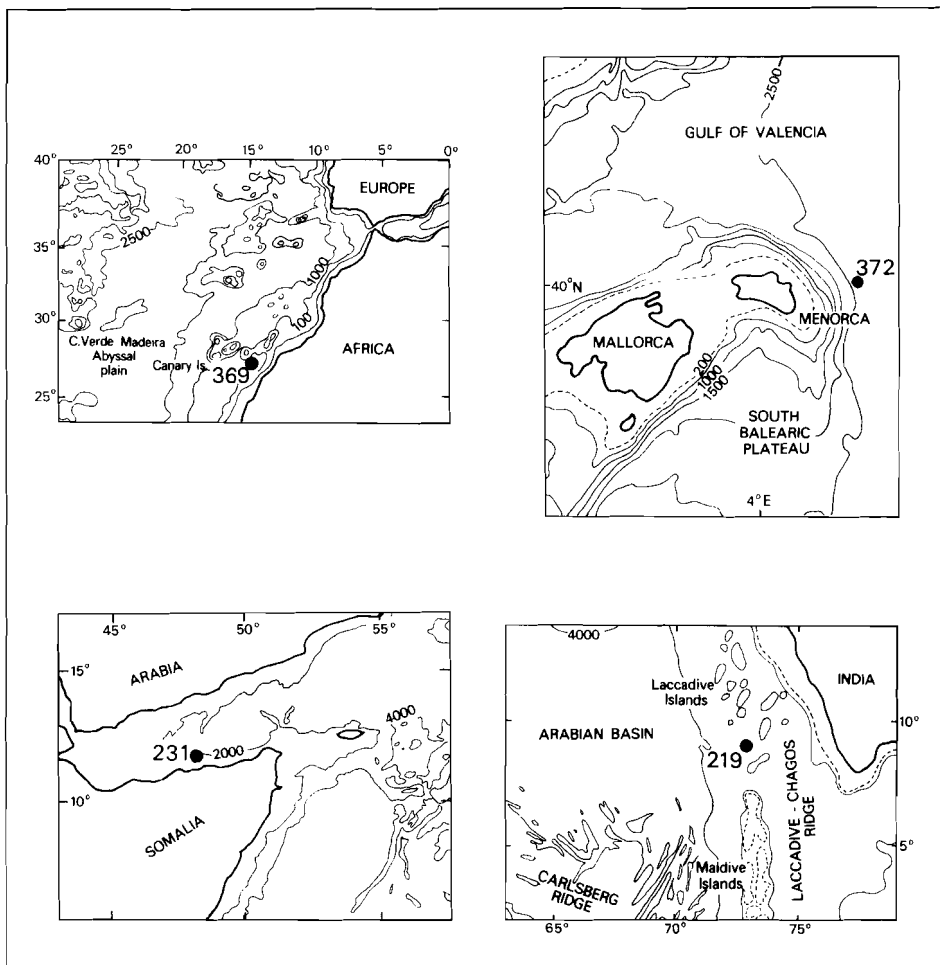


Fig. 3. Location of the D.S.D.P. sites.

and the underlying Siliceous Nannofossil Subunit 1b. The two subunits differ mainly in the abundance of siliceous fossils.

The planktonic foraminifera of cores 4 to 13 have been studied by Krascheninnikov and Pflaumann (In. Repts. D.S.D.P., vol. 41, 1978). They assigned these cores to the interval from the *Globigerinoides primordius* and *Globorotalia kugleri* Zones (combined) to the *Globorotalia peripheroacuta* Zone.

Bukry (In. Repts. D.S.D.P., vol. 41, 1978) studied the nannofossil associations of this site. According to this author, cores 1 to 13 belong to the interval from NN1 to NN15.

NN11. This author indicated a hiatus within core 9 ranging through Zones NN9 and NN10.

Our investigation did not reveal the presence of a hiatus at any level of this site. Furthermore, all samples of core 4 contained common *H. walbersdorfensis* and rare *R. floridana*, indicating the presence of the *H. intermedia* Subzone (nearest equivalent of upper NN6) in the uppermost part of the investigated sequence. The section ranges as low as the *E. deflandrei* Subzone.

D.S.D.P. Site 231, cores 29 to 57 (figs. 3, 6)

D.S.D.P. Site 231 is situated in the Gulf of Aden, South of the Sheba Ridge and 70 km north of the Somalia Coast. The investigated cores of this site constitute a 275-metre-thick succession of greyish to olive-green nannofossil ooze. The whole succession falls within the lithological Unit 5 as defined in the D.S.D.P. shipboard report (In. Repts. D.S.D.P., vol. 24, 1974).

The planktonic foraminiferal zonal assignments in the same D.S.D.P. report were based on the observations of Vincent et al., 1974. Cores 50 to 45 – which are also included in our study – were placed by these authors within the interval from N14/N13 to N17/N16.

The average sample distance in the studied part of site 231 is 2.5 m. All samples yield slightly etched nannofossil assemblages which explains their high discoaster content and the relatively low numbers of dissolution-prone helicospheres.

The calcareous nannofossils from this site have been studied by Roth (In. Repts. D.S.D.P., vol. 24, 1974) who based his zonal assignments for the Miocene on the zonations of Bukry (1971, 1973) and Bramlette and Wilcoxon (1967).

Our investigation produced results comparable to those of Roth. The section has been assigned to the interval from the *E. kugleri* Subzone through the *C. leptoporus* Zone and contains the complete succession of subzones described for this interval in the Integrated Miocene Zonation.

D.S.D.P. Site 219, cores 8 to 14 (figs. 3, 7)

Site 219 is located on the crest of the Laccadive-Chagos Ridge to the North of the Maldive islands. Only cores 8 through 14 were selected for our study because they are the only part of this site that contains sediments of Miocene Age. Cores 8 through 12 belong to lithological Unit I (Detrital clay-rich nannofossil ooze) whereas cores 13 and 14 constitute Unit II consisting of foraminiferal ooze with thin intercalations of foraminiferal chalk (In. Repts. D.S.D.P., vol. 23, 1974). The change in lithology from Unit I to Unit II is marked by an abrupt change of colour from grey to white, by a sudden increase in the number of foraminifera and by the total disappearance of detrital elements.

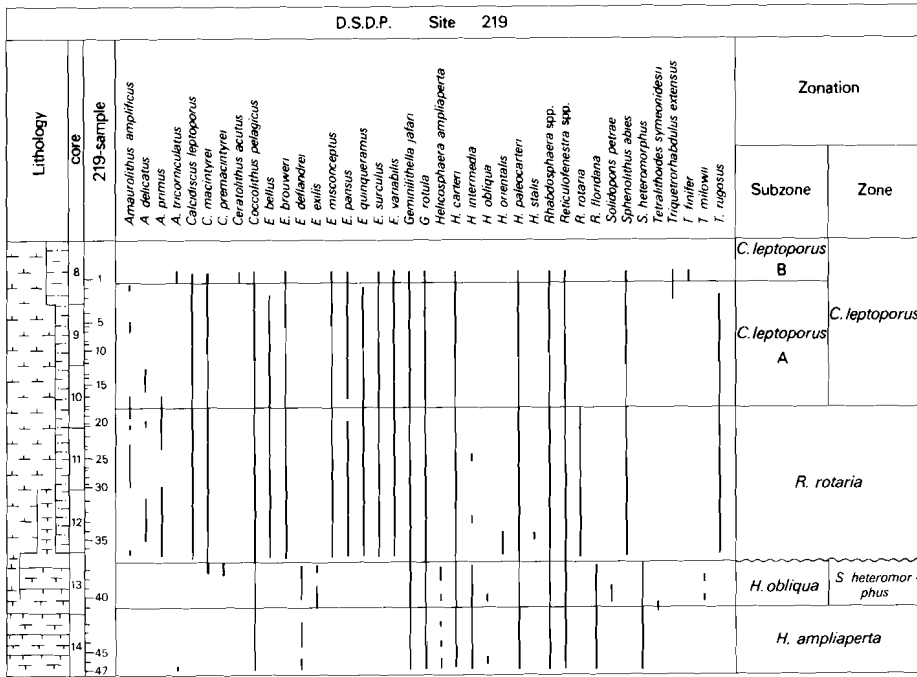


Fig. 7. D.S.D.P. Site 219; lithology, distribution of species and biozonation.

Cores 8 to 14 have been assigned by Fleischer (In. Repts. D.S.D.P., vol. 23, 1974) to the interval represented by the planktonic foraminiferal zones N7 to N18. Two hiatuses, one corresponding to Zone N9 and the other corresponding to zones N11 through N16, were detected by this author at the top of core 13.

The nannofossil content of site 219 has been studied by Boudreaux (In. Repts. D.S.D.P., vol. 23, 1974). Although our results concerning the total range of the studied interval are comparable with those of that author, we disagree about the number of zones present within this interval.

Cores 13 and 14 fall within the *H. ampliaperta* Zone and the *H. obliqua* Subzone of the Integrated Miocene Zonation which together are nearly equivalent to the *H. ampliaperta* Zone of Bramlette and Wilcoxon. Thus no equivalent of the *S. heteromorphus* Zone of Bramlette and Wilcoxon is present in cores 13 and 14, which conclusion is in contrast to the observations of Boudreaux. Furthermore, the simultaneous first occurrences of *Amaurolithus* species, *E. bellus*, *E. quinqueramus*, and *R. rotaria* in the lowermost sample of core 12 indicate a considerable hiatus between this core and the underlying one. All samples above this hiatus yield assemblages typical for

the *R. rotaria* and *C. leptoporus* Zones of the Integrated Miocene Zonation both of which are comparable to the upper part of the *E. quinquedentatus* Zone of Gartner.

LAND SECTIONS

Sicily (fig. 8)

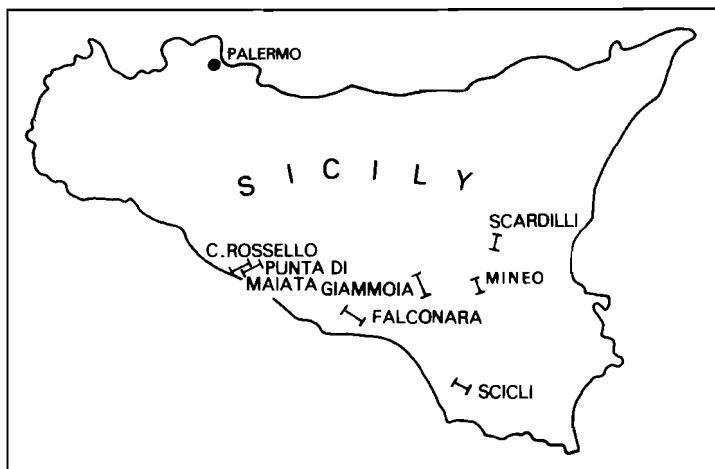


Fig. 8. Location of the sections on Sicily.

The Giammoia sections (fig. 9)

A sequence of Miocene sediments which is a few hundred metres thick is exposed along the slopes of the Monte Giammoia at about one kilometre to the West of the highway Piazza Armerina – Passo di Piazza.

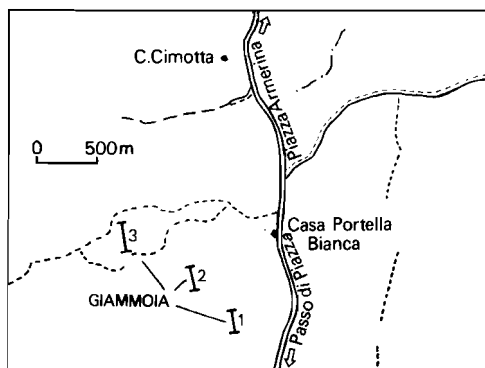


Fig. 9. Location of the Giammoia sections.

The entire sequence consists of homogeneous brownish-grey marls with thin intercalations (10–50 cm each) of laminated brown clays. The number of clayey intercalations increases in upward direction in the section; they form the dominant feature of the uppermost 90 metres.

The planktonic and benthonic foraminifera of parts of the Giammoia sequence have been studied by Zachariasse and Spaak (1983) and by Van der Zwaan and Den Hartog Jager (1983).

The Giammoia sequence was sampled in three sections – Giammoia 1, 2 and 3 – with no apparent lithological correlation in the field.

Giammoia 1 (fig. 10)

This is the lowermost part of the Giammoia sequence consisting of at least 23 metres of brownish grey marls. The section is underlain by a chaotic mixture of several lithotypes referred to as “Argille Scagliose” in the Italian literature.

The section ranges from the *H. vedderi* Subzone to the *H. perch-nielsenae* Subzone. The *T. milowii* Zone was not recorded in this section, but this zone might be present in a poorly exposed – and therefore not sampled – interval of several metres between samples CP3602 and CP3603.

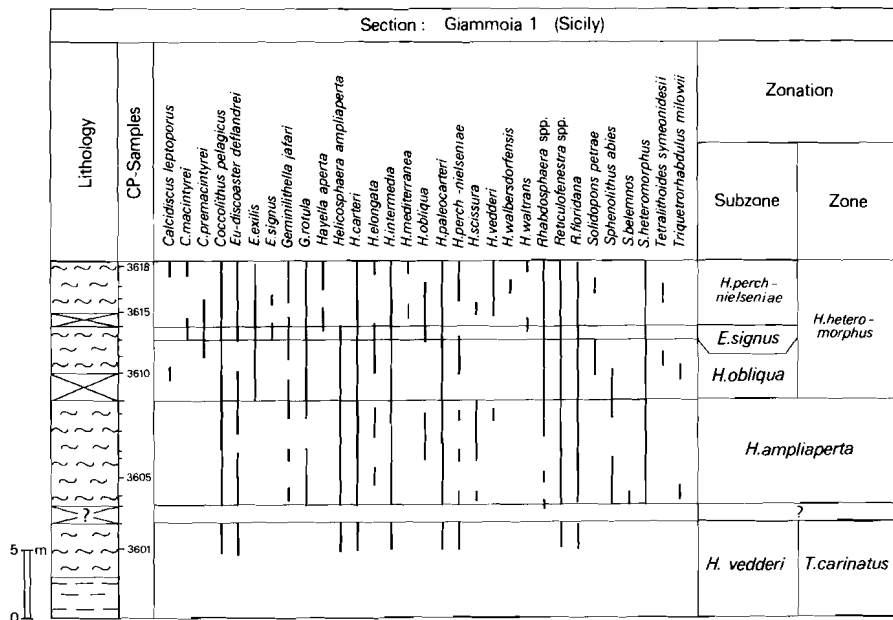


Fig. 10. Section Giammoia 1; lithology, distribution of species and biozonation.

Giammoia 2 (fig. 11)

This section represents the middle part of the Giammoia sequence. It consists of a 96-metre-thick succession of marls with a few intercalations of laminated, brown clays in its lower part. The laminated intervals increase in number and are closer spaced in the top part of the section.

Giammoia 2 ranges from the *E. musicus* Subzone to the *E. bellus* Subzone. A biostratigraphic gap occurs between the top of the underlying Giammoia 1 and the base of Giammoia 2. The gap corresponds to the *H. waltrans* Subzone.

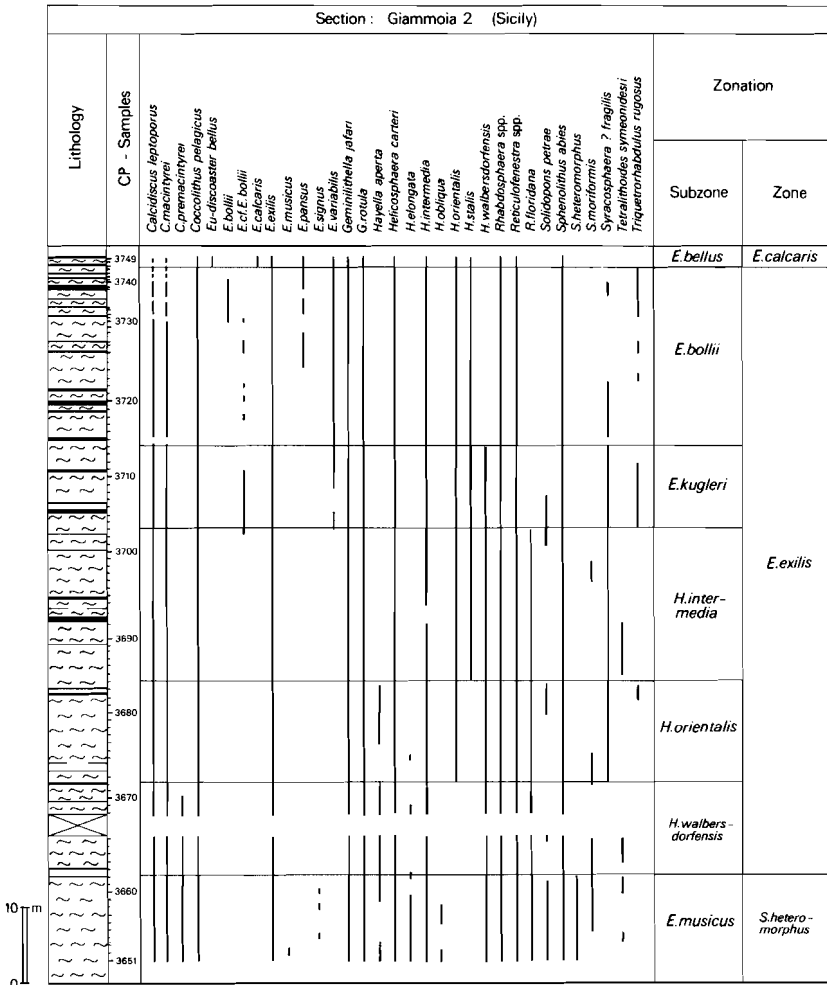


Fig. 11. Section Giammoia 2; lithology, distribution of species and biozonation.

Giammoia 3 (fig. 12)

The uppermost part of the Giammoia sequence is represented by the section Giammoia 3. This section consists of 88 metres of marls alternating with closely spaced laminated brown clays. The section ranges from the *E. kugleri* Subzone to the *C. pelagicus* Zone.

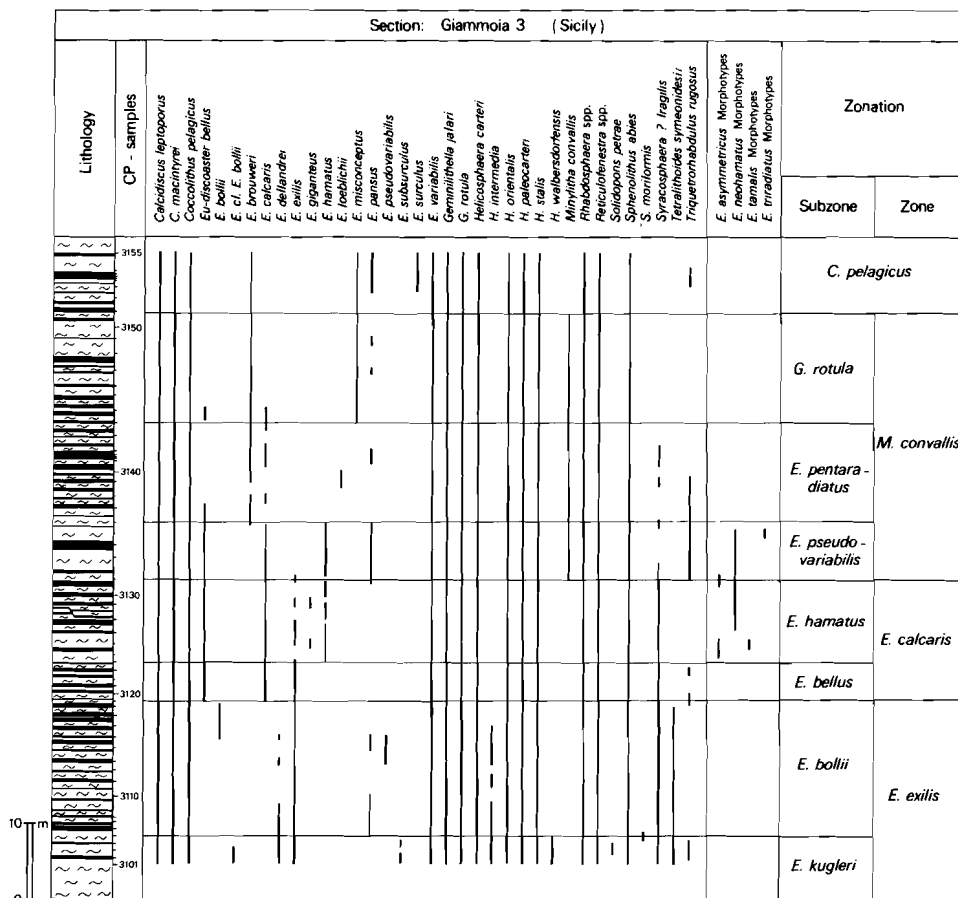


Fig. 12. Section Giammoia 3; lithology, distribution of species and biozonation.

Section Mineo (figs. 13, 14)

The section is exposed along the road Mineo-Palagonia to the East of the village of Mineo. It consists of nearly 19 metres of clayey marls and marly clays. The whole section falls within the *E. musicus* Subzone.

Section Scicli (figs. 15, 16)

The section is exposed in a clay-pit in the outskirts of the village of Scicli.

It consists of greenish-grey marls with a few intercalations of laminated brown clays.

The section Scicli ranges from the *H. walbersdorfensis* Subzone up to the *C. pelagicus* Zone. A normal fault, between samples CP4610 and CP4501, has created a biostratigraphic gap that ranges from the *E. bellus* Subzone to the *E. pentaradiatus* Subzone.

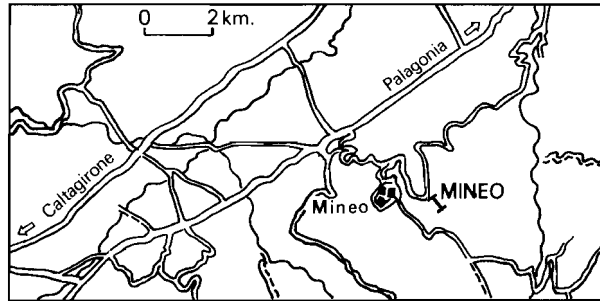


Fig. 13. Location of the section Mineo.

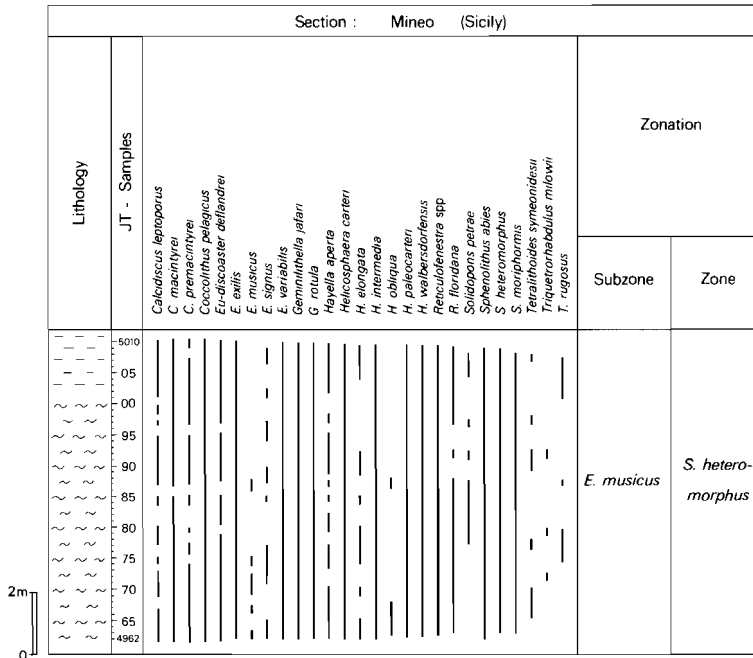


Fig. 14. Section Mineo; lithology, distribution of species and biozonation.

The Falconara sections (fig. 17)

The sections Falconara 1 and 2 are complementary and overlapping parts of a 130-metres-thick Miocene sequence which is exposed along the southern slope of the Monte Cantigaglione at about 5 km NW of the Castello di Falconara in SW Sicily. This sequence consists mainly of blue-grey clays to clayey marls with regular intercalations of brown, sometimes laminated clay beds of varying thicknesses. Within the uppermost 30 metres of the sequence the homogeneous sediments become more calcareous, whereas laminated intervals are represented mainly by diatomites. The sequence is overlain by the "Calcare di Base" limestones.

The planktonic foraminifera and calcareous nannofossils of the upper part of the Falconara sequence – roughly corresponding to our Falconara 2 section – have been studied by Colalongo et al., 1979. These authors proposed the section as the Tortonian/Messinian boundary stratotype.

Quantitative and isotopic studies of planktonic and benthonic foraminifera from the upper part of the Falconara sequence have been carried out by Van der Zwaan (1979 and 1982). The samples studied by that author have been used in our study too and form the set of samples of Falconara 2.

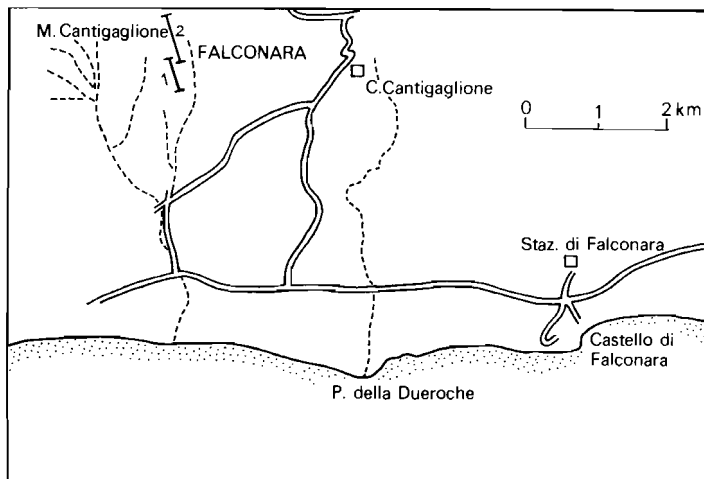


Fig. 17. Location of the Falconara sections.

Falconara 1 (fig. 18)

This section contains the lower 70 metres of the total sequence and ranges from the *E. kugleri* Subzone up to the *C. pelagicus* Zone. A fault between samples JT3069 and JT3068 has resulted in a biostratigraphic gap equivalent to the *E. bollii* Subzone.

Zwaan and Den Hartog Jager (1983). Our study of this section was based on the same set of samples.

The lowermost sampled part of the section (18 metres) consists of alternating sand and clay beds varying in thickness from 25 to 40 cm. The sand beds often exhibit a cm-scale cross lamination.

On top there are 25 metres of bluish to greenish-grey, silty clays.

The next higher unit consists almost entirely of sands with thin intercalations of clays. This sand unit has a thickness of nearly 85 metres of which the uppermost 20 metres are not well exposed.

The sand unit is overlain by 22 metres of dark-grey clays. A thin interval of diatomite beds has been observed at the top of these clays.

The section Scardilli can be assigned to the interval from the *G. rotula* Subzone to the *C. leptoporus* Subzone MA.

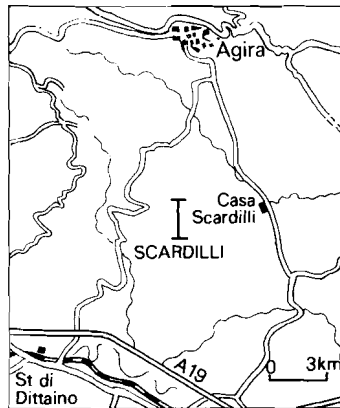


Fig. 20. Location of the section Scardilli.

Gozo (fig. 22)

Section Reqqa Point (figs. 22, 23)

The Reqqa Point section is exposed along the cliffs of the northern coast of the Island of Gozo at about 2.2 km to the west of the village of Marsalforn. It consists of nearly 30 metres of compact, yellow marls to marly limestones and it contains two hardgrounds with a dark brown colour. The section belongs to the Globigerina Limestone Formation (Felix, 1973).

The section ranges from the *E. deflandrei* Subzone to the *H. waltrans* Subzone. The lower hardground (between samples MT718B and MT721) coincides with a hiatus corresponding to the *H. vedderi* Subzone. The upper hardground horizon corresponds to a hiatus equivalent to the *H. obliqua* and *E. signus* Subzones.

Section Marsalforn (figs. 22, 24)

The section is exposed in the cliffs along the beach of the village of Marsalforn (northern coast of Gozo).

The lower 21 metres of the section consist of yellow, homogeneous marls with some intercalations of compact marly limestones. Near the base of this part and, above the level of sample MT744 there is an interval nearly one metre thick with hardgrounds. The marls are overlain by a few metres of blue-grey clays (samples MT771 to MT774). The transition from the yellow marls to the blue clays is marked by an interval of greyish marls. The marly part of the section belongs to the Globigerina Limestone Formation, and the clayey part to the Blue Clay Formation (the reader is referred to Felix, 1973 for detailed lithological descriptions of the formations).

The section ranges from the *H. ampliaperta* Zone to the *E. musicus* Subzone. The hardground interval coincides with a hiatus corresponding to the *H. obliqua* and the *E. signus* Subzones.

Malta (fig. 22)

Section Ras Il Pelegrin (figs. 22, 25)

The section has been studied by Felix (1973) whose samples have been

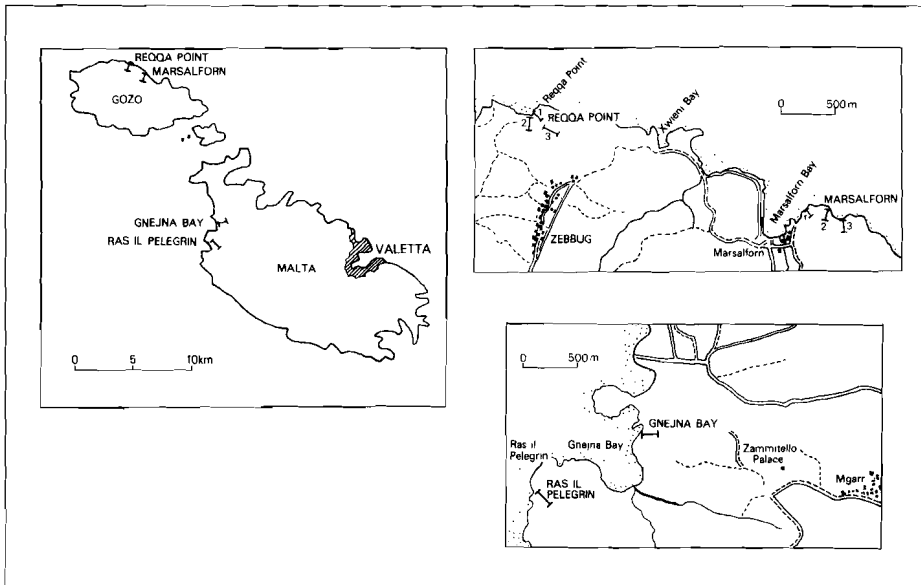


Fig. 22. Location of the sections on Gozo and Malta. The sections Regqa Point and Marsalforn are composite sections with lithological correlation.

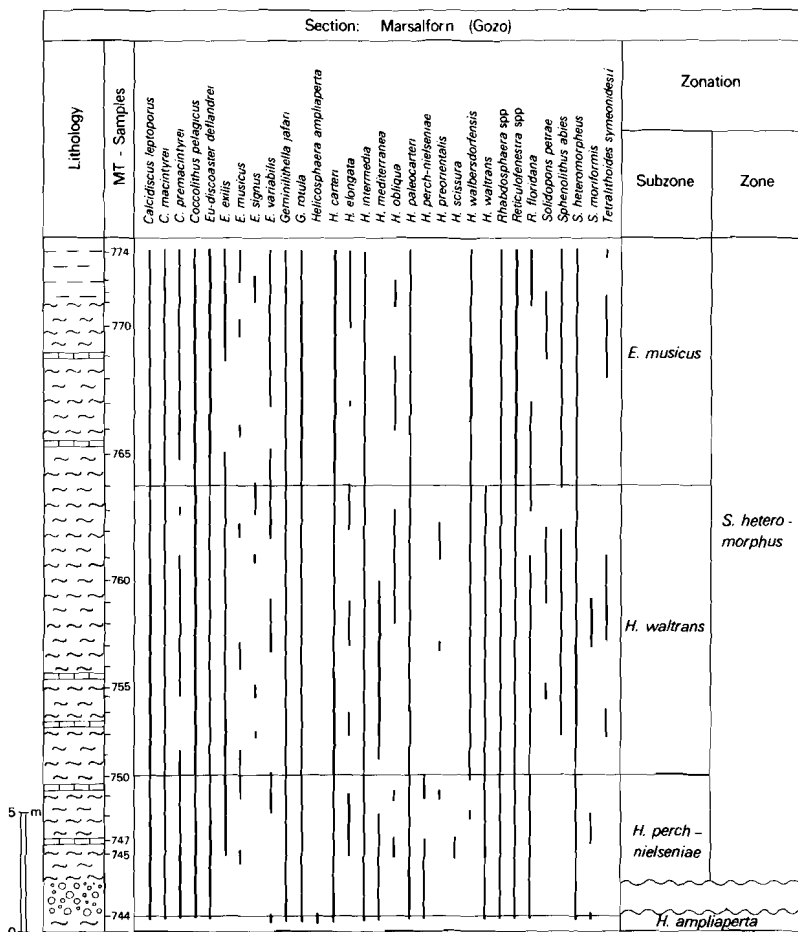


Fig. 24. Section Marsalforn; lithology, distribution of species and biozonation.

The section ranges from the *H. ampliaperta* Zone to the *H. orientalis* Subzone. The two hardground horizons in the section correspond to a hiatus from the *H. ampliaperta* to the *E. signus* Subzone.

Section Gnejna Bay (figs. 22, 26)

The section consists of 50 metres of bluish-grey clays belonging to the Blue Clay Formation (Felix, 1973). It is exposed along Gnejna Bay on the West coast of Malta and at about 3 kilometres to the West of the village of Mgarr.

The section has been assigned to the interval from the *E. musicus* Subzone up to the *H. orientalis* Subzone.

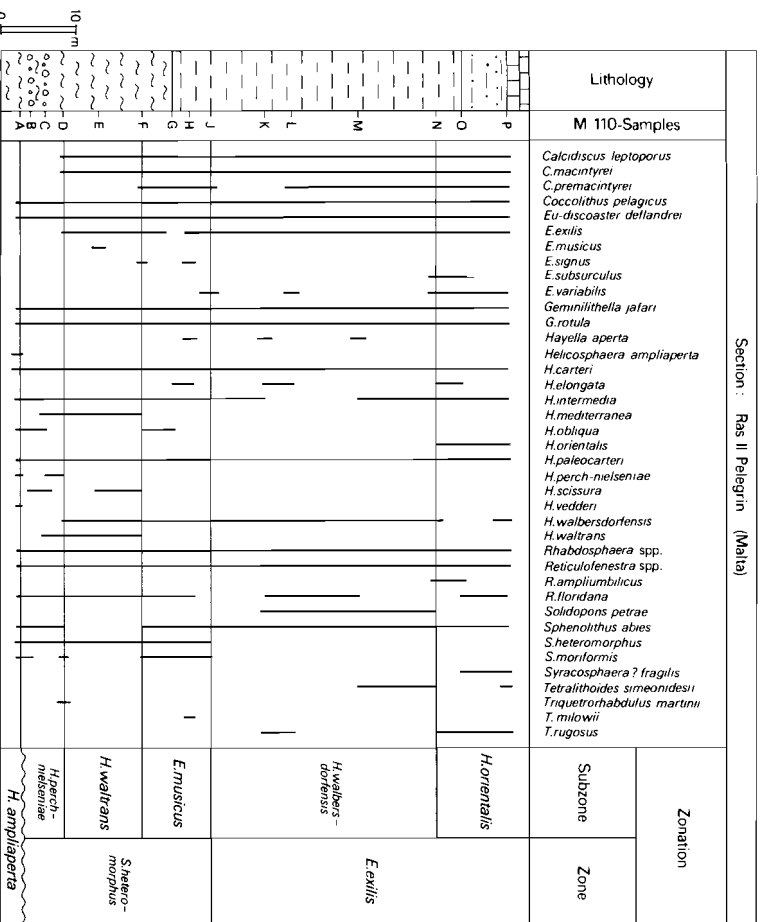


Fig. 25. Ras Il Pelegrin; lithology, distribution of species and biozonation.

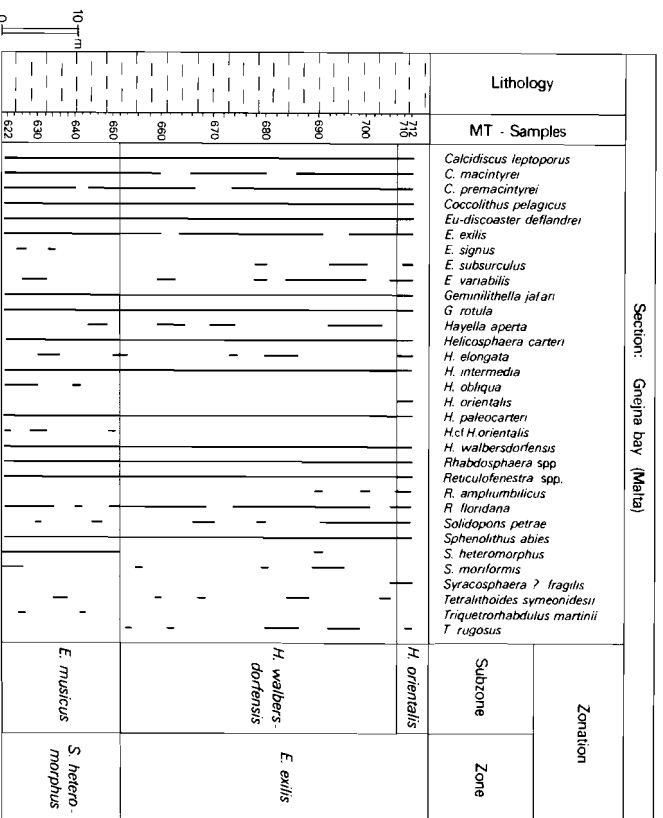


Fig. 26. Gnejna Bay; lithology, distribution of species and biozonation.

Zakynthos

Section Limin Kieri (figs. 27, 28)

The planktonic and benthonic foraminifera of this section have been studied by Dermitzakis (1978), who also gives a detailed lithological description. The section is exposed along a small coastal cliff to the south-west of the bay of Limin Kieri on the southern coast of Zakynthos.

The sampled part of the section is only part of that described by Dermitzakis and consists of 6.5 metres of bluish- to greenish-grey clays with three distinct bituminous clay beds in its lower part. The section contains the *E. hamatus* and the *E. pseudovariabilis* Subzones.

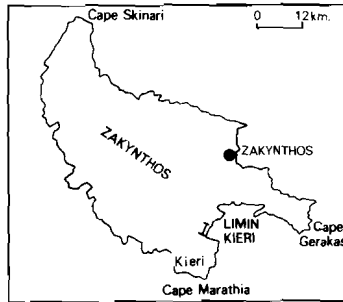


Fig. 27. Location of the section Limin Kieri.

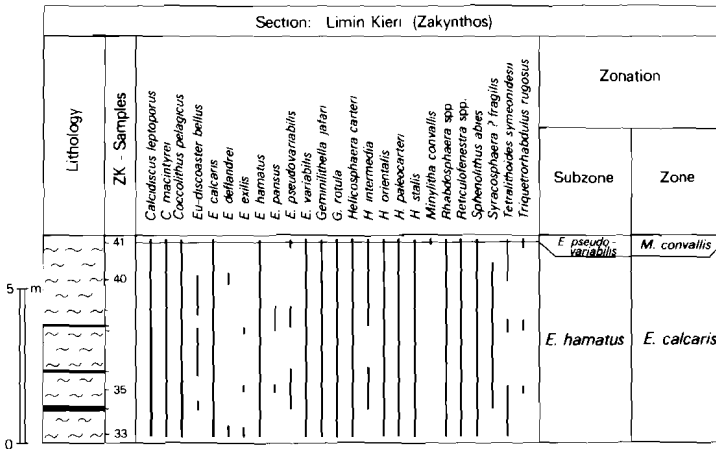


Fig. 28. Section Limin Kieri; lithology, distribution of species and biozonation.

Crete (fig. 29)

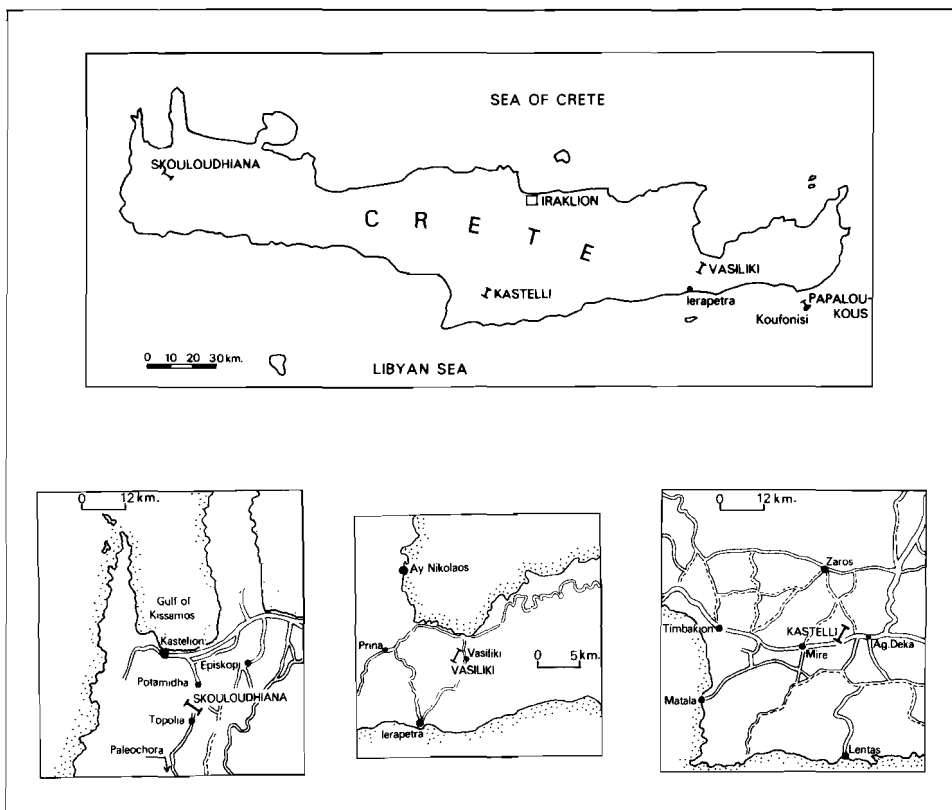


Fig. 29. Locations of the sections on Crete.

Section Vasiliki (figs. 29, 30)

The section is located in the outskirts of the village of Vasiliki in the Ierapetra province (Eastern Crete). It consists of 21 metres of grey, silty clays with a few intercalations of thin sand seams.

The section ranges through the *E. bellus* and the *E. hamatus* Subzones.

Section Skouloudhiana (figs. 29, 31)

The section is located in western Crete near the village of Skouloudhiana and has been included in the magneto-biostratigraphic study of Langereis, Zachariasse and Zijdeveld (1984). The samples used for our investigation are the same as the ones used by these authors.

The section consists of a 42-metre-thick succession of blue-grey homoge-

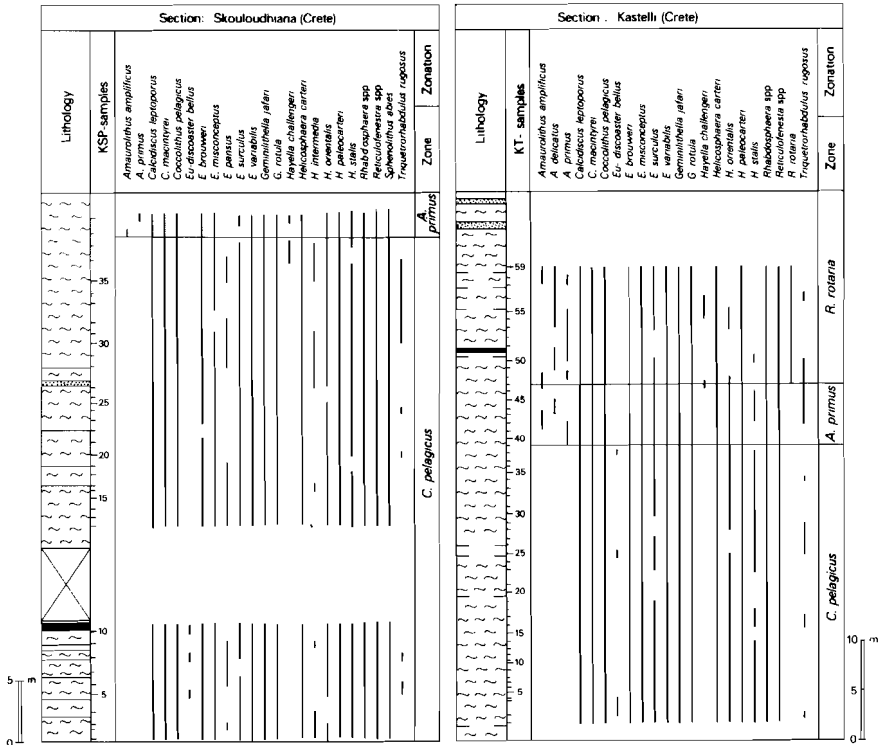


Fig. 31. Section Skouloudhiana and section Kastelli; lithology, distribution of species and biozonation.

Java

Section Solo-River (fig. 32)

The section is exposed along the Solo river valley in central Java. Data on the geology and stratigraphy of that area can be found in Van Bemmelen (1949), Marks (1957) and De Genevraye and Samuel (1972). The biostratigraphic position of the section derived on the basis of the planktonic foraminifera has been discussed by Van Gorsel and Troelstra (1981). The samples of these authors from the lower part of the section have been incorporated in our study. The studied part of the Solo-River section corresponds to the interval from the *G. rotula* Subzone (Zonule b) to the *C. leptoporus* Subzone B.

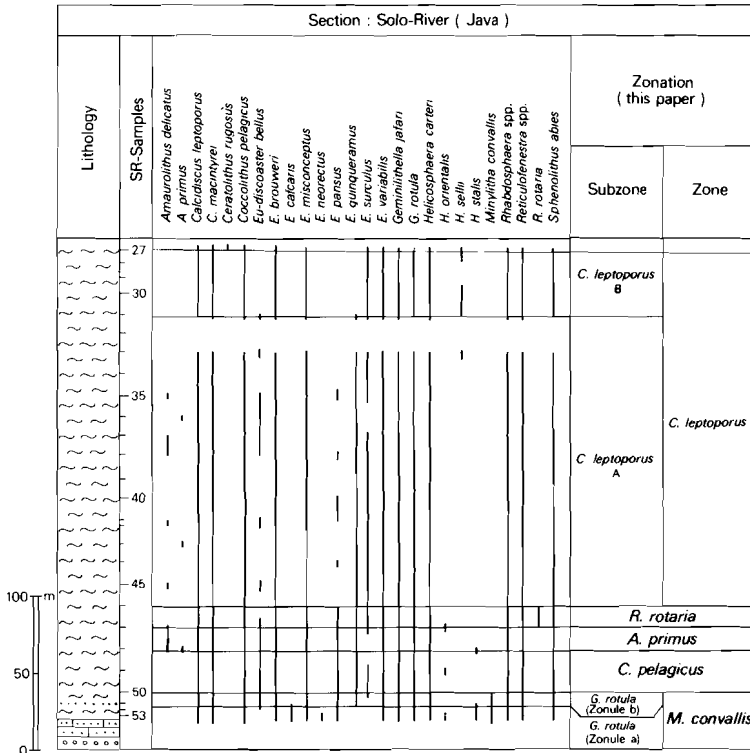


Fig. 32. Section Solo-River; lithology, distribution of species and biozonation.

Individual samples (fig. 33)

Samples from Trinidad

These samples belong to the Cipero and Lengua Formations from the type localities of the Miocene zones introduced by Bramlette and Wilcoxon (1967). The samples represent all zones from the *T. carinatus* Zone to the *E. hamatus* Zone of these authors. The biostratigraphic position of each of these samples in terms of the Integrated Miocene Zonation is given in figure 33.

Samples from the Paratethys

A small number of samples from Hungarian localities have also been studied. The geographical and biostratigraphic position of these samples is presented in figure 33.

Biostratigr. position	Sample	Geographic position	
Pleistocene (CN13-CN14)	154A-6-1 206-7-1	154A-sample:	DSDP Site 154A (Colombian Basin)
Pleistocene (CN13)	397-15-3	206-sample:	DSDP Site 206 (Tasman Sea)
Miocene (<i>E. bollii</i> S.)	TR23422	397-sample:	DSDP Site 397 (Cape Bojador)
		TR-samples:	Trinidad
Miocene (<i>E. kugleri</i> S.)	TR355	TK-samples:	Tekeres borehole (Hungary)
Miocene (<i>E. musicus</i> S.)	TK1 TK5 TR202	DR-samples:	Dregelypalank (Hungary)
		NB-samples:	Nagiborzsony (Hungary)
Oligocene (CP19)	TR291 DR3 DR5 NB1 NB2	PL-samples:	Calabria (S. Italy)
		WEPCO- and UM- samples:	Umbarca (Egypt)
Oligocene (CP16-CP19)	PL24 PL25		
Oligocene (CP16)	PL18 PL24		
Eocene-Oligocene (CP13-CP19)	WEPCO2500-2530 UM2000-2010 UM2990-3000 UM3070-3100		

Legend
S.: Subzone
CP-code numbers: after Okada and Bukry (1980)

Fig. 33. Biostratigraphic and geographical position of individual samples.

NON-MIOCENE MATERIAL

Sections Nahal Avdat, Caravaca and Aspe (figs. 34-37)

The reader is referred to Romein (1979) for lithological descriptions, range charts and literature concerning these sections. The samples studied here are the same as the ones used by that author.

According to Romein, the combined range of the sections Caravaca and Aspe falls within the interval from the *B. sparsus* Zone (Romein, Lower

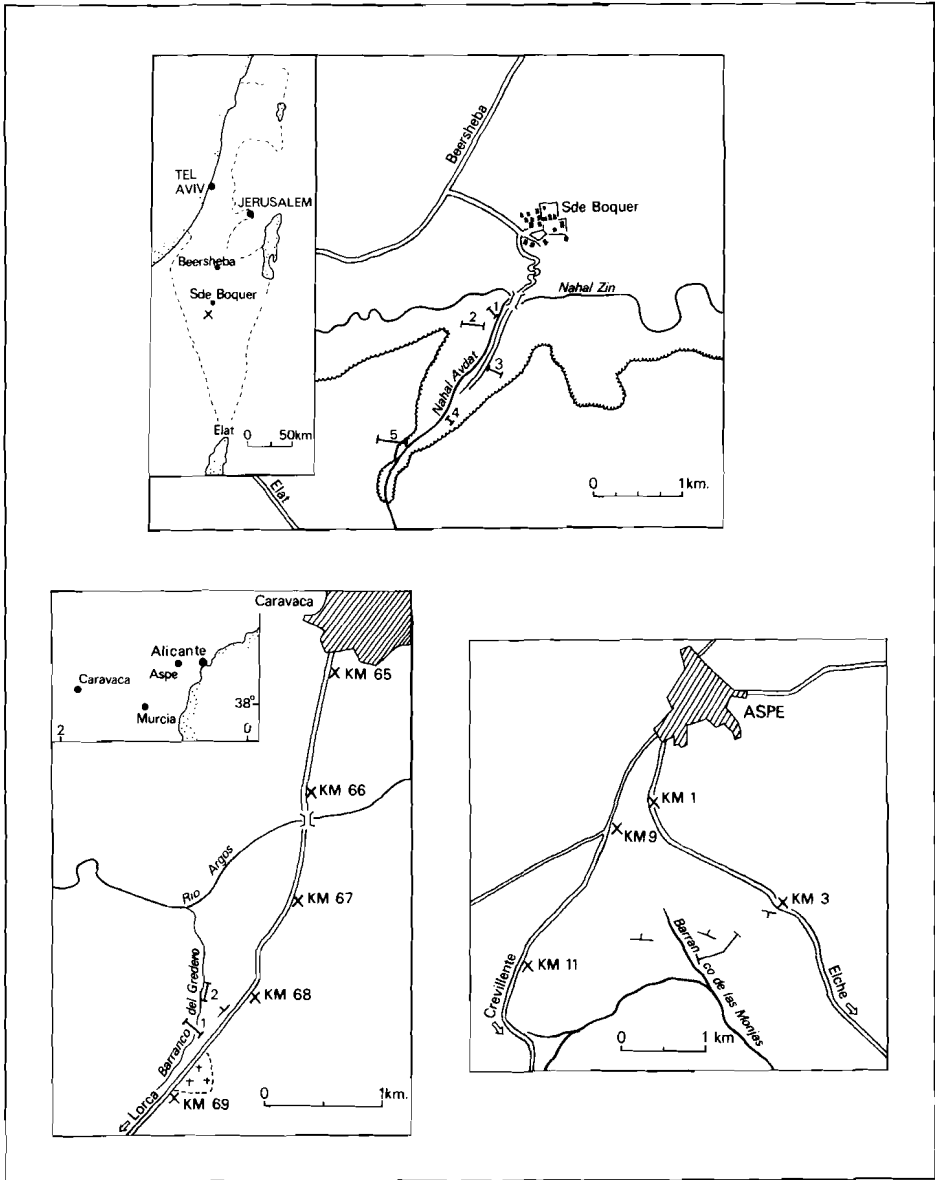


Fig. 34. Location of the sections Nahal Avdat (Israel), Caravaca and Aspe (Spain) (after Romein, 1979).

Paleocene) to the *N. fulgens* Zone (Romein, Middle Eocene). Section Nahal Avdat has an identical lower limit but its uppermost part falls within the *H. subladoensis* Zone.

All three sections contain fairly well preserved discoaster associations and were useful in the reconstruction of the discoaster lineages.

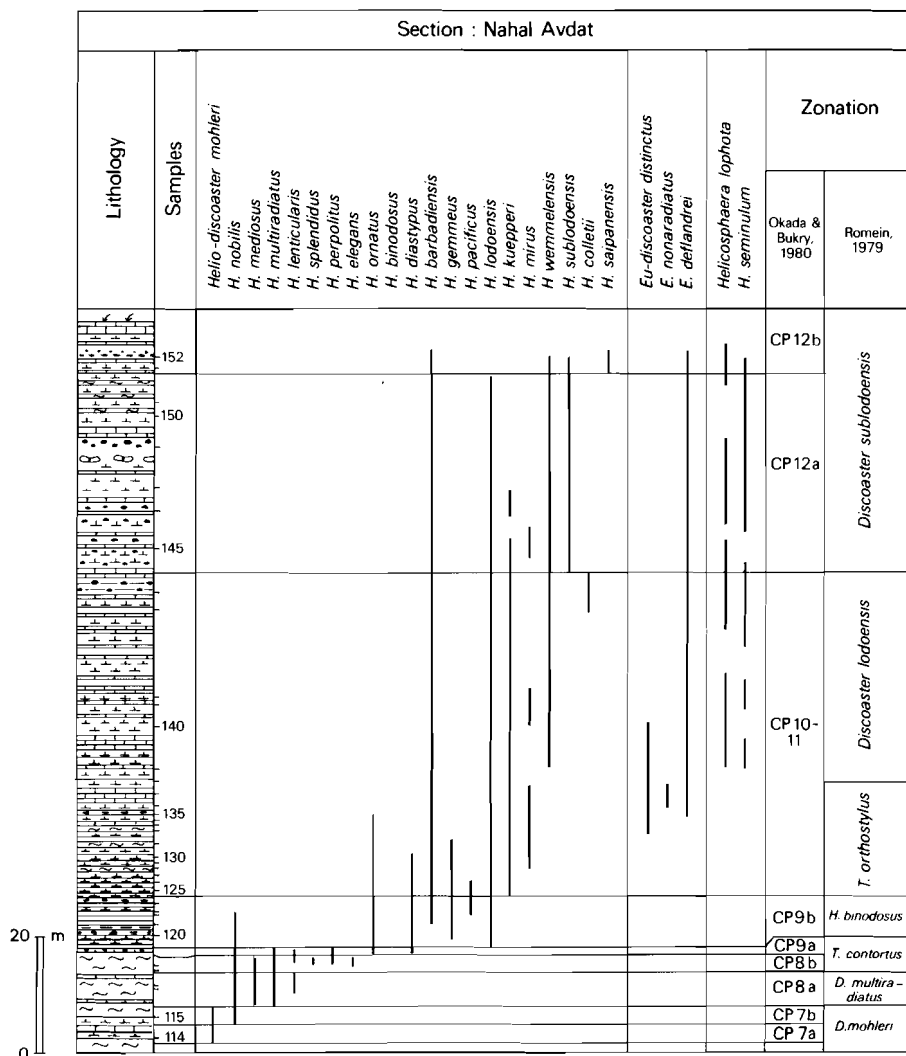


Fig. 35. Section Nahal Avdat; lithology, distribution of helicoliths, discoasters and biozonation. The lithology and the zonal assignments are after Romein (1979).

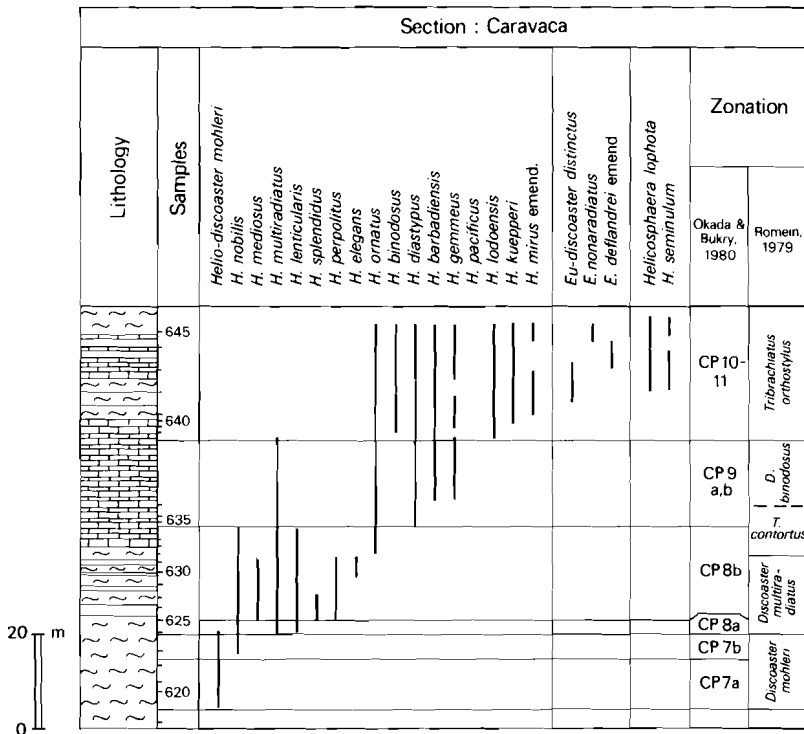


Fig. 36. Section Caravaca; lithology, distribution of helicoliths, discoasters and biozonation. The lithology and the zonal assignments are after Romein (1979).

Koufounisi Island (S.E. of Crete)

Section Papaloukous (fig. 38)

The planktonic foraminifera and the calcareous nannofossils from this section have been studied by Dermitzakis and Theodoridis (1978). The section comprises 23 metres of cream-coloured homogeneous marls with several intercalations of brown, laminated beds of clay. It corresponds to zones NN13–NN15 and it contains well-preserved Pliocene associations of discoasters and helicospheres.

Sicily (fig. 8)

Section Capo Rossello (figs. 39, 40)

The section consists of 40 metres of white calcareous marls (Trubi) and it is underlain by grey clastic sediments (Arenazzolo). An interval nearly 8 metres thick with finely laminated diatomites occurs about 27 metres above the base of the Trubi. This interval has been used by Zachariasse et al.

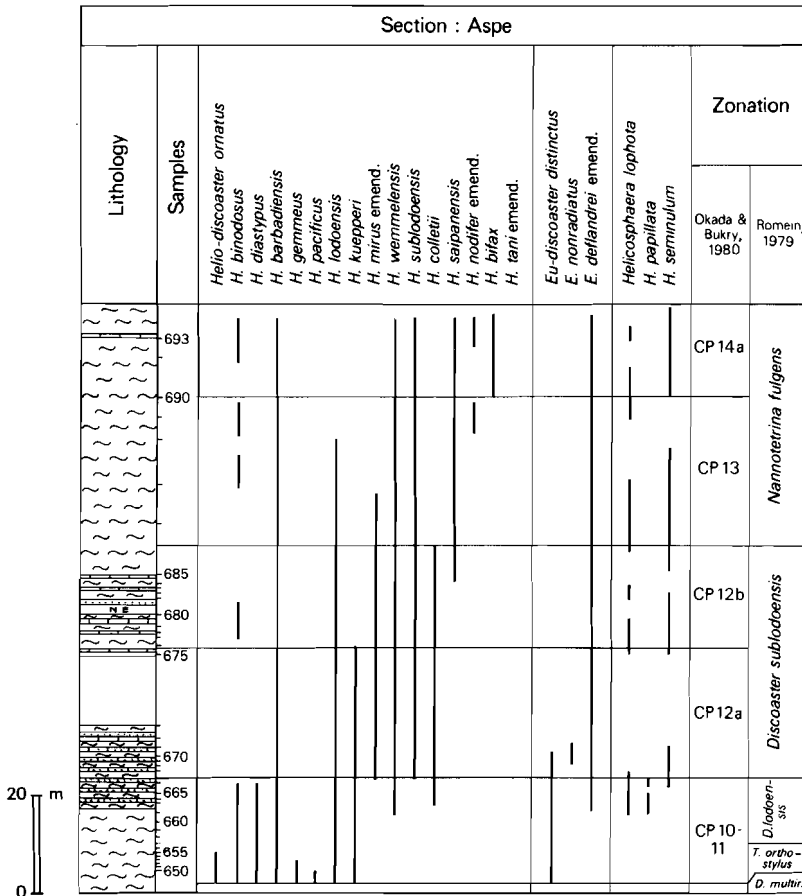


Fig. 37. Section Aspe; lithology, distribution of helicoliths, discoasters and biozonation. The lithology and the zonal assignments are after Romein (1979).

(1978) for the exercise in counting methods and techniques carried out on various microfossil groups, within the framework of the "Accuracy in Time" Project.

Sampling of this section was terminated approximately 5 metres above the highest diatomaceous bed.

The section corresponds to the lower 40 metres of the Capo Rossello section of Spaak (1983) who has studied the planktonic foraminifera, but we used a different set of samples.

The Capo Rossello section is assigned here to the *C. leptoporus* Subzone MC.

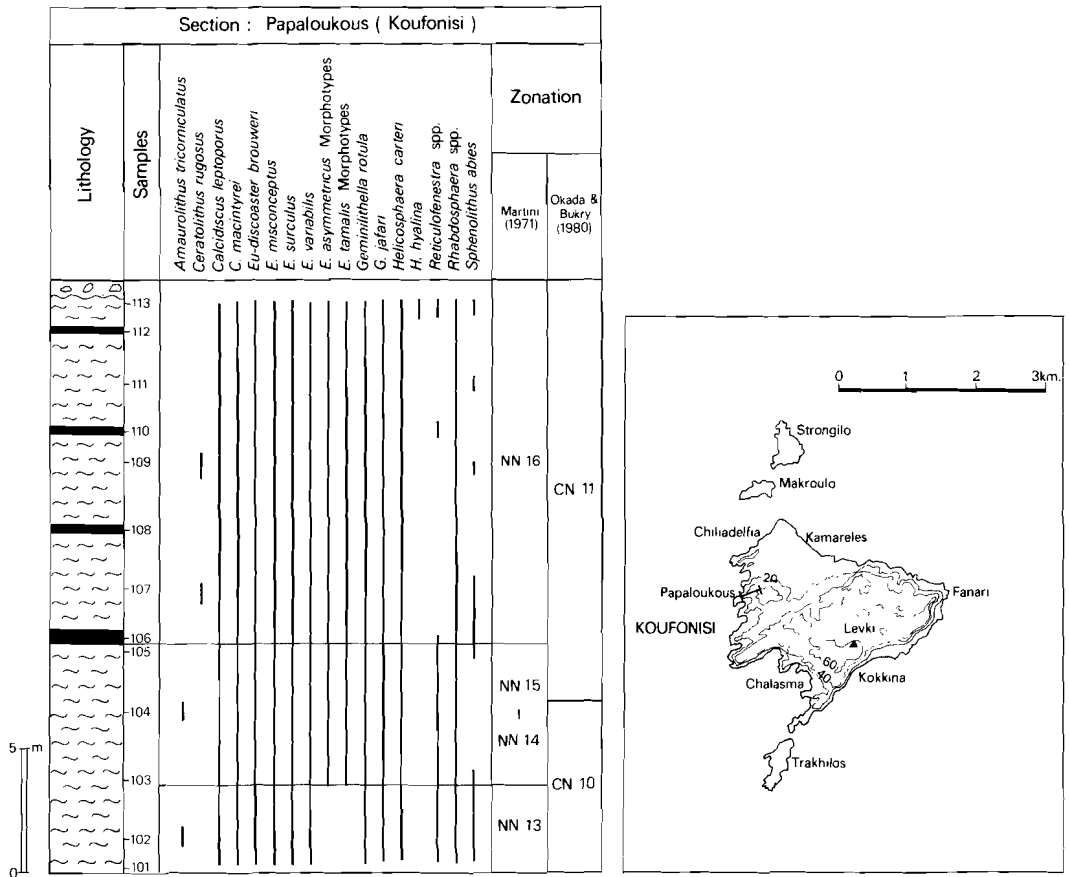


Fig. 38. Section Papaloukous; location of the section, lithology, distribution of selected species and biozonation.

Section Punta di Maiata (figs. 39, 40)

The discoaster associations of this section have been studied by Driever (1981). Spaak (1983) studied the planktonic foraminifera using the same set of samples as Driever.

The section consists of approximately 30 metres of white marls (Trubi) overlain by nearly 70 metres of grey marls of the Monte Narbone Formation. Part of our section overlaps with the lower 70 metres of the Punta di Maiata section of Driever and Spaak, but our investigation was carried out on a different set of samples. The Punta di Maiata section ranges from the *C. leptoporus* Subzone MC to the *E. brouweri* Zone of Bukry.

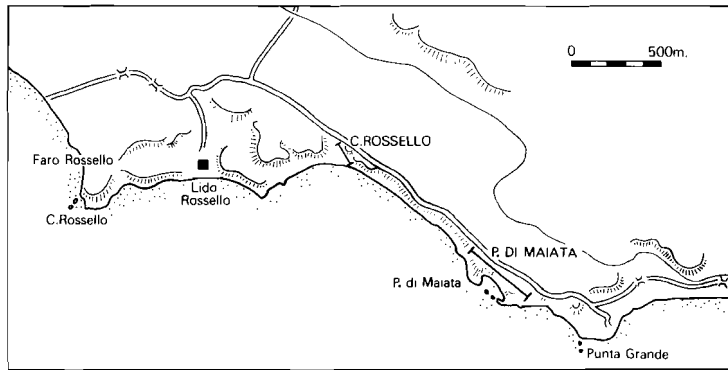


Fig. 39. Location of the sections Capo Rossello and Punta di Maiata.

Egypt

Umbarca (fig. 33)

This set of samples consists of cuttings from the “Umbarca” borehole in Egypt; all samples contain a mixture of Oligocene and Eocene nannofossil associations – contaminated possibly by caving. Despite their dubious biostratigraphic position the samples were useful as they contained highly diverse and well-preserved associations of helicospheres and discoasters.

Calabria (fig. 33)

A small number of samples from Calabria (S. Italy) were incorporated in our study because of their diverse content of helicospheres and discoasters. These samples were collected about 10 kilometres to the North of Capo Spartivento. They belong to zones CP16 to CP19.

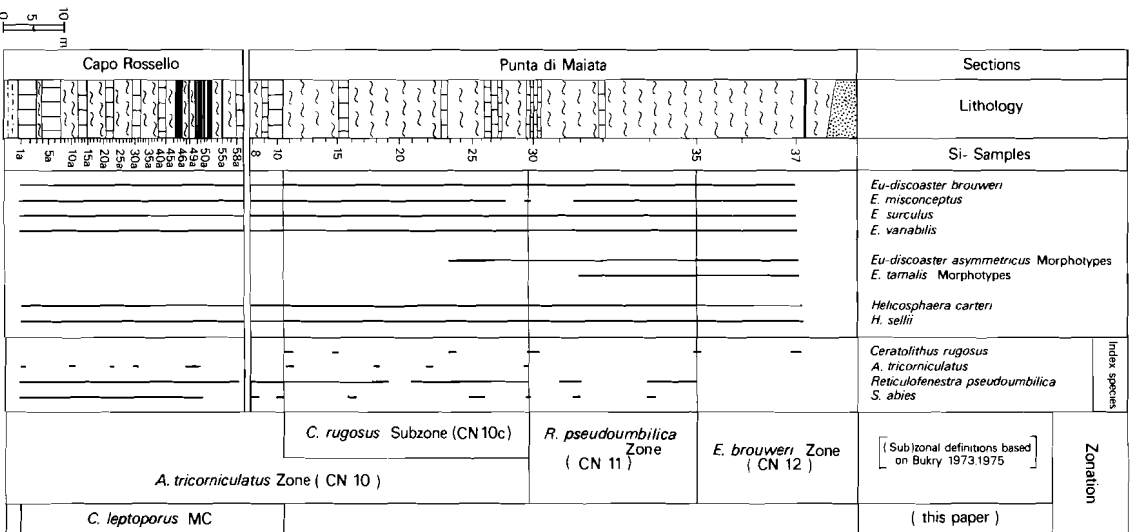


Fig. 40. Sections Capo Rossello and Punta di Maiata; lithology, distribution of selected species and biozonation.

Chapter 3

BIOZONATION

INTRODUCTION

Nearly all biozonal schemes (figs. 41, 42) currently in use for the subdivision of the Miocene are based on data which can be traced back to the zonations of Bramlette and Wilcoxon (1967) and Gartner (1969). The incorporation of these data in one comprehensive scheme by Martini and Worsley (1970) resulted in a zonation which is still in use in an almost unaltered form. The most thorough contribution to our knowledge of the Cenozoic biostratigraphy since the "standard" zonations of Martini and Worsley (1970) and Martini (1970) comes from the compilations of Bukry (1973 and 1975). The latter author introduced a very refined subdivision of the entire Cenozoic, but the Miocene part of his zonation (in terms of zones and zonal markers) is nearly identical to the previous zonations.

Zonation (Bukry 1975)			Zones recognizable in the Mediterranean sections	
Zone	Subzone	Index species	Subzone	Zone
<i>C. tricorniculatus</i>	<i>T. rugosus</i>	<i>C. oculus</i> *		
		<i>E. quinquaramus</i> †		
<i>D. quinquaramus</i>	<i>C. primus</i>	<i>A. primus</i> *		
	<i>D. berggrenii</i>	<i>E. quinquaramus</i> *		
<i>D. neohamatus</i>	<i>D. neorectus</i>	<i>E. neorectus</i> *		
	<i>D. bellus</i>	<i>E. hamatus</i> †		
<i>D. hamatus</i>	<i>C. calyculus</i>	<i>E. calyculus</i> *		<i>D. hamatus</i>
	<i>H. carteri</i>	<i>E. hamatus</i> *		
<i>C. coalitus</i>		<i>E. kugleri</i> † <i>E. coalitus</i> *		
<i>D. exilis</i>	<i>D. kugleri</i>	<i>E. kugleri</i> *		
	<i>C. miopelagicus</i>	<i>S. heteromorphus</i> †		
<i>S. heteromorphus</i>		<i>H. ampliaperta</i> †		<i>S. heteromorphus</i>
<i>H. ampliaperta</i>		<i>S. belemnus</i> † <i>S. heteromorphus</i> *		<i>H. ampliaperta</i>
<i>S. belemnus</i>		<i>T. carinatus</i> †		
<i>T. carinatus</i>	<i>D. druggii</i>	<i>E. druggii</i> *		
	<i>D. deflandrei</i>	<i>C. abisectus</i> Acme †		

* First occurrence † Last occurrence

Fig. 43. The recognizability of the conventional biozonal schemes in the Mediterranean sections is demonstrated in this figure. Bold letters indicate index species that are absent, atypical or extremely rare in the Mediterranean region. The names of the index species have been modified to comply with the nomenclatural changes in this paper.

Originally we did not intend to question the applicability of the established biozonal schemes. The study of the Mediterranean sections and D.S.D.P. cores, however, was largely impeded by the lack of the conventional zonal markers (fig. 43). Eventually the creation of a new “Mediterranean Miocene Zonation” (fig. 44) was unavoidable.

A weakness of the new zonal scheme is the fact that several new, emended, or hitherto neglected species have been used as datum-level-indicators. We

Epoch	Stages	Other Zonations		Mediterranean Miocene Zonation				
		Martini & Worsley (1970)	Okada & Bukry (1980)	Zone	Subzone	Datum - level indicators		
PLIO-CENE	TABIANIAN	NN 12	CN 10 a/b	<i>C. leptoporus</i>	<i>C. leptoporus</i> MC	<i>C. rugosus</i> *		
					<i>C. leptoporus</i> MB			
					<i>C. leptoporus</i> MA			
MIOCENE	MESSINIAN	NN 11	CN 9	<i>R. rotaria</i>		<i>R. rotaria</i> †		
					<i>A. primus</i>		<i>R. rotaria</i> *	
						<i>C. pelagicus</i>		<i>Amaurolithus</i> spp.*
								<i>M. convallis</i> †
	TORTONIAN	NN 10	CN 8	<i>M. convallis</i>	<i>G. rotula</i>	<i>E. misconceptus</i> *		
					<i>E. pentaradiatus</i>	<i>E. hamatus</i> †		
					<i>E. pseudovariabilis</i>	<i>M. convallis</i> *		
		NN 9	CN 7	<i>E. calcaris</i>	<i>E. hamatus</i>	<i>E. hamatus</i> *		
					<i>E. bellus</i>	<i>E. calcaris</i> * <i>E. bellus</i> *		
		SERRAVALIAN	NN 8	CN 6	<i>E. exilis</i>	<i>E. bollii</i>	<i>H. walberdorfensis</i> †	
						<i>E. kugleri</i>	<i>R. floridana</i> †	
	NN 7		b	<i>H. intermedia</i>		<i>H. stalis</i> *		
				<i>H. orientalis</i>		<i>H. orientalis</i> * <i>S. fragilis</i> *		
				<i>H. walberdorfensis</i>		<i>S. heteromorphus</i> †		
	LANGHIAN	NN 5	CN 4	<i>S. heteromorphus</i>	<i>E. musicus</i>	<i>H. waltrans</i> †		
					<i>H. waltrans</i>	<i>H. perch-nielseniae</i> †		
					<i>H. perch-nielseniae</i>	<i>H. ampliaperta</i> †		
	BURDIGALIAN	NN 4	CN 3	<i>H. ampliaperta</i>	<i>E. signus</i>	<i>E. signus</i> *		
					<i>H. obliqua</i>	<i>E. exilis</i> *		
AQUITANIAN	NN 3	CN 2	<i>T. milowii</i>		<i>S. heteromorphus</i> *			
				NN 2	c	<i>H. vedderi</i>	<i>G. rotula</i> *	
						<i>E. druggii</i>	<i>H. ampliaperta</i> *	
CHATTIAN	NN 1	CN 1	<i>E. deflandrei</i> (Bukry)	<i>E. druggii</i> *				
OLIGO-CENE					<i>R. abisecta</i> Acme †			

* First occurrence † Last occurrence

Fig. 44. Boundary definitions of the zones and subzones of the “Mediterranean Miocene Zonation”. The Tortonian/Messinian boundary is set here at the level of F.O. of *R. rotaria* which nearly coincides with the F.O. of the *Globorotalia conomiozea* group (see also Langereis, Zachariasse and Zijdeveld, 1984). The position of all other stage boundaries is based on data from Haq (1984).

hope, however, that the presented descriptions and pictorial documentation will compensate for this shortcoming.

A second problem may arise in respect to the names given to the subzones and zones. Many of the names have been used already for completely different zones. Obviously, this is a consequence of the limited number of suitable names. In order to avoid confusion every previously used zonal name is mentioned in the text and in the figures with the name(s) of the original author(s).

Our new Mediterranean Miocene Zonation was applied to closely sampled D.S.D.P. cores which contained both the new and the conventional markers. The D.S.D.P. Sites 369 (cores 1 to 13), 231 (cores 29 to 57) and 219 (cores 8 to 14) proved to be suitable for this part of the investigation. This helped us to determine the position of the Mediterranean Miocene biohorizons relative to those employed in the conventional zonations. Intermingling of the conventional datum levels with those introduced here for the Mediterranean sections led to finer subdivisions of some intervals.

The results led to the composition of an "Integrated Miocene Zonation" (fig. 45) which might be useful for correlations of middle latitude Miocene sections. It will be evident that the Integrated Miocene Zonation is based on a mixture of cosmopolitan and provincial datum levels. The provincial datum levels are used here only for subzonal subdivisions. This was prompted by the need to avoid zonal hiatuses introduced artificially by the absence or the sporadic occurrence of the provincial markers.

COMPARISON BETWEEN THE TWO BIOZONAL SCHEMES

The "Integrated Miocene Zonation" and the "Mediterranean Miocene Zonation" are identical in number and names of zones, but they differ in the number of smaller subdivisions.

More precisely, the *T. martinii* and *S. belemnos* Subzones are not applicable in the Mediterranean area and, therefore, are presented only in the "Integrated Miocene Zonation". The same applies to the zonules to which the *E. pseudovariabilis* and the *G. rotula* Subzones have been subdivided. On the other hand, the *C. leptoporus* Zone of the "Mediterranean Miocene Zonation" is subdivided into three subzones (MA, MB and MC) that can only be used in the Mediterranean area. The same zone appears, in the Integrated Miocene Zonation, with two different subzones (A and B). The upper boundary of the *C. leptoporus* Subzone A falls possibly within the *C. leptoporus* Subzone MB.

The reader is referred to figures 44 and 45 for differences in the datum-level indicators used in the two zonal schemes.

Epoch	Stages	Other Zonations		Integrated Miocene Zonation			
		Martini & Worsley (1970)	Okada & Bukry (1980)	Zone	Subzone	Datum-level indicators	
PLIO-CENE	TABIANIAN	NN 12	CN 10 a/b	<i>C. leptoporus</i>	<i>C. leptoporus</i> B	<i>C. rugosus</i> *	
					<i>C. leptoporus</i> A	<i>C. acutus</i> *, <i>E. quinquaramus</i> †, <i>T. rugosus</i> †	
MIOCENE	MESSINIAN	NN 11	CN 9	<i>R. rotaria</i>		<i>R. rotaria</i> †	
						<i>R. rotaria</i> *	
						<i>A. primus</i>	<i>Amaurolithus</i> spp.*
						<i>C. pelagicus</i>	<i>M. convallis</i> †
	TORTONIAN	NN 10	CN 8	<i>M. convallis</i>	<i>G. rotula</i> b	<i>E. quinquaramus</i> *	
					<i>E. pentaradiatus</i> a	<i>E. pentaradiatus</i> †, <i>E. misconceptus</i> *	
		NN 9	CN 7	<i>E. pseudo-variabilis</i>	<i>E. pseudo-variabilis</i> b	<i>E. hamatus</i> †	
					<i>E. pseudo-variabilis</i> a	<i>E. pentaradiatus</i> *	
	SERRAVALIAN	NN 8	CN 6	<i>E. calcaris</i>	<i>E. hamatus</i>	<i>M. convallis</i> *	
					<i>E. bellus</i>	<i>E. hamatus</i> *	
		NN 7	b	<i>E. exilis</i>	<i>E. bollii</i>	<i>E. calcaris</i> *, <i>E. bellus</i> *	
					<i>E. kugleri</i>	<i>H. walbersdorfensis</i> †, <i>E. kugleri</i> †, <i>E. coalitus</i> *	
		NN 6	CN 5	<i>E. exilis</i>	<i>H. intermedia</i>	<i>E. kugleri</i> * <i>R. floridana</i> †	
					<i>H. orientalis</i>	<i>H. stalis</i> *	
					<i>H. walbersdorfensis</i>	<i>H. orientalis</i> *	
					<i>S. heteromorphus</i>	<i>S. heteromorphus</i> †	
		LANGHIAN	NN 5	CN 4	<i>S. heteromorphus</i>	<i>E. musicus</i>	<i>H. waltrans</i> †
						<i>H. waltrans</i>	<i>H. perch-nielseniae</i> †
	BURDIGALIAN	NN 4	CN 3	<i>H. ampliaperta</i>	<i>H. perch-nielseniae</i>	<i>H. ampliaperta</i> †	
					<i>E. signus</i>	<i>E. signus</i> *	
NN 3		CN 2	<i>T. milowii</i>	<i>H. obliqua</i>	<i>E. exilis</i> *		
				<i>S. belemnus</i>	<i>S. heteromorphus</i> *, <i>S. belemnus</i> †		
AQUITANIAN	NN 2	CN 1	<i>T. carinatus</i>	<i>T. carinatus</i>	<i>T. carinatus</i> †, <i>S. belemnus</i> *		
				<i>H. vedderi</i>	<i>G. rotula</i> *		
OLIGO-CENE	CHATTIAN	NN 1	a	<i>E. druggii</i>	<i>H. ampliaperta</i> *		
				<i>E. deflandrei</i> (Bukry)	<i>E. druggii</i> †, <i>T. martinii</i> *		
					<i>R. abisecta</i> Acme†		

* First occurrence † Last occurrence

Fig. 45. Boundary definitions of the zones, subzones and zonules of the "Integrated Miocene Zonation" (see also the legend of fig. 44).

BIOSTRATIGRAPHIC PROBLEMS RELATED TO THE MEDITERRANEAN MIOCENE

Early zonations devised particularly for the Mediterranean Miocene were rough and partial (fig. 46). Cati and Borsetti (1970) introduced several zones based on discoaster assemblages. The species used, however, are possibly preservational morphotypes of long-ranging discoasters such as *E. variabilis*, *E. exilis* and *E. brouweri*.

Schmidt (1973) presented a zonation for the Neogene of the southern Aegean area. He divided the interval Middle to Upper Miocene into three zones, but these zones are hard to recognize as they are defined either on the basis of "preservational" species such as *E. aulakos* and *E. divaricatus* or species such as *E. quinqueramus*, which is rare in the Mediterranean area, if not absent.

Stradner (1973) used the standard nannofossil zonation of Martini (1971) for his age determinations of the D.S.D.P. Leg 13. He admitted, however, that the "assignments of Miocene assemblages to a certain Zone was complicated by the lack of some index species" and mentioned *E. coalitus* (= *C. coalitus*) as one of them. Cita (1973) who summarized the results of Stradner offered some indirect evidence about the possible absence of *E. quinqueramus*. She implied that the *E. quinqueramus* Zone was not determined by the presence of the nominal index species but by the position of this zone – in the deep sea sequences – in relation to the *E. calcaris* and *C. tricorniculatus* Zones. The assignment by Martini (1971) of the type Tortonian to the *E. hamatus* and *E. calcaris* Zones provided a "logical" basis for assuming that

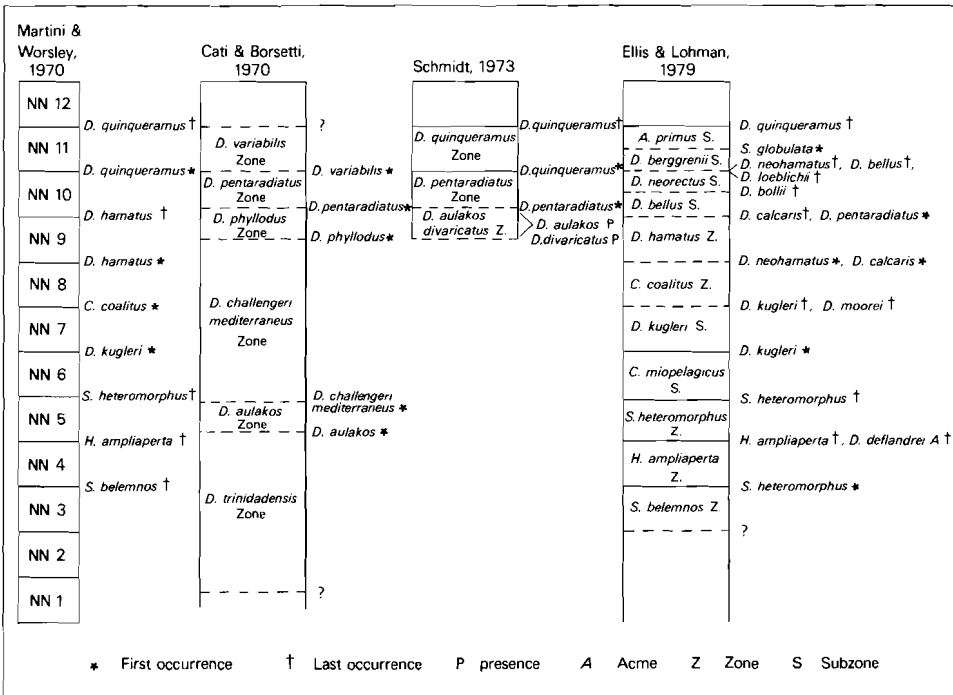


Fig. 46. Early nannofossil zonations for the Mediterranean Miocene.

the Messinian evaporitic succession corresponded to the *E. quinqueramus* Zone.

Barbieri and Rio (1974) in their study of the nannofossil content of the clay intercalations in the gypsum series reported the presence of *E. quinqueramus*. Nevertheless, the single specimen they depicted (pl. 1, fig. 14) is atypical and resembles an asymmetrical *E. bellus* rather than the characteristic *E. quinqueramus* such as observed in typical associations of the species in extra-Mediterranean areas.

More evidence about the absence of some Miocene index species from the Mediterranean is provided by Bizon and Müller (1979). More specifically, *T. carinatus* and *E. quinqueramus* are mentioned as rare or missing.

Müller (1978) mentioned having used successfully the standard nannofossil zonation of Martini (1971) by basing her zonal assignments on the whole assemblages and not on the presence of the index species, most of which appeared to be too scarce or missing. In her introductory description of the zones, *T. carinatus*, *S. belemnos*, *E. coalitus*, *E. hamatus* and *E. quinqueramus* are reported as extremely scarce or absent, whereas *E. kugleri* is mentioned as atypically developed. Similar statements were made by Müller, in Bizon and Müller (1979).

Moshkovitz and Ehrlich (1980) who studied the Neogene nannofossil associations from the Jaffa-1 borehole (Israel) also discussed the sporadic occurrence or absence of *T. carinatus*, *E. druggii*, *S. belemnos*, *E. coalitus* and *E. hamatus*. Furthermore they mentioned the difficulty they had in recognizing *E. kugleri*.

We experienced comparable difficulties when we tried to apply the conventional zonations to the Mediterranean sections and D.S.D.P. cores (the reader is referred to the preceding chapters); of all zones presented in the conventional zonal schemes of Martini and Worsley (1970) and Bukry (1973, 1975) only the *S. heteromorphus* Zone is easily recognizable in the Mediterranean area, as both of its zonal markers are abundantly present (fig. 43). The identification of the *E. hamatus* Zone is more problematical because of the sporadic, but nevertheless consistent, occurrence of *E. bellus* below and above the range of *E. hamatus*. The recognition of this zone however is only possible if we confine our species concept of *E. hamatus* to typical pentaradial forms with clearly bent arm tips and without birefringence. All other zones can only be inferred on the basis of their position relative to the *S. heteromorphus* and *E. hamatus* Zones. Species such as *S. belemnos* and *T. carinatus* were extremely rare and sporadic, whereas the typical forms of *E. kugleri*, *E. coalitus*, *E. calyculus* and *E. quinqueramus* were entirely absent.

Atypical forms of the latter four species could best be assigned to preservational morphotypes of *E. deflandrei*, *E. musicus* and *E. bellus* respectively.

Special attention should be paid to the biostratigraphic studies of the eastern Mediterranean region by Ellis (1979) and Ellis and Lohman (1979). In both studies the zonations are based on the low latitude zonation of Bukry (1973, 1975), but some modifications of the original scheme are also introduced.

An advantage of their zonation is that it includes as datum levels the first occurrences of *E. exilis* and *E. calcaris*. Both species have continuous ranges and their first occurrences are not obscured by preceding homeomorphic discoasters. The use of datum levels – and auxiliary datum levels – such as the first occurrence of *E. kugleri* and the last occurrences of *E. kugleri*, “*E. moorei*”, *H. intermedia*, *E. calcaris*, *E. bollii*, “*E. neohamatus*”, *E. bellus* and *E. quinqueramus* as suggested in their Mediterranean zonation is disadvantageous, however, because:

“*E. moorei*” and “*E. neohamatus*” are dubious taxonomic units. The first “species” is possibly a mixture of asymmetric pentaradial variants of *E. deflandrei* and *E. variabilis* and therefore it has been observed to occur repeatedly at various biostratigraphic intervals. “*E. neohamatus*”, on the other hand, is a taxonomic category possibly made of preservational morphotypes of *E. calcaris* and/or *E. brouweri* with bent arm tips.

The last occurrence of *E. calcaris* is not biostratigraphically helpful because the last representatives of the species have less pronouncedly curved arm tips. Their identification, therefore, is impeded by the presence of the first representatives of *E. brouweri*.

E. bollii very often has a discontinuous range. Its last presence, therefore, does not always correspond with the end of the range of the species.

H. intermedia and *E. bellus* have been observed at higher biostratigraphic intervals than the interval indicated by Ellis and Lohman.

E. kugleri and *E. quinqueramus* are not suitable as index species in the Mediterranean area for reasons discussed earlier in this chapter.

DESCRIPTION OF THE MIOCENE ZONATIONS: THE MEDITERRANEAN MIOCENE ZONATION AND THE INTEGRATED MIOCENE ZONATION

In order to avoid repetitive definitions of zones and subzones both zonal schemes are discussed together. The zones and the subzones are described in the order given in the Integrated Miocene Zonation (fig. 45). All subdivisions must be considered as present also in the Mediterranean Miocene Zonation (fig. 44) unless otherwise indicated.

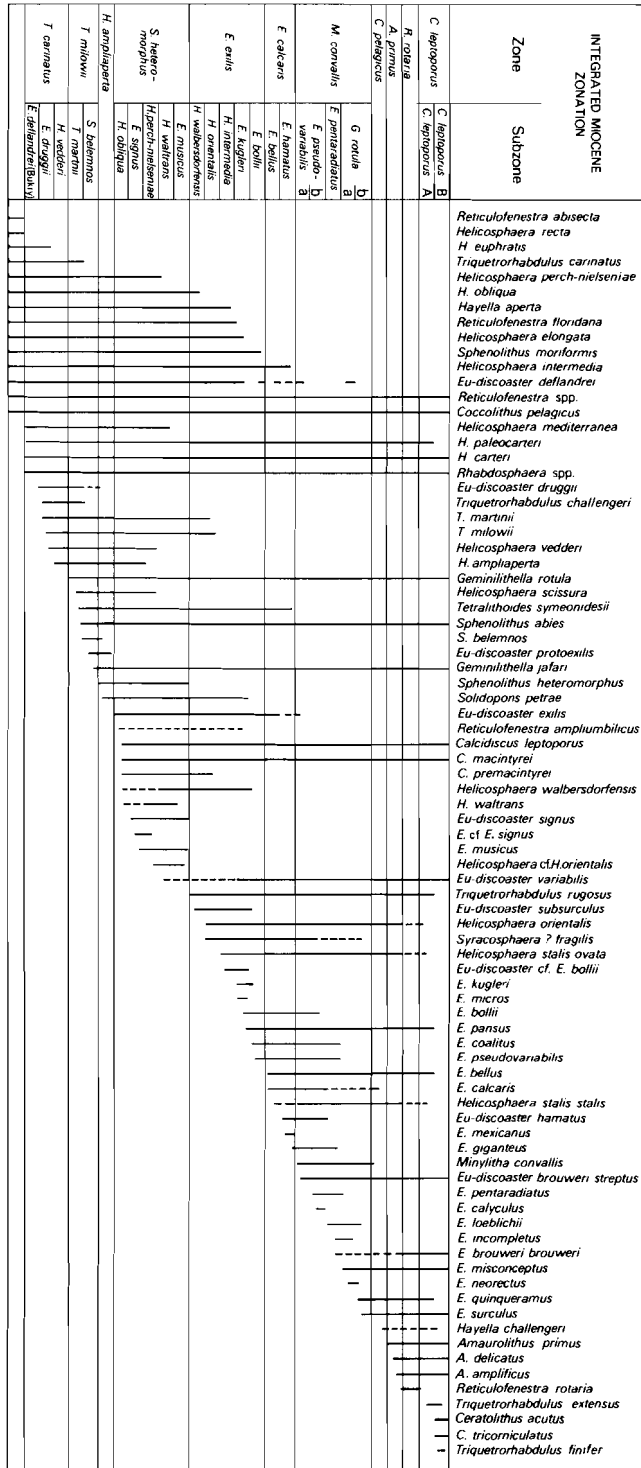


Fig. 47. Maximum ranges of the Miocene species which are mentioned in the text, arranged in order of first occurrences.

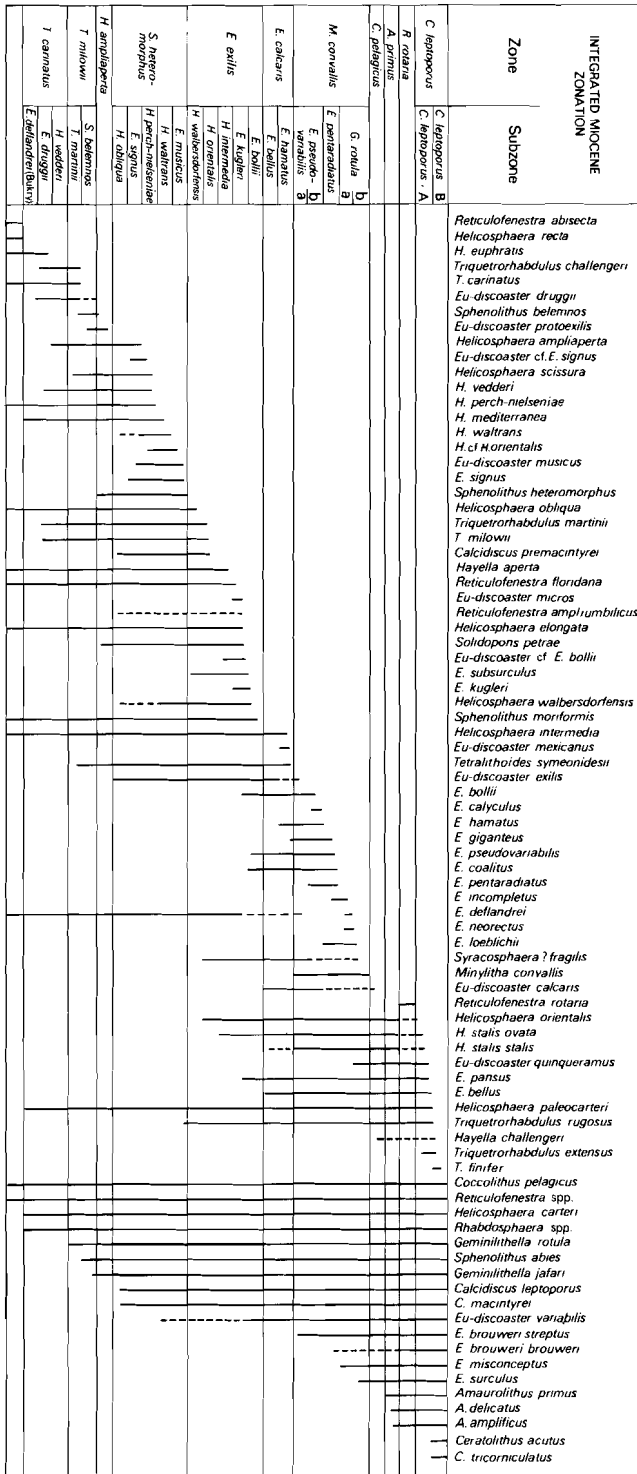


Fig. 48. Maximum ranges of the Miocene species which are mentioned in the text, arranged in order of last occurrences.

Age	Martini & Worsley 1970		Integrated Miocene Zonation (this paper)		Bukry 1973, 1975			
	Zone	Datum levels in common	Zone	Subzone	Datum levels in common	Subzone	Zone	
PLIO-CENE	<i>C. tricorniculatus</i> (Gartner) NN12	<i>C. rugosus</i> *	<i>C. leptoporus</i>	<i>C. leptoporus</i> B	<i>C. rugosus</i> *	<i>C. acutus</i> (Bukry)	<i>C. tricorniculatus</i> (Bukry) CN 10	
	MIOCENE	<i>D. quinqueramus</i> (Gartner)		<i>E. quinqueramus</i> †	<i>R. rotaria</i>	<i>C. leptoporus</i> A		<i>E. quinqueramus</i> †
<i>A. primus</i>			<i>C. primus</i> (Bukry)				<i>D. quinqueramus</i> (Gartner) CN 9	
<i>C. pelagicus</i>			<i>D. berggrenii</i> (Bukry)					
NN 11			<i>E. quinqueramus</i> *				<i>M. convallis</i>	
<i>D. calcaris</i> (Martini) NN 10		<i>E. hamatus</i> †	<i>E. pentaradiatus</i>	<i>D. bellus</i> (Bukry)				
<i>D. hamatus</i> (Braml. & Wilcox.) NN 9			<i>E. hamatus</i> *	<i>E. pseudo-variabilis</i> b	<i>E. hamatus</i> †	<i>C. calyculus</i> (Bukry)	<i>D. hamatus</i> (Braml. & Wilcox.) CN 7	
		<i>E. hamatus</i> *		<i>E. hamatus</i>		<i>H. kamptneri</i> (Bukry)		
<i>C. coalitus</i> (Braml. & Wilcox.) NN 8		<i>E. coalitus</i> *	<i>E. calcaris</i>	<i>E. bellus</i>	<i>E. hamatus</i> *	<i>C. coalitus</i> (Braml. & Wilcox.) CN 6		
<i>D. kugleri</i> (Braml. & Wilcox.)		<i>E. kugleri</i> *		<i>E. bollii</i>			<i>E. kugleri</i> †	<i>D. kugleri</i> (Bukry) b
<i>D. exilis</i> (Martini & Worsley) NN 6		<i>E. kugleri</i> *		<i>E. exilis</i>			<i>E. kugleri</i>	
	<i>H. intermedia</i>						<i>E. kugleri</i> *	<i>R. floridana</i> †
<i>S. heteromorphus</i> (Braml. & Wilcox.) NN 5	<i>S. heteromorphus</i> †	<i>S. heteromorphus</i>	<i>H. walbersdorffensis</i>	<i>S. heteromorphus</i> †	<i>C. miopelagicus</i> (Bukry) a	<i>D. exilis</i> (Martini & Worsley) CN 5		
<i>H. ampliaperta</i> (Braml. & Wilcox.) NN 4	<i>H. ampliaperta</i> †		<i>H. walbersdorffensis</i>				<i>H. ampliaperta</i> †	<i>S. heteromorphus</i> *
			<i>H. perch-nielseniae</i>					
<i>S. belemnus</i> (Braml. & Wilcox.)	<i>S. heteromorphus</i> *		<i>H. obliqua</i>				<i>H. ampliaperta</i>	<i>H. ampliaperta</i> (Braml. & Wilcox.) CN 3
<i>T. carinatus</i> (Martini & Worsley) NN 2	<i>T. carinatus</i> †	<i>T. milowii</i>	<i>E. signus</i>	<i>S. heteromorphus</i> *	<i>S. belemnus</i> (Braml. & Wilcox.) CN 2			
<i>T. carinatus</i> (Martini & Worsley) NN 1	<i>E. druggii</i> *		<i>S. belemnus</i>			<i>H. obliqua</i>	<i>D. druggii</i> (Bukry) c	
		<i>T. martinii</i>	<i>H. vedderi</i>	<i>D. deflandrei</i> (Bukry) b				
		<i>T. carinatus</i>	<i>E. druggii</i>		<i>E. druggii</i> *	<i>T. carinatus</i> (Bukry)		
			<i>E. deflandrei</i> (Bukry)	<i>R. abisecta</i> Acme †				
OLIGOCENE						CN 1		

* First occurrence † Last occurrence

Fig. 49. Correlation of the Integrated Miocene Zonation with the zonal compilations of Martini and Worsley (1970) and Bukry (1973, 1975), CN-code numbers after Okada and Bukry (1980). Correlation lines between the zonal schemes are drawn along common datum levels. The names of the index species have been modified according to the nomenclatural changes in this paper.

Several boundaries of the (sub)zones are based on more than one zonal marker; these markers are considered to be of equal importance.

The assemblages of the zones are given through the descriptions of their subzones. Figures 47 and 48 present an overview of the nannofossil content of every unit of the Integrated Miocene Zonation.

In order to avoid confusion between new units and units given the same names by other authors, a correlation scheme is presented in figure 49. Correlation lines are drawn only when the zonal schemes have markers in common. Furthermore, references in our text to homonymous (sub)zones of other authors are accompanied by the names of those authors.

The *C. leptoporus* Zone is subdivided into subzones indicated by a capital letter which follows the name of the zone. An M is added prior to that indication when these parts are present only in the Mediterranean region.

The *E. pseudovariabilis* and the *G. rotula* Subzones in the extra-Mediterranean sections can be subdivided into zonules. The zonules are indicated by small letters following the names of the subzones.

The distribution of all the new zones and subzones in our Miocene sections is given in figure 50.

Triquetrorhabdulus carinatus Zone

Definition: Interval zone from the end of the acme of *Reticulofenestra abisecta* (= *Cyclicargolithus abisectus*) (bottom) to the first occurrence of *Geminilithella rotula* (top).

Comparison: The *T. carinatus* Zone, as defined here, differs in the definition of the upper and lower boundaries from the similarly named zones of Bramlette and Wilcoxon (1967), Bukry and Bramlette (1970), Hay (1970), Martini (1971), Roth, Baumann and Bertolini (1971), Gartner (1974), Roth (1973) and Bukry (1973, 1975).

Subdivision: *Eu-discoaster deflandrei* Subzone, *Eu-discoaster druggii* Subzone and *Helicosphaera vedderi* Subzone. All three subzones are recognizable both in the Mediterranean and the extra-Mediterranean sections.

Remarks: Bramlette and Wilcoxon (1967) defined the *Triquetrorhabdulus carinatus* Zone by the range of the nominal species above the last occurrence of *Helicosphaera recta*, but since then the zonal definition has undergone modifications. A summary of the different versions of the *T. carinatus* Zone has been presented by Bukry (1978). Datum levels such as the *T. carinatus* L.O., *S. belemnos* F.O., *H. ampliapertura* F.O., and *E. druggii* F.O. have been used either individually or in combination for the definition of the upper boundary of the Zone (Bukry and Bramlette, 1970; Martini and Worsley, 1970; Martini, 1971; Roth, Baumann and Bertolini, 1971; Gartner, 1974; Roth, 1973; Bukry, 1973 and 1975).

INTEGRATED MIOCENE ZONATION (This paper)		MEDITERRANEAN									
Zone	Subzone	SIERRA LEONE RISE	MENORCA RISE	SICILY							
		Leg. 41, Site 369 A cores: 1-13 369A - samples	Leg. 42A, Site 372 cores: 1-13 372 - samples	Giammoia 1 CP - samples	Giammoia 2 CP - samples	Giammoia 3 CP - samples	Mineo JT - samples	Scicli CP - samples	Falconara 1 JT - and CP - samples	Falconara 2 JT - samples	Scardilli CP - samples
<i>C. leptoporus</i>	<i>C. leptoporus</i> A									1942	4364
<i>R. rotaria</i>										1916	4360
<i>A. primus</i>										1905	4354
<i>C. pelagicus</i>						3155		4560	3034	1900	4345
						3151		4555	3030	1945	4308
<i>M. convallis</i>	<i>G. rotula</i> b										
	a										
	<i>E. pentara-diatius</i>					3138		4501	3018	1946	4301
	<i>E. pseudo-variabilis</i> b					3136			3009		
	a										
<i>E. calcaris</i>	<i>E. hamatus</i>					3130				3060	
	<i>E. bellus</i>										
<i>E. exilis</i>	<i>E. bollii</i>					3749				3067	
	<i>E. kugleri</i>					3743				3068	
	<i>H. intermedia</i>					11 m		4610			
	<i>H. orientalis</i>					3714		4601		3069	
	<i>H. walbersdorfensis</i>					8.4 m		3105		3073	
<i>S. heteromorphus</i>	<i>E. musicus</i>					3703		4595			
	<i>H. waltrans</i>					20 m					
	<i>H. perch-nielseniae</i>					3683		4592			
	<i>E. signus</i>					14 m					
	<i>H. obliqua</i>					3671		4565			
						12.2 m		4561			
						3662					
<i>H. ampliaperta</i>							4508				
<i>T. milowii</i>	<i>S. belemnos</i>							4962			
	<i>T. martinii</i>										
<i>T. carinatus</i>	<i>H. vedderi</i>										
	<i>E. druggii</i>										
	<i>E. deflandrei</i>										

Fig. 50. Distribution of the units of the Integrated Miocene Zonation in our sections. The uppermost sample of each unit is used as a boundary (between adjacent units). The thicknesses of the units (bold numbers) are given only in the type localities.

Here the upper boundary of the *T. carinatus* Zone is set at the first occurrence of *G. rotula*, which has a continuous record; it is more abundant and occurs consistently in both the Mediterranean and the extra-Mediterranean sections.

Distribution: D.S.D.P. Site 369A, Sierra Leone Rise, Atlantic Ocean, samples: 369A-79 to 369A-65. Reqqa Point, Gozo, samples: MT713 to MT721.

Eu-discoaster deflandrei Subzone

Definition: Interval from the end of the acme of *R. abisecta* (bottom) to the first occurrence of *E. druggii* (top).

Author: Bukry, 1971.

Assemblage: *Coccolithus pelagicus*, *Eu-discoaster deflandrei*, *Helicosphaera carteri*, *H. elongata* (sporadic), *H. euphratis*, *H. intermedia*, *H. mediterranea* (rare and sporadic), *H. perch-nielseniae* (sporadic), *Reticulofenestra* spp., *R. abisecta*, *R. floridana*, *Sphenolithus moriformis*, *Triquetrorhabdulus carinatus*, *T. challengerii*.

Remarks: The lowermost Miocene samples of our sections (D.S.D.P. Sites 372 and 369A) represent only the upper part of this interval. The definition of the lower boundary, therefore, is based on data presented by Bukry (1973, 1975). Rare specimens of *H. recta* were encountered in both D.S.D.P. sections. The scarcity of these helicoliths makes it hard to decide whether we are dealing with indigenous or reworked specimens. Neither *T. carinatus* nor *T. challengerii* has been observed in the Mediterranean assemblage of the *E. deflandrei* Subzone.

Distribution: D.S.D.P. Site 369A, Sierra Leone Rise, Atlantic Ocean, samples: 369A-79 to 369A-74. D.S.D.P. Site 372, Menorca Rise, samples: 372-148 to 372-145. Reqqa Point, Gozo, within the interval MT713 to MT721 (the upper boundary of this subzone was not recognized at this locality).

Eu-discoaster druggii Subzone

Definition: Interval from the first occurrence of *Eu-discoaster druggii* (bottom) to the first occurrence of *Helicosphaera ampliaptera* (top).

Comparison: The *E. druggii* Subzone as defined here has the same lower boundary as the similarly named zones and subzones of other authors, but it represents a shorter biostratigraphic interval.

Assemblage: *Coccolithus pelagicus*, *Eu-discoaster deflandrei*, *E. druggii*, *Helicosphaera carteri*, *H. elongata* (sporadic), *H. euphratis*, *H. paleocarteri*, *H. perch-nielseniae*, *H. recta* (rare), *H. vedderi* (rare), *Reticulofenestra* spp., *R. abisecta*, *R. floridana*, *Sphenolithus moriformis*, *Triquetrorhabdulus carinatus*, *T. challengerii*, *T. martinii* (= *Orthorhabdus serratus*), *T. milowii*.

Remarks: *E. druggii* is a species that occurs sporadically in the Mediterranean area (Müller, 1978, 1979; Moshkovitz and Ehrlich, 1980) and in high latitude regions (Perch-Nielsen, 1977). Therefore, its first occurrence is not

used here to define a zonal boundary. The species, however, is considered as a useful marker for the low-latitude D.S.D.P. cores (Bukry, 1971, 1973) and therefore we retain this marker in our zonation.

Müller (1978) substituted the first (rare) occurrence of *H. ampliaperta* for the first occurrence of *E. druggii*. In our study of the material from D.S.D.P. Site 372 *E. druggii* was rare but consistently present well below the first (rare) occurrence of *H. ampliaperta*.

The first occurrence of *T. martinii* (= *Orthorhabdus serratus*) was noted to be very close to the first occurrence of *E. druggii* (D.S.D.P. Site 369). This is in agreement with the suggestion of Bukry (1973) that it can be used as an auxiliary marker. The species, however, was absent from the Mediterranean Site 372. The first rare occurrence of *H. vedderi* has been noted in the upper part of the *E. druggii* Subzone.

Reference locality: D.S.D.P. Site 372, Menorca Rise, samples: 372-144 to 372-125. The thickness of this subzone in this site is 235 metres.

Distribution: D.S.D.P. site 369A, Sierra Leone Rise, samples: 369A-73 to 369A-65. Reqqa Point, Gozo, within the interval from sample MT713 to MT721 (the lower boundary of this subzone was not recorded in the section Reqqa Point).

Helicosphaera vedderi Subzone

Definition: Interval from the first occurrence of *Helicosphaera ampliaperta* (bottom) to the first occurrence of *Geminilithella rotula* (top).

Assemblage: *Coccolithus pelagicus*, *Eu-discoaster deflandrei*, *E. druggii*, *Helicosphaera ampliaperta*, *H. carteri*, *H. elongata*, *H. euphratis*, (rare) *H. intermedia*, *H. mediterranea* (sporadic), *H. obliqua*, *H. paleocarteri*, *H. perch-nielseniae*, *H. vedderi*, *Reticulofenestra* spp., *R. abisecta*, *R. floridana*, *Sphenolithus moriformis*, *Triquetrorhabdulus carinatus*, *T. challengeri*, *T. milowii*.

Remarks: *Helicosphaera ampliaperta* was found to be a useful guide species with a continuous record in all the Mediterranean sections. In the D.S.D.P. Site 372 and the sections Giammoia 1 (Sicily) and Reqqa Point (Malta) the first occurrence of *H. ampliaperta* was noted below but very close to the first occurrence of *G. rotula*, thus allowing the distinction of the *H. vedderi* Subzone. This subzone represents a very thin biostratigraphic interval and may be absent in areas with low sedimentation rates.

Backman (1980) reported the first occurrence of *G. rotula* close to but below the first occurrence of *H. ampliaperta* in D.S.D.P. Site 116. This is possibly due to the presence of specimens of *Hayella* sp. which have been noted to occur sporadically in our sections below the range of *H. ampliaperta*.

In the D.S.D.P. Site 369A the first occurrences of *H. ampliaperta* and *G. rotula* coincide. This is possibly the result of a hiatus at that level. The presence of such a hiatus is also indicated by the nearly simultaneous first occurrences of *S. heteromorphus* and *E. exilis* at the same level, and by the lack of *S. belemnos*.

Reference locality: D.S.D.P. Site 372, samples: 372-124 to 372-122. Thickness: 43 m.

Distribution: Giammoia 1, Sicily, samples: CP3601 to CP3602.

Triquetrorhabdulus milowii Zone

Definition: Interval zone from the first occurrence of *Geminilithella rotula* (bottom) to the first occurrence of *Sphenolithus heteromorphus* and/or the last occurrence of *Sphenolithus belemnos* (top).

Subdivision: *Triquetrorhabdulus martinii* Subzone and *Sphenolithus belemnos* Subzone. Both subzones are based on literature data. They are not recognizable in the Mediterranean area.

Remarks: This zone contains the last occurrence of *T. carinatus* and the first occurrence of *S. belemnos*, neither of which can be used for zonal assignments in the Mediterranean area. The *T. carinatus* L.O. and the *S. belemnos* F.O. are used instead as subzonal markers to be utilized only in extra-Mediterranean regions.

Reference locality: D.S.D.P. Site 372, Menorca Rise, samples: 372-121 to 372-115. The thickness of the *T. milowii* Zone in this locality is 28 metres.

Distribution: Reqqa Point, Gozo, samples: MT721 to MT730.

Triquetrorhabdulus martinii Subzone

Definition: Interval from the first occurrence of *Geminilithella rotula* (bottom) to the last occurrence of *Triquetrorhabdulus carinatus* and the first occurrence of *Sphenolithus belemnos* (top).

Assemblage: *Coccolithus pelagicus*, *Eu-discoaster deflandrei*, *E. druggii*, *Geminilithella rotula*, *Helicosphaera ampliaperta*, *H. carteri*, *H. elongata*, *H. intermedia*, *H. mediterranea* (sporadic), *H. obliqua*, *H. paleocarteri*, *H. perch-nielseniae*, *H. scissura*, *H. vedderi*, *Reticulofenestra* spp., *R. floridana*, *Sphenolithus* cf. *S. abies*, *S. moriformis*, *Tetralithoides symeonidesii*, *Triquetrorhabdulus carinatus*, *T. challengerii*, *T. martinii*, *T. milowii*.

Remarks: *T. challengerii* is present throughout the interval that falls within the Miocene part of the range of *T. carinatus* in the D.S.D.P. Site 369A.

S. belemnos was not recorded in the D.S.D.P. Site 369. The suggestion here that the first occurrence of *S. belemnos* can be regarded as an alterna-

tive for the last occurrence of *T. carinatus* is based on the data of Bukry and Bramlette (1970).

Sphenolithus belemnus Subzone

Definition: Interval from the last occurrence of *Triquetrorhabdulus carinatus* and/or the first occurrence of *Sphenolithus belemnus* (bottom) to the first occurrence of *Sphenolithus heteromorphus* (top).

Comparison: The *Sphenolithus belemnus* Subzone is identical to the homonymous zone of Bramlette and Wilcoxon (1967).

Assemblage: *Coccolithus pelagicus*, *Eu-discoaster deflandrei*, *E. druggii*, *Geminilithella rotula*, *Helicosphaera ampliaperta*, *H. carteri*, *H. elongata*, *H. intermedia*, *H. mediterranea* (sporadic), *H. obliqua*, *H. paleocarteri*, *H. perch-nielseniae*, *H. scissura*, *H. vedderi*, *Reticulofenestra* spp., *R. floridana*, *Sphenolithus* cf. *S. abies*, *S. belemnus*, *S. moriformis*, *Tetralithoides symeonidesii*, *Triquetrorhabdulus carinatus*, *T. martinii*, *T. milowii*.

Remarks: There is some disagreement in the literature concerning the position of the *S. belemnus* L.O. relative to the *S. heteromorphus* F.O. Some investigators consider the two events as isochronous (Bramlette and Wilcoxon, 1967; Bukry, 1973). However, in Martini and Worsley (1971), Ellis (1975) and Gartner (1977), an overlap is indicated between the ranges of the two species. We are not in a position to decide which of the two opinions is more reliable because *S. belemnus* was not recorded in our sections. Therefore we use only the F.O. of *S. heteromorphus* as an indicator of the upper boundary of this subzone.

Helicosphaera ampliaperta Zone

Definition: Interval zone from the first occurrence of *Sphenolithus heteromorphus* (bottom) to the first occurrence of *Eu-discoaster exilis* (top).

Comparison: Only the definition of the lower boundary of this zone is the same as the one of the *H. ampliaperta* zone of Bramlette and Wilcoxon (1967). The upper boundary is different.

Assemblage: *Calcidiscus leptoporus* s.l., *Coccolithus pelagicus*, *Eu-discoaster deflandrei*, *E. protoexilis*, *Geminilithella jafari*, *G. rotula*, *Helicosphaera ampliaperta*, *H. carteri*, *H. elongata*, *H. intermedia*, *H. mediterranea*, *H. obliqua*, *H. paleocarteri*, *H. perch-nielseniae*, *H. scissura*, *H. vedderi*, *H. walbersdorfensis* s.l., *Reticulofenestra* spp., *R. floridana*, *Solidopons petrae*, *Sphenolithus abies*, *S. belemnus*, *S. heteromorphus*, *S. moriformis*, *Tetralithoides symeonidesii*, *Triquetrorhabdulus martinii*, *T. milowii*.

Remarks: In the definition by Bramlette and Wilcoxon (1967) the upper

boundary of their *H. ampliaperta* Zone was placed at the last occurrence of the nominal species. As can be inferred from the D.S.D.P. reports, *H. ampliaperta* may be absent in many parts of the oceanic areas. The species is missing in the western Indian Ocean (Müller, 1974) and was not encountered in the D.S.D.P. Sites of Leg 39 from the western South Atlantic (Perch-Nielsen, 1977) and Sites 400A and 406 from the North Atlantic (Müller, 1979).

Martini (1976) suggested the use of a combined NN4/NN5 zone in areas where *H. ampliaperta* is missing. Such a combination of zones, however, results in a relatively large biostratigraphic interval which can be subdivided further by the first occurrence of *E. exilis*, which appears to be a more cosmopolitan species than *H. ampliaperta*.

In our sections the last occurrence of *H. ampliaperta* was noted well above the first occurrence of *E. exilis* and above the first occurrence of *E. signus*. This justifies the use of the last occurrence of *H. ampliaperta* as a subzonal boundary within the next zonal unit (i.e. the *S. heteromorphus* Zone).

Bukry (1971, 1981), Ellis (1979) and Ellis and Lohman (1979) suggested that the last occurrence of *Triquetrorhabdulus milowii* is very close to the first occurrence of *S. heteromorphus* and considered it as an indication of the lower part of the *H. ampliaperta* Zone of Bramlette and Wilcoxon. In our sections, *T. milowii* persists higher than the last occurrence of *S. heteromorphus*. The last occurrence of *T. milowii* was recorded very close to the first occurrence of *Helicosphaera orientalis*. This is in accordance with the range of this species presented by Biolzi et al. (1981).

Reference locality: D.S.D.P. Site 372, samples: 372-114 to 372-108. Thickness in the reference locality: 52 metres.

Distribution: D.S.D.P. Site 369A, Sierra Leone Rise, Atlantic, sample: 369A-64; Giammoia 1, Sicily, samples: CP3603 to CP3609; Reqqa Point, Gozo, samples: MT731 to MT733; Marsalforn, Gozo, samples: MT744 to MT745; Ras il Pelegrin, Malta, samples: M110-A to M110-B; D.S.D.P. Site 231, Gulf of Aden, Indian Ocean, samples: 219-47 to 219-43.

Sphenolithus heteromorphus Zone

Definition: Interval zone from the first occurrence of *Eu-discoaster exilis* (bottom) to the last occurrence of *Sphenolithus heteromorphus* (top).

Comparison: The *S. heteromorphus* Zone as defined here covers a longer biostratigraphic interval than the similarly named zone of Bramlette and Wilcoxon (1967) with which it shares the upper boundary. The lower boundary has been shifted lower to the first occurrence of *E. exilis*.

Subdivision: *Helicosphaera obliqua* Subzone, *Eu-discoaster signus* Sub-

zone, *Helicosphaera Perch-nielseniae* Subzone, *Helicosphaera waltrans* Subzone, and *Eu-discoaster musicus* Subzone. All subzones are recognizable in the Mediterranean and the extra-Mediterranean sections.

Remarks: This interval is characterized by the continuous presence of *S. heteromorphus* and *E. exilis*. It contains the first occurrences of *C. macintyreii*, *C. premacintyreii*, *Hayella aperta* and *E. signus* emend. (*E. signus* (Bukry) including *E. petaliformis* (Moshkovitz and Ehrlich)). *H. ampliapertura*, *H. perch-nielseniae*, *H. vedderi* and *H. scissura* have their last occurrence in the lower part of this zone.

Helicosphaera waltrans occurs sporadically below the extinction level of *H. ampliapertura* but becomes common or abundant above it.

H. walbersdorfensis was noted sporadically from the base of the *S. heteromorphus* Zone (as defined here) but it becomes common close to the last occurrence of *H. ampliapertura*. This is much lower than the first occurrence indicated for *H. walbersdorfensis* by Müller (1981). Such an early occurrence of *H. walbersdorfensis* (= *H. californiana* Bukry) has been given also by Bukry (1981) who mentioned *H. californiana* from his CN4 zone.

Eu-discoaster musicus (= *E. sanmiguelensis* (Bukry)) has its total range in our sections within the *S. heteromorphus* Zone. The range of this species above the *S. heteromorphus* L.O. mentioned by Bukry (1981) – for *E. sanmiguelensis* – could not be confirmed.

Reference locality: D.S.D.P. Site 369A, Sierra Leone Rise, Atlantic, samples: 369A-63 to 369A-20. Thickness in this locality: 63.9 metres.

Distribution: D.S.D.P. Site 372, Menorca Rise, samples: 372-107 to 372-57; Giammoia 1, Sicily, samples: CP3610 to CP3618; Giammoia 2, Sicily, samples: CP3651 to CP3662; Mineo, Sicily, samples: JT4962 to JT4508; Reqqa Point, Gozo, samples: MT734 to MT743; Marsalforn, Gozo, samples: MT745 to MT774; Ras il Pelegrin, Malta, samples: M110-B to M110-J; Gnejna Bay, Malta, samples: MT622 to MT650; D.S.D.P. Site 219, Laccadive-Chagos Ridge, Indian Ocean, samples: 219-42 to 219-37.

Helicosphaera obliqua Subzone

Definition: Interval from the first occurrence of *Eu-discoaster exilis* (bottom) to the first occurrence of *E. signus* (top).

Assemblage: *Calcidiscus leptoporus*, *C. macintyreii*, *C. premacintyreii*, *Coccolithus pelagicus*, *Eu-discoaster deflandrei*, *E. exilis*, *Geminilithella jafari*, *G. rotula*, *Helicosphaera ampliapertura*, *H. carteri*, *H. elongata*, *H. intermedia*, *H. mediterranea*, *H. obliqua*, *H. perch-nielseniae*, *H. scissura*, *H. vedderi*, *H. walbersdorfensis* (rare), *H. waltrans* (rare), *Reticulofenestra* spp.,

R. ampliumbilicus (rare), *R. floridana*, *Solidopons petrae*, *Sphenolithus abies*, *S. heteromorphus*, *S. moriformis*, *Tetralithoides symeonidesii*, *Triquetrorhabdulus milowii*, *T. martinii*.

Reference locality: D.S.D.P. Site 369A, Sierra Leone Rise, Atlantic, samples: 369A-63 to 369-A61. Thickness in this site: 4.5 metres.

Distribution: D.S.D.P. Site 372, samples: 372-108 to 372-98; Giammoia 1, samples: CP3610 to CP3612; D.S.D.P. Site 219, Laccadive Chagos Ridge, samples: 219-42 to 219-37.

Eu-discoaster signus Subzone

Definition: Interval from the first occurrence of *Eu-discoaster signus* (bottom) to the last occurrence of *Helicosphaera ampliaperta* (top).

Assemblage: *Calcidiscus leptoporus*, *C. macintyreii*, *C. premacintyreii*, *Coccolithus pelagicus*, *Eu-discoaster deflandrei*, *E. exilis*, *E. musicus*, *E. signus*, *E. cf. E. signus*, *Geminilithella jafari*, *G. rotula*, *Hayella aperta*, *Helicosphaera ampliaperta*, *H. carteri*, *H. elongata*, *H. intermedia*, *H. mediterranea*, *H. obliqua*, *H. perch-nielseniae*, *H. scissura*, *H. vedderi*, *H. walbersdorfensis* (rare), *H. waltrans* (rare), *Reticulofenestra* spp., *R. ampliumbilicus* (rare), *R. floridana*, *Solidopons petrae*, *Sphenolithus abies*, *S. heteromorphus*, *S. moriformis*, *Tetralithoides symeonidesii*, *Triquetrorhabdulus milowii*, *T. martinii*.

Remarks: Questionable specimens of *Hayella* Gartner were recorded sporadically from the lowest Miocene samples of the D.S.D.P. Sites 369A and 372. Nannoliths of this genus with a short cone, named here *H. aperta*, became common from this interval onwards.

Reference locality: D.S.D.P. Site 369A, Sierra Leone Rise, samples: 369A-60 to 369A-46. The thickness of the *E. signus* Subzone in the reference locality is 21.1 metres.

Distribution: D.S.D.P. Site 372, samples: 372-97 to 372-94; Giammoia 1, Sicily, samples: CP3613 and CP3614.

Helicosphaera perch-nielseniae Subzone

Definition: Interval from the last occurrence of *Helicosphaera ampliaperta* (bottom) to the last occurrence of *H. perch-nielseniae* (top).

Assemblage: The same as in the *E. signus* Subzone with the addition of *Helicosphaera* cf. *H. orientalis* and the common occurrence of *H. waltrans*.

Remarks: *Eu-discoaster* cf. *E. signus* and *Helicosphaera scissura* have their last occurrence within this interval. *Helicosphaera vedderi* has been observed within this subzone too. This species persists possibly within the next higher

subzone but it becomes extremely rare and sporadic. A very small species of *Helicosphaera*, named here *H. cf. H. orientalis*, has its first rare occurrence within the *H. perch-nielseniae* Subzone.

Reference locality: D.S.D.P. Site 369A, Sierra Leone Rise, samples: 369A-45 to 369A-40. The thickness of the *H. perch-nielseniae* Subzone at this locality is 9 metres.

Distribution: D.S.D.P. Site 372, samples 372-93 to 372-89; Giammoia 1, Sicily, samples: CP3615 to CP3618; Reqqa Point, Gozo, samples: MT734 to MT736. Marsalforn, samples: MT745 to MT750; Ras il Pelegrin, Malta, samples: M110-B to M110-D.

Helicosphaera waltrans Subzone

Definition: Interval from the last occurrence of *Helicosphaera perch-nielseniae* (bottom) to the last occurrence of *Helicosphaera waltrans* (top).

Assemblage: *Calcidiscus leptoporus*, *C. macintyreii*, *C. premacintyreii*, *Coccolithus pelagicus*, *Hayella aperta*, *Eu-discoaster deflandrei*, *E. exilis*, *E. musicus*, *E. signus*, *E. variabilis*, *Geminolithella jafari*, *G. rotula*, *H. mediterranea*, *H. obliqua*, *H. paleocarteri*, *H. cf. H. orientalis* (rare), *H. walbersdorfensis* s.s., *H. waltrans*, *Reticulofenestra* spp., *R. ampliumbilicus* (rare), *R. floridana*, *Solidopons petrae*, *Sphenolithus abies*, *S. heteromorphus*, *S. moriformis*, *Tetralithoides symeonidesii*, *T. martinii*, *T. milowii*.

Remarks: The last occurrence of *H. mediterranea* was noted within this subzone. This position is much higher than the last occurrence indicated for this species by Müller (1981), i.e. top NN3.

Bukry (1981) recorded *H. mediterranea* (= *H. crouchii*) in Zones CN2–CN4 which is similar to the range of this species in our sections.

Reference locality: D.S.D.P. Site 369A, Sierra Leone Rise, Atlantic, samples: 369A-39 to 369A-36. Thickness at this site: 6.7 metres.

Distribution: D.S.D.P. Site 372, samples: 372-88 to 372-77; Reqqa Point, samples MT737 to MT743; Marsalforn, Gozo, samples: MT751 to MT764; Ras il Pelegrin, Malta, samples: M110-E and M110-F.

Eu-discoaster musicus Subzone

Definition: Interval from the last occurrence of *Helicosphaera waltrans* (bottom) to the last occurrence of *Sphenolithus heteromorphus* (top).

Assemblage: *Calcidiscus leptoporus*, *C. macintyreii*, *C. premacintyreii*, *Coccolithus pelagicus*, *Hayella aperta*, *Eu-discoaster deflandrei*, *E. exilis*, *E. musicus*, *E. signus*, *E. variabilis*, *Geminolithella jafari*, *G. rotula*, *H. mediterranea*, *H. obliqua*, *H. paleocarteri*, *H. cf. H. orientalis* (rare), *H. walbers-*

dorfensis s.s., *Reticulofenestra* spp., *R. ampliumbilicus* (rare), *R. floridana*, *Solidopons petrae*, *Sphenolithus abies*, *S. heteromorphus*, *S. moriformis*, *Tetralithoides symeonidesii*, *T. martinii*, *T. milowii*.

Remarks: *Eu-discoaster musicus* and *E. signus* have their last occurrence in this interval.

Reference locality: D.S.D.P. Site 369A, Sierra Leone Rise, samples: 369A-35 to 369A-20. The *E. musicus* Subzone has a thickness of 22.5 metres at this locality.

Distribution: D.S.D.P. Site 372, samples: 372-76 to 372-57; Giammoia 2, Sicily, samples: CP3651 to CP3662; Mineo, Sicily, samples: JT4962 to JT4508; Marsalforn, Gozo, samples: MT765 to MT774; Ras il Pelegrin, Malta, samples: M110-G to M110-J; Gnejna Bay, Malta, samples: MT622 to MT650.

Eu-discoaster exilis Zone

Definition: Interval zone from the last occurrence of *Sphenolithus heteromorphus* (bottom) to the first occurrence of *Eu-discoaster calcaris* and/or the first occurrence of *Eu-discoaster bellus*.

Comparison: The *E. exilis* Zone as introduced here comprises a larger biostratigraphic interval than the *E. exilis* Zones of other authors. It has no boundaries in common with the *E. exilis* Zone of Hay (1970) which was defined as the interval from the first occurrence of *E. exilis* to the first occurrence of *E. kugleri*.

The *E. exilis* Zone as it appears in Martini, 1971, Bukry, 1973, 1975 and Roth, 1973, is based on the definition of Martini and Worsley (1970), namely that it is the interval from the last occurrence of *S. heteromorphus* to the first occurrence of *E. kugleri*. Thus the *E. exilis* Zone of the latter authors has only the lower boundary in common with the *E. exilis* Zone as defined here.

Subdivision: *Helicosphaera walbersdorfensis* Subzone, *Helicosphaera orientalis* Subzone, *Helicosphaera intermedia* Subzone, *Eu-discoaster kugleri* Subzone, *Eu-discoaster bollii* Subzone. All subzones are recognizable in the Mediterranean and in extra-Mediterranean sections.

Remarks: Hay (1970) introduced the *E. exilis* Zone to fill in an interval which remained unnamed in the zonal scheme of Bramlette and Wilcoxon (1967). The *E. exilis* Zone of Hay, however, extends below the last occurrence of *S. heteromorphus* which was the base of the unnamed interval of Bramlette and Wilcoxon.

Martini and Worsley (1970) modified the *E. exilis* Zone of Hay by using the last occurrence of *S. heteromorphus* as the lower boundary.

Bukry (1971, 1973 and 1975) extended the top of the *E. exilis* Zone upwards to the first occurrence of *E. coalitus* (= *C. coalitus*) in order to include the *E. kugleri* Zone of Bramlette and Wilcoxon as a subzone within the *E. exilis* Zone of Bukry. He did this in order to avoid the stratigraphic hiatuses which might occur if the sporadic *E. kugleri* were absent (Bukry, 1973).

Here the upper boundary of the *E. exilis* Zone is extended upward, to the first occurrence of *E. calcaris* and/or the first occurrence of *E. bellus*. In this way we avoid using of *E. coalitus* as a zonal marker and we assign a more cosmopolitan datum level to the upper boundary of this zone. The first occurrence of *E. coalitus* and/or the last occurrence of *E. kugleri* are used here for the definition of the lower boundary of the *H. walbersdorfensis* Subzone in the Mediterranean area.

Reference locality: Giammoia 2, Sicily, samples: CP3663 to CP3743. The thickness of this zone at this locality is 65.6 metres.

Distribution: D.S.D.P. Site 369A, Sierra Leone Rise, samples: 369A-19 to 369A-3; D.S.D.P. Site 372, samples: 372-56 to 372-1; Giammoia 3, Sicily, samples: CP3101 to CP3118; Scicli, samples: CP4561 to CP4601; Falconara 1, Sicily, samples: JT3073 to JT3069; D.S.D.P. Site 231, Gulf of Aden, samples: 231-135 to 231-130.

Helicosphaera walbersdorfensis Subzone

Definition: Interval from the last occurrence of *Sphenolithus heteromorphus* (bottom) to the first occurrence of *Helicosphaera orientalis* and/or the first occurrence of *Syracosphaera? fragilis* (the F.O. of *S.? fragilis* is applicable only in the Mediterranean area).

Assemblage: *Calcidiscus leptoporus*, *C. macintyreii*, *C. premacintyreii*, *Coccolithus pelagicus*, *Hayella aperta*, *Eu-discoaster deflandrei*, *E. exilis*, *E. subsurculus*, *E. variabilis*, *Geminilithella jafari*, *G. rotula*, *Helicosphaera carteri*, *H. elongata* (rare), *H. intermedia*, *H. obliqua*, *H. walbersdorfensis* (abundant), *Reticulofenestra* spp., *R. amplumbilicus* (rare), *R. floridana*, *Solidopons petrae*, *Sphenolithus abies*, *S. moriformis*, *Tetralithoides symeonidesii*, *Triquetrorhabdulus martinii*, *T. milowii*, *T. rugosus*.

Remarks: The first rare specimens of *E. subsurculus* were observed in this subzone. It is hard to pinpoint the first occurrence of this species, however, because *E. subsurculus* closely resembles *E. exilis* which is already present earlier.

Reference locality: Giammoia 2, Sicily, samples: CP3663 to CP3671. Thickness of the subzone at this locality: 12.2 metres.

Distribution: D.S.D.P. Site 369A, Sierra Leone Rise, samples: 369A-19 to 369A-18; D.S.D.P. Site 372, samples: 372-56 to 372-11; Scicli, samples: CP4561 to CP4565; Ras il Pelegrin, Malta, samples: M110-K to M110-M; Gnejna Bay, Malta, samples: MT651 to MT708.

Helicosphaera orientalis Subzone

Definition: Interval from the first occurrence of *Helicosphaera orientalis* and/or the first occurrence of *Syracosphaera? fragilis* (bottom) to the first occurrence of *Helicosphaera stalis* (top).

Assemblage: *Calcidiscus leptoporus*, *C. macintyreii*, *C. premacintyreii*, *Coccolithus pelagicus*, *Eu-discoaster deflandrei*, *E. exilis*, *E. subsurculus*, *E. variabilis*, *Geminolithella jafari*, *G. rotula*, *Hayella aperta*, *Helicosphaera carteri*, *H. elongata* (rare), *H. intermedia*, *H. obliqua*, *H. orientalis*, *H. walbersdorfensis* (abundant), *Reticulofenestra* spp., *R. ampliumbilicus* (rare), *R. floridana*, *Solidopons petrae*, *Sphenolithus abies*, *S. moriformis*, *Syracosphaera? fragilis*, *Tetralithoides symeonidesii*, *Triquetrorhabdulus martinii*, *T. milowii*, *T. rugosus*.

Remarks: The definition of this subzone is based on dissolution-prone species and, therefore, it may not be recognizable in badly preserved samples. In such cases the *H. orientalis* Subzone should be used in combination with the *H. walbersdorfensis* and the *H. intermedia* Subzones.

Rounded specimens of *Syracosphaera?*, named here *S.? fragilis*, have been observed only in the Mediterranean sections where their first common occurrence coincides with the first occurrence of *H. orientalis*.

The last rare occurrences of *Calcidiscus premacintyreii*, *Triquetrorhabdulus martinii* and *T. milowii* have been observed within the *H. orientalis* Subzone.

Reference locality: Giammoia 3, Sicily, samples: CP3672 to CP3683. Thickness in the reference locality: 14 metres.

Distribution: D.S.D.P. Site 369A, Sierra Leone Rise, samples: 369A-17 to 369A-16; D.S.D.P. Site 372, samples: 372-10 to 372-4; Scicli, samples: CP4566 to CP4592; Ras il Pelegrin, Malta, samples: M110-N to M110-P; Gnejna Bay, Malta, samples: MT709 to MT712.

Helicosphaera intermedia Subzone

Definition: Interval from the first occurrence of *Helicosphaera stalis* (bottom) to the last occurrence of *Reticulofenestra floridana* and/or the first occurrence of *Eu-discoaster kugleri* (top).

Assemblage: *Calcidiscus leptoporus*, *C. macintyreii*, *Hayella aperta*, *Eu-discoaster* cf. *E. bollii*, *E. deflandrei*, *E. exilis*, *E. subsurculus*, *E. variabilis*,

Geminilithella jafari, *G. rotula*, *Hayella aperta* (rare), *Helicosphaera carteri*, *H. elongata*, *H. intermedia*, *H. orientalis*, *H. paleocarteri*, *H. stalis*, *H. walbersdorfensis*, *Reticulofenestra* spp., *R. ampliumbolicus*, *R. floridana*, *Solidopons petrae*, *Sphenolithus abies*, *S. moriformis*, *Syracosphaera?* *fragilis*, *Tetralithoides symeonidesii*, *Triquetrorhabdulus rugosus*.

Remarks: The coincidence of the first occurrence of *E. kugleri* with the last occurrence of *R. floridana*, as suggested by Bukry (1975 and 1978), was confirmed in D.S.D.P. Site 369A. Furthermore, both species were observed within the interval between the first occurrence of *H. stalis* and the last occurrence of *H. walbersdorfensis*.

The interval from the F.O. of *H. stalis* to the L.O. of *H. walbersdorfensis* was used to estimate the position of the last occurrence of *R. floridana* in the absence of *E. kugleri* (Mediterranean sections); the last occurrence of *R. floridana* was recorded consistently within our subzone.

Reference locality: Giammoia 2, Sicily, samples: CP3684 to CP3703. Thickness in the reference locality: 20 metres.

Distribution: D.S.D.P. Site 369A, Sierra Leone Rise, samples: 369A-15 to 369A-10; D.S.D.P. Site 372, Menorca Rise, samples: 372-3 to 372-1; Scicli, samples: CP4593 to CP4595.

Eu-discoaster kugleri Subzone

Definition: Interval from the first occurrence of *Eu-discoaster kugleri* and/or the last occurrence of *Reticulofenestra floridana* (bottom) to the last occurrence of *Eu-discoaster kugleri* and/or the last occurrence of *Helicosphaera walbersdorfensis* and/or the first occurrence of *Eu-discoaster coalitus* (top).

Comparison: The *E. kugleri* Subzone as defined here represents an interval identical to the *E. kugleri* Zone of Bramlette and Wilcoxon (1967) and the *E. kugleri* Subzone of Bukry (1973, 1975). The last occurrence of *H. walbersdorfensis* is introduced here as an alternative marker for the upper boundary of this interval.

Assemblage: *Calcidiscus leptoporus*, *C. macintyreii*, *Coccolithus pelagicus*, *Eu-discoaster bollii*, *E. cf. E. bollii*, *E. deflandrei*, *E. exilis*, *E. micros*, *E. pansus*, *E. subsurculus*, *E. variabilis*, *Geminilithella jafari*, *G. rotula*, *Helicosphaera carteri*, *H. elongata* (rare), *H. intermedia*, *H. orientalis*, *H. pacifica*, *H. stalis*, *H. walbersdorfensis*, *Reticulofenestra* spp., *R. ampliumbolicus*, *Solidopons petrae*, *Sphenolithus abies*, *S. moriformis*, *Syracosphaera?* *fragilis*, *Triquetrorhabdulus rugosus*.

Remarks: The last occurrence of *H. walbersdorfensis* may serve as an upper boundary of the *E. kugleri* Subzone when *E. kugleri* and *E. coalitus* are absent (e.g. Mediterranean region).

H. walbersdorfensis was abundantly present in all our sections throughout its range. The last occurrence of this species was recorded close to, but above the last occurrence of *E. kugleri* in the D.S.D.P. Site 369A, whereas in the D.S.D.P. Site 231 it coincided with the last occurrence of *E. kugleri* and the first occurrence of *E. coalitus*. A similar level for the last occurrence of *H. walbersdorfensis* was indicated by Müller (1981).

Reference locality: Giammoia 2, Sicily, samples: CP3704 to CP3714. The *E. kugleri* Subzone has a thickness of 8.4 metres in this locality.

Distribution: D.S.D.P. Site 369A, Sierra Leone Rise, samples: 369A-9 to 369A-4; Giammoia 3, Sicily, samples: CP3101 to CP3105; Scicli, samples: CP4596 to CP4601; Falconara 1, samples: JT3073 to JT3069; D.S.D.P. Site 231, Gulf of Aden, samples: 231-135 to 231-132.

Eu-discoaster bollii Subzone

Definition: Interval from the last occurrence of *Eu-discoaster kugleri* and/or the last occurrence of *Helicosphaera walbersdorfensis* and/or the first occurrence of *Eu-discoaster coalitus* (bottom) to the first occurrence of *Eu-discoaster calcaris* and/or the first occurrence of *Eu-discoaster bellus* (top).

Assemblage: *Calcidiscus leptoporus*, *C. macintyreii*, *Coccolithus pelagicus*, *Eu-discoaster bollii*, *E. coalitus*, *E. deflandrei*, *E. exilis*, *E. pansus*, *E. pseudo-variabilis*, *E. variabilis*, *Geminolithella jafari*, *G. rotula*, *Helicosphaera carteri*, *H. intermedia*, *H. orientalis*, *H. pacifica*, *H. paleocarteri*, *H. stalis*, *Reticulofenestra* spp., *Sphenolithus abies*, *S. moriformis*, *Syracosphaera? fragilis*, *Tetralithoides symeonidesii*, *Triquetrorhabdulus rugosus*.

Reference locality: Giammoia 2, Sicily, samples: CP3715 to CP3743. Thickness of the subzone at this locality: 11 metres.

Distribution: D.S.D.P. Site 369A, Sierra Leone Rise, samples: 369A-3; Giammoia 3, Sicily, samples: CP3106 to CP3118; Scicli, samples: CP4602 to CP4610; D.S.D.P. Site 231, Gulf of Aden, samples: 231-131 to 231-130.

Eu-discoaster calcaris Zone

Definition: Interval zone from the first occurrence of *Eu-discoaster calcaris* and/or the first occurrence of *Eu-discoaster bellus* (bottom) to the first occurrence of *Minylitha convallis* (top).

Comparison: Our *E. calcaris* Zone represents a lower biostratigraphic interval than the *E. calcaris* Zone of Martini (1969).

Subdivision: *Eu-discoaster bellus* Subzone and *Eu-discoaster hamatus* Subzone.

Remarks: The *E. calcaris* Zone as defined here is introduced in order to

create a zone based on cosmopolitan markers within which the first occurrence of *E. hamatus* can be used for a subzonal boundary.

In this zone and in the next higher biostratigraphic intervals of the Upper Miocene a succession of the pentaradial discoasters *E. bellus*, *E. hamatus* and *E. quinqueramus* is introduced. *E. hamatus* as well as *E. quinqueramus* exhibit very characteristic features and, when present, they are excellent biostratigraphic markers. The atypical specimens of these two discoasters, however, cannot be distinguished from *E. bellus*.

It is hard to define the actual range of *E. bellus* as it is never certain whether we are dealing with this species or with the preservational morphotypes of the other two. *E. bellus* is present, however, below the first occurrence of *E. hamatus* and it persists higher up within the range of *E. quinqueramus*. This consequently obscures the ranges of the latter two species. For this reason *E. hamatus* and *E. quinqueramus* are used in the present zonation to make a subzonal subdivision recognizable only when typical forms of these species are present.

Reference locality: D.S.D.P. Site 231, Gulf of Aden, samples: 231-130 to 231-117. Thickness in the reference locality: 31.5 metres.

Distribution: Giammoia 2, Sicily, samples: CP3744 to CP3749; Giammoia 3, samples: CP3119 to CP3130; Falconara 1, Sicily, samples: JT3068 to JT3060; Limin Kieri, Zakynthos, samples: ZK33 to ZK40; Vasiliki, Crete, samples: GR2921 to GR2963.

Eu-discoaster bellus Subzone

Definition: Interval from the first occurrence of *Eu-discoaster calcaris* and/or the first occurrence of *Eu-discoaster bellus* (bottom) to the first occurrence of *Eu-discoaster hamatus* (top).

Comparison: The *E. bellus* Subzone as defined here represents a lower biostratigraphic interval than the *E. bellus* Subzone of Bukry (1973, 1975) and Roth (1973).

Assemblage: *Calcidiscus leptoporus*, *C. macintyreii*, *Coccolithus pelagicus*, *Eu-discoaster bellus*, *E. bollii*, *E. calcaris*, *E. coalitus*, *E. deflandrei*, *E. exilis*, *E. pansus*, *E. pseudovariabilis*, *E. variabilis*, *Geminolithella jafari*, *G. rotula*, *Helicosphaera carteri*, *H. intermedia*, *H. orientalis*, *H. pacifica*, *H. paleocarteri*, *H. stalis*, *Reticulofenestra* spp., *Sphenolithus abies*, *Syracosphaera fragilis*, *Tetralithoides symeonidesii*, *Triquetrorhabdulus rugosus*.

Remarks: The first occurrence of *E. calcaris* was recorded in all our sections consistently below the first occurrence of *E. hamatus* s.s.. *E. bellus* is rare and sporadic near this level and therefore it is of a secondary importance as a boundary indicator.

Reference locality: D.S.D.P. Site 231, Gulf of Aden, samples: 231-130 to 231-125. The thickness of this subzone is 11.7 metres at the reference locality.

Distribution: Giammoia 2, Sicily, samples: CP3744 to CP3749; Giammoia 3, samples: CP3117 to CP3123; Falconara 1, Sicily, samples: JT3068 to JT3066; Vasiliki, samples: GR2929 to GR2928.

Eu-discoaster hamatus Subzone

Definition: Interval from the first occurrence of *Eu-discoaster hamatus* s.s. (bottom) to the first occurrence of *Minylitha convallis* (top).

Comparison: The *E. hamatus* Subzone as defined here has a common lower boundary with the *E. hamatus* Zone of Bramlette and Wilcoxon (1967) but it represents a shorter biostratigraphic interval.

Assemblage: *Calcidiscus leptoporus*, *C. macintyreii*, *Coccolithus pelagicus*, *Eu-discoaster bellus*, *E. bollii*, *E. calcaris*, *E. coalitus*, *E. deflandrei*, *E. exilis*, *E. hamatus*, *E. pansus*, *E. pseudovariabilis*, *E. variabilis*, *Geminilithella jafari*, *G. rotula*, *Helicosphaera carteri*, *H. intermedia*, *H. orientalis*, *H. pacifica*, *H. paleocarteri*, *H. stalis*, *Reticulofenestra* spp., *Sphenolithus abies*, *Syracosphaera? fragilis*, *Tetralithoides symeonidesii*, *Triquetrorhabdulus rugosus*.

Reference locality: D.S.D.P. Site 231, Gulf of Aden, samples: 231-124 to 231-117. The thickness of the subzone at the reference locality is 19.8 metres.

Distribution: Giammoia 3, Sicily, samples: CP3124 to CP3130; Falconara 1, samples: JT3066 to JT3060; Limin Kieri, Zakynthos, samples: ZK33 to ZK40; Vasiliki, samples: GR2929 to GR2963.

Minylitha convallis Zone

Definition: Total range zone defined by the range of *Minylitha convallis*.

Comparison: The *M. convallis* Zone represents the interval from the upper part of the *E. hamatus* Zone of Bramlette and Wilcoxon (1967) to the lower part of the *E. quinqueramus* Zone of Gartner (1969).

Subdivision: *Eu-discoaster pseudovariabilis* Subzone, *Eu-discoaster pentaradiatus* Subzone and *Geminilithella rotula* Subzone.

Remarks: *Minylitha convallis* Bukry, 1973, is a very characteristic nanolith which was encountered as common or abundant in all our sections that contain its range. This species has been neglected so far, possibly because of the incomplete description by the original author who described only the less characteristic – and less birefringent side view – of *M. convallis* (see the description of *M. convallis*, this paper).

The first occurrences of *E. pentaradiatus* (= *E. prepentaradiatus* (Bukry)), *E. misconceptus* (i.e. birefringent pentaradial discoasters) and *E. quinqueramus* (i.e. *E. quinqueramus* (Gartner) including *E. berggrenii* (Bukry)), as well as the last occurrences of *E. hamatus* and *E. pentaradiatus* fall within the range of *M. convallis* and are used here for subzonal subdivisions.

Reference locality: D.S.D.P. Site 231, Gulf of Aden, samples 231-116 to 231-80. This zone has a thickness of 59.1 metres at the reference locality.

Distribution: D.S.D.P. Site 369A, Sierra Leone Rise, samples: 369A-2 to 369A-1; Giammoia 3, Sicily, samples: CP3131 to CP3151; Scicli, samples: CP4501 to CP4555; Falconara 1, Sicily, samples: JT3059 to CP3030; Falconara 3, samples: JT1946 to JT1945; Scardilli, Sicily, samples: CP4301 to CP4308; Solo River, samples: SR53 to SR50.

Eu-discoaster *pseudovariabilis* Subzone

Definition: Interval from the first occurrence of *Minylitha convallis* (bottom) to the last occurrence of *E. hamatus* (top).

Assemblage: *Calcidiscus leptoporus*, *C. macintyreii*, *Coccolithus pelagicus*, *Eu-discoaster bellus*, *E. bollii*, *E. brouweri*, *E. calcaris*, *E. calyculus*, *E. coalitus*, *E. deflandrei* (rare), *E. exilis* (rare), *E. giganteus*, *E. hamatus*, *E. pansus*, *E. pentaradiatus*, *E. pseudovariabilis*, *E. variabilis*, *Geminilithella jafari*, *G. rotula*, *Helicosphaera carteri*, *H. orientalis*, *H. pacifica*, *H. paleocarteri*, *H. stalis*, *Minylitha convallis*, *Reticulofenestra* spp., *Sphenolithus abies*, *Syracosphaera? fragilis*, *Tetralithoides symeonidesii*, *Triquetrorhabdulus rugosus*.

Subdivision: A further subdivision of this interval into two parts is possible in areas where *E. pentaradiatus* (= *E. prepentaradiatus* (Bukry)) is present:

A) *E. pseudovariabilis* Subzone, Zonule a

Definition: Interval from the first occurrence of *Minylitha convallis* (bottom) to the first occurrence of *Eu-discoaster pentaradiatus* (= *E. prepentaradiatus* (Bukry)) (top). *Reference locality*: D.S.D.P. Site 231, Gulf of Aden, samples: 231-116 to 231-114. Thickness at this locality: 3.5 metres.

B) *E. pseudovariabilis* Subzone, Zonule b

Definition: Interval from the first occurrence of *E. pentaradiatus* (= *E. prepentaradiatus* (Bukry)) (bottom) to the last occurrence of *E. hamatus* (top). *Reference locality*: D.S.D.P. Site 231, Gulf of Aden, samples: 231-113 to 231-110. Thickness: 6.3 metres.

Remarks: The suggested subdivision of the *E. pseudovariabilis* Subzone is

not applicable in the Mediterranean sections due to the scarcity of *E. pentaradiatus*. It may be useful, however, in extra-Mediterranean localities.

Reference locality: D.S.D.P. Site 231, Gulf of Aden, samples: 231-116 to 231-110. Thickness at this locality: 9.8 metres.

Distribution: D.S.D.P. Site 369A, Sierra Leone Rise, samples: 369A-2 to 369A-1; Giammoia 3, Sicily, samples: CP3131 to CP3136; Falconara 1, Sicily, samples: JT3059 to CP3009; Limin Kieri, Zakynthos, sample: ZK41.

Eu-discoaster pentaradiatus Subzone

Definition: Interval from the last occurrence of *E. hamatus* bottom to the last occurrence of *E. pentaradiatus* (= *E. prepentaradiatus* (Bukry)) and/or the first occurrence of *E. misconceptus* (i.e. birefringent pentaradial asteroliths), (top).

Assemblage: *Calcidiscus leptoporus*, *C. macintyreii*, *Coccolithus pelagicus*, *Eu-discoaster bellus*, *E. brouweri*, *E. calcaris* (sporadic), *E. coalitus*, *E. giganteus*, *E. incompletus*, *E. loeblichii*, *E. neorectus*, *E. pansus*, *E. pentaradiatus*, *E. pseudovariabilis*, *E. surculus*, *E. variabilis*, *Geminilithella jafari*, *G. rotula*, *Helicosphaera carteri*, *H. orientalis*, *H. pacifica*, *H. paleocarteri*, *H. stalis*, *Minylitha convallis*, *Reticulofenestra* spp., *Sphenolithus abies*, *Syracosphaera? fragilis* (rare), *Tetralithoides symeonidesii*, *Triquetrorhabdulus rugosus*.

Reference locality: D.S.D.P. Site 231, samples: 231-109 to 231-100. Thickness at the reference locality: 10.8 metres.

Distribution: Giammoia 3, Sicily, samples: CP3137 and CP3138; Falconara 1, Sicily, samples: CP3010 to CP3018.

Geminilithella rotula Subzone

Definition: Interval from the last occurrence of *E. pentaradiatus* (= *E. prepentaradiatus* (Bukry)) and/or the first occurrence of *E. misconceptus* (i.e. birefringent pentaradial asteroliths) (bottom) to the last occurrence of *Minylitha convallis* (top).

Assemblage: *Calcidiscus leptoporus*, *C. macintyreii*, *Coccolithus pelagicus*, *Eu-discoaster bellus*, *E. brouweri*, *E. calcaris* (sporadic), *E. giganteus*, *E. incompletus*, *E. loeblichii*, *E. misconceptus*, *E. neorectus*, *E. pansus*, *E. pseudovariabilis*, *E. quinquaramus*, *E. surculus*, *E. variabilis*, *Geminilithella jafari*, *G. rotula*, *Helicosphaera carteri*, *H. orientalis*, *H. pacifica*, *H. paleocarteri*, *H. stalis*, *Minylitha convallis*, *Reticulofenestra* spp., *Sphenolithus abies*, *Syracosphaera? fragilis* (rare), *Tetralithoides symeonidesii*, *Triquetrorhabdulus rugosus*.

Subdivision: The *G. rotula* Subzone is subdivided in two zonules which are recognizable only in extra-Mediterranean areas.

A) Geminilithella rotula Subzone, Zonule a

Definition: Interval from the last occurrence of *E. pentaradiatus* and/or the first occurrence of *E. misconceptus* (bottom) to the first occurrence of *E. quinqueramus* (top). Reference locality: D.S.D.P. Site 231, Gulf of Aden, samples: 231-99 to 231-89. Thickness: 27.9 metres.

B) Geminilithella rotula Subzone, Zonule b

Definition: Interval from the first occurrence of *E. quinqueramus* (bottom) to the last occurrence of *Minylitha convallis* (top). Reference locality: D.S.D.P. Site 231, Gulf of Aden, samples: 231-88 to 231-80. Thickness: 10.8 metres.

Reference locality: D.S.D.P. Site 231, samples: 231-99 to 231-80. Thickness at the reference locality: 38.7 metres.

Distribution: Giammoia 3, Sicily, samples: CP3130 to CP3136; Falconara 1, Sicily, samples: JT3061 to CP3009; Limin Kieri, Zakynthos, sample: ZK41.

Coccolithus pelagicus Zone

Definition: Interval zone from the last occurrence of *Minylitha convallis* (bottom) to the first occurrence of the genus *Amaurolithus* (top).

Assemblage: *Calcidiscus leptoporus*, *C. macintyreii*, *Coccolithus pelagicus*, *Eu-discoaster bellus*, *E. brouweri*, *E. misconceptus*, *E. pansus*, *E. quinqueramus*, *E. surculus*, *E. variabilis*, *Geminilithella jafari*, *G. rotula*, *Helicosphaera carteri*, *H. orientalis*, *H. pacifica*, *H. stalis*, *Reticulofenestra* spp., *Sphenolithus abies*, *Tetralithoides symeonidesii*, *Triquetrorhabdulus rugosus*.

Reference locality: D.S.D.P. Site 231, Gulf of Aden, samples: 231-80 to 231-69. Thickness at this locality: 24.3 metres.

Distribution: Giammoia 3, Sicily, samples: CP3152 to CP3155; Scicli, Sicily, samples: CP4556 to CP4560; Falconara 2, Sicily, samples: CP3031 to CP3034; Falconara 3, samples: JT1944 to JT1900; Scardilli, Sicily, samples: CP4307 to CP4345; Skouloudhiana, Crete, samples: KSP1 to KSP36; Kastelli, Crete, samples: KT1 to KT38; Solo River, sample: SR49.

Amaurolithus primus Zone

Definition: Interval from the first occurrence of species of *Amaurolithus* – generally *A. primus* – (bottom) to the first occurrence of *Reticulofenestra rotaria* (top).

Assemblage: *Amaurolithus primus*, *A. delicatus*, *Calcidiscus leptoporus*, *C. macintyreii*, *Coccolithus pelagicus*, *Eu-discoaster bellus*, *E. brouweri*, *E. misconceptus*, *E. pansus*, *E. quinquaramus*, *E. surculus*, *E. variabilis*, *Geminilithella jafari*, *G. rotula*, *Helicosphaera carteri*, *H. orientalis*, *H. pacifica*, *H. paleocarteri*, *H. stalis*, *Tetralithoides symeonidesii*, *Triquetrorhabdulus rugosus*.

Reference locality: D.S.D.P. Site 231, Gulf of Aden, samples: 231-68 to 231-57. Thickness at the reference locality: 20.7 metres.

Distribution: Falconara 3, Sicily, samples: JT1901 to JT1905; Scardilli, Sicily, samples: CP4346 to CP4355; Skouloudhiana, Crete, samples KSP37 to KSP39; Kastelli, Crete, samples: KT39 to KT47; Solo River, samples: SR48 to SR47.

Reticulofenestra rotaria Zone

Definition: Total range zone defined by the range of *Reticulofenestra rotaria*.

Assemblage: *Amaurolithus primus*, *A. amplificus*, *A. delicatus*, *Calcidiscus leptoporus*, *C. macintyreii*, *Coccolithus pelagicus*, *Eu-discoaster bellus*, *E. brouweri*, *E. misconceptus*, *E. pansus*, *E. quinquaramus*, *E. surculus*, *E. variabilis*, *Geminilithella jafari*, *G. rotula*, *Helicosphaera carteri*, *H. orientalis*, *H. pacifica*, *H. paleocarteri*, *H. stalis*, *Reticulofenestra* spp., *R. rotaria*, *Tetralithoides symeonidesii*, *Triquetrorhabdulus rugosus*.

Remarks: The last rare occurrences of *Helicosphaera orientalis*, *H. pacifica* and *H. stalis* have been recorded in this zone.

Reference locality: D.S.D.P. Site 231, Gulf of Aden, samples: 231-56 to 231-49. Thickness at this locality: 18.9 metres.

Distribution: Falconara 3, Sicily, samples: JT1906 to JT1916; Scardilli, Sicily, samples: CP4355 to CP4360; Kastelli, Crete, samples: KT47 to KT59; D.S.D.P. Site 219, Laccadive Chagos Ridge, samples: 219-35 to 219-18; Solo River, samples: SR45 to SR46.

Calcidiscus leptoporus Zone

Definition: Interval zone from the last occurrence of *Reticulofenestra rotaria* (bottom) to the first occurrence of *Ceratolithus rugosus* (top).

Subdivision:

1. In Extra-Mediterranean areas:

A) *Calcidiscus leptoporus* Subzone A

Definition: Interval from the last occurrence of *R. rotaria* (bottom) to

the last occurrence of *E. quinquerramus* and/or the first occurrence of *Ceratolithus acutus* and/or the last occurrence of *Triquetrorhabdulus rugosus* (top).

Assemblage: *Amaurolithus amplificus*, *A. delicatus*, *A. primus*, *Calcidiscus leptoporus*, *C. macintyreii*, *Coccolithus pelagicus*, *Ceratolithus acutus*, *A. tricorniculatus*, *Eu-discoaster bellus*, *E. brouweri*, *E. misconceptus*, *E. pansus*, *E. quinquerramus*, *E. surculus*, *E. variabilis*, *Geminilithella jafari*, *G. rotula*, *Helicosphaera carteri*, *H. paleocarteri*, *Reticulofenestra* spp., *Tetralithoides symeonidesii*, *Triquetrorhabdulus rugosus*.

Reference locality: D.S.D.P. Site 231, Gulf of Aden, samples: 231-48 to 231-5. Thickness: 67.5 metres.

Distribution: D.S.D.P. Site 219, Laccadive-Chagos Ridge, Indian Ocean, samples: 219-17 to 219-2; Solo River, Java, samples: SR45 to SR31.

B) *Calcidiscus leptoporus* Subzone B

Definition: Interval from the last occurrence of *E. quinquerramus* and/or the first occurrence of *Ceratolithus acutus* (bottom) to the first occurrence of *Ceratolithus rugosus* (top).

Assemblage: *Amaurolithus delicatus*, *A. primus*, *Calcidiscus leptoporus*, *C. macintyreii*, *Coccolithus pelagicus*, *Ceratolithus acutus*, *A. tricorniculatus*, *Eu-discoaster bellus*, *E. brouweri*, *E. misconceptus*, *E. pansus*, *E. surculus*, *E. variabilis*, *Geminilithella jafari*, *G. rotula*, *Helicosphaera carteri*, *H. paleocarteri*, *Reticulofenestra* spp.

Reference locality: D.S.D.P. Site 231, Gulf of Aden, samples: 231-4 to 231-1. Thickness: 9 metres.

Distribution: D.S.D.P. Site 219, Laccadive Chagos Ridge, Indian Ocean, sample: 219-1; Solo River, Java, samples: SR30 to SR28.

2. In the Mediterranean area:

A) *Calcidiscus leptoporus* Subzone MA

Definition: Interval from the last occurrence of *R. rotaria* to the beginning of the barren interval which starts at the base of the "Calcare di base" (top).

Assemblage: *Amaurolithus amplificus*, *A. delicatus*, *A. primus*, *Calcidiscus leptoporus*, *C. macintyreii*, *Coccolithus pelagicus*, *Eu-discoaster bellus* (rare), *E. brouweri*, *E. misconceptus*, *E. pansus*, *E. surculus*, *E. variabilis*, *Geminilithella jafari*, *G. rotula*, *Helicosphaera carteri*, *H. paleocarteri*, *Reticulofenestra* spp., *Tetralithoides symeonidesii*, *Triquetrorhabdulus rugosus*.

Reference locality: Falconara 3, Sicily, samples: JT1917 to the base of the "Calcare di base". The thickness in this locality is estimated to be 30 metres.

B) *Calcidiscus leptoporus* Subzone MB

Definition: Barren interval corresponding to the Messinian evaporite succession.

C) *Calcidiscus leptoporus* Subzone MC

Definition: Interval from the top of the evaporites to the first occurrence of *Ceratolithus rugosus*.

Assemblage: *Amaurolithus delicatus*, *A. primus*, *Calcidiscus leptoporus*, *C. macintyreii*, *Coccolithus pelagicus*, *A. tricorniculatus*, *E. brouweri*, *E. misconceptus*, *E. pansus*, *E. surculus*, *E. variabilis*, *Geminilithella jafari*, *G. rotula*, *Helicosphaera carteri*, *H. paleocarteri*, *Reticulofenestra* spp.

Reference locality: Capo Rossello section, Sicily, samples: SI1A to SI1O. Thickness in this section: 35 metres.

TAXONOMIC NOTES

Information about all species of *Helicosphaera*, *Eu-discoaster* and *Helio-discoaster* is presented in chapters 4 and 5. Here we confine our taxonomic notes to all other nannofossil species mentioned in the descriptions of the Miocene zones. The descriptions of these species are arranged in alphabetical order of the generic names. The species are depicted in plates 1–11. Plates 12 and 13 present the index species of *Eu-discoaster* and *Helicosphaera*.

Genus *Amaurolithus* Gartner and Bukry, 1975

Amaurolithus amplificus (Bukry and Percival) Gartner and Bukry
(Pl. 1, figs. 3–8)

Ceratolithus amplificus Bukry and Percival, 1971, p. 125, pl. 1, figs. 9–11.

Amaurolithus amplificus (Bukry and Percival) Gartner and Bukry, 1975, pp. 454–456, figs. 6g-1.

Amaurolithus delicatus Gartner and Bukry
(Pl. 1, figs. 9–11)

Amaurolithus delicatus Gartner and Bukry, 1975, pp. 456–457, figs. 7a-f.

Amaurolithus primus (Bukry and Percival) Gartner and Bukry
(Pl. 1, figs. 1, 2)

Ceratolithus primus Bukry and Percival, 1971, p. 126, pl. 1, figs. 12–14.

Amaurolithus primus (Bukry and Percival) Gartner and Bukry, 1975, p. 457, figs. 7g-1.

Amaurolithus tricorniculatus (Gartner) Gartner and Bukry

Ceratolithus tricorniculatus Gartner, 1967, p. 5, pl. 10, figs. 4–6.

Amaurolithus tricorniculatus (Gartner) Gartner and Bukry, 1975, pp. 457–458, figs. 8c-h.

Remarks: The close similarities among the earlier species of *Amaurolithus* mean that these species cannot be used as individual markers. The first occurrence of representatives of the genus gives a useful datum-level in the Upper Miocene.

Genus *Calcidiscus* Kamptner, 1950

Synonyms: *Cyclococcolithus* Kamptner, 1954; *Tiarolithus* Kamptner, 1958; *Cycloplacolithus* Kamptner, 1963; *Cycloplacolithella* Haq, 1968; *Cyclococcolithina* Wilcoxon, 1970.

Calcidiscus leptoporus (Murray and Blackman) Loeblich and Tappan

Coccosphaera leptopora Murray and Blackman, 1898, pp. 430, 493, pl. 15, figs. 1–7.

Calcidiscus leptoporus (Murray and Blackman) Loeblich and Tappan, 1978, p. 1391.

Calcidiscus macintyre (Bukry and Bramlette) Loeblich and Tappan (Pl. 2, figs. 4–6)

Cyclococcolithus macintyre Bukry and Bramlette, 1969, p. 132, pl. 1, figs. 1–3.

Calcidiscus macintyre (Bukry and Bramlette) Loeblich and Tappan, 1978, p. 1392.

Remarks: The first rare occurrence of both *C. leptoporus* and *C. macintyre* was recorded in the *H. obliqua* Subzone.

Calcidiscus premacintyre n. sp. (Pl. 2, figs. 1–3)

? *Cyclococcolithus leptoporus centrovalis* Stradner and Fuchs, 1980, partim, pl. 5, figs. 1–3, non: pl. 5, figs. 4–9, pl. 6, figs. 2–6, pl. 7, figs. 1–6.

Etymology: From pre- and macintyre.

Description: Large placoliths with subelliptical outline and an elliptical central tube which has a relatively large opening and usually lacks calcareous filling. The placoliths have a non-birefringent distal shield and a birefringent proximal one. The extinction bands of the birefringent proximal shield curve sinistrally in proximal view.

Differential diagnosis: *C. premacintyre* can be distinguished from *C. macintyre* and *C. leptoporus* by the elliptical wall, the larger central opening and the subelliptical outline. It differs from *Coccolithus pelagicus* by the more rounded outline and the sinistral curvature of the extinction bands (in proxi-

mal view). Large species of *Reticulofenestra* differ from *C. premacintyreii* by having birefringent proximal as well as distal shields.

Remarks: Placoliths with the morphology of *C. premacintyreii* have also been reported by Bukry (1973) from his *S. heteromorphus* Zone as *C. cf. C. macintyreii* or as *C. macintyreii* with elliptic central areas.

Occurrence: The species was recorded from the *H. obliqua* Subzone to the *H. orientalis* Subzone.

Holotype: Pl. 2, fig. 1, sample: CP3656, coordinates: 108, 2/4, 9.

Isotypes: Pl. 2, fig. 2, sample: CP3656; Pl. 2, fig. 3, sample: MT750.

Type level: *E. musicus* Subzone.

Type locality: Giammoia 2, Sicily.

Genus *Ceratolithus* Kamptner, 1950

Ceratolithus acutus Gartner and Bukry (Pl. 1, fig. 12)

Ceratolithus acutus Gartner and Bukry, 1974, p. 115, pl. 1, figs. 1–4.

Remarks: The species is absent in the Mediterranean sections, but it was recorded as rare in the D.S.D.P. Sites 231 and 219. In both sites the first occurrence of *C. acutus* coincides with the last occurrence of *E. quinqueramus*.

Ceratolithus rugosus Bukry and Bramlette

Ceratolithus rugosus Bukry and Bramlette, 1968, p. 152, pl. 1, figs. 5–9.

Genus *Hayella* Gartner, 1969

Homonym: *Hayella* Roth, 1969

Synonym: *Nannocorbis* Müller, 1974.

Hayella aperta n. sp. (Pl. 3, figs. 3–8)

Etymology: From aperture.

Description: Calcareous body resembling a short conical tube. It consists of 30 to 35 elements which imbricate dextrally (when observed from the smaller base of the cone); at both ends of the tube they terminate radially and form two narrow shields.

Differential diagnosis: *Hayella aperta* is distinguished from *H. situliformis* Gartner by the shorter cone and the large opening at the narrow end of the

tube. *H. gauliformis* Troelsen and Quadros has comparable openings but a longer cone. *H. challengerii* (Müller) n. comb. is much smaller.

H. aperta superficially resembles *G. rotula*, in plane view, but it is easily distinguished by its brighter birefringence and its conical shape which becomes apparent when the level of focus of the light microscope is changed.

Occurrence: From the *T. carinatus* Zone to the *H. intermedia* Subzone.

Holotype: Pl. 3, fig. 3, sample: 369A-18, coordinates: 104.0/11.6.

Isotypes: Pl. 3, fig. 4, sample: 369A-27; Pl. 3, fig. 5, sample: 369A-18; Pl. 3, fig. 6, sample: 369A-21; Pl. 3, fig. 7, sample: 369A-22; Pl. 3, fig. 8, sample: 369A-22.

Type level: *H. walbersdorfensis* Subzone.

Type locality: D.S.D.P. Site 369A, Sierra Leone Rise, Atlantic Ocean.

Hayella challengerii (Müller) n. comb.

Nannocorbis challengerii Müller, 1974, p. 593, pl. 15, figs. 4, 5.

Hayella sp. Perch-Nielsen, 1977, p. 750, pl. 41, fig. 10.

Remarks: This species was recorded from the *C. pelagicus* Zone to the *C. leptoporus* Zone. It has been reported to range into the Lower Pliocene (Müller, 1974).

Genus *Geminilithella* Backman, 1980

Geminilithella jafari (Müller) Backman

Umbilicosphaera jafari Müller, 1974, p. 394, pl. 1, fig. 3.

Geminilithella jafari (Müller) Backman, 1980, p. 52, pl. 1, figs. 16–17.

Geminilithella rotula (Kamptner) Backman (Pl. 3, figs. 1, 2)

Cyclococcolithus rotula Kamptner, 1956, p. 7.

Geminilithella rotula (Kamptner) Backman, 1980, p. 52, pl. 1, figs. 14, 15, pl. 8, fig. 3.

Genus *Minylitha* Bukry, 1973, emended

Type species: *Minylitha convallis* Bukry, emend. this paper.

Description: Nannoliths consisting of two concavo-convex calcite elements attached to each other by their convex surfaces.

Emendation: The generic diagnosis is emended to include nannoliths that consist of a pair of calcite elements. The emendation is complementary to the description of Bukry (1973) who based his diagnosis on only one of the two elements that compose the nannoliths of this genus.

Minylitha convallis Bukry, emended
(Pl. 4, figs. 1–7)

Minylitha convallis Bukry, 1973, p. 679, pl. 3, figs. 12–18.

Description: Nannoliths consisting of two polygonal convexo-concave calcite elements. The elements are usually four-sided with the two adjacent sides long and the other two sides short. The two elements are attached to each other by their convex surfaces, the attachment being along their longer axis. Between crossed nicols, the basal or apical view of *M. convallis* roughly resembles the letter X and in this view the specimens show maximum birefringence.

Remarks: Bukry (1973) observed only the side view of *M. convallis*. His description is, therefore, incomplete and does not permit the identification of specimens in basal (or apical) view.

The construction of *M. convallis* does not indicate a "relation" with a pentolith as suggested by Bukry. It is more likely that the nannolith of *M. convallis* is a complete nannolith and not a fragment of a larger structural unit such as a placolith or a pentolith.

Occurrence: The species is common or abundant throughout the *M. convallis* Zone.

Genus Reticulofenestra Hay, Mohler and Wade, 1966

Synonym: *Cyclicargolithus* Bukry, 1971.

Reticulofenestra ampliumbilicus n. sp.
(Pl. 5, figs. 5–7)

Etymology: From *amplus* (= spacious, Lat) and *umbilicus*.

Description: Large placoliths with subcircular and often circular outline, a large central opening, and birefringent distal and proximal shields.

Differential diagnosis: The placoliths of *R. ampliumbilicus* have a larger central opening, narrower shields and a more circular outline than those of *R. pseudoumbilicus*.

Occurrence: *R. ampliumbilicus* occurs sporadically throughout the *S. heteromorphus* and the *E. exilis* Zones.

Holotype: Pl. 5, fig. 5, sample: CP4579, coordinates: 104.6/10.7.

Isotypes: Pl. 5, fig. 6, sample: CP4580; pl. 5, fig. 7, sample: CP4579.

Type level: *H. orientalis* Subzone.

Type locality: Scicli, Sicily.

Reticulofenestra floridana (Roth and Hay) n. comb.

(Pl. 5, fig. 8)

Coccolithus floridanus Roth and Hay, 1967, p. 445, pl. 6, fig. 1–4.

Cyclicargolithus floridanus (Roth and Hay) Bukry, 1971, p. 312.

Remarks: Bukry introduced the genus *Cyclicargolithus* (type species: *Cyclicargolithus floridanus*) for circular placoliths with a birefringent proximal and distal shield. In doing so he disregarded the genus *Reticulofenestra* whose placoliths have identical optical properties and ultrastructure and often a circular outline.

Reticulofenestra rotaria n. sp.

(Pl. 5, figs. 1–4)

Etymology: From *rota* (= wheel, Lat.). The name refers to the circular outline of the species.

Description: Small (5–7 microns) circular placoliths with a relatively large circular central opening. Both proximal and distal shield are brightly birefringent between crossed nicols.

Differential diagnosis: *R. rotaria* differs from all other species of *Reticulofenestra* by the circular outline and the relatively large and rounded central opening.

Occurrence: The species is common throughout the *R. rotaria* Zone.

Holotype: Pl. 5, fig. 1, sample: 219-12, coordinates: 119.6/9.6.

Isotypes: Pl. 5, fig. 2, sample: 219-30; Pl. 5, fig. 3, sample: JT1910; Pl. 5, fig. 4, sample: 219-25.

Type level: *R. rotaria* Zone.

Type locality: D.S.D.P. Site 219, Laccadive-Chagos Ridge, Indian Ocean.

Reticulofenestra spp.

Remarks: This taxonomic label is given to all other Miocene *Reticulofenestra* species (e.g. *R. pseudoumbilicus*, *R. gelidus*, *R. minutula*, *R. haqii*, *R. minuta*). These species comprised the largest part of the nannofossil content of our samples, but because of their gradational morphological features they could not always be identified.

Genus Rhabdosphaera Haeckel, 1894

Rhabdosphaera spp.

Remarks: In our Miocene samples the rhabdolites are represented mainly

by *Rhabdosphaera claviger* Murray and Blackman, 1898 and *Rhabdosphaera procera* Martini, 1969. No attempt was made, however, to distinguish these two species which are presented in our range charts as *Rhabdosphaera* spp.,

Genus *Solidopons* n. gen.

Etymology: Combination of the words *solidus* (= solid, Lat.) and *pons* (= bridge, Lat.).

Diagnosis: Placoliths with an elliptical outline, a central opening, a birefringent proximal shield and a non-birefringent distal one. The central opening is spanned by a single, arched bridge. The bridge is highly birefringent and it is optically discontinuous from the main body of the placolith from which it is separated by two distinct sutures. The bridge consists of microcrystals that merge into a single element.

Differential diagnosis: Cenozoic placoliths with a bridge (or bridges) transversing their central opening are classified in the genera *Chiasmolithus* Hay, Mohler and Wade, *Cruciplacolithus* Hay and Mohler, *Placozygus* Hoffman and *Gephyrocapsa* Kamptner. The bridges of these genera, however, are distinguished from the bridge of *Solidopons* by being composed of two or several segments that meet along a suture at the centre of the bridge.

Type species: *Solidopons petrae* n. sp.

Solidopons petrae n. sp.

(Pl. 6, figs. 1–7)

Etymology: In honour of Miss Petra van der Schaar for her moral support and her valuable technical assistance during the completion of this publication.

Description: Elliptical placoliths with a large central opening. The bridge is (sub)parallel to the shorter axis of the placolith and it is highly arched in distal direction. The distal shield is not birefringent in contrast to the proximal shield and the bridge which are bright between crossed nicols.

Occurrence: This species occurs sporadically from the *H. ampliaperta* Zone to the *E. exilis* Zone.

Holotype: Pl. 6, fig. 1, sample: 219-39, coordinates: 104.1/6.2.

Isotypes: Fig. 2, sample: CP4566; fig. 3, sample: 369A-17; fig. 4, sample: 369A-57; fig. 5, sample: 219–39; fig. 6, sample: 369A-59; fig. 7, sample: 369A-12. All figures in plate 6.

Type level: *H. obliqua* Subzone.

Type locality: D.S.D.P. Site 219, Laccadive-Chagos Ridge, Indian Ocean.

Genus *Sphenolithus* Deflandre, 1952

Sphenolithus abies Deflandre, 1954

(Pl. 8, figs. 8, 9)

Sphenolithus abies Deflandre, in Deflandre and Fert, 1954, p. 164, pl. 10, figs. 1–4.

Sphenolithus neobabies Bukry and Bramlette, 1969, p. 140, pl. 3, figs. 9–11.

Sphenolithus belemnus Bramlette and Wilcoxon, 1967

(Pl. 7, figs. 1–4)

Sphenolithus belemnus Bramlette and Wilcoxon, 1967, p. 118, pl. 2, figs. 1–3.

Sphenolithus heteromorphus Deflandre, 1953

(Pl. 7, figs. 5–12)

Sphenolithus heteromorphus Deflandre, 1953, p. 1786, figs. 1, 2.

Sphenolithus moriformis (Brönnimann and Stradner) Bramlette and Wilcoxon

(Pl. 8, figs. 1–3)

Nannoturbella moriformis Brönnimann and Stradner, 1960, p. 7, figs. 11–16.

Sphenolithus pacificus Martini, 1965, p. 407, pl. 36, figs. 1–6.

Sphenolithus moriformis (Brönnimann and Stradner) Bramlette and Wilcoxon, 1967, pp. 124–126, pl. 3, figs. 1–6.

Genus *Syracosphaera* Kamptner, 1941

Syracosphaera? *fragilis* n. sp.

(Pl. 9, figs. 1–4)

Etymology: The name refers to the fragile appearance of these nannoliths.

Description: Circular coccoliths with a narrow rim. The central area is filled with elongated bars which radiate from the centre towards the rim and are separated by slits. The slits that separate the bars become narrower towards the centre. A short stem is visible at the centre of the coccolith.

Differential diagnosis: The only other species with comparable outline is *Syracosphaera beogradiensis* Jercovic (1971). However, neither slits nor a central stem are visible in the picture presented by Jercovic.

Occurrence: *S?* *fragilis* was found only in the Mediterranean sections from the *H. orientalis* Subzone to the *G. rotula* Subzone.

Holotype: Pl. 9, fig. 1, sample: CP4581, coordinates: 118.5/6.2.

Isotypes: Pl. 9, fig. 2, sample: AU163; Pl. 9, fig. 3, sample: CP4581; Pl. 9, fig. 4, sample: CP4561.

Type level: *H. orientalis* Subzone.

Type locality: Scicli, Sicily.

Genus *Tetralithoides* n. gen.

Etymology: Combination of the words tetras (= group of four, Gr.), lithos (= stone, Gr.) and the suffix -oides (latin modification of -ooides = similar to, Gr.).

Diagnosis: Calcareous bodies consisting of a narrow outer ring of low-birefringent elements surrounding four polygonal segments.

Type species: *Tetralithoides symeonidesii*.

Tetralithoides symeonidesii n. sp.

(Pl. 9, figs. 5–12)

Etymology: In honour of Prof. Dr. N. Symeonides of the Department of Geology of the State University of Athens, Greece.

Description: A species of *Tetralithoides* with an elliptical and lowbirefringent outer cycle of elements. The central area is optically discontinuous from the outer ring. The four segments that fill the central area of the ring are arranged in pairs of two relatively larger elements along the longer axis of the ellipse and two relatively smaller ones along the shorter axis. The optical behaviour of the two pairs is slightly different; they appear alternatively darker or brighter upon rotation.

Occurrence: The species occurs from the *T. milowii* Zone to the *R. rotaria* Zone.

Holotype: Pl. 9, fig. 5, sample: 372-101, coordinates 120.9/6.2.

Isotypes: Pl. 9, fig. 6, sample: 369A-13; Pl. 9, fig. 7, sample: 369A-63; Pl. 9, fig. 8, sample: 369A-15; Pl. 9, fig. 9, sample: 369A-63; Pl. 9, fig. 10, sample: 369A-64; Pl. 9, fig. 11, sample: 369A-25; Pl. 9, fig. 12, sample: 369A-25.

Type level: *H. obliqua* Subzone.

Type locality: D.S.D.P. Site 372, Menorca Rise, W. Mediterranean.

Genus *Triquetrorhabdulus* Martini 1965

Triquetrorhabdulus carinatus Martini

(Pl. 10, figs. 1, 2, 5, 6)

Triquetrorhabdulus carinatus Martini, 1965, pp. 394–411, pls. 33–37, text-fig. 153.

Remarks: The species is common in the samples of D.S.D.P. Site 369A but it is absent from the Mediterranean sections.

Triquetrorhabdulus challenger Perch-Nielsen
(Pl. 10, figs. 9, 10)

Triquetrorhabdulus challenger Perch-Nielsen, 1977, p. 749, pl. 36, figs. 3, 7, 8, 10, 11, pl. 49, fig. 1.

Remarks: *T. challenger* was recorded as rare only in the D.S.D.P. Site 369A.

Triquetrorhabdulus extensus n. sp.
(Pl. 11, figs. 4–6)

Etymology: The name refers to the extended third (“apical”) blade of the nannoliths of this species.

Descriptions: A species of *Triquetrorhabdulus* consisting of two smaller equal blades and a third one which is much larger and roughly triangular. The surface of the larger blade shows a slight striation perpendicular to the smaller blades. The species is not birefringent between crossed nicols.

Occurrence: This species was recorded only in the *C. leptoporus* Subzone A and B of the D.S.D.P. Site 219.

Holotype: Pl. 11, figs. 4–6, sample: 219-3, coordinates: 112.8/7.5.

Type level: *C. leptoporus* Zone.

Type locality: D.S.D.P. Site 219, Laccadive-Chagos Ridge, Indian Ocean.

Triquetrorhabdulus finifer n. sp.
(Pl. 11, figs. 7–10)

Etymology: Combination of the words fin and fero (= bear, Gr.) referring to the fin-like apical blade of this species.

Description: A species of *Triquetrorhabdulus* with a very large and crescent-shaped apical blade. The species lacks birefringence.

Differential diagnosis: *T. finifer* is distinguished from *T. extensus* by the larger and crescent-shaped apical blade.

Occurrence: *T. finifer* was recorded as rare in the *C. leptoporus* Subzone B of the D.S.D.P. Site 219.

Holotype: Pl. 11, figs. 7, 8, sample: 219-1, coordinates: 117.9/7.6.

Isotype: Pl. 11, figs. 9, 10, sample: 219-1.

Type level: *C. leptoporus* Subzone B.

Type locality: D.S.D.P. Site 219, Laccadive-Chagos Ridge, Indian Ocean.

Triquetrorhabdulus martinii Gartner

(Pl. 10, figs. 11–16)

Triquetrorhabdulus sp. Martini, 1965, p. 408, pl. 36, figs. 4–6.

Triquetrorhabdulus martinii Gartner, 1967, pp. 6, pl. 10, figs. 1a–c, 2a–c, 3a–b.

Orthorhabdus serratus Bramlette and Wilcoxon, 1967, p. 114, pl. 9, figs. 5–10; Müller, 1974, pl. 12, fig. 12.

Remarks: This species is distinguished from all other species of *Triquetrorhabdulus* by the strong curvature at one of its ends. When observed in polarized light it shows highest contrast at an orientation of 90 degrees to the polarization plane, which is in contrast to all other birefringent species of *Triquetrorhabdulus* which show highest contrast at a position parallel to the plane of polarization (compare pl. 10, figs. 14–16 with pl. 10, figs. 5–8).

Triquetrorhabdulus milowii Bukry

(Pl. 10, figs. 3, 4, 7, 8)

Triquetrorhabdulus milowii Bukry, 1971, p. 325, pl. 7, figs. 9–12.

Remarks: The nannoliths of this species are short and broad and they are often curved. The curvature of *T. milowii* is less pronounced than that of *T. martinii*.

Triquetrorhabdulus rugosus Bramlette and Wilcoxon

(Pl. 11, figs. 1–3)

Triquetrorhabdulus rugosus Bramlette and Wilcoxon, 1967, p. 128, pl. 9, figs. 17, 18.

Chapter 4

HELICOLITHS

INTRODUCTION

Excellent electron micrographs of most species of *Helicosphaera* have been presented by many authors (e.g. Haq, 1968, 1971, 1973; Hay et al., 1967; Boudreaux and Hay, 1969; Clocchiatti, 1969; Müller, 1970; Bukry, 1971; Gartner, 1971; Perch-Nielsen, 1971). In spite of the extensive pictorial documentation of this genus, our knowledge of the ultrastructure of the "helicolith" remains, nonetheless, incomplete. This is reflected by the poor definitions of most species – which are often based only on the size and on the general outline.

Haq (1973) presented an outline of the evolution of most species of *Helicosphaera*. Our revision of the specific and the generic characters of this genus, however, has resulted in another picture of the connections between the different species based on their structural similarities.

In the lineages presented in figure 60 the ranges of the pre-Neogene species are based on the ranges given by Haq.

TERMINOLOGY

A number of terms have been introduced in order to facilitate the descriptions. These terms are explained in figure 51.

STRUCTURE OF THE HELICOLITHS

All helicoliths are composite constructions consisting of three, closely appressed, structural units: the blanket, the flange and the proximal plate. A "dismantled" helicolith has been drawn in figure 52 to demonstrate the spatial interrelationship of these units and to give insight into their structure. In reality the three structural units of the helicolith do not have such distinct boundaries as those drawn in figure 52 but they fuse at the surfaces along which they are attached to each other.

The proximal plate (fig. 52a)

This is the simplest structural unit of the helicolith. It consists of "radi-

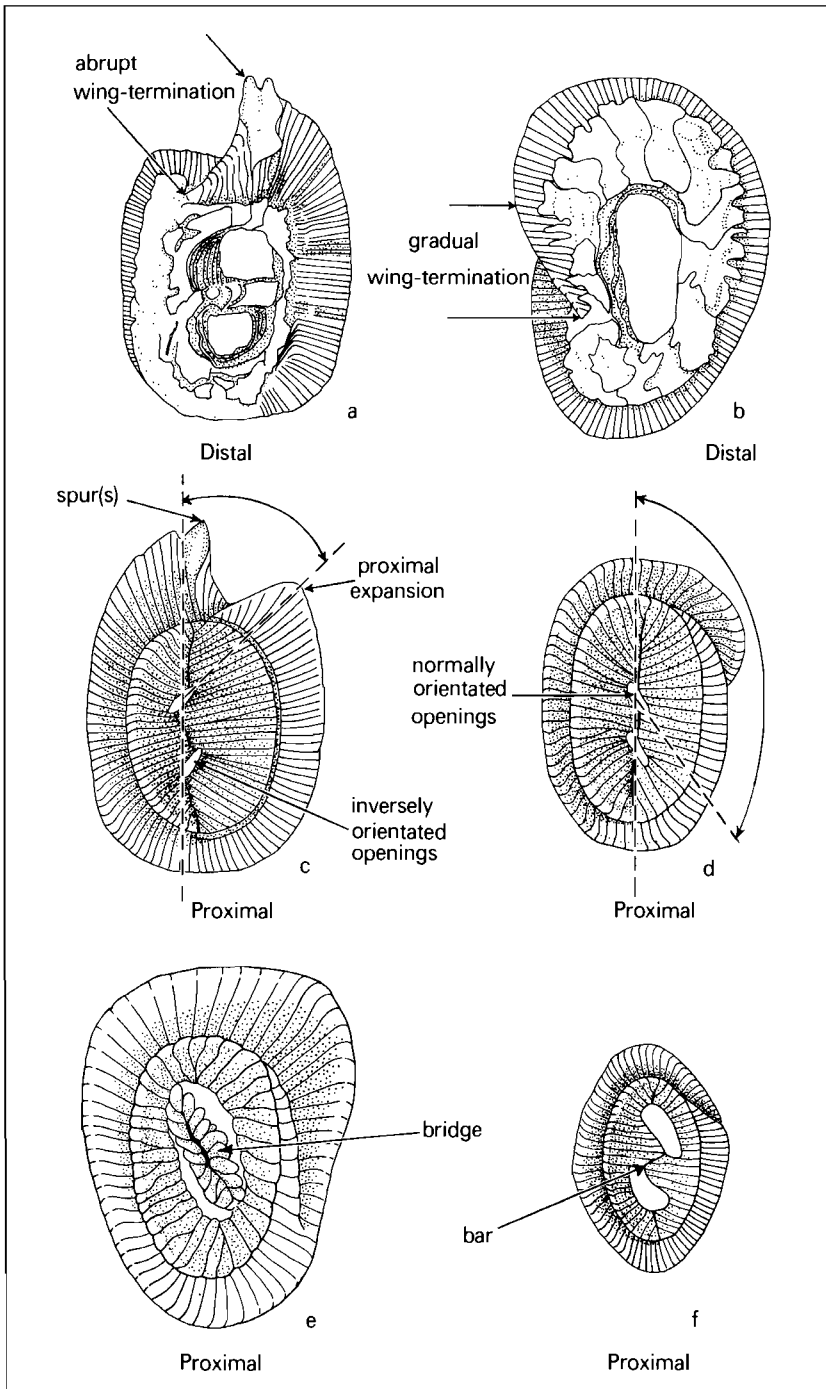
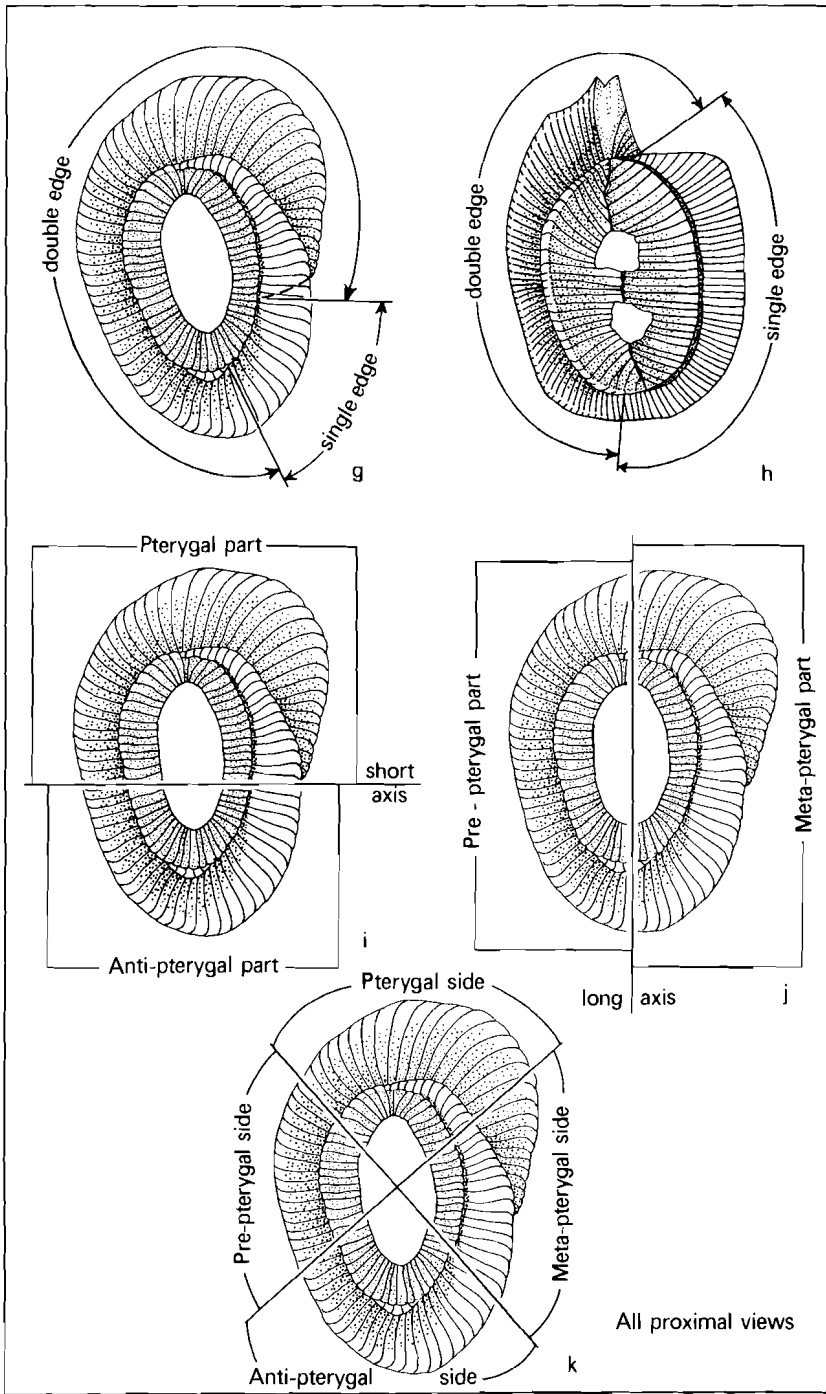


Fig. 51. Explanation of the terms used to describe the helicoliths.



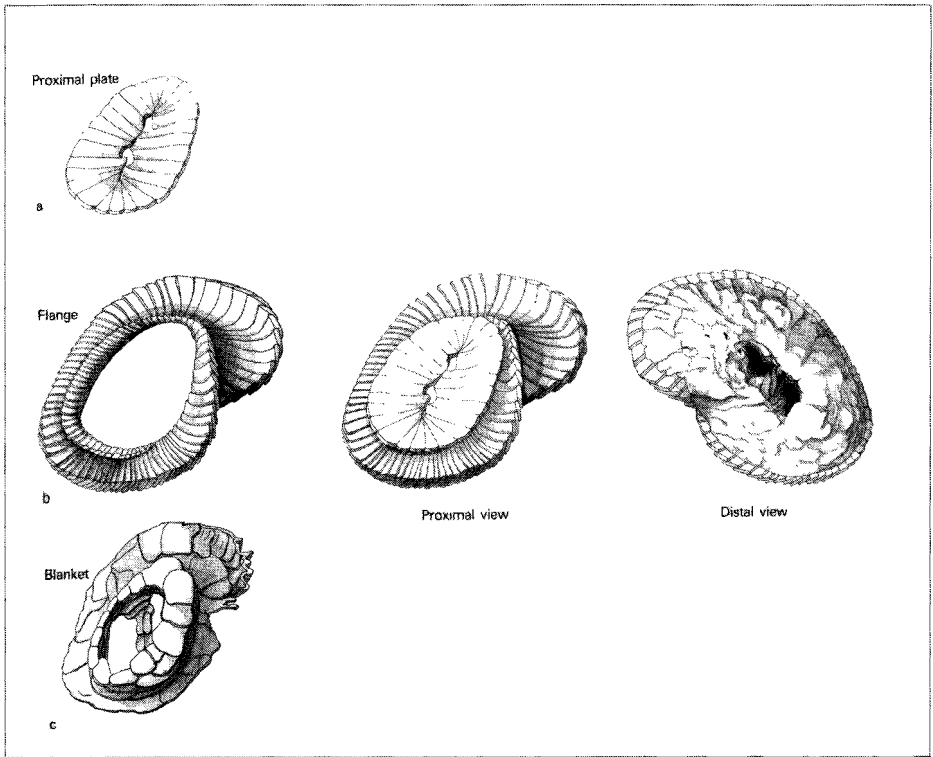


Fig. 52. Structural units of the helicoliths.

ally” arranged wedge-shaped and lath-like elements. The elements are juxtaposed without imbrication. Three different types of proximal plates can be distinguished:

Type I. Proximal plates without central opening(s). The elements of the opposite long sides of the elliptical plate meet along the longer axis of the ellipse and form a suture (principal suture), fig. 53a, or a slit (fig. 53b).

Type II. Proximal plates with a large central opening. The elements do not meet at the centre of the plate, leaving a large central opening (fig. 53c). The central opening may be transversed by a set of elements whose orientation is different from that of the elements of the plate and which are defined here as the “bridge” (fig. 53d).

The elements that constitute the bridge are usually assembled into two composite segments divided by a suture. These segments may be roughly triangular or roughly rectangular.

Type III. Proximal plates with central openings and a bar. Some of the ele-

ments of this type of proximal plates meet at the centre of the plate and form a “bar” (i.e. a bridge-like structure but composed of elements that belong to the plate) which is flanked by two central openings. The central openings may be rounded (fig. 53e) or elongated (fig. 53f). When elongated the central openings may or may not make an angle with the longer axis of the plate. This angle may be “inverse” or “normal” as demonstrated by figures 51c and 51d respectively.

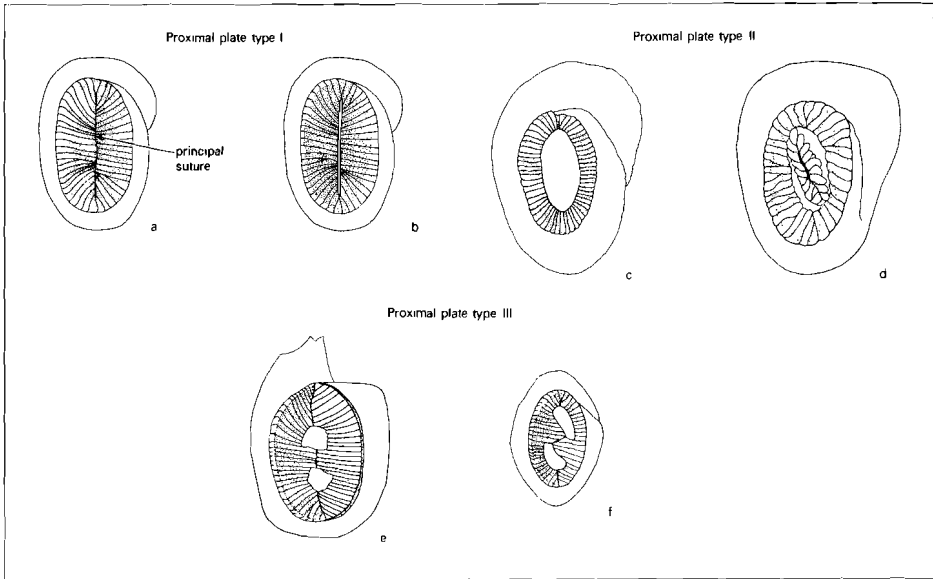


Fig. 53. Types of proximal plate. Explanations in the text.

The blanket (fig. 52c)

This unit is situated on the distal surface of the proximal plate, extends through the opening of the flange (fig. 52b) and covers the distal surface of the flange. Cross-sections of the blanket reveal a multi-layered construction of lamellar elements superimposed like bricks in a wall (pl. 14, figs. 4,6). This organization of the elements of the blanket is not directly visible in intact specimens however, because the elements of the uppermost layer of the blanket are usually fused (pl. 14, fig. 1). Three types of blankets are distinguished on the basis of the degree in which they cover the distal surface of the helicolith:

Type I. Blankets that cover only the central area of the helicolith (fig. 54a).

Type II. Blankets that cover the metapterygial part (fig. 51j) and the central area of the helicolith (fig. 54b).

Type III. Blankets that cover the entire distal surface of the helicolith (fig. 54c).

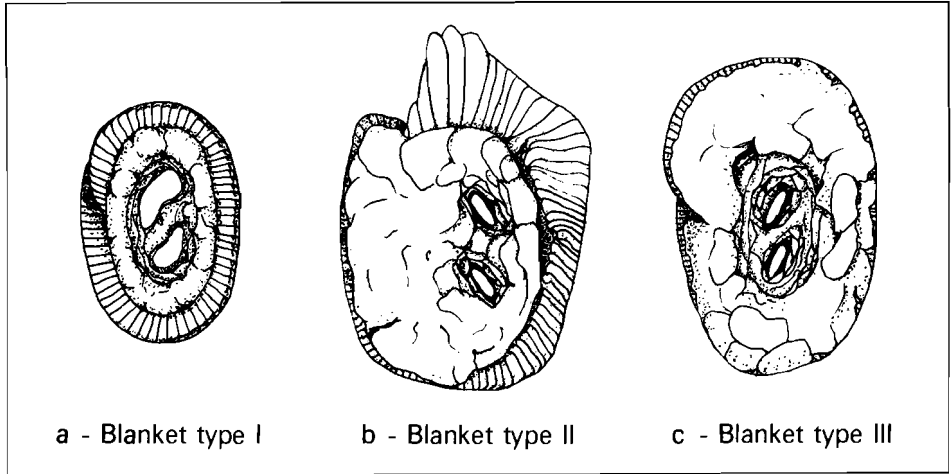


Fig. 54. Types of blanket. (a) Type I with a blanket confined to the central area of the helicolith, (b) Type II with a blanket covering the central area and the metapterygial part and (c) Type III with a blanket covering the entire distal surface.

The flange (fig. 52b)

This is the structural unit that gives the helicoid appearance to the helicoliths. The periphery of the flange extends beyond the peripheries of the previously described structural units and therefore the outline of the flange con-

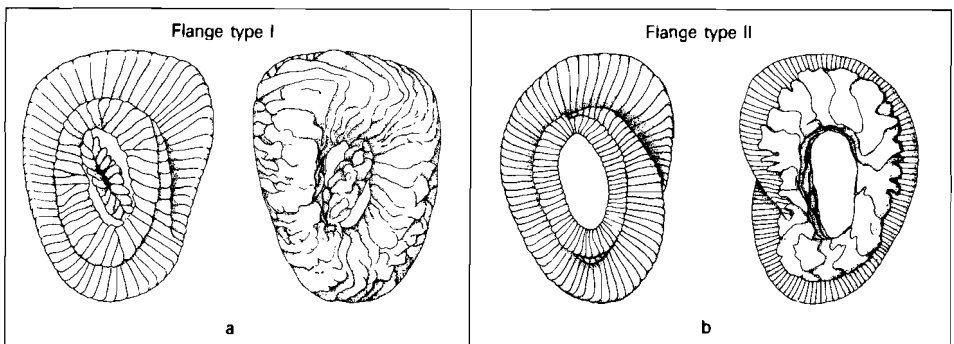


Fig. 55. Proximal and distal views of *H. lophota* (a) and *H. ampliaperta* (b). The two species are drawn here to represent helicoliths with flange type I and flange type II, respectively.

trols the outline of the helicolith. The flange is sandwiched between the blanket and the proximal plate.

Two different types of flange have been observed. Figures 55 a and b present helicoliths with a flange type 1 and a flange type 2 respectively, and figures 56 and 57 illustrate the structural characteristics of each type.

Common characteristics of the two types of flanges

Two different types of elements are involved in the construction of both flange types:

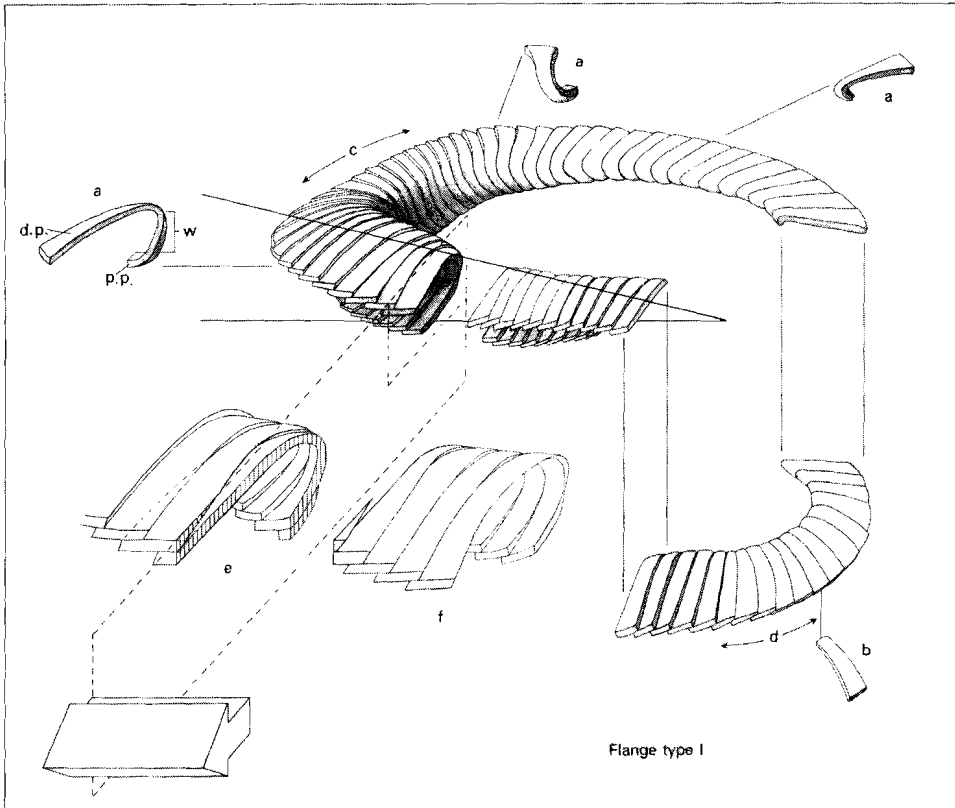


Fig. 56. Structural characteristics of flange type I. (a) curved elements, (b) lath-like elements, (c) double edge, (d) single edge, (e) and (f) enlarged cross-sections demonstrating the mode of imbrication of the curved elements, (p.p.) proximal portion of the curved elements (d.p.) distal portion of the curved elements, (w) wall of the curved elements. The walls of the curved elements diminish gradually in height in anti-clockwise direction, whereas the length of their proximal and distal portions remains nearly constant.

a) Curved elements (figs. 56a, 57a and Pl. 14, fig. 5):

These elements are roughly U-shaped in cross-section and exhibit a distal portion, a wall and a proximal portion. They are juxtaposed in such a way that their walls show no imbrication, but both their proximal and distal portions imbricate sinistrally (figs. 56e, 57e). The parts of the flange which are composed of the curved elements produce a double edge in side view. This will be referred to in the following as the “double edge” of the flange (figs. 56c, 69c).

b) Lath-like elements (figs. 56b, 57b):

These elements make up the smallest part of the flange in the majority of

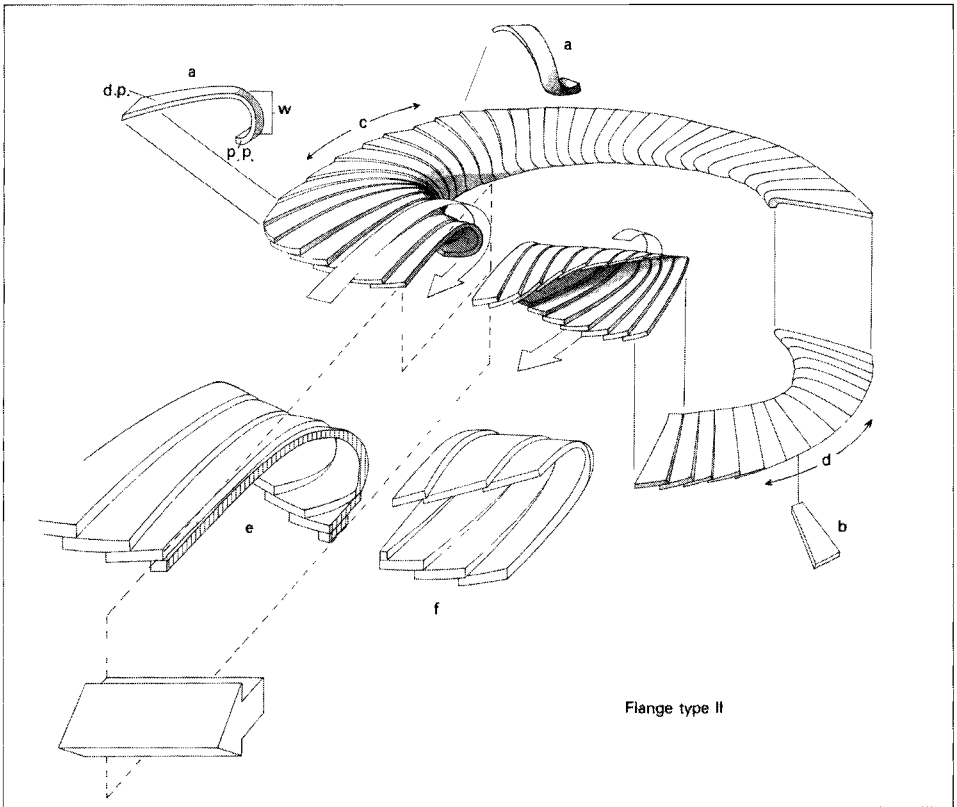


Fig. 57. Structural characteristics of flange type II. (a) curved elements, (b) lath-like elements, (c) double edge, (d) single edge, (e) and (f) enlarged cross-sections demonstrating the mode of imbrication of the curved elements, (p.p.) proximal portion of the curved elements (d.p.) distal portion of the curved elements, (w) wall of the curved elements. The height of the walls of the curved elements remains nearly constant in anti-clock wise direction, whereas the proximal portions become longer at the expense of the distal ones.

helicoliths. They are arranged with sinistral imbrication and form a “single edge” in side view (figs. 56d, 57d).

The characteristic helicoid appearance of both types of flanges is created by a gradual transformation of the curved elements into the lath-like ones. The mode of this gradual modification is demonstrated in figures 56 and 57.

Differences between flange types

The difference between the two types of flange can be observed in distal view.

Flange type I (fig. 56)

The elements of this type of flange have a nearly uniform length in distal view. Consequently, the helicoliths with this type of flange have a continuous distal surface, an elliptical distal periphery, do not have a wing and do not look helicoidal in distal view (fig. 55a). In side view of the metapterygial part, the walls of the curved elements diminish in length towards the single edge.

Flange type II (fig. 57)

The flanges of type II show a gradual or abrupt diminution of the distal portions of their curved elements; this takes place from the widest part of the flange (the wing) towards the position of “termination of the wing” (i.e. the position where the distal portions of the elements of the wing obtain their shortest size, figs. 51a, b). This results in a discontinuous distal surface of the flange and in the helicoid appearance of the flange in distal view (fig. 55b). The walls of the curved elements of flange type II remain nearly constant.

OPTICAL PATTERN OF THE HELICOLITHS

All helicoliths are birefringent between crossed nicols. The bright part of the interference figure is restricted to that area of the helicolith which is covered by the blanket (figs. 58a, b, c). This part of the interference figure, therefore, is useful for an indirect observation of the type of the blanket in the light microscope.

The optical behaviour of the “bridge” of the proximal plate differs from that of the rest of the helicolith and, as a rule, the bridge appears bright and dark alternately upon rotation of the specimens between crossed nicols. Two distinct and usually V-shaped sutures mark the places where the bridge is attached to the proximal plate. “Bars”, on the contrary, are optically continuous with the rest of the helicolith.

The interference figures of the helicoliths are classified in the following categories:

Interference figure type I (fig. 58a)

Interference figures that consist of a highly birefringent area at the centre, surrounded by an area with lower birefringence. This area of lower birefringence will be referred to in the following as the “optical rim”.

Interference figure type II (fig. 58b)

Figures with an optical rim only along the periphery of the prepterygal part of the helicolith. In crossed nicols the lighted area of the helicoliths with this type of interference figure often appears dimmer than the lighted area of helicoliths with interference figures of types I and III.

Interference figure type III (fig. 58c)

Interference figures without an optical rim.

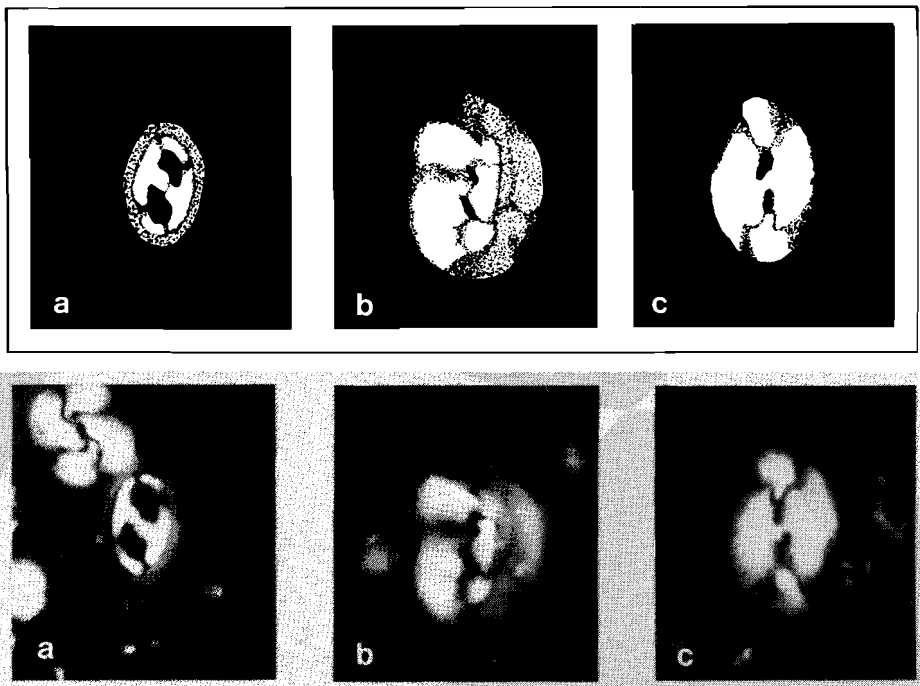


Fig. 58. Optical pattern of the helicoliths; Light micrographs (lower half of figure) and interpretation (upper half). For explanation see text.

GENERIC AND SPECIFIC CHARACTERISTICS OF THE HELICOLITHS

The presence of the flange consisting of two different types of elements is the main feature which distinguishes the helicoliths from all other nannofos-

sil genera. The type of flange can be used for a subdivision of the helicoliths into two structural groups:

The helicoliths with a flange type I are the earliest forms and all, except *H. gertae*, are confined to the Eocene and Oligocene (fig. 61). They are classified here as *Helicosphaera* Group I.

The helicoliths with flange type II are classified as *Helicosphaera* Group II. The helicoliths of Group II have their first appearance in the Late Eocene and persist up to the present.

Transitional types between the two groups of *Helicosphaera* have not been observed.

All other structural and morphological features of the helicoliths (i.e. the outline of the flange, the type of the blanket, the features of the proximal plate and the type of the interference figure) are used here for a specific classification.

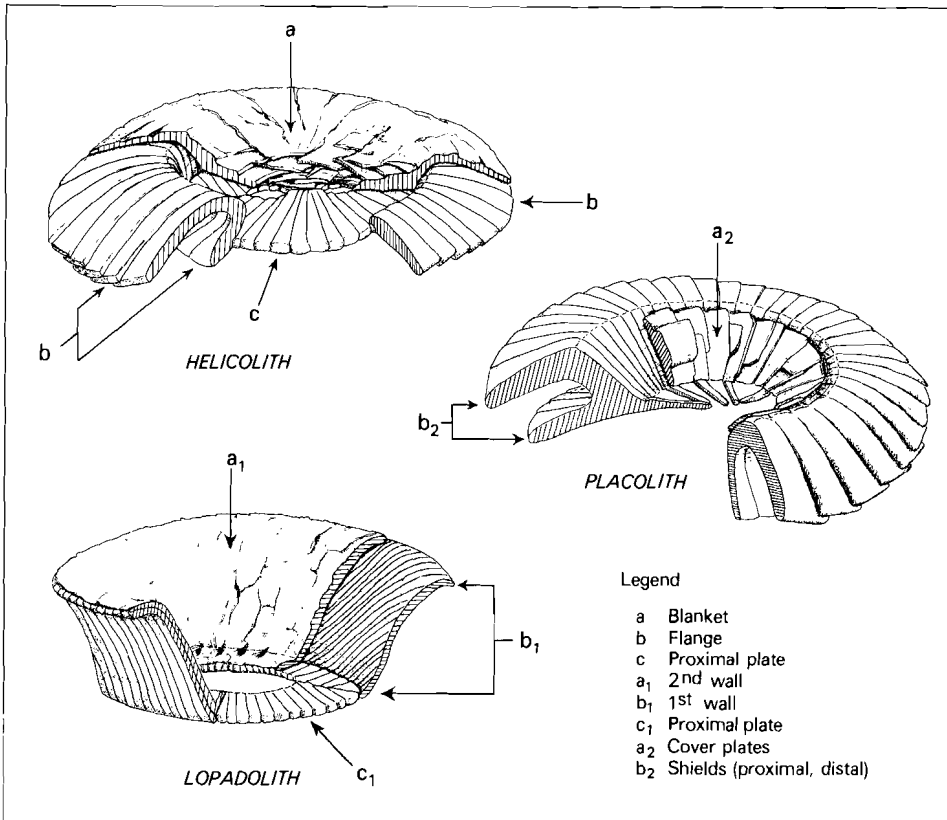


Fig. 59. Comparison of the structural units of the helicoliths, the lopadoliths and the placoliths. Equivalent units are indicated by the same letter.

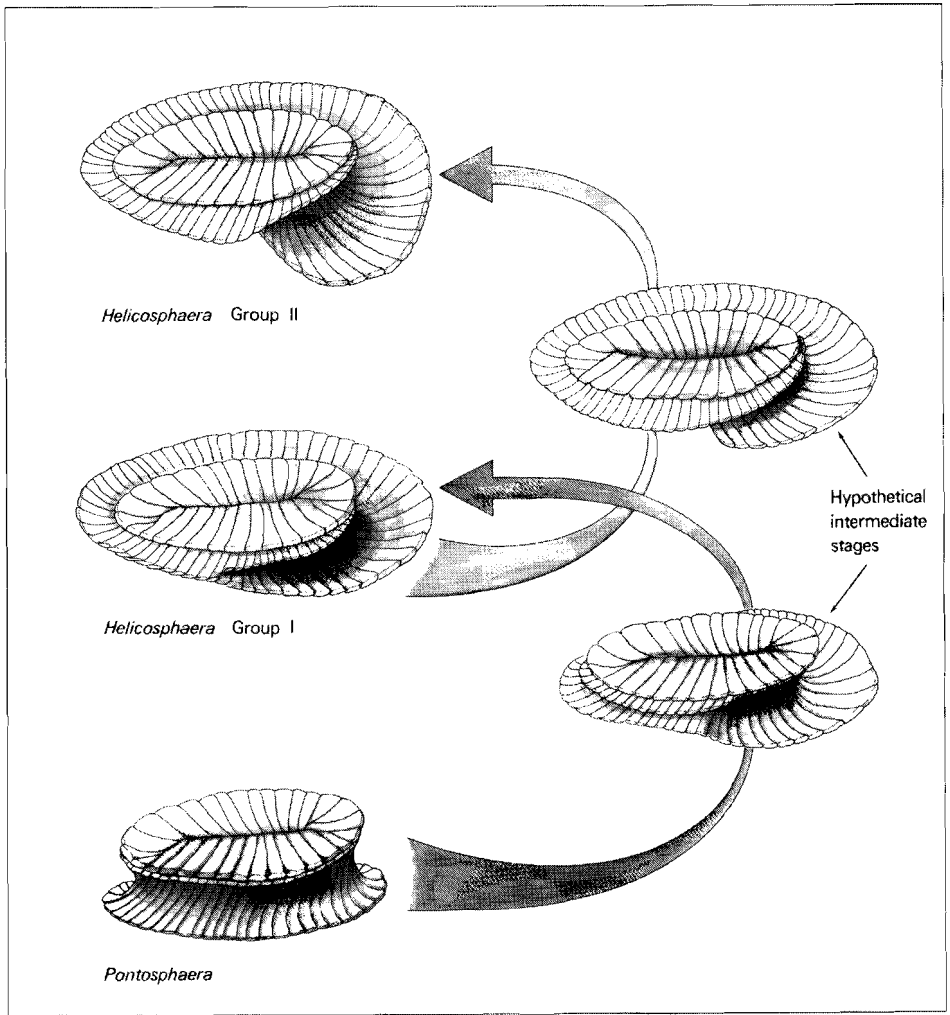


Fig. 60. Model demonstrating the possible steps in the development of the two groups of helicoliths from the lopadoliths of *Pontosphaera*. The helicoliths of Group I might have developed from the lopadoliths by asymmetric compression and subsequent fusion of the elements of the rim of *Pontosphaera*. The helicoliths of Group II might have developed from those of Group I by the formation of a "wing" giving the helicoliths a helicoid appearance in distal view. The features of the proximal plate (e.g. bridge, central openings) have been intentionally omitted; this was done in order to draw attention to the rim-flange modification which is fundamental in the development of the helicolith.

ORIGIN OF HELICOSPHAERA

The lopadoliths of *Pontosphaera* usually consist of a proximal plate simi-

distal portion of the flange of the helicoliths, generally shows a dextral imbrication.

Figure 60 presents our opinion about the possible morphological transformations through which the helicoliths of the two groups of *Helicosphaera* may have been derived from the lopadoliths of *Pontosphaera*.

SPECIFIC EVOLUTION OF THE HELICOLITHS

The ranges of all *Helicosphaera* species are presented in figure 61 where they are arranged in groups of species with close structural similarities. The ranges of the pre-Neogene species have been compiled from the literature (Haq, 1973).

TAXONOMY

Family PONTOSPHAERACEAE Lemmermann, 1908

Definition: Coccolithophores which bear lopadoliths.

Subfamily Helicosphaeroidae new subfamily

Definition: Shallow lopadoliths with two walls (i.e. flange and blanket) and a proximal plate. The flange is modified to a single and a double edge.

Type genus: *Helicosphaera* Kamptner emended, this paper.

Discussion: Black (1971, p. 615) introduced the monogeneric family Helicosphaeraceae. His concept of the flange as being constructed of petaloid elements arranged in a "single spiral band" has been incorporated in his diagnosis of the family. Such a concept is not in agreement with our interpretation of the construction of the flange.

Jafar and Martini (1975, pp. 388; 389) emended the family Helicosphaeraceae Black, 1971, by introducing a diagnosis based on the overall morphology of the coccosphere. Such a diagnosis, however, is not practical as the number of observed coccospheres is very limited. In the entire literature only fourteen coccospheres have been depicted (Clocchiatti, 1969; Gaarder, 1970; Jafar, 1975; Jafar and Martini, 1975; Okada and McIntyre, 1977; and Nishida, 1979) and nearly all of them belong to the same species (*H. carteri* sensu lato, except a few of *H. hyalina* by Gaarder and *H. pavimentum* by Okada and McIntyre). The definition of the family based on the shape of the coccosphere, as suggested by Jafar and Martini, is, therefore, ahead of the evidence.

Genus *Helicosphaera* Kamptner emended

Diagnosis: Shallow lopadoliths possessing a flange with a helicoid appearance at least in proximal view.

Type species: *Helicosphaera carteri* (Wallich) Kamptner, 1954; Basionym: *Coccosphaera carteri* Wallich, 1877.

Emendation: The generic diagnosis is emended to comply with the structure of the helicoliths as described in the preceding paragraphs. More precisely, the elements of the flange are arranged radially and not in the helicoid manner described by Kamptner (1954).

Remarks: In introducing the genus *Helicosphaera*, Kamptner (1954, pp. 21, 73; figs. 17–19) attempted to interpret the construction of the helicoliths. His concept of the flange as a spiral of lath-shaped elements that winds around a “central plate” (“... Spirale um das elliptische Mittelstück...”) is clearly demonstrated by his drawings which are reproduced in figure 62. What seems to be one and a half whorls of lath-like elements in his figure 17a is further exaggerated in figure 17c where he draws a double edge on the metapterygial side. The double edge could have been present in that position only if the elements had been wound for two and a quarter whorls.

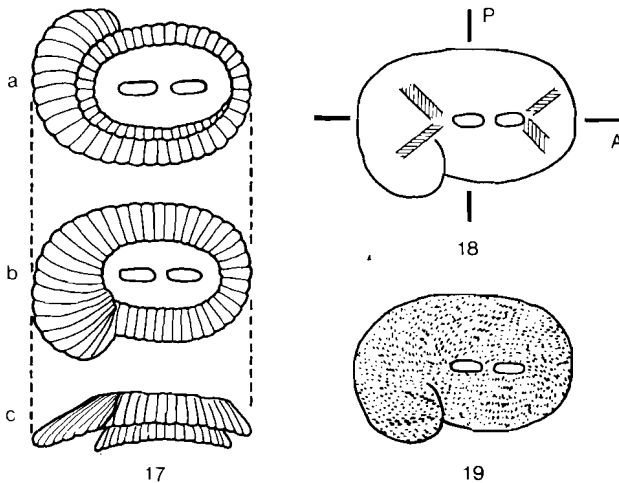


Fig. 62. Reproduction of the original drawings of Kamptner (1954) accompanying his description of *Helicosphaera*.

Kamptner's interpretation of the flange is reflected in most of the literature. The flange is described as winding for one and a half convolutions (Black and Barnes, 1961; Hay and Towe, 1962; Roth, 1970; Ellis, Lohman

and Wray, 1972), or as overlapping (Romein, 1979) or as being composed of petaloid or cuneate – in any case non curved – elements (Deflandre and Fert, 1954; Okada and McIntyre, 1977). All three descriptions carry the same implication: a flange built by a single band of linear elements, which spirals around an axis.

In the analysis of the structure of the helicolith we demonstrated that all elements of the flange are arranged radially and not as a spiral. The helicoid appearance of the flange is induced simply by a gradual modification of the elements – from curved to lath-like.

Nomenclatural notes: The first valid publication of the generic name *Helicosphaera* is in Kamptner, 1954. The lack of a formal diagnosis does not invalidate the name as suggested by Hay and Towe (1962), as the original publication of Kamptner contains an extensive description and thus complies with I.C.B.N. articles 32.1.c and 41.1.a (the reader is referred also to Loeblich and Tappan, 1966 and to Jafar and Martini, 1975).

Hay and Mohler (1967) introduced *Helicopontosphaera* as a substitute for *Helicosphaera* Kamptner which they considered, erroneously though, to be invalid as not being typified.

Clocchiatti (1969) and Jafar and Martini (1975) showed that *Helicosphaera* Kamptner did not lack a type species. These authors used identical arguments (i.e. *Coccosphaera carteri* Wallich is identical to *Helicosphaera carteri* (Wallich) Kamptner on the basis of the shape and the coccolith arrangement in their coccospheres), and rejected *Helicopontosphaera* as being superfluous.

The name *Helicopontosphaera* has not been rejected unanimously, however, and it is found in more recent publications (e.g. Gartner, 1977).

Here the name *Helicopontosphaera* is regarded as a junior synonym of *Helicosphaera*.

Subdivision: The genus is subdivided into two structural groups.

HELICOSPHAERA GROUP I

Diagnosis: Helicoliths with a helicoid appearance only in proximal view (i.e. helicoliths with flange type I).

Remarks: *H. bramlettei* Müller (synonym: *Helicopontosphaera wilcoxonii* Gartner) is the only species in Group I that does not have a smooth, elliptical outline; a strong serration of the periphery of the flange results in the formation of a wing-like expansion. In spite of this wing-like expansion the flange of this species has a continuous distal surface and it does not appear helicoid in distal view.

Helicosphaera seminulum Bramlette and Sullivan
(pl. 15, fig. 1, pl. 24, fig. 2)

Helicosphaera seminulum seminulum Bramlette and Sullivan, 1961, p. 144, pl. 4, figs. 1a–c, 2; Hay and Towe, 1962, partim, p. 512, pl. 1, fig. 1, non pl. 1, fig. 2.

Helicosphaera seminulum Bramlette and Sullivan. Black, 1968, p. 802, pl. 147, fig. 4; Miller, 1981, p. 433, pl. 1, fig. 2.

Helicopontosphaera seminulum (Bramlette and Sullivan) Stradner, 1969, p. 419, pl. 87, figs. 19, 20; Perch-Nielsen, 1971, partim, p. 44, pl. 34, fig. 4, pl. 35, figs. 1, 2, pl. 36, fig. 2, non pl. 35, figs. 5, 6, pl. 36, figs. 4, 7, 8; Haq, 1973, p. 46, pl. 1, fig. 4, pl. 3, figs. 7, 8; Perch-Nielsen, 1977, pl. 21, fig. 4, pl. 22, fig. 7.

non: *Helicosphaera seminulum* Bramlette and Sullivan; Gartner, 1967, p. 5, pl. 7, figs. 1–4; Stradner and Edwards, 1968, p. 38, pl. 39, fig. 1, pl. 40, figs. 1–5.

Description: The outline of the helicoliths of this species is symmetrically elliptical. The proximal plate is elliptical with a large central opening spanned by a subhorizontal to normally inclined bridge. The bridge is divided into two rows of elements by a suture along its longer axis. In SEM observations this suture is visible only in proximal view, as the distal side of the bridge is covered by the elements of the blanket. The blanket covers completely the distal surface of the helicolith (blanket-type III). The periphery of the flange is usually smooth but specimens with a slight serration of their metapterygial part have also been observed. The ratio of the double edge to the single edge of the flange is approximately 3 : 1.

Optical pattern: The helicoliths of this species have an interference pattern of type III. The bridge is optically discontinuous from the main body of the helicolith.

Differential diagnosis: *Helicosphaera seminulum* is distinguished from *H. lophota* by its more symmetrical outline, the thinner and lesser inclined (usually subhorizontal) bridge and the larger and more rounded central openings. *H. dinesenii* and *H. heezenii* have blankets that cover the central openings. *H. bramlettei* is closely related to *H. seminulum* but it is easily distinguished from it by the pointed wing-like expansion of the flange. *H. compacta* has a nearly round outline and possesses a bar instead of a bridge. *H. papillata* is easily distinguished from *H. seminulum* by the characteristic pits of the blanket.

Remarks: No specimens with a reticulum at the central opening have been observed. Roth (1970) mentioned a “grille” among the characteristics of this species but it is likely that he observed specimens of *H. gartneri* n. sp. which often possess such a structure.

Occurrence: *H. seminulum* ranges within the interval from the CP10 through the CP14 Zone. The species was rare in section Caravaca and common in sections Aspe and Nahal Avdat.

***Helicosphaera bramlettei* (Müller) Jafar and Martini**
(Pl. 15, figs. 2–7, pl. 24, fig. 6)

- Helicosphaera seminulum* (Bramlette and Sullivan) *seminulum* Bramlette and Sullivan. Hay and Towe, 1962, partim, p. 512, pl. 1, fig. 2, non pl. 1, fig. 1.
- Helicosphaera* aff. *H. seminulum* Bramlette and Sullivan. Bramlette and Wilcoxon, 1967, p. 106, pl. 5, figs. 11, 12.
- Helicopontosphaera bramlettei* Müller, 1970, partim, p. 114, pl. 5, figs. 5, 6, non pl. 5, fig. 4; Haq, 1973, p. 36, pl. 3, figs. 3, 4; Baldi-Beke, 1977, pl. 4, figs. 3, 9, 10.
- Helicopontosphaera wilcoxonii* Gartner, 1971, p. 110, pl. 2, figs. 1–4; Haq, 1973, pp. 46, 47, pl. 34, figs. 1, 2.
- Helicopontosphaera lophota* (Bramlette and Sullivan) Bukry. Perch-Nielsen, 1971, partim, p. 43, pl. 34, figs. 1, 2, pl. 36, fig. 1, non pl. 36, fig. 2.
- Helicopontosphaera seminulum* (Bramlette and Sullivan) Stradner. Perch-Nielsen, 1971, partim, p. 44, pl. 35, fig. 5, pl. 36, figs. 4, 7, 8, non pl. 34, fig. 4, pl. 35, figs. 1, 2, 6, pl. 36, fig. 2.
- Helicopontosphaera* (?) *lophota* (Bramlette and Sullivan) Bukry. Haq, 1971, p. 116, pl. 10, figs. 8, 9.
- Helicosphaera bramlettei* (Müller) Jafar and Martini, 1975, p. 390.
- Helicosphaera wilcoxonii* (Gartner) Jafar and Martini, 1975, p. 391.
- Helicosphaera seminulum* Bramlette and Sullivan. Müller, 1979, pl. 8, fig. 7.
- Helicosphaera* sp. aff. *H. seminulum* Bramlette and Sullivan. Miller, 1981, p. 433, pl. 1, fig. 3.

Description: The helicoliths of this species are asymmetrically elliptical (i.e. broader at their pterygal part). The flange is not smoothly rounded (in contrast to the flanges of the other species of Group I) but it has a crescent-shaped wing-like expansion which exhibits several pointed projections (spurs). The size of this expansion varies from as small as that of *Helicosphaera* aff. *H. seminulum* of Bramlette and Wilcoxon (1967) to as large as that of *Helicopontosphaera wilcoxonii* Gartner, 1971.

The proximal plate is elliptical with a large central opening which is transversed by a diabolo-like bridge. The outline of the remaining parts of the opening (on both sides of the bridge) depends entirely upon the orientation of the bridge, appearing elongated to kidney-shaped when the bridge is inclined, or round when the bridge is (sub)horizontal.

The bridge is formed by two rows of elements. A suture is present along the longer axis of the bridge in proximal view. The attachment of the bridge to the proximal plate is marked by two V-shaped sutures. The bridge is obscured, distally, by the elements of the blanket.

The blanket is of type III. The ratio of the double edge to the single edge is approximately 3 : 1.

Optical pattern: Interference figure type III. The bridge is optically discontinuous from the rest of the helicolith with two distinct extinction bands at the attachment to the flange. A fainter extinction band is often seen along the axis of the bridge.

Differential diagnosis: *Helicosphaera bramlettei* (Müller) differs from all other species of the *Helicosphaera* Group I by the pointed wing-like expansion at the periphery of the flange.

The wing of *H. bramlettei* is comparable but not identical to the wings of the species of *Helicosphaera* Group II; it resembles a “break” or an “irregularity” of the periphery of the flange and does not give the helicolith a helicoid appearance in distal view.

Emendation: We emend the concept of *Helicosphaera bramlettei* to exclude forms resembling the specimen of plate 5, fig. 4 of Müller (1970) and to include specimens comparable to *H. wilcoxonii* (Gartner).

Remarks: The isotype (Müller, 1970, pl. 5, fig. 4, SEM micrograph) in the introduction of *Helicopontosphaera bramlettei* has a flange of type II and its outline is narrower and more symmetrically elliptical than the holotype of the species. This isotype is assigned here to *H. gartneri* n. sp.

Both Müller (1970) and Gartner (1971) considered their new species (*H. bramlettei* and *H. wilcoxonii*, respectively) to be similar to *Helicosphaera* aff. *H. seminulum* of Bramlette and Wilcoxon and both depicted specimens similar to those of Bramlette and Wilcoxon (cf. holotype of *H. bramlettei* and isotype of *H. wilcoxonii*, pl. 2, fig. 3). In our opinion, *H. wilcoxonii* and *H. bramlettei* should be regarded as variants of one species with a variable configuration of the wing.

Occurrence: This species ranges from the CP15 Zone to the CP19 Zone. *H. bramlettei* was recorded as common in the Umbarca samples, Egypt.

Helicosphaera lophota Bramlette and Sullivan

(Pl. 24, fig. 1)

Helicosphaera seminulum lophota Bramlette and Sullivan, 1961, p. 144, pl. 4, figs. 3a, b, 4.

Helicopontosphaera lophota (Bramlette and Sullivan) Bukry et al., 1971, p. 1300; Haq, 1973, p. 40, pl. 1, figs. 1–3, pl. 3, figs. 9, 10; Perch-Nielsen, 1977, pl. 21, figs. 2, 5, 6, pl. 22, fig. 6.

Helicosphaera lophota (Bramlette and Sullivan) Jafar and Martini, 1975, p. 391; Miller, 1981, p. 433, pl. 1, fig. 1.

non: *Helicopontosphaera lophota* (Bramlette and Sullivan) Bukry et al., Perch-Nielsen, 1971, p. 43, pl. 34, figs. 1, 2, pl. 36, figs. 1, 2.

Description: The helicoliths are large and asymmetrically elliptical (broader at their pterygal part). The proximal plate is elliptical with a large central opening spanned by a bridge. The bridge is nearly parallel to the longer axis of the helicolith and consists of two rows of elements arranged in a fish-bone pattern. The two rows are divided by a suture aligned with the axis of the bridge.

The flange and the proximal plate are constructed of relatively robust and often irregular crystal elements. The blanket covers the entire distal surface of the helicolith (type III). The elements of the blanket imbricate dextrally. The ratio of the double edge to the single edge is approximately 3 : 1.

Optical pattern: Interference pattern type III.

Differential diagnosis: *Helicosphaera lophota* is distinguished from all other helicosphaeres of Group I by being more robust and by its more strongly asymmetrical outline. *H. seminulum* and *H. bramlettei* have thinner and lesser inclined bridges flanked by larger openings. Furthermore the flange of *H. bramlettei* possesses a pointed wing-like expansion. *H. heezenii* and *H. dinesenii* have a rhomboidal proximal plate and possess a blanket that covers the entire central opening distally. *H. papillata* has a multiperforated blanket. *H. compacta* has a nearly circular outline and a bar instead of a bridge.

Occurrence: According to Haq (1973) *H. lophota* ranges from the CP10 Zone to the CP15 Zone. This species was common in the interval from the CP11 to the CP14 Zone of the sections Caravaca, Aspe and Nahal Avdad.

***Helicosphaera papillata* (Bukry and Bramlette) Jafar and Martini**
(Pl. 16, fig. 2, pl. 24, fig. 5)

Helicopontosphaera papillata Bukry and Bramlette, 1969, pp. 133, 134, pl. 2, figs. 1, 2; Haq, 1973, pp. 40–42, pl. 2, figs. 2, 3, pl. 7, fig. 9; Perch-Nielsen, 1977, partim, pl. 21, fig. 1, non pl. 21, fig. 3.

Helicosphaera papillata (Bukry and Bramlette) Jafar and Martini, 1975, p. 391.

Description: The helicoliths of this species are asymmetrically elliptical to broadly rhomboidal. The proximal plate is rhomboidal to broadly elliptical and its central opening is transversed by a bridge with a strong normal inclination. Both the bridge and the central opening are covered distally by the blanket.

The blanket is of type III and is ornamented by numerous perforations. The perforations do not penetrate the flange and the proximal plate, and therefore are visible only in distal view in the SEM.

The ratio of the double edge to the single edge is approximately 3 : 1.

Optical pattern: The interference figure is of type III with an optically discontinuous bridge. The fine perforations of the blanket appear as darker spots.

Differential diagnosis: The fine perforations of the blanket are very characteristic of this species. *H. dinesenii* and *H. heezenii* also possess perforated blankets but their pores are less numerous and confined to the central area of the blanket.

Emendation: The perforations of the blanket of *H. papillata* have been mistaken by the original authors for nipple-like protuberances (= papillae). No such projections have been observed on the surface of the helicolith.

Occurrence: From the CP11 to the CP13 Zone. The species was rare in the CP11 Zone of section Aspe.

Helicosphaera dinesenii (Perch-Nielsen) Jafar and Martini
(Pl. 24, fig. 4)

Helicopontosphaera dinesenii Perch-Nielsen, 1971, partim, pp. 42, 43, pl. 35, figs. 3, 4, pl. 36, figs. 3, 9, 11, pl. 61, figs. 6, 7, non pl. 36, fig. 6; Haq, 1973, p. 37, pl. 1, fig. 6, pl. 2, figs. 4, 5, pl. 3, figs. 11, 12.

Helicosphaera dinesenii (Perch-Nielsen) Jafar and Martini, 1975, p. 390.

Helicopontosphaera papillata Bukry and Bramlette. Perch-Nielsen, 1977, partim, pl. 21, fig. 3, non pl. 21, fig. 1.

non: *Helicosphaera dinesenii* (Perch-Nielsen) Jafar and Martini, Müller, 1979, pl. 8, fig. 8.

Description: The helicoliths are asymmetrically or symmetrically elliptical. The proximal plate is rhomboidal or broadly elliptical and has a large central opening transversed by a bridge. The bridge is nearly aligned with the longer axis of the plate and consists of two composite segments separated by a suture.

The blanket is of type III and covers, distally, the central opening of the proximal plate. The central area of the blanket is multiperforated.

Optical pattern: The interference figure of *H. dinesenii* is of type III. The perforations of the blanket can be seen as darker spots in the central area of the specimens.

Differential diagnosis: This species closely resembles *H. heezenii* from which it differs in the number of perforations of the blanket (the latter has only two rows of perforations) and in the narrower bridge. *H. papillata* is perforated all over the surface of the blanket.

Occurrence: This species is restricted to the zones CP13 and CP14. *H. dinesenii* was rare in the Umbarca samples, Egypt. Very few, possibly re-worked specimens, were encountered at a higher interval (CP15) in sample PL16 from Calabria, S. Italy.

Helicosphaera heezenii (Bukry) Jafar and Martini
(Pl. 16, fig. 1, pl. 24, fig. 3)

Helicopontosphaera heezenii Bukry, 1971, pp. 318–320, pl. 5, figs. 1–5; Haq, 1973, p. 37, pl. 1, fig. 5, pl. 3, figs. 5, 6.

Helicopontosphaera salebroza Perch-Nielsen, 1971, partim, pp. 43, 44, pl. 34, fig. 5, non pl. 36, figs. 5, 10, pl. 37, fig. 5, pl. 61, figs. 8, 9.

Helicosphaera heezenii (Bukry) Jafar and Martini, 1975, p. 390.

Description: The helicoliths are asymmetrically elliptical, being slightly broader at their pterygal part. The proximal plate is nearly rhomboidal and its central area is filled entirely by a bridge. The bridge consists of two rows of elongated elements separated by a suture along the longer axis of the bridge.

The blanket is of type III and is ornamented by two rows of perforations which are situated along the longer sides of the underlying bridge. These perforations are consistently present on the helicoliths of this species and are not the result of dissolution as speculated by Bukry (1971).

Optical pattern: The interference pattern is of type III.

Differential diagnosis: *Helicosphaera heezenii* differs from *H. lophota* in the alignment of the bridge with the longer axis of the helicolith and in possessing a perforated blanket. It differs from *H. dinesenii* in having a broader bridge and only two rows of perforations in the central area of the blanket.

Occurrence: Haq (1973) reported this species from zones CP13 and CP14. It was rare in the Umbarca samples, Egypt.

***Helicosphaera compacta* Bramlette and Wilcoxon** (Pl. 16, figs. 6–8, pl. 24, fig. 7)

Helicosphaera compacta Bramlette and Wilcoxon, 1967, p. 105, pl. 6, figs. 5–8.

Helicopontosphaera compacta (Bramlette and Wilcoxon) Hay, 1970, p. 458; Roth, 1970, partim, pp. 861, 862, pl. 10, fig. 2, non pl. 10, fig. 4; Haq, 1971, pp. 114, 115, pl. 7, figs. 4, 5, pl. 8, figs. 6–8, pl. 9, figs. 1–3; Haq, 1973, pp. 36, 37, pl. 7, figs. 1, 2; Baldi-Beke, 1977, partim, pl. 4, figs. 5, 6, non pl. 4, figs. 1, 2.

Helicosphaera moorkensii Steurbaut, 1983, pp. 328, pl. 1, figs. 1–9.

Description: The helicoliths of this species are large with a broadly elliptical to round outline. The proximal plate is elliptical and bears two small central openings which are aligned with its longer axis and are separated by a short bar with no inclination. Specimens with only a principal suture, although rare, have also been observed.

The majority of the specimens of this species have blankets confined to the central area and the metapterygial part of the helicolith (blanket-type II).

The ratio of the double edge to the single edge is approximately 3 : 1.

Optical pattern: The interference figure of *H. compacta* is usually of type II. Specimens with interference figure of type III have also been observed, but this might be the result of overgrowth.

Differential diagnosis: *H. compacta* is the only species of Group I of *Helicosphaera* with a bar instead of a bridge.

Occurrence: This species ranges from CP14 to CP19. *H. compacta* was common in all the samples from Calabria, S. Italy and Umbarca, Egypt.

***Helicosphaera gertae* Bukry**

Helicosphaera gertae Bukry, 1981, p. 463, pl. 5, figs. 5–13, pl. 6, figs. 1–4.

Remarks: This species has not been observed in our samples but it has

been included here in order to complete the lineages of *Helicosphaera*. According to the pictures of Bukry *Helicosphaera gertae* has close morphological and optical similarities to *H. compacta*; it can be distinguished from it, however, by the characteristic proximal expansion of the flange (cf. Bukry, 1981, pl. 6, fig. 1).

Occurrence: Bukry (1981) reported this species from the Lower Miocene (CN1).

HELICOSPHERA GROUP II

Diagnosis: Helicoliths with a helicoid appearance both in proximal and in distal view (helicoliths with flange type II).

Helicosphaera reticulata Bramlette and Wilcoxon (Pl. 16, figs. 3–5, pl. 24, fig. 8)

Helicosphaera reticulata Bramlette and Wilcoxon, 1967, p. 106, pl. 6, fig. 15.

Helicopontosphaera reticulata (Bramlette and Wilcoxon) Roth, 1970, p. 863, pl. 10, fig. 5; Haq, 1973, pp. 42, 44, pl. 2, fig. 1, pl. 3, figs. 1, 2; Perch-Nielsen, 1977, pl. 22, fig. 4.

Helicopontosphaera salebroza Perch-Nielsen, 1971, partim, pp. 43, 44, pl. 36, figs. 5, 10, pl. 61, figs. 8, 9, pl. 37, fig. 5, non: pl. 34, fig. 5.

Helicopontosphaera dinesenii Perch-Nielsen, 1971, partim, pp. 42, 43, pl. 36, fig. 6, non: pl. 35, figs. 3, 4, pl. 36, figs. 3, 9, 11.

Description: The helicoliths of *H. reticulata* are large and have a rhomboidal to broadly rectangular outline. A short and usually pointed wing protrudes at the middle of the pterygal side of the helicolith. The distal surface of the helicolith is pitted.

The proximal plate is of type II; it has a rhomboidal outline and bears a large central opening spanned by a normally inclined bridge. The bridge consists of two roughly triangular, composite segments and it is separated from the proximal plate by lateral sutures.

Proximally and close to the wing the flange forms a short proximal expansion.

The blanket covers only part of the helicolith, leaving the metapterygal margin of the flange exposed distally. The blanket is penetrated by two rows of perforations situated along the sides of the bridge. The exposed metapterygal margin of the flange is ornamented by one or two rows of pits which follow roughly the periphery of this margin.

The ratio of the double edge to the single edge of the flange is approximately 1 : 1.

Optical pattern: The helicoliths of *H. reticulata* have an interference figure of type II with a highly birefringent bridge.

Differential diagnosis: *H. reticulata* is readily distinguished from all other helicospaeres by the rhomboidal outline and the characteristic ornamentation of its distal surface.

Occurrence: *H. reticulata* ranges from the CP14 Zone to the CP16 Zone. It was common in the Umbarca samples and the samples from Calabria. A few specimens were found in the CP14 Zone of the section Aspe.

Helicospaera recta (Haq) Jafar and Martini
(Pl. 17, figs. 1–2, pl. 25, fig. 2)

Helicospaera seminulum Bramlette and Sullivan subsp. *recta* Haq, 1966, p. 34, pl. 2, fig. 6, pl. 3, fig. 4.

Helicospaera truncata Bramlette and Wilcoxon, 1967, pp. 106, 107, pl. 6, figs. 13, 14.

Helicopontosphaera recta (Haq) Martini, 1969, p. 136; Müller, 1970, p. 115, pl. 5, figs. 1–3, pl. 6, fig. 2; Haq, 1971c, partim, pp. 116, 117, pl. 6, figs. 8–12, pl. 7, figs. 1–3, pl. 8, figs. 1, 2, pl. 10, figs. 1–4, non: pl. 6, fig. 13; Haq, 1973, p. 42, pl. 4, fig. 1, pl. 5, figs. 3, 4; Perch-Nielsen, 1977, pl. 22, fig. 1, pl. 23, figs. 1–3, pl. 26, figs. 1, 3, 5; Baldi-Beke, 1977, pl. 4, fig. 4.

Helicospaera recta (Haq) Jafar and Martini, 1975, p. 391.

Description: The helicoliths of this species are relatively large and have a rectangular outline. They are most often asymmetrical with the pterygal part of the helicolith broader than the antipterygal one.

The proximal plate is of type III with two large, rounded central openings and a (sub)horizontal bar.

The distal portions of the elements of the flange form a pointed wing which protrudes on the pterygal side of the helicolith. On the same side of the helicolith (the proximal portions of) the flange elements form a proximal expansion which gives the characteristic rectangular outline to the helicolith. The longest elements of the wing often fuse into one or two thick and pointed “spur(s)”.

The blanket covers only the metapterygal part of the helicolith and leaves the prepterygal periphery of the flange exposed distally. The elements of the flange which are exposed along that periphery often show dissolution features such as pits or perforations.

The ratio of the double edge to the single edge is approximately 1 : 1.

Optical pattern: The helicoliths of *H. recta* are weakly birefringent between crossed nicols. Their interference figure is of type II.

Differential diagnosis: *H. recta* is distinguished from both *H. perch-nielseniae* and *H. obliqua* by the larger central openings and the normal inclination of the bar. Further differences can be observed in the shape and position of the proximal expansion of these three species.

Occurrence: This species occurs from Zone CP19 to Subzone CN1a.

***Helicosphaera perch-nielseniae* (Haq) Jafar and Martini, emended**
(Pl. 13, fig. 3, pl. 17, figs. 3, 4, pl. 25, fig. 1)

- Helicopontosphaera compacta* (Bramlette and Wilcoxon) Hay. Roth, 1970, partim, pp. 861, pl. 10, fig. 4, non: pl. 10, fig. 2; Baldi-Beke, 1977, partim, pl. 4, figs. 1, 2, non: pl. 4, figs. 5, 6.
Helicopontosphaera perch-nielsenasae Haq, 1971, partim, p. 116, pl. 10, figs. 5, 6, non: pl. 10, fig. 7.
Helicopontosphaera perch-nielseniae Haq. Haq, 1973, p. 42, pl. 4, fig. 5, pl. 5, figs. 5, 6.
Helicosphaera perch-nielseniae (Haq) Jafar and Martini, 1975, p. 391.
non: *Helicopontosphaera perch-nielseniae* Haq. Perch-Nielsen, 1977, pl. 23, fig. 9.

Description: The helicoliths of this species are relatively large. Their outline is asymmetrically rectangular, the pterygal part being broader than the antipterygal side.

The proximal plate is of type III with two elongated central openings and a bar inversely inclined.

The distal portions of the elements of the flange form a pointed wing which terminates abruptly, close to the middle of the pterygal side. On the same side, proximal portions of the elements of the flange extend outwards and form a proximal expansion. The longest elements of the wing are fused into a thick and pointed spur.

The blanket is confined to the central area and the metapterygial part of the helicolith. The elements of the prepterygal margin of the flange are exposed distally.

The ratio of the double edge to the single edge is approximately 1 : 1.

Optical pattern: The helicoliths of *H. perch-nielseniae* are weakly birefringent and have an interference figure of type II.

Differential diagnosis: *H. perch-nielseniae* (Haq) emended differs from *H. obliqua* by the larger size and the broader and more rectangular outline of the helicoliths. It is distinguished from *H. recta* by the inversely inclined bar and central openings. *H. orientalis* (syn. *H. philippinensis* Müller) is much smaller, has a symmetrically rectangular outline, lacks a proximal expansion and usually shows an optical rim all along the periphery of the interference figure. *H. preorientalis* n. sp. is much smaller than *H. perch-nielseniae* and is less elongated and nearly square. *H. elongata* n. sp., on the other hand, is a much more elongated form and symmetrically rectangular.

Emendation: We emend the diagnosis of this species to include only large and broadly rectangular helicoliths with the bar and central openings inclined inversely.

Remarks: In the original diagnosis of *H. perch-nielseniae* Haq (1971) took into consideration only the pointed wing and the closed central openings of the proximal plate. The pointed wing is a common feature of a number of *Helicosphaera* species (e.g. *H. recta*, *H. obliqua*, *H. elongata* n. sp., *H. ori-*

entalis, *H. acuta* n. sp.), all of which, except *H. recta* may possess closed central openings. The characteristics described by Haq, therefore, can be used for the determination of this species, only in conjunction with the inverse inclination of the bar (and of the central openings), the broadly rectangular outline, and the proximal expansion of the helicoliths.

Occurrence: According to Haq (1973) this species has its first occurrence in the Middle Oligocene (NP23). It has been recorded in our samples (Umbarca, Egypt) from as low as zone CP17 and it ranges up to the top of the *H. perch-nielseniae* Zone of our zonation.

***Helicosphaera obliqua* Bramlette and Wilcoxon** (Pl. 17, fig. 5, pl. 25, fig. 4)

Helicosphaera obliqua Bramlette and Wilcoxon, 1967, p. 106, pl. 5, figs. 13, 14; Miller, 1981, p. 433, pl. 3, fig. 8.

Helicopontosphaera perch-nielsenasae Haq, 1971, partim, p. 116, pl. 10, fig. 7, non: pl. 10, figs. 5, 6.

Helicopontosphaera obliqua (Bramlette and Wilcoxon) Haq, 1971, p. 116; Haq, 1973, p. 40, pl. 4, fig. 6, pl. 5, figs. 7, 8; Perch-Nielsen, 1977, pl. 23, figs. 4–8, pl. 24, fig. 2.

Description: The helicoliths are small to medium sized and have a spindle-like outline. The proximal plate is of type III with two inversely orientated central openings and a bar. The central openings vary from broad to slit-like.

The elements of the flange form a pointed and abruptly terminating wing and a pointed proximal expansion which protrude at the middle of the pterygal side making that side look like a swallow's tail. The longest elements of the wing form a spur.

The blanket reaches as far as the periphery of the prepterygal part of the flange. Along this periphery, the distal surface of the flange remains exposed.

The ratio of the single edge to the double edge is approximately 1 : 1.

Optical pattern: The interference figure of *H. obliqua* is of type II and is dimly birefringent.

Differential diagnosis: *H. obliqua* is distinguished from *H. perch-nielseniae* by the smaller size and the spindle-like outline.

H. elongata n. sp. is more elongated and has a rectangular outline. *H. recta* is consistently larger, has an asymmetrically rectangular outline, rounded central openings and a horizontal to normally inclined bar.

Occurrence: This species ranges from the CP19 Zone to the Miocene *H. orientalis* Subzone of our zonation.

***Helicosphaera elongata* n. sp.**
(Pl. 17, figs. 6–9, pl. 25, fig. 3)

Helicopontosphaera perch-nielseniae Haq; Perch-Nielsen, 1977, pl. 23, fig. 9.

Etymology: Because it is elongated.

Diagnosis: A species of *Helicosphaera* Kamptner emended with an elongated rectangular outline, an abrupt, pointed wing and inversely inclined central slits.

Description: The rectangular outline of the helicolith is elongated and symmetrical. The wing is pointed and terminates at the middle of the pterygal side. A pointed proximal expansion can be seen on the same side. A spur is often present on the wing. The proximal plate is of type III with a bar and two central openings varying from slits to more open elongated. The central openings are inclined inversely and their direction makes an acute angle with the longer axis of the helicolith. Less frequently the central openings are aligned with the longer axis of the proximal plate. The blanket is confined to the central area and the metapterygal part of the helicolith. The periphery of the flange along the prepterygal part remains exposed distally.

Optical pattern: The interference figure of *H. elongata* is of type II and appears weakly birefringent between crossed nicols.

Differential diagnosis: For differentiation of *H. elongata* from *H. acuta* n. sp. the reader is referred to the differential diagnosis of the latter species. The two species are well separated in time; *H. elongata* n. sp. has its last occurrence in the Middle Miocene, whereas the first occurrence of *H. acuta* is in the Late Pliocene. *H. elongata* n. sp. differs from the related *H. perch-nielseniae*, *H. obliqua* and *H. recta* in the more elongated rectangular outline.

Occurrence: The earliest presence of *H. elongata* in our samples has been recorded in the *E. deflandrei* Subzone. The species ranges upwards to the *H. intermedia* Subzone. It is sporadic in all our Mediterranean sections. In D.S.D.P. Site 369A, Atlantic, it is common throughout most of its range. *H. elongata* was absent from the Lower Miocene samples of D.S.D.P. Site 219, Indian Ocean.

Holotype: Pl. 17, fig. 6, sample: 369A-10, coordinates: 111, 3/7, 5.

Isotypes: Pl. 17, fig. 7, sample: 369A-10; Pl. 17, fig. 8, sample: 369A-41; Pl. 17, fig. 9, sample: 369A-49.

Type level: *H. intermedia* Subzone.

Type locality: D.S.D.P. Site 369A, Sierra Leone Rise, Atlantic Ocean.

Helicosphaera orientalis Black

(Pl. 13, fig. 4, pl. 17, fig. 11, pl. 18, figs. 2–5, pl. 25, fig. 6)

Helicosphaera orientalis Black, 1971, p. 619, pl. 45, 3, fig. 22.

Helicopontosphaera orientalis (Black) Jafar, 1975, pp. 77, 78, pl. 9, figs. 16–17, 19–21.

Helicosphaera philippinensis Müller, 1981, p. 429, pl. 1, figs. 7–12.

Description: This species is small and symmetrically rectangular. The wing is pointed and terminates abruptly at the beginning of the metapterygial side. The central openings are slits of variable width and are inclined inversely.

The blanket leaves the distal margin of the flange exposed (blanket type I).

Optical pattern: The bright area of the interference figure is highly birefringent and it is surrounded by an optical rim (interference pattern type I). The optical rim is broader along the periphery of the prepterygial part.

Differential diagnosis: The wings of the related *H. recta*, *H. perch-nielseniae*, *H. obliqua* and *H. elongata* show a limited number of elements of decreasing length, that follow the longest and usually pointed element of the flange (spur). The wing of *H. orientalis* does not possess such a succession of gradually shorter elements but terminates directly after the pointed portion.

H. orientalis is closely related to *H. pacifica* Müller and Brönnimann, but it does not have a porous centre.

Remarks: The holotype of *H. orientalis* Black (1971, pl. 45, 3, fig. 22) is clearly a badly preserved specimen. Nevertheless, the essential characters (i.e. the rectangular outline, the pointed wing and the inverse central slits) are clearly visible. The principal suture, however, has been broadened by dissolution. *H. philippinensis* Müller has been introduced as a species with a "central field" which differs from that of *H. orientalis* (Müller, 1981, p. 429). We believe that this difference is due only to the state of preservation.

Occurrence: From the *H. orientalis* Subzone to the *R. rotaria* Zone. *H. orientalis* is abundant or common in all our Mediterranean sections as well as in the D.S.D.P. Site 369A and the samples from Trinidad. It is scarce in the D.S.D.P. sites from the Indian Ocean.

Helicosphaera cf. *H. orientalis* Black

(Pl. 17, fig. 10, pl. 18, fig. 1, pl. 25, fig. 5)

Remarks: This name is given to helicoliths with characteristics intermediate between *H. orientalis* and *H. perch-nielseniae*. These helicoliths are larger and more square than *H. orientalis* but nevertheless they are too small to be included within *H. perch-nielseniae*. Such helicoliths are restricted to the *S. heteromorphus* Zone but they are extremely rare.

Helicosphaera pacifica Müller and Brönnimann
(Pl. 18, figs. 6–8, pl. 25, fig. 7)

Helicosphaera pacifica Müller and Brönnimann, 1974, pp. 661, 662, pl. 1, figs. 1–10.

Description: The helicoliths are small with a symmetrically rectangular outline. The wing terminates abruptly at the beginning of the metapterygial side but it is not pointed. The central area is perforated by numerous pores which create the impression of a reticulum. Two slits with inverse inclination are present in the multiperforate central area. The blanket is of type I.

Optical pattern: The bright area of the interference figure of *H. pacifica* is surrounded by a narrow optical rim. The perforated central area of the helicolith remains dark between crossed nicols.

Differential diagnosis: *H. pacifica* can be easily confused with partly dissolved specimens of *H. orientalis*. Perfect specimens of *H. orientalis*, however, are distinguished by their non-porous centre which appears bright between crossed nicols, and by their pointed wing. For the differentiation of *H. pacifica* from *H. inversa*, the reader is referred to the description of the latter species.

Occurrence: Müller (1981) reported this species from NN7 to NN11.

Helicosphaera acuta n. sp.
(Pl. 18, figs. 9–11, pl. 25, fig. 8)

Etymology: From *acutus* (= acute, Lat.).

Diagnosis: A species of *Helicosphaera* Kamptner, emended, narrow and long elliptical and with an abruptly terminating wing. It possesses one or more often two inversely orientated central openings.

Description: The helicoliths are medium-sized, narrow and symmetrically long, elliptical. The wing terminates abruptly close to the middle of the pterygial side and does not possess a spur. The proximal plate is of type III with two small and slightly elongated central openings and a bar which are inclined in inverse direction. Rare specimens exhibit either a single opening, or two openings aligned with the longer axis of the helicolith. In such cases identification is still possible on the basis of the outline of the helicolith and the typically abrupt wing. The distance between the two central openings is variable. The elements of the blanket cover the entire distal surface of the helicolith, except part of the wing.

Optical pattern: The interference figure of *H. acuta* is of type III and it is brightly birefringent.

Differential diagnosis: *H. acuta* n. sp. is distinguished from all earlier

helicospheres with abrupt wings and inversed central openings (e.g. *H. obliqua*, *H. orientalis*, *H. elongata* n. sp.) by the elliptical outline and the different type of interference pattern. *H. inversa* has the same type of interference figure as *H. acuta*, but it is smaller, it has larger central openings and a more rectangular outline. Specimens of *H. acuta* with central openings aligned with the longer axis of the helicolith are distinguishable from *H. carteri* by their different outline and the pointed wing.

Occurrence: This species has been observed only in samples belonging to CN12–CN13 from the D.S.D.P. Site 397.

Holotype: Pl. 18, fig. 10, sample: 397-15-3, coordinates: 111.4/10.6.

Isotypes: Pl. 18, fig. 9, pl. 18, fig. 11. Both isotypes from sample 397-15-3.

Type level: Pleistocene, CN13 Zone.

Type locality: D.S.D.P. Site 397, off Cape Bojador (W. Africa).

Helicosphaera inversa (Gartner) n. comb.

(Pl. 25, fig. 9)

Helicopontosphaera inversa Gartner, 1977, p. 23, pl. 1, figs. 4a, b, 5a–c. Invalid, ICBN art. 37.

Helicosphaera inversa (Gartner) Haq and Berggren, 1978, p. 1192. Invalid, ICBN art. 43.

Helicopontosphaera inversa Gartner, 1977 ex Gartner 1979, INA newsl., vol. 1, no. 1, p. C2. Invalid, ICBN art. 45.

Helicopontosphaera inversa Gartner 1977 ex Gartner 1980, INA newsl., vol. 2, no. 1, p. 35.

Description: The helicoliths are medium-sized and have a symmetrical, rectangular outline. The wing terminates abruptly at the beginning of the metapterygial side. The proximal plate is of type III with large and rounded central openings and a bar with inverse inclination. The blanket is of type III.

Optical pattern: The interference figure of *H. inversa* is of type III.

Differential diagnosis: *H. inversa* is distinguished from *H. sellii* (Bukry and Bramlette) emend. by the rectangular outline and the inversely inclined bar and central openings. *H. orientalis* has a more pointed wing and an interference pattern of type I or II. *H. pacifica* has an interference pattern similar to that of *H. orientalis* and in addition its central area is multiperforated having a grid-like appearance. Furthermore, both *H. orientalis* and *H. pacifica* are confined to the Miocene.

Helicosphaera acuta n. sp. differs from *H. inversa* in having a long-elliptical outline and much smaller central opening(s).

Occurrence: Gartner recorded this species in Upper Pleistocene samples from D.S.D.P. Sites 154 (Caribbean) and 206 (Tasman Sea).

Helicosphaera euphratis Haq
(Pl. 22, figs. 1, 2, pl. 27, fig. 3)

- Helicosphaera euphratis* Haq, 1966, p. 33, pl. 2, figs. 1, 3; Miller, 1981, p. 433, pl. 3, fig. 6.
Helicosphaera parallela Bramlette and Wilcoxon, 1967, p. 106, pl. 5, figs. 9, 10.
Helicopontosphaera euphratis (Haq) Martini, 1969, p. 136; Haq 1971, p. 115, pl. 6, fig. 4, pl. 9, figs. 7–9; 1971b, p. 86, pl. 3, fig. 13; Moshkovitz and Ehrlich, 1980, pl. 3, figs. 10, 11.
Helicopontosphaera rhomba Bukry, 1971, p. 320, pl. 5, figs. 6–9; Haq 1973, p. 44, pl. 4, fig. 2, pl. 7, fig. 10.
Helicosphaera rhomba (Bukry) Jafar and Martini, 1975, p. 391.

Description: The helicoliths are large and symmetrically elliptical. The wing terminates gradually at the beginning of the metapterygial side. The proximal plate is of type II with a bridge which seals its central opening completely. The bridge is divided by a suture into two roughly triangular segments which consist of elements with a random arrangement. The blanket covers the entire distal surface of the helicolith. The ratio of the double edge to the single edge of the flange is approximately 3 : 1.

Optical pattern: The interference figure of *H. euphratis* is of type III with an optically discontinuous bridge.

Differential diagnosis: This species shows close affinities to *H. intermedia* Martini but it differs in having a bridge that covers the entire central opening of the proximal plate.

Occurrence: *H. euphratis* has its first occurrence in the Upper Eocene (CP15) and persists up to the *H. vedderi* Subzone (Lower Miocene).

Helicosphaera intermedia Martini
(Pl. 22, fig. 3, pl. 27, fig. 4)

- Helicosphaera intermedia* Martini, 1965, p. 404, pl. 35, figs. 1, 2; Bramlette and Wilcoxon, 1967, p. 105, pl. 6, figs. 11, 12; Biolzi and Perch-Nielsen, 1982, pl. 1, figs. 9, 10.
Helicopontosphaera intermedia Martini, Hay and Mohler, 1967, p. 448; Roth, 1970, p. 862, pl. 10, fig. 6; Haq, 1971, pl. 3, figs. 10, 11; Haq, 1971, p. 115, pl. 8, figs. 3, 4, pl. 9, figs. 4–6; Haq, 1983, p. 38, pl. 4, fig. 3, pl. 5, figs. 9–10; Baldi-Beke, 1977, pl. 4, figs. 7, 8; Moshkovitz and Ehrlich, 1980, pl. 3, fig. 14.
Helicopontosphaera euphratis (Haq) Martini, Perch-Nielsen, 1977, pl. 22, fig. 5.
Helicopontosphaera rhomba Bukry, Perch-Nielsen, 1977, pl. 24, figs. 3, 5, 6.

Description: The helicoliths of *H. intermedia* are symmetrically elliptical with a wing that terminates gradually at the beginning of the metapterygial side. The proximal plate is of type II with a large central opening transversed by a sigmoid bridge which is inclined in a normal direction. A diagonal suture divides the bridge into two roughly triangular segments consisting of equidimensional elements without apparent orientation. The suture of the bridge is visible only in proximal view.

The blanket covers the entire distal surface of the helicolith.

The ratio of the double edge to the single edge is approximately 3 : 1.

Optical pattern: The interference figure of the helicoliths of *H. intermedia* is of type III. The bridge becomes brightest when the helicoliths are orientated with their longer axis at 45 degrees to the polarization direction.

Differential diagnosis: *H. intermedia* is distinguished from *H. euphratis* by the s-shaped bridge. *H. gartneri* n. sp. has larger central openings, and a sub-horizontal bridge which is divided by a suture into two rectangular, elongated segments.

Occurrence: The first occurrence of *H. intermedia* is in the Oligocene zone CP16. In our samples this species has a common occurrence as high as the *E. hamatus* Subzone. In section Falconara 2, Sicily, rare specimens of *H. intermedia* were recorded up to the *C. leptoporus* Subzone MA.

Helicosphaera mediterranea Müller

(Pl. 22, figs. 4–9, pl. 27, fig. 5)

? *Helicopontosphaera recta* (Haq) Martini, Haq, 1971, partim, pp. 116, 117, pl. 6, fig. 13, non: pl. 6, figs. 8–12, pl. 7, figs. 1–3, pl. 8, figs. 1, 2, pl. 10, figs. 1–4.

Helicosphaera intermedia Martini, Ellis and Lohman, 1979, pl. 3, fig. 12.

Helicopontosphaera cf. *H. sellii* Bukry and Bramlette, Baldi-Beke, 1980, partim, p. 171, pl. 4, figs. 16, 19, 20, non: pl. 4, figs. 11–13.

Helicopontosphaera recta (Haq) Martini, Baldi-Beke, 1980, pl. 4, figs. 17, 18.

Helicosphaera mediterranea Müller, 1981, p. 428, pl. 1, figs. 13, 14.

Helicosphaera crouchii Bukry, 1981, p. 462, pl. 5, figs. 1–4.

Description: The helicoliths of this species are large with a symmetrically elliptical outline. The wing terminates at the beginning of the metapterygial side. The proximal plate is of type II with broad central openings and a horizontal bar. The two portions of the bar are slightly offset, which gives the bar a sigmoid appearance. In some specimens, the two portions of the bar overlap and appear brighter at the point of overlap between crossed nicols.

The elements of the blanket cover the entire distal surface of the helicolith.

The ratio of the double edge to the single edge is approximately 3 : 1.

Optical pattern: The interference figure of *H. mediterranea* is of type III.

Differential diagnosis: *H. mediterranea* differs from *H. waltrans* n. sp. in having a horizontal bar and central openings that are larger and nearly circular. The bar of the latter species is broader and strongly inclined, while its openings are elongated, appearing nearly triangular between crossed nicols.

H. mediterranea is distinguished from *H. sellii* by the larger size and the relatively broader central openings. The distinction is facilitated further by the non-concurrent ranges of the two species.

H. vedderi Bukry and *H. stalis* n. sp. are considerably smaller and have different interference-pattern types.

Occurrence: Müller (1981) reported *H. mediterranea* from the Lower Miocene zones NN2 and NN3. In our samples this species has been observed from the *E. deflandrei* Subzone to the *H. waltrans* Subzone.

H. mediterranea has a sporadic occurrence in the sections on Gozo and Sicily and in the D.S.D.P. Sites 372 (Mediterranean) and 369A (Atlantic).

Helicosphaera vedderi Bukry
(Pl. 20, figs. 1–4, pl. 26, fig. 3)

Helicosphaera vedderi Bukry, 1981, p. 463, pl. 6, figs. 8–17.

Description: The helicoliths of this species are small and symmetrically elliptical. The proximal plate is of type III with a normally inclined bar, flanked by two large and angular openings. The wing is small but distinct and terminates at the beginning of the metapterygial side.

The blanket is restricted to the centre of the distal surface of the helicolith.

The ratio of the double edge to the single edge is approximately 3 : 1.

Optical pattern: The interference figure of *H. vedderi* is of type I.

Differential diagnosis: *Helicosphaera walbersdorfensis* Müller emend. is distinguished from *H. vedderi* Bukry by the larger wing that terminates close to the beginning of the antipterygial side of the helicolith. Furthermore, the bar of *H. walbersdorfensis* is thinner, less resistant and low-birefringent, if birefringent at all.

H. stalis n. sp. has a wing that does not extend beyond the periphery of the proximal cycle of the flange. The wing therefore is invisible in LM observation, whereas in SEM observation it is visible only in distal view. The wing of *H. vedderi*, on the other hand, is easily distinguished both in proximal and distal view. In addition to these morphological differences, the two species have different, non-overlapping ranges. *H. vedderi* is distinguished from *H. waltrans* n. sp. by its much smaller size.

Remarks: Bukry (1981, insert) considered *H. vedderi* to be a junior synonym of *H. minuta* Müller “by age, size and morphology”. The specimens described by Müller as *H. minuta*, however, are distinguished from *H. vedderi* by the non-extended wings, the weak birefringence of their bars, and their higher stratigraphic occurrence. In our opinion they can best be assigned to *H. walbersdorfensis*.

Occurrence: Bukry reported this species from zones CN3 and CN4. In our samples *H. vedderi* ranges from as low as the *E. druggii* Subzone to the *H.*

perch-nielseniae Subzone. It was recorded in the sections from Sicily, Malta and Gozo and in the Lower Miocene samples of the D.S.D.P. Sites 372, (Mediterranean), and 369A (Atlantic).

Helicosphaera waltrans n. sp.

(Pl. 13, fig. 2, pl. 20, figs. 5–9, pl. 26, fig. 2)

Etymology: Combination of the words Walbersdorf and transverse.

Diagnosis: A large species of *Helicosphaera* Kamptner emend. with a wide and normally inclined bar and two central openings that appear triangular between crossed nicols.

Description: The helicoliths are large and have an asymmetrically elliptical outline and a prominent wing which terminates near the middle of the meta-ptyergal side. The bar is broad and normally inclined, leaving two central openings which have a characteristic triangular outline between crossed nicols.

The elements of the blanket cover only the central area of the helicolith.

The ratio of double edge to single edge of the flange is approximately 3 : 1.

Optical pattern: The interference figure of *H. waltrans* is of type I.

Differential diagnosis: *H. waltrans* is distinguished from *H. vedderi* by the more prominent wing, the larger central openings and the much larger size of the helicoliths.

Occurrence: *H. waltrans* is restricted to the *S. heteromorphus* Zone (from the *H. obliqua* Subzone to the *H. waltrans* Subzone). It becomes common within the *H. perch-nielseniae* and *H. waltrans* Subzones. This species was recorded in all our sections.

Holotype: Pl. 20, fig. 5, sample: MT740, coordinates: 114.9/5.4.

Isotypes: Pl. 13, fig. 2, sample: CP3656; pl. 20, fig. 6, sample: MT740; pl. 20, fig. 7, sample: MT739; Pl. 20, fig. 8, sample: MT741; Pl. 20, fig. 9, sample: MT737.

Type level: *H. waltrans* Subzone.

Type locality: Reqqa Point, Gozo.

Helicosphaera ampliaperta Bramlette and Wilcoxon, emended

(Pl. 13, fig. 1, pl. 19, figs. 1–4, pl. 26, fig. 1)

Helicosphaera ampliaperta Bramlette and Wilcoxon, 1967, p. 105, pl. 6, figs. 1–4; Ellis and Lohman, 1979, pl. 3, fig. 10; Miller, 1981, p. 432, pl. 3, figs. 7a, b.

Helicopontosphaera ampliaperta (Bramlette and Wilcoxon) Hay, 1970, p. 458; Perch-Nielsen, 1971, pp. 41, 42, pl. 34, fig. 3; Haq, 1973, p. 36, pl. 6, figs. 4, 5, pl. 7, figs. 3, 4; Baldi-Beke, 1980, pl. 2, fig. 3, pl. 4, figs. 6, 7, 8; Moshkovitz and Ehrlich, 1980, pl. 3, figs. 12, 13.

Diagnosis: A species of *Helicosphaera* with a proximal plate of type II without a bridge and with a wing of variable size.

Description: The outline of these helicoliths varies from elliptical to roughly triangular, depending on the width of the wing of the specimens. The proximal plate is of type II without a bridge. The shape of the central opening of the proximal plate corresponds to the shape of the periphery of the flange. Thus, more rounded specimens exhibit relatively more rounded central openings. Two nodes are occasionally present, one at each end of the shorter axis of the central opening.

The wing terminates gradually near the middle of the metapterygial side. The blanket covers only the central area of the helicolith, leaving exposed the periphery of the distal surface of the flange.

The ratio of the double edge to the single edge is approximately 3 : 1.

Optical pattern: The interference figure is of type I.

Emendation: We emend the original description to include morphotypes with an extended wing.

Remarks: Bramlette and Wilcoxon (1967, p. 105) confined their description to specimens with a "nearly oval outline, normally showing little of the terminal flare of the larger (distal) shield". A reduced "terminal flange" or "subdued rim-flare" is attributed to *H. ampliaperta* by Haq (1973, p. 36) and Bukry (1973, p. 698). Although this character can be ascribed to the most common variant of the species, specimens with distinctly extended wings are common.

Occurrence: *H. ampliaperta* ranges from the *H. vedderi* Subzone to the *E. signus* Subzone. The species was consistently present in all our sections covering this interval.

***Helicosphaera scissura* Miller** (Pl. 19, figs. 5–8)

Helicosphaera scissura Miller, 1981, p. 433, pl. 3, figs. 10a–c, 11a–b; Bukry, 1981, p. 463, pl. 6, figs. 8–10.

Description: Long, elliptical helicoliths with a proximal plate of type II without a bridge. The central opening of the proximal plate is narrow and very often it has a weakly birefringent filling. The blanket is of type I. The flange has an extended wing.

Optical pattern: The interference figure of *H. scissura* is of type I.

Occurrence: From the *T. martinii* Subzone to the *E. signus* Subzone.

Helicosphaera walbersdorfensis Müller, emended
(Pl. 13, fig. 5, pl. 14, fig. 3, pl. 19, figs. 9–11, pl. 26, fig. 4)

Helicosphaera walbersdorfensis Müller, 1974, pp. 392, 393, pl. 2, fig. 15, pl. 4, figs. 35–37, 45, 46.

Helicosphaera minuta Müller, 1981, pp. 428, 429, pl. 1, figs. 1–6.

Helicosphaera californiana Bukry, 1981, p. 462, pl. 4, figs. 7–12.

Description: The helicoliths are small and their outline varies from roughly triangular to symmetrically elliptical, depending on the width of the wing. The proximal plate is of type III with two narrow central openings and a thin bar with normal inclination.

The wing is usually large and terminates close to the antipterygal side. Specimens with less prominent wings are less frequent, but they occur throughout the range of the species. The bar is characteristically thin and it may be dissolved or broken off even in otherwise first-class samples. In these cases, either a straight or a zigzag opening remains at the centre of the helicolith. The blanket is confined to the central area of the distal surface of the helicolith.

Optical pattern: The interference figure of *H. walbersdorfensis* is of type I. The bar of the proximal plate appears weakly birefringent.

Differential diagnosis: *Helicosphaera walbersdorfensis* is easily distinguished from *H. stalis* n. sp. by the thinner and less birefringent bar, the different position of termination of the wing, and the usually larger wing.

Emendation: We emend the diagnosis of *H. walbersdorfensis* to include specimens with reduced wings comparable to *H. minuta* Müller, and with slits comparable to *H. californiana* Bukry.

The type of the interference pattern, the small size, and the thin and weakly birefringent bar are considered as characteristic features of the species.

Remarks: The electron micrographs Müller presented when introducing *H. walbersdorfensis* and *H. minuta* are not directly comparable because of the different position of the specimens. It is necessary, therefore, to point out some of the common features; the holotype of *H. walbersdorfensis* (Müller, 1974, pl. 2, fig. 15) has a wing which terminates close to the antipterygal side of the helicolith and in this aspect it is similar to the isotype of *H. minuta* (Müller, 1981, pl. 1, fig. 1). The holotype of *H. minuta* (pl. 1, fig. 2) on the other hand lies on its distal surface with the wing away from the observer; the size of the wing is therefore hard to estimate, but the size and shape of the central openings are identical to those of the paratype of *H. walbersdorfensis* on pl. 4, fig. 36. Moreover, the light microscope figures of both species have similar interference figures (compare Müller, 1974, pl. 4, fig. 46 with Müller, 1981, pl. 1, figs. 4–6).

Occurrence: From the *H. obliqua* Subzone to the top of the *E. kugleri* Subzone. *H. walbersdorfensis* was common or abundant in all our Mediterranean sections. In D.S.D.P. Site 369A this species was less frequent but consistently present.

***Helicosphaera stalis* n. sp.**

(Pl. 13, fig. 6, pl. 20, figs. 10–12, pl. 21, figs. 1–12, pl. 26, figs. 5, 6)

Etymology: From *stalis* (Greek metaphor for anything very small).

Description: A very small species of *Helicosphaera* Kamptner emend., with an oval or rhomboidal outline and a broad, straight or sigmoid bar which is inclined normally. The wing does not extend beyond the periphery of the proximal portions of the elements of the flange and, therefore, it is visible only in distal view (in S.E.M. observation). The proximal plate is of type III with central openings that vary in size and may be round or kidney-shaped. The bar of the proximal plate is inclined in a normal direction. The elements of the blanket cover only the central area of the distal surface of the helicolith.

Optical pattern: The interference figure of *H. stalis* is of type I. The bar is in optical continuity with the rest of the helicolith and it is distinctly bright.

Differential diagnosis: *H. stalis* is distinguished from *H. vedderi* by the smaller wing. The differentiation of the two species is facilitated by their different biostratigraphic ranges. It differs from variants of *H. walbersdorfensis* with small wings, in the larger central openings, and the thicker and brighter bar.

Remarks: The bar of this minute species is noticeably resistant. In extremely dissolved assemblages it has been observed to outlast parts of the periphery of the helicolith.

Subdivision: Two subspecies are introduced here: *Helicosphaera stalis stalis* n. subsp. and *Helicosphaera stalis ovata* n. subsp.

Holotype: See *H. stalis stalis*.

Occurrence: From the *H. intermedia* Subzone to the *R. rotaria* Zone. *H. stalis* is abundant or common in all our sections covering this interval except those from the Indian Ocean where the species has a sporadic occurrence.

***Helicosphaera stalis stalis* n. subsp.**

(Pl. 21, figs. 8–12, pl. 26, fig. 5)

Diagnosis: A subspecies of *H. stalis* n. sp. with large kidney-shaped central openings, a sigmoid bar and a rhomboidal outline.

Holotype: Pl. 21, fig. 9, sample: CP3018, coordinates: 107.8/10.

Isotypes: Pl. 21, figs. 8, 10, 11, all from sample: 369A-15; Pl. 21, fig. 12, sample: CP3020.

Type level: *E. pentaradiatus* Subzone.

Type locality: Falconara, Sicily.

Occurrence: From the *E. calcaris* Zone to the *R. rotaria* Zone.

Helicosphaera stalis ovata n. subsp.

(Pl. 13, fig. 6, pl. 20, figs. 10–12, pl. 21, figs. 1–7, pl. 26, fig. 6)

Diagnosis: A subspecies of *Helicosphaera stalis* n. sp. with small central openings, a straight bar and a massive central area.

Remarks: The distinction of the two subspecies is difficult within the *E. calcaris* Zone because of the presence of transitional morphotypes. Below this zone and as low as the *H. intermedia* Subzone, however, *H. stalis stalis* is absent, whereas in the interval from the *E. calcaris* Zone to the *R. rotaria* Zone *H. stalis ovata* becomes sporadic and is gradually replaced by *H. stalis stalis*.

Holotype: Pl. 21, fig. 1, sample: CP4609, coordinates: 115.6/13.7.

Isotypes: Pl. 13, fig. 6, sample: CP3118; pl. 20, figs. 10–12, all from sample CP3122; pl. 21, figs. 3–4, sample: CP3068; pl. 21, figs. 5–7, sample CP3059.

Type level: *E. bollii* Subzone.

Type locality: Scicli, Sicily.

Occurrence: From the *H. intermedia* Subzone to the *R. rotaria* Zone.

Helicosphaera sellii (Bukry and Bramlette) Jafar and Martini, emended (Pl. 26, fig. 7)

Helicopontosphaera sellii Bukry and Bramlette, 1969, p. 134, pl. 2, figs. 3–7; Perch-Nielsen, 1972, pl. 18, figs. 4, 6; Haq, 1973, pp. 44, 46, pl. 6, fig. 3, pl. 7, figs. 5, 6; Gartner, 1977, pl. 1, figs. 6a, b, 7a, b, pl. 4, figs. 1, 2; partim, pl. 3, fig. 15, non: pl. 3, fig. 20.

Helicosphaera sellii (Bukry and Bramlette) Jafar and Martini, 1975, p. 391; Haq and Berggren, 1978, pl. 2, figs. 17, 20; Backman, 1980, pl. 8, figs. 2, 6.

non: *Helicosphaera sellii* (Bukry and Bramlette) Jafar and Martini, Ellis and Lohman, 1979, p. 76.

non: *Helicopontosphaera inversa* Gartner, 1977, ex Gartner, 1980, p. 23, pl. 1, figs. 4a–b, 5a–c.

Description: The helicoliths are small to medium sized and symmetrically elliptical in outline. The wing is short and terminates gradually close to the beginning of the metapherygal side. The proximal plate is of type III with a subhorizontal to normally inclined bar and large central openings.

Most specimens of *H. sellii* possess a blanket that covers the entire distal

surface of the helicoliths. Specimens with a blanket confined to the centre of the helicolith (type I) have also been encountered.

Optical pattern: Interference pattern types I and III have both been observed.

Differential diagnosis: *H. sellii* is distinguished from *Helicosphaera inversa* (Gartner) n. comb. by the elliptical outline and the normally inclined bar. All other similar helicospheres (e.g. *H. mediterranea*, *H. waltrans* n. sp., *H. vedderi* and *H. stalis* n. sp. differ in size and/or stratigraphic range.

Emendation: We emend the diagnosis of *H. sellii* to restrict the species to specimens with subhorizontal to normally inclined bars, elliptical outline and a gradually terminating wing.

Remarks: Ellis and Lohman (1979) remarked that the orientation of the bar was not mentioned in the original description of this species. They concluded, therefore, that specimens with inversely inclined bars, such as *H. inversa* (Gartner), should be included in the concept of *H. sellii*. In our opinion the orientation of the bars of the helicoliths shows no such variation within a species.

Occurrence: *H. sellii* ranges from the *C. leptoporus* Zone to zone CN14

***Helicosphaera gartneri* n. sp.**
(Pl. 15, figs. 8–12, pl. 27, fig. 1)

Helicosphaera seminulum Bramlette and Sullivan; Gartner, 1967, p. 5, pl. 7, figs. 1–4; Stradner and Edwards, 1968, p. 38, pl. 39, fig. 1, pl. 40, figs. 1–5.

Helicopontosphaera bramlettei Müller, 1970, partim, p. 114, pl. 5, fig. 4, non: pl. 5, figs. 5, 6.

Helicopontosphaera seminulum (Bramlette and Sullivan) Stradner; Perch-Nielsen, 1971, partim, p. 44, pl. 35, fig. 6, non: pl. 34, fig. 4, pl. 35, fig. 1, 2, 5, pl. 36, figs. 4, 7, 8, pl. 37, fig. 6.

Etymology: In honour of Dr. S. Gartner who was the first to depict specimens resembling this species.

Diagnosis: A species of *Helicosphaera* Kamptner emend. with a symmetrically elliptical outline, large central openings and a bridge. The bridge is divided into two equidimensional segments by a suture aligned with its axis. The outline of the bridge varies from roughly rectangular to sigmoidal.

Description: The helicoliths are medium sized, symmetrically elliptical and relatively elongated. The wing is small and terminates close to the beginning of the metapterygial side. The proximal plate is of type II with a bridge. The bridge consists of two nearly rectangular, composite segments separated by a suture. The orientation of the bridge may vary from (sub)horizontal to normally inclined. The central openings are relatively large, vary in shape from round to kidney-shaped, and they are often filled by a fine grid.

The blanket covers the entire distal surface of the helicolith.

The ratio of the double edge to the single edge is approximately 3 : 1.

Optical pattern: The interference figure of *H. gartneri* is of type III with a bright and optically discontinuous bridge.

Differential diagnosis: Specimens of *H. gartneri* have been assigned to either *H. seminulum* or *H. bramlettei* both of which are distinguished from *H. gartneri* by their flange of type I.

Helicosphaera gartneri n. sp. is distinguished from *H. intermedia* by the larger central openings and the suture which is situated along the axis of the bridge. In contrast, the suture of the bridge of *H. intermedia* is diagonal.

H. truempyi Biolzi and Perch-Nielsen is the only other helicosphere with a bridge similar to that of *H. gartneri* but it is much larger and has a different stratigraphic range.

Remarks: Excellent electron micrographs of this species have been presented by Gartner, 1967, Stradner and Edwards, 1968 and Müller 1970 (the reader is referred also to *H. bramlettei*, this paper).

Holotype: Pl. 15, fig. 8, sample: WEPCO 2500–2530, coordinates: 111.6/15.3.

Isotypes: Pl. 15, figs. 9–12, sample: WEPCO 2500–2530.

Type level: Oligocene.

Type locality: Umbarca, Egypt.

Occurrence: The total range of *H. gartneri* is yet to be defined. It was encountered in Oligocene samples (Umbarca, Egypt).

***Helicosphaera truempyi* Biolzi and Perch-Nielsen**
(Pl. 27, fig. 2)

Helicosphaera truempyi Biozi and Perch-Nielsen, 1982, pp. 171–175, pl. 1, figs. 1–8.

Remarks: This is one of the few species of Group II of *Helicosphaera* with a proximal plate of type II and a bridge consisting of two nearly rectangular composite segments. Specimens of *H. truempyi* were not observed in our samples. According to the authors it is a very large helicosphere and in that aspect it differs from *H. gartneri* n. sp. which is a medium to small species. Moreover the two species are distinguished by their different outlines and the different biostratigraphic occurrence.

The figures presented in this paper are interpretations based on the original figures of the species.

The original authors speculated that *H. truempyi* has developed from *H. intermedia* by a rotation of the bridge from oblique to axial. Species of *Helicosphaera* with an axial bridge are present, however, earlier than the first occurrence of *H. intermedia* (e.g. *H. seminulum*, *H. bramlettei* and probably

H. gartneri). In our lineages *H. truempyi*, therefore, is connected with *H. gartneri*.

Occurrence: Biolzi and Perch-Nielsen (1982) have reported this species from the Lower Miocene zone CN1a.

***Helicosphaera paleocarteri* n. sp.**
(Pl. 23, figs. 1–4, pl. 27, fig. 6)

Helicosphaera carteri (Wallich) Kamptner, Bramlette and Wilcoxon, 1967, p. 105, pl. 6, figs. 9, 10.

Helicopontosphaera kamptneri Hay and Mohler, 1967, p. 38, pl. 7, fig. 12.

Etymology: From palaeos (= ancient, old, Gr.) and carteri.

Diagnosis: Helicoliths with an interference figure showing two dark points not aligned with the extinction line of the principal suture.

Description: The helicoliths are large- to medium-sized, they may be symmetrically or asymmetrically elliptical and they have a prominent wing.

The proximal plate is of type I with a suture along the median longer axis of the plate (“principal suture”). The blanket spreads all over the distal surface of the helicolith and its centre is ornamented by two shallow pits. The pits usually do not penetrate the proximal plate. Observation in transmitted light reveals that the pits are offset relatively to the position of the principal suture.

The ratio of the double edge to the single edge is approximately 3 : 1.

Optical pattern: The interference figure of this species is of type III.

Differential diagnosis: *Helicosphaera paleocarteri* n. sp. is distinguished from *H. carteri* by the lack of central openings aligned with the principal suture.

Remarks: So far these helicoliths have been included within *H. carteri*.

Holotype: Pl. 23, fig. 1, sample: CP3682, coordinates: 112.3/4.5.

Isotypes: Pl. 23, figs. 2–4, sample: CP3670.

Type level: *H. orientalis* Subzone.

Type locality: Giammoia 2, Sicily.

Occurrence: *H. paleocarteri* ranges throughout the Miocene and most of the Pliocene. Within the Pliocene this species has a sporadic occurrence.

***Helicosphaera carteri* (Wallich) Kamptner, emended**
(Pl. 23, figs. 5–9, pl. 27, fig. 7)

Coccosphaera carteri Wallich, 1877, p. 348, pl. 17.

Coccolithophora wallichii Lohmann, 1902, p. 138, pl. 5, figs. 58, 58b, 59, 60.

Helicosphaera carteri (Wallich) Kamptner, 1954, pp. 21, 73, figs. 17–19.

Helicopontosphaera kamptneri Hay and Mohler, 1967, p. 448, pl. 10, fig. 5, pl. 11, fig. 5.

Helicosphaera burkei Black, 1971, pp. 618, 619, pl. 45.3, fig. 23.

Helicopontosphaera neogranulata Gartner, 1977, pp. 22, 23, pl. 2, figs. 2a, b.

Helicopontosphaera colombiana Gartner, 1977, p. 22, pl. 2, figs. 5a–c.

Description: The helicoliths are symmetrically to asymmetrically elliptical and vary in size. The proximal plate may be of type I with only a principal suture, or of type III with two central openings and a bar which are slightly inclined in normal direction, or may be aligned with the longer axis of the helicolith.

The blanket covers the entire distal surface of the helicolith except the tip of the wing. The wing varies in size.

The ratio of the double edge to the single edge is approximately 3 : 1.

Optical pattern: The helicoliths are intensely birefringent between crossed nicols. Their interference figure is of type III.

Differential diagnosis: Morphotypes of *H. carteri* with central openings are distinguished from *H. sellii* by the smaller size of the openings. The bar of *H. carteri*, when present, is either horizontal or normally inclined, which distinguishes the species from *H. inversa*.

Emendation: The concept of this species is enlarged to include morphotypes with only a principal suture and morphotypes with inclined central openings.

Remarks: The specimens depicted by Kamptner (1954) as *H. carteri* have their central openings aligned with the longer axis of the helicolith. On the basis of the figures and the description of Kamptner later authors restricted the species concept of *H. carteri* to the helicoliths with such an alignment of their openings, while all other obviously related forms with inclined central openings (*H. wallichii*) or only a principal suture (*H. burkei*) have been distinguished as different species. These three "species" are considered here as varieties of *H. carteri* (Wallich) Kamptner emended.

Occurrence: From the *E. deflandrei* Subzone to the Recent. Three varieties are present throughout the range of the species.

***Helicosphaera carteri* var. *carteri* n. var.**

(Pl. 23, fig. 5)

Coccosphaera carteri Wallich, 1877, p. 348, pl. 17.

Coccolithophora pelagica (Wallich) Lohmann, 1902, p. 139, pls. 4–6.

Coccolithus carteri (Wallich) Kamptner, 1944, pp. 141–144.

Helicosphaera carteri (Wallich) Kamptner, 1954, pp. 21, 73, fig. 17–19; Deflandre and Fert, 1954, partim, p. 32, text-fig. 75, non: figs. 9–11; Black and Barnes, 1961, partim, pp. 139, 140, pl. 23, fig. 2, non: pl. 22, fig. 1, pl. 23, fig. 1; McIntyre and Bé, 1967, p. 571, pl. 11, fig. a; McIntyre, Bé and Preikstas, 1967, partim, pp. 12, 13, pl. 6, fig. b, non: pl. 6, fig. a; Kamptner, 1967, pp. 141, 143, pl. 7, figs. 45, 46, 48, 49; Black, 1968, partim, pp. 801, 802, pl. 147, figs. 1, 3, non: pl. 147,

fig. 2; Clocchiatti, 1969, pp. 77, 79, pl. 1, figs. 1–5, pl. 2, figs. 1–3, pl. 3, figs. 1, 2; Gaarder, 1970, figs. 1h, 2e, 2f; Gaarder and Hasle, 1971, figs. 9a, b, e; Haq and Berggren, 1978, pl. 2, figs. 7, 8; Conley, 1979, partim, p. 29, pl. 2, fig. 17, non: pl. 1, fig. 18; Nishida, 1979, pl. 9, figs. 4a–d; Backman, 1980, pl. 8, fig. 1; Miller, 1981, pl. 3, fig. 9.

Helicopontosphaera kamptneri Hay and Mohler, 1967, p. 448, pl. 10, fig. 5, pl. 11, fig. 5; Boudreaux and Hay, 1969, p. 272, pl. 6, figs. 8, 10–15; Nishida, 1970, p. 364, pl. 40, figs. 14, 15; Nishida, p. 152, pl. 17, figs. 17, 18; Bukry, 1971, pl. 1, fig. 2; Martini and Müller, 1972, partim, p. 68, pl. 2, figs. 13, 14, non: pl. 1, fig. 2; Ellis, Lohman and Wray, 1972, partim, p. 29, pl. 6, figs. 1, 2, non: pl. 5, fig. 6; Sachs and Skinner, 1973, pl. 3, figs. 21–24; Gartner, 1977, pl. 2, figs. 4a, b.

Helicopontosphaera wallichii (Lohmann) Boudreaux and Hay, 1969, pp. 272–273, pl. 6, fig. 9; Perch-Nielsen, 1972, pl. 18, figs. 1–3, 8, 11.

Helicosphaera wallichii (Lohmann) Okada and McIntyre; Haq and Berggren, 1978, pl. 2, figs. 21, 22; Conley, 1979, p. 29, pl. 1, fig. 19, pl. 2, fig. 18.

Helicosphaera sp. cf. *H. carteri* (Wallich) Kamptner; Black, 1971, pl. 45. 2, fig. 21.

Helicopontosphaera sp. cf. *H. intermedia* Martini; Sachs and Skinner, 1973, pl. 3, figs. 18–20.

Helicopontosphaera sp. cf. *H. wallichii* (Lohmann) Boudreaux and Hay; Moshkovitz and Ehrlich, 1980, pl. 3, fig. 8.

Helicopontosphaera carteri (Wallich) Moshkovitz and Ehrlich, 1980, partim, pl. 3, figs. 16–19, 23, non: pl. 3, fig. 22.

Diagnosis: Variants of *H. carteri*, with their central openings, aligned with the longer axis of the proximal plate.

Helicosphaera carteri var. *burkei* n. var.

(Pl. 23, figs. 6–7)

Helicosphaera carteri (Wallich) Kamptner; Black and Barnes, 1961, partim, pp. 139, 140, pl. 22, fig. 1, pl. 23, fig. 1, non: pl. 23, fig. 2; McIntyre, Bé and Preikstas, 1967, partim, p. 12, 13, pl. 6, fig. A, non: pl. 6, fig. B; Conley, 1979, partim, p. 29, pl. 1, fig. 18, non: pl. 2, fig. 17.

Helicosphaera burkei Black, 1971, pp. 618, 619, pl. 45.3, fig. 23.

Helicopontosphaera kamptneri Hay and Mohler; Perch-Nielsen, 1972, partim, pl. 18, figs. 9, 12, non: pl. 18, fig. 5; Ellis, Lohman and Wray, 1972, partim, p. 29, pl. 5, non: pl. 6, figs. 1, 2; Martini and Müller, 1972, partim, p. 68, pl. 1, fig. 2, non: pl. 2, figs. 13, 14; Müller, 1974, pl. 3, fig. 4; McIntyre and Imbrie, 1975, pl. 1, fig. D; Jafar, 1975, pp. 76, 77, pl. 9, figs. 4–7.

Helicopontosphaera carteri (Wallich) Moshkovitz and Ehrlich, 1980, partim, pl. 3, fig. 22, non: pl. 3, figs. 16–19, 23.

Diagnosis: Variants of *H. carteri*, without central openings, exhibiting only a principal suture.

Helicosphaera carteri var. *wallichii* n. var.

(Pl. 23, figs. 8, 9, pl. 27, fig. 7)

Coccolithophora wallichii Lohmann, 1902, p. 138, pl. 5, figs. 58, 58b, 59, 60.

Helicopontosphaera wallichii (Lohmann) Boudreaux and Hay; Perch-Nielsen, 1977, pl. 24, fig. 1.

Helicosphaera wallichii (Lohmann) Okada and McIntyre, 1977, pp. 14, 15, fig. 8.

Diagnosis: Variants of *H. carteri* with normally inclined central openings.

Helicosphaera granulata (Bukry and Percival) Jafar and Martini

Helicopontosphaera granulata Bukry and Percival, 1973, p. 37, pl. 6, figs. 1, 2, pl. 7, figs. 7, 8; Perch-Nielsen, 1977, partim, pl. 25, figs. 3–5, pl. 26, figs. 2, 4, non: pl. 25, figs. 1, 2, 6, pl. 26, fig. 6.

Helicosphaera granulata (Bukry and Percival) Jafar and Martini, 1975, p. 390; Haq and Berggren, 1978, pl. 2, fig. 9, 10.

Helicosphaera sp. aff. *H. granulata* (Bukry and Percival) Jafar and Martini, Haq and Berggren, 1978, pl. 2, figs. 11–12.

Remarks: In our material the helicoliths of *H. granulata* are consistently found in samples with preservational conditions unfavourable for helicospheres. In our opinion, *H. granulata* is a preservational form of other *Helicosphaera* species such as *H. carteri* and/or *H. paleocarteri*.

Occurrence: *H. granulata* is found at various levels in the Miocene and the Pliocene.

Helicosphaera hyalina Gaarder

Helicosphaera carteri (Wallich) Kamptner. Black, 1968, partim, pp. 801, 802, pl. 147, fig. 2, non: pl. 147, figs. 1, 3.

Helicosphaera hyalina Gaarder, 1970, pp. 113–119, figs. 1a–e, 2a–d, 3a; Gaarder and Hasle, 1971, figs. 9c, d, f; Conley, 1979, p. 29, pl. 1, fig. 20; Ellis and Lohman, 1979, pl. 3, fig. 11; Nishida, 1979, pl. 9, fig. 1.

Description: These small helicoliths have a symmetrically elliptical outline and a wing that terminates within the metapterygial side. The proximal plate is of type I.

The blanket is confined to the central area of the helicolith, leaving the periphery of the flange exposed distally.

Optical pattern: *H. hyalina* is weakly birefringent between crossed nicols. Its interference figure is of type I.

Differential diagnosis: *H. hyalina* is distinguished from *H. pavementum* by a larger wing which terminates at the metapterygial side.

Occurrence: Specimens with affinities to *H. hyalina* have been observed in samples from zone CN11. The species ranges up to the Recent.

Chapter 5

DISCOASTERS

INTRODUCTION

References to stellate nannoliths can be found in the very early micro-paleontological literature (e.g. Ehrenberg, 1854; Sorby, 1861; Jukes-Browne and Harrison, 1892; Haupt, 1906). The formal introduction of the calcareous "asterisks", however, is attributed to Tan Sin Hok (1926, 1927 and 1931) who was the first to speculate about their possible organic origin and who subsequently attempted to classify these nannoliths into genera.

Since the pioneering studies of Tan numerous "Discoaster" species have been introduced, many of which are excellent biostratigraphic markers.

Stradner contributed much to our knowledge of the discoasters by his tentative study in Stradner and Papp (1961). Although many of the figures do not represent the exact morphology of the species, his paper was the first to deal exclusively with the discoasters and it formed a useful basis for the further study of these nannoliths.

Prins (1971) presented the first detailed study of the morphological evolution of the asteroliths and discussed some of the nomenclatural problems caused by the generic definitions of Tan Sin Hok.

Romein (1979) revised the phylogeny of the Early Paleogene discoasters, basing his lineages mainly on the optical pattern of the asteroliths.

Our study of the discoaster associations from numerous land sections and D.S.D.P. cores revealed that these nannoliths can be separated into two major groups. These groups are regarded here as genera, firstly because they have profound structural differences and occur in different biostratigraphic intervals, and secondly because we can make use of the valid generic names which were originally introduced by Tan Sin Hok.

EMENDATION OF THE DISCOASTER GENERA INTRODUCED BY TAN SIN HOK

For the classification of the discoasters Tan used as diagnostic features (a) the outline (rosette-shaped or stellate) (b) the degree of differentiation of the segments and (c) the number of arms. Consequently, the genus *Eu-discoaster* was introduced to include all stellate discoasters with arms distinguished from each other "until the centre of the disc". *Helio-discoaster* included all rosette-shaped forms with non-separated segments. *Hemi-dis-*

coaster was used for discoasters with arms that have grown together “without joints” in groups of three.

The generic names *Helio-discoaster* and *Eu-discoaster* are retained here because the species, assigned to them by Tan, are discoasters with an essentially different structure. The diagnoses of these genera, however, are emended in order to disregard some preservational characteristics which were included by Tan in their original descriptions. *Hemi-discoaster* is rejected as being a preservational type of either of the two aforementioned genera (see also Bramlette and Riedel, 1954, pp. 394–395).

All discoasters consist of segments that are attached to each other along well-defined sutures. Whether or not these sutures are visible (*Eu-discoaster* versus *Helio-discoaster* sensu Tan) depends mainly on the state of preservation.

The shape and the relative position of the sutures of the central area of the discoasters are considered here to be the essential criteria for a generic classification of this group of nannoliths.

All discoasters with curved, hook-shaped or subradial sutures are assigned to the genus *Helio-discoaster* Tan emend., whereas discoasters with straight and radial sutures are ascribed to the genus *Eu-discoaster* Tan emend.

The chosen generic characters can be distinguished easily both in the light microscope and the electron microscope and the two genera are clearly separable in time. The asteroliths of *Helio-discoaster* are the dominant forms of the Paleogene. The asteroliths of *Eu-discoaster* (with the exception of *E. deflandrei*, *E. nonaradiatus* and *E. distinctus*) are confined to the Neogene.

A further subdivision of the genera into subgenera based on the characteristics and/or the position of the ornamentation (Prins, 1971) is not attempted here. In our opinion such criteria should be reserved for a classification at the species level or for a further grouping of the discoasters into informal groups. Moreover, a grouping of the asteroliths of *Helio-discoaster* based on whether or not they show extinction crosses (Romein, 1979) is avoided because forms with obvious morphological similarities may exhibit dissimilar optical properties.

STRUCTURE OF THE DISCOASTERS

All discoasters consist of wedge-shaped crystal elements (segments) arranged radially around an axis. The attachment of the segments results in sutures which are present on both faces of the central area of the asteroliths (central area: the part around the centre of an asterolith which is confined to a circle with a radius equal to the length of the sutures).

The segments may be confined entirely to the central area (rosette-shaped discoasters) or they may extend beyond it, producing free portions. The free portions of the segments (arms) may be simple pointed protrusions or they may be more elaborately shaped.

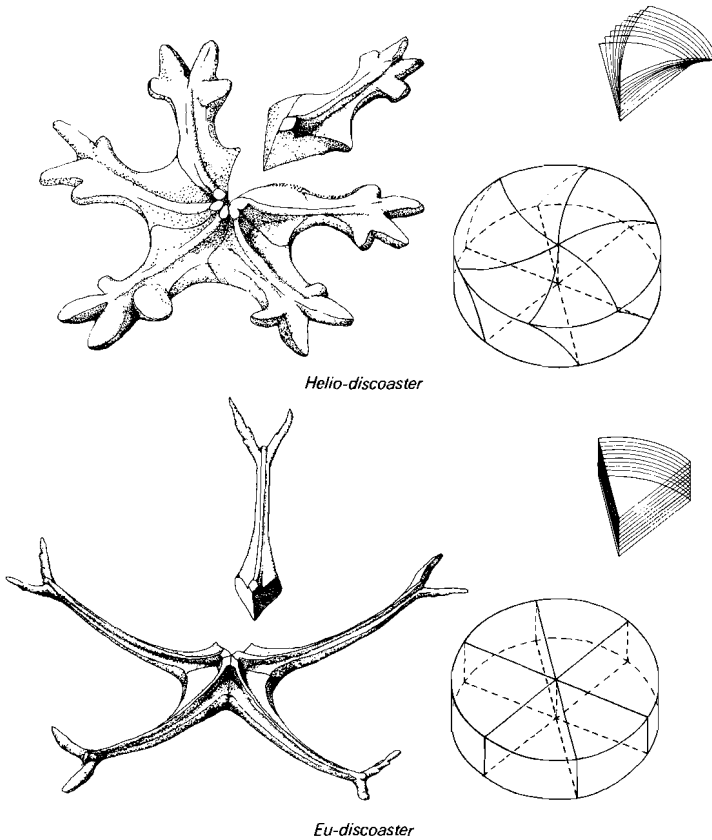


Fig. 63. Models of the discoasters of *Helio-discoaster* and *Eu-discoaster* showing their morphological differences. One segment of each discoaster has been removed to show the shape of the attachment surfaces.

Helio-discoaster Tan emended

The sutures of discoasters of this genus differ in shape and position when the two faces of the same asterolith are compared; they are curved, hook-shaped or subradial (tangential to some ill-defined central area) on one face (superior face) and straight or less curved on the opposite side (inferior face). Moreover, the two sets of sutures do not lie directly above each other. This

arrangement of the sutures can only be explained if we assume that the attachment surfaces of the segments are concave (or convex) (fig. 63). Such a shape of the attachment surface of the segments of *Helio-discoaster* leads to a slight imbrication of the adjoining segments and an increase of the overall area of attachment.

Eu-discoaster Tan emended

The asteroliths of *Eu-discoaster* possess straight sutures on both their faces. The corresponding sutures of the opposite faces are situated directly above each other. As a consequence the segments have flat attachment surfaces and lack imbrication (fig. 63).

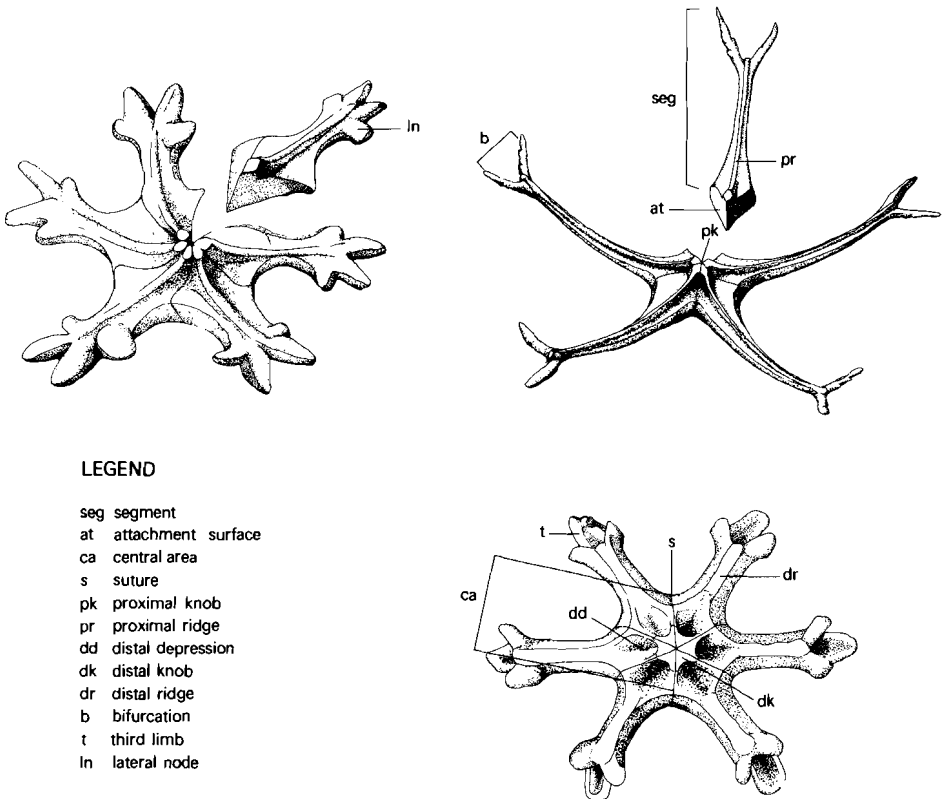


Fig. 64. Terminology of the discoasters.

TERMINOLOGY

For the description of the two sides (faces) of the discoasters of *Helio-discoaster* we use the terms “inferior” and “superior” of Stradner (in Stradner and Papp, 1961) to refer to the face (or view) of the asterolith with straight and with curved (or subradial) sutures respectively. These terms are not applicable to the discoasters of *Eu-discoaster* as they possess straight sutures on both their faces. In this case, the terms “proximal” and “distal” are used instead and they are defined as the concave and the convex side of the discoaster, respectively.

The meaning of some of the terms used in the description of the discoasters is presented in figure 64.

LINEAGES IN THE GENERA HELIO-DISCOASTER AND EU-DISCOASTER

In figures 65 and 66 the ranges of the discoasters have been arranged in groups of species with close morphological similarities. Each morphological group has been named after a representative species. A brief account of the common characteristics of the species in each group is given as a “diagnosis” of each group in the course of the taxonomic descriptions.

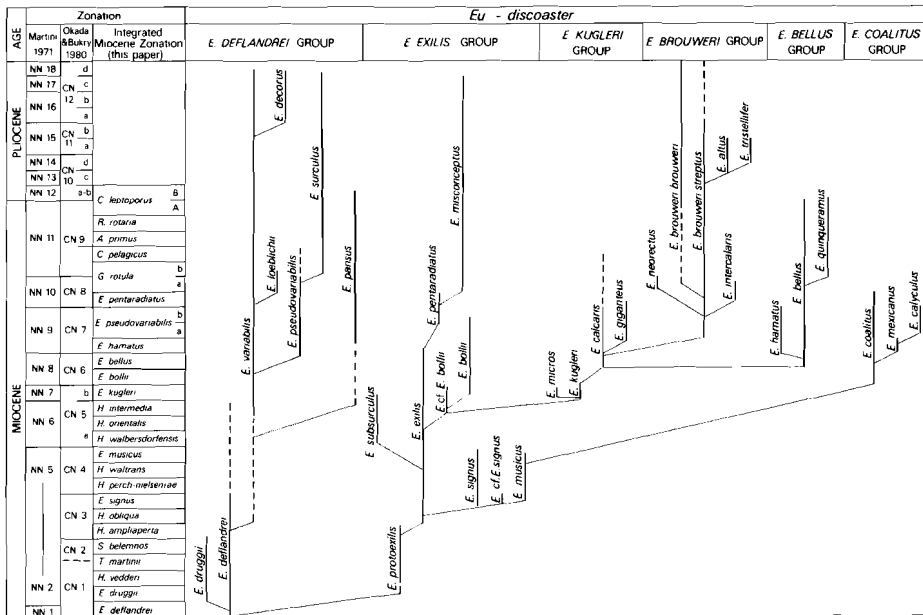


Fig. 65. Lineages in the genus *Eu-discoaster*.

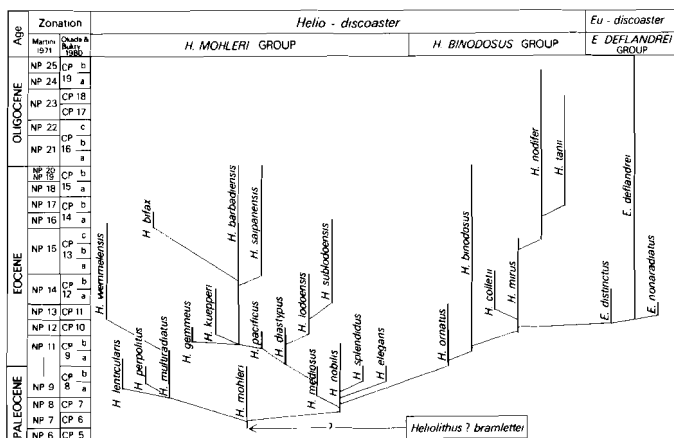


Fig. 66. Lineages in the genus *Helio-discoaster*.

TAXONOMY

Notation: The name *Discoaster* Tan has been replaced by *Eu-discoaster* Tan and *Helio-discoaster* Tan (Theodoridis, 1983). The name *discoaster* is retained here as a morphological term equivalent to *asterolith*.

Family EU-DISCOASTERACEAE Prins, 1971

Genus *Helio-discoaster* Tan Sin Hok, 1927, emended

Synonyms: *Discoasteroides* Bramlette and Sullivan, 1961. *Agalmatoaster* Klumpp, Prins, 1971. *Turbo-discoaster* Prins, 1971. *Radiodiscoaster* Prins, 1971.

Diagnosis: Asteroliths with curved, hooked or subradial sutures on at least one face of their central area.

Subdivision: *Helio-discoaster* is subdivided into the *H. mohleri* group and the *H. binodosus* group.

Type species: *Helio-discoaster barbadiensis* (Tan Sin Hok) Theodoridis, *Basionym:* *Discoaster barbadiensis* Tan Sin Hok, 1931.

HELIO-DISCOASTER MOHLERI GROUP

Diagnosis: Rosette-like asteroliths of *Helio-discoaster*, mostly multi-segmented. The free portions of the segments, when present, are tapering and pointed, without lateral ornamentation.

Helio-discoaster mohleri (Bukry and Percival) Theodoridis

(Pl. 28, figs. 1, 2)

- Discoaster gemmeus* Stradner, Hay and Mohler, 1967, p. 1538, pl. 204, figs. 19–21, pl. 205, figs. 1–3, pl. 206, figs. 3, 5, 6, 8; Haq, 1971, pp. 37, 38, pl. 12, fig. 5, pl. 13, figs. 1, 3, pl. 14, fig. 1.
- Discoaster mohleri* Bukry and Percival, 1971, p. 128, pl. 3, figs. 3–5; Kappelos and Schaub, 1973, p. 728, pl. 6, fig. 11; Haq and Lohmann, 1976, pl. 2, figs. 1, 2; Perch-Nielsen, 1977, pl. 13, figs. 3, 4, 8; Romein, 1979, pp. 160, 161, pl. 5, fig. 9.
- Radiodiscoaster *gemmeus gemmeus* (Stradner) Prins, 1971, pl. 3, fig. 12, pl. 7, figs. 7A–B. (Invalid combination, art. 33, 2 ICBN).
- Discoaster salisburgensis* Stradner, Kappelos 1973, p. 113, pl. 10, figs. 10, 11.
- Helio-discoaster mohleri* (Bukry and Percival) Theodoridis, 1983, p. 19.

Descriptions: *H. mohleri* consists of 9 to 19 segments without free portions.

The superior face of the asterolith is flat or slightly convex with a shallow depression and/or a pore usually present in the centre. The sutures are curved in the centre of this face but straighten out towards the periphery. The segments do not possess ridges on their superior face.

The inferior face is strongly convex to conical. As a rule, a well-defined depression appears at its centre. The segments possess median ridges on this face and they are separated from each other by straight sutures.

Differential diagnosis: The asteroliths of *H. mohleri* differ from those of *H. multiradiatus* in having a smaller number of segments and in being more conical in cross-section. The related *H. nobilis* is flatter and its segments extend further beyond the central area of the asterolith. *H. gemmeus* has a comparable morphology but it is more conical and its segments imbricate strongly in inferior view. Furthermore the latter species occurs at a higher stratigraphic interval.

Occurrence: From CP6 to CP8. It is common in sections Caravaca and Nahal Avdat.

Helio-discoaster nobilis (Martini) Theodoridis

(Pl. 28, figs. 5, 6)

- Discoaster nobilis* Martini, 1961, p. 11, pl. 2, fig. 23, pl. 5, fig. 51; Hay and Mohler, 1967, p. 1538, pl. 204, fig. 16, pl. 205, figs. 6–9; Haq and Lohmann, 1976, pl. 2, fig. 7.
- Discoaster falcatus* Bramlette and Sullivan, 1961, p. 159, pl. 11, figs. 14a, b, 15; Sullivan, 1964, p. 190, pl. 11, figs. 10–12; Kappelos, 1973, p. 111, pl. 11, fig. 12, pl. 6, fig. 11.
- Discoaster lubinaensis* Bystrická, 1966, p. 237, figs. 1–3.
- Discoaster* sp. aff. *D. mediosus* Bramlette and Sullivan, Haq and Lohmann, 1976, pl. 2, fig. 8.
- Discoaster* sp. aff. *D. falcatus* Bramlette and Sullivan, Haq and Lohmann, 1976, pl. 5, figs. 10, 11.
- Helio-discoaster nobilis* (Martini) Theodoridis, 1983, p. 20.

Description: The asteroliths of this species are almost flat and consist of

7 to 13 segments. The segments have free portions which extend well beyond the central area. The tips of the free portions may be blunt or pointed. The sutures are deeply incised on both faces of the central area.

On the superior face the sutures curve in an anticlockwise direction. A shallow depression has been observed occasionally at the centre of the inferior face. Well-preserved specimens have depressions also along the median axis of each segment in the inferior face, which leads to the morphology of *D. falcatus*.

Differential diagnosis: Specimens with a morphology intermediate between *H. mohleri* and *H. nobilis* are common in the interval in which the ranges of the two species overlap. *H. nobilis* is flatter, and its segments have longer free portions than those of *H. mohleri*. Furthermore, the curvature of the sutures of *H. nobilis* is stronger and can be observed on the whole surface of the central area in the superior face. The sutures on the same face of the central area of *H. mohleri* are straighter and curve only at the very centre.

Occurrence: *H. nobilis* ranges within the interval from zone CP7 to CP9a.

Helio-discoaster mediusus (Bramlette and Sullivan) Theodoridis (Pl. 28, figs. 7–9)

Discoaster mediusus Bramlette and Sullivan, 1961, p. 161, pl. 12, figs. 7, 8; Hay and Mohler, 1967, p. 1539, pl. 204, figs. 17, 18, pl. 206, fig. 2; Kapellos, 1973, pl. 7, figs. 7, 8, pl. 9, fig. 3, pl. 10, figs. 8, 9; Haq and Lohmann, 1976, pl. 2, fig. 11, Müller, 1979, pl. 1, fig. 5.

Helio-discoaster mediusus (Bramlette and Sullivan) Theodoridis, 1983, p. 19.

Description: The asteroliths of *H. mediusus* consist of 7 to 12 segments which terminate in short and blunt free portions. The interray areas are U-shaped.

On their inferior face, the segments are ornamented with characteristic depressions along their median axis. As a consequence, ridges are present along the sutures between adjacent segments (sutural ridges). A circle of nodes surrounds the centre of the asterolith.

On their superior face the segments bear ridges along their median axis. The sutures of the superior face are curved only at the centre of the asterolith. At the position of curvature a low knob-like protuberance may be present.

Differential diagnosis: *Helio-discoaster mediusus* has very characteristic U-shaped interray areas and segments with parallel-sided free portions by which it can easily be differentiated from the related *H. nobilis*. *H. elegans* and *H. splendidus* exhibit V-shaped interray areas and the free portions of their segments are pointed.

Occurrence: This species is restricted to zone CP8 in sections Nahal Avdat and Caravaca.

Helio-discoaster splendidus (Martini) Theodoridis

Discoaster splendidus Martini, 1960, p. 80, pl. 10, figs. 25, 26, 29; Martini, 1961, p. 11, pl. 2, fig. 21.
Discoaster helianthus Bramlette and Sullivan, 1961, p. 160, pl. 11, figs. 18a, b; Sullivan, 1965, p. 42, pl. 10, fig. 7; Kapellos, 1973, p. 112, pl. 4, figs. 2, 3; Haq and Lohmann, 1976, pl. 2, fig. 12; Wise and Wind, 1977, pl. 17, fig. 6.

Helio-discoaster splendidus (Martini) Theodoridis, 1983, p. 20.

Description: The asteroliths of this species consist of 8 to 15 segments with short and pointed free portions. The interray areas are V-shaped.

Deep depressions can be observed along the median axis of each segment in the inferior face. A broad circle of nodes surrounds the centre of this face.

Differential diagnosis: *H. splendidus* differs from *H. mediosus* in having a circle of nodes of a larger diameter, V-shaped interray areas and pointed free portions of segments.

The asteroliths of *H. elegans* can be differentiated from those of *H. splendidus* only in an inferior view. In that view *H. elegans* shows a prominent knob instead of a circle of nodes and its depressions are ornamented by concentric arrays of nodes.

Occurrence: *H. splendidus* ranges within subzone CP8b

Helio-discoaster elegans (Bramlette and Sullivan) Theodoridis (Pl. 28, figs. 10–12)

Discoaster elegans Bramlette and Sullivan, 1961, p. 159, pl. 11, figs. 16a, b; Black, 1968, pl. 153, fig. 2; Perch-Nielsen, 1971, p. 63, pl. 51, figs. 2, 3; Haq and Lohmann, 1976, pl. 5, fig. 3; Müller, 1979, pl. 4, figs. 3, 4, 6.

Discoaster stradneri Martini, 1961, p. 10, pl. 2, fig. 22, pl. 5, fig. 52.

Discoaster limbatus Bramlette and Sullivan, 1961, p. 160, pl. 12, figs. 3a, b; Sullivan, 1965, p. 42, pl. 10, figs. 8, 9; Haq and Lohmann, 1976, pl. 2, fig. 10.

Discoaster boulangeri Lézaud, 1968, p. 23, pl. 1, figs. 9–12, pl. 2, fig. 14; Perch-Nielsen, 1971, p. 62, pl. 52, fig. 1.

Helio-discoaster elegans (Bramlette and Sullivan) Theodoridis, 1983, p. 19.

Description: The discoasters of this species consist of 8 to 15 segments with short and pointed free portions. The segments are caved with deep depressions flanked by sutural ridges on their inferior face. The central area may be ornamented by concentric arrays of nodes or ridges. In the centre of this face the segments bend and form a slender but prominent knob. The knob portions of the segments often show grooves which are in continuity with the corresponding depressions. The knob portions do not imbricate in inferior view.

The superior face of *H. elegans* bears a low central knob and it is often ornamented by shallow pits. On this face, the sutures are subradial and curve strongly near the centre of the central area. The segments show ridges with flat crests.

Differential diagnosis: *Helio-discoaster elegans* possesses a very characteristic ornamentation by which it can easily be distinguished from related species such as *H. mediosus* and *H. splendidus*.

Occurrence: This species occurs in subzone CP8b.

Helio-discoaster multiradiatus (Bramlette and Riedel) Theodoridis (Pl. 28, fig. 3)

Discoaster multiradiatus Bramlette and Riedel, 1954, p. 396, pl. 38, fig. 10; Bramlette and Sullivan, 1961, p. 161, pl. 12, fig. 10; Sullivan, 1965, p. 43, pl. 10, figs. 13, 15; Hay and Mohler, 1967, p. 1539, pl. 204, fig. 22, pl. 206, figs. 1, 4, 7; Kapellos, 1973, pp. 112, 113, pl. 3, figs. 10–12, pl. 5, fig. 1, pl. 6, figs. 4, 5, pl. 8, fig. 8, pl. 24, fig. 1, pl. 25, figs. 5, 6, pl. 28, fig. 6, pl. 38, fig. 1; Kapellos and Schaub, 1973, p. 728, pl. 2, fig. 3, pl. 7, fig. 6, pl. 8, fig. 1, pl. 11, fig. 12, pl. 10, fig. 7; Haq and Lohmann, 1976, pl. 2, figs. 4–6; Wise and Wind, 1977, pl. 17, fig. 2; Romein, 1979, pp. 165, 166, pl. 6, figs. 1–3.

Helio-discoaster multiradiatus (Bramlette and Riedel) Theodoridis, 1983, p. 19.

Description: The number of segments varies greatly (16 to 35). The segments exhibit no free portions. They are flat and imbricate dextrally in inferior view. At the centre of the inferior face a depression of variable diameter is present. Whether the inferior face is convex or concave depends on the diameter of this depression. The superior face is concave to flat and at the centre; it bears a short knob that results from the extension of the segments in a direction perpendicular to the disc.

Occurrence: *H. multiradiatus* is restricted to zones CP8 and CP9a.

Helio-discoaster lenticularis (Bramlette and Sullivan) Theodoridis

Discoaster lenticularis Bramlette and Sullivan, 1961, p. 160, pl. 12, figs. 1, 2; Sullivan, 1964, p. 191, pl. 11, fig. 1; Sullivan, 1965, p. 42, pl. 10, fig. 10.

Discoaster sp. Edwards and Perch-Nielsen, 1975, pl. 4, fig. 3.

Helio-discoaster lenticularis (Bramlette and Sullivan) Theodoridis, 1983, p. 19.

Description: The asteroliths are small (5–8 microns) and consist of 18 to 27 segments which lack free portions. A low central knob is present on both faces of the disc.

Occurrence: This species is confined to zones CP8 and CP9.

Helio-discoaster perpolitus (Martini) Theodoridis

Discoaster perpolitus Martini, 1961, p. 9, pl. 2, fig. 20, pl. 5, fig. 50; Sullivan, 1965, p. 43, pl. 10, fig. 12; Romein, 1979, p. 167, pl. 6, fig. 4.

Discoaster multiradiatus Bramlette and Riedel var., Bramlette and Sullivan, 1961, p. 162, pl. 12, fig. 11.

Discoaster elegans Bramlette and Sullivan, Perch-Nielsen, 1972, pl. 14, fig. 6.

Helio-discoaster perpolitus (Martini) Theodoridis, 1983, p. 20.

Description: The discoasters of *H. perpolitus* consist of 17 to 32 segments which lack free portions. Each segment is thinner along its median axis due to an elongated depression on its inferior face. Very often a faint ornamentation of concentric ridges is visible. A small knob is present at the centre of the inferior face.

The superior face of this species has not been observed.

Differential diagnosis: *Helio-discoaster perpolitus* differs from *H. multiradiatus* in being ornamented by concentric ridges on the inferior face. This ornamentation is observed also on the inferior face of asteroliths such as *H. elegans* and *H. kuepperi*. These species can be easily distinguished by their different outline, smaller number of segments and pronounced stems.

Occurrence: This species was rare in our sections. It has been recorded in zone CP8 of the sections Caravaca and Nahal Avdat.

Helio-discoaster wemmelensis (Achuthan and Stradner) Theodoridis

Discoaster wemmelensis Achuthan and Stradner, 1967, p. 5, pl. 4, figs. 3, 4, text-fig. 2; Perch-Nielsen, 1971, p. 65, pl. 2, figs. 1, 2, pl. 53, figs. 5, 6; Perch-Nielsen, 1977, pl. 14,

Radiodiscoaster wemmelensis (Achuthan and Stradner) Prins, 1971, pl. 3, fig. 14. Invalid: ICBN art. 33, 2.

Helio-discoaster wemmelensis (Achuthan and Stradner) Theodoridis, 1983, p. 20.

Description: The asteroliths of *H. wemmelensis* consist of 20 to 25 segments without free portions. The inferior face of the asteroliths has a large knob that covers almost two thirds of the disc. The knob has a concave surface.

Differential diagnosis: *H. wemmelensis* is distinguished from *H. multiradiatus* by the smaller size and by the large knob on its inferior face.

Occurrence: This species ranges from CP11 to CP14.

Helio-discoaster diastypus (Bramlette and Sullivan) Theodoridis (Pl. 29, figs. 1–3)

Discoaster diastypus Bramlette and Sullivan, 1961, p. 159, pl. 11, figs. 6–8; Perch-Nielsen, 1971, p. 62, pl. 51, figs. 8–10; Haq and Lohmann, 1976, pl. 5, fig. 12.

Discoaster aff. *D. diastypus* Bramlette and Sullivan, 1961, p. 159, pl. 11, figs. 9, 10.

Helio-discoaster diastypus (Bramlette and Sullivan) Theodoridis, 1983, p. 19.

Description: The number of segments varies from 9 to 17. The segments possess only one sutural ridge on the right side of their inferior face. The tips

of the segments of some specimens point in anticlockwise direction (in inferior view). Around the centre of the asterolith, elevated portions of each segment join each other to form a tube. The tube portions of the segments imbricate dextrally.

In superior view the segments show ridges close to their median axis. The segments show a strong imbrication at the centre of the superior face, where they form a knob with a narrow pore. The knob of the superior face has a smaller diameter and a narrower pore than the tube on the inferior face.

Differential diagnosis: *Helio-discoaster diastypus* is the first species of this group with sutural ridges on only one side of the segments and in that aspect it differs from all earlier forms such as *H. mediosus*, *H. splendidus* and *H. elegans*. Furthermore, it possesses well-defined knobs on both faces of its asteroliths.

Occurrence: *H. diastypus* occur in zones CP9 and CP10.

Helio-discoaster pacificus (Haq) Theodoridis

Discoaster pacificus Haq, 1969, p. 11, pl. 4, figs. 4–7, text-fig. 3.

Helio-discoaster pacificus (Haq) Theodoridis, 1983, p. 20.

Description: The discoasters of *H. pacificus* consist of 11 to 15 segments with relatively long and often pointed free portions. In the inferior face the segments extend vertically near the centre of the asterolith and form a hollow knob. The knob portions of the segments show a dextral imbrication in this view. Blade-like ridges can be observed on the inferior faces of the segments. The ridges occur on the right of the median axis of the segments in inferior view. A knob with smaller diameter is present at the centre of the superior faces of the asterolith.

Differential diagnosis: *H. pacificus* can be differentiated from *H. diastypus* by the longer and more straight free portions of the segments and by the smaller diameter of its knobs. It resembles very closely *H. diastypus*, however, and differentiation of atypical specimens of the two species is not always possible.

Occurrence: This species has been recorded in zones CP9 and CP10.

Helio-discoaster barbadiensis (Tan) Theodoridis

(Pl. 29, figs. 4–8)

“Kalkerdige Krystaldrusen” Ehrenberg, 1854, p. 155, pl. 24, fig. 67, pl. 25, figs. 13–15.

“Crystalloids” Jukes-Browne and Harrison, 1892, p. 178, text-figs. 4–6.

Discoaster barbadiensis Tan, 1927, p. 119 invalid (ICBN art. 43.1)

Discoaster barbadiensis Tan, 1931, p. 93; Bramlette and Riedel, 1954, p. 398, pl. 39, figs. 5a–b;

Stradner, 1958, p. 183, fig. 11; Martini, 1958, p. 366, pl. 5, figs. 24a–c; Bramlette and Sullivan, 1961, p. 158, pl. 11, fig. 2; Stradner and Papp, 1961, p. 95, pl. 28, figs. 1, 2, text-figs. 9/7, 18/6, 24/3; Hay and Towe, 1962, p. 515, pl. 10, figs. 3, 5; Sullivan, 1965, p. 41; Levin and Joerger, 1967, p. 172, pl. 3, figs. 17a–b; Haq, 1967, p. 63, pl. 7, figs. 1, 2; Black, 1968, pl. 153, fig. 3; Haq, 1969, pp. 6, 7, pl. 3, figs. 4–7, text-fig. 1A; Perch-Nielsen, 1971, p. 61, pl. 51, fig. 5; Müller, 1974, pl. 6, fig. 10; Müller, 1979, pl. 4, figs. 1, 2; Romein, 1979, pp. 168, 169, pl. 7, fig. 1.

Helio-discoaster barbadiensis (Tan) Theodoridis, 1983, p. 19.

Description: The number of segments varies from 11 to 20. The segments have very short, pointed free portions and longitudinal ridges on both their faces. In the centre of the inferior face the segments bend perpendicular to the surface of the asterolith to form a long and slender stem.

A smaller knob-like protrusion is present at the centre of the superior face of the asterolith.

Occurrence: The first occurrence of *H. barbadiensis* was recorded in our sections in zone CP9. The last occurrence of this species as reported by Bukry (1973) is in zone CP15b.

Helio-discoaster gemmeus (Stradner) Theodoridis (Pl. 28, fig. 4)

Discoaster gemmeus Stradner, 1959, p. 1086, text-fig. 21; Müller, 1974, pl. 6, figs. 1–3.

Discoaster robustus Haq, 1969, p. 12, pl. 5, fig. 7, text-fig. 1c; Haq and Lohmann, 1976, pl. 5, figs. 4, 5; Wise and Wind, 1977, pl. 17, fig. 1.

Helio-discoaster gemmeus (Stradner) Theodoridis, 1983, p. 19.

Description: The asterolith consists of 8 to 11 thick segments that form a pyramid-like construction. In the inferior face the segments imbricate dextrally. The segments do not possess free portions.

Differential diagnosis: *H. mohleri* is comparable to *H. gemmeus*. This first species, however, possesses larger asteroliths with more segments but there is no imbrication of its segments in the inferior face. The differentiation of the two taxa is facilitated by their different stratigraphic range.

Remarks: In his description of the species, Stradner referred to the conical shape of the asteroliths. Furthermore he correctly attributed the gleaming emerald colour of the asteroliths to their robustness. These characteristics, in addition to the number of segments and the identical biostratigraphic range of *H. gemmeus* and *H. robustus* (Haq), indicate that the latter species should be considered as a junior synonym of *H. gemmeus*.

Occurrence: *H. gemmeus* is restricted to zones CP9 and CP10.

Helio-discoaster kuepperi (Stradner) Theodoridis (Pl. 29, figs. 9–13)

Discoaster kuepperi Stradner, 1959, p. 478, figs. 17–21; Martini, 1961, p. 14, pl. 3, fig. 29; Stradner

and Papp, 1961, p. 93, pl. 27, figs. 1–6, text-figs. 9/6, 16; Perch-Nielsen, 1971, p. 64, pl. 51, figs. 6, 7, 9, 11, 12; Perch-Nielsen, 1972, pl. 13, figs. 5, 6.

Discoasteroides kuepperi (Stradner) Bramlette and Sullivan, 1961, p. 163, pl. 13, figs. 16–19; Hay and Towe, 1962, p. 515, pl. 10, fig. 1; Sullivan, 1965, p. 44; Haq, 1967, p. 62, pl. 4, figs. 1–6; Haq, 1968, p. 47, pl. 10, fig. 6; Kapellos, 1973, p. 114, pl. 14, figs. 10–12, pl. 15, fig. 7, pl. 29, fig. 4; Haq and Lohmann, 1976, pl. 6, fig. 3; Haq, 1969, pp. 15, 16, pl. 3, figs. 1–3.

Helio-discoaster kuepperi (Stradner) Theodoridis, 1983, p. 19.

Description: The asteroliths of this species are composed of 8 to 10 petaloid segments. The segments have short and pointed free portions. In inferior view the segments show depressions on their surface and they are often ornamented by concentric ridges. On the same face a large stem is present at the centre of the asterolith. The tip of the stem flares outwards to form a funnel-like structure. The portions of the segments that form this stem extend helicoidally around an axis perpendicular to the surface of the asterolith. As a result, the sutures on the funnel-like tip of the stem are offset to the right relative to the sutures of the central area.

The sutures on the superior face of the asterolith are curved in anticlockwise direction. A small knob is present at the centre of this face.

Occurrence: From zone CP10 to zone CP12.

Helio-discoaster lodoensis (Bramlette and Riedel) Theodoridis (Pl. 30, figs. 4–6)

Discoaster lodoensis Bramlette and Riedel, 1954, p. 398, pl. 39, figs. 3a, b; Stradner, 1958, p. 182, fig. 8; Martini, 1958, p. 366, pl. 6, figs. 28a–d; Stradner, 1959, p. 1083, fig. 5; Martini, 1961, p. 11; Bramlette and Sullivan, 1961, p. 161, pl. 12, figs. 4, 5; Stradner and Papp, 1961, p. 92, pl. 25, 26, text-figs. 9/3, 24/9; Hay and Towe, 1962, p. 514, pl. 10, figs. 2, 4, 6; Sullivan, 1965, p. 42, pl. 10, fig. 14; Black, 1965, fig. 20; Haq, 1967, p. 63, pl. 7, figs. 3, 6, 7; Haq, 1969, p. 10, pl. 2, figs. 1–4, text-figs. 4e–g; Kapellos, 1973, p. 112, pl. 12, figs. 1–12, pl. 15, fig. 3, pl. 16, figs. 1–3, pl. 27, fig. 2, pl. 28, figs. 1, 2, pl. 29, fig. 1; Müller, 1974, pl. 6, fig. 11; Haq and Lohmann, 1976, pl. 5, figs. 8, 9; Müller, 1979, pl. 4, figs. 7–9.

Helio-discoaster lodoensis (Bramlette and Riedel) Theodoridis, 1983, p. 19.

Description: The number of segments varies from 5 to 7. The segments terminate in long and pointed free portions. The free portions of the segments curve sinistrally when the specimens are observed from their inferior side. On the inferior face the segments show ridges along their right sides. The ridges extend to the tips of the free portions. At the centre of the inferior face the ridges meet to form a knob. A less pronounced knob can be seen on the superior face.

Differential diagnosis: *H. lodoensis* is easily distinguished from *H. sublo-doensis* by the generally larger size and the curved free portions of its segments.

Occurrence: *H. lodoensis* has been recorded in our sections from zone CP10 to zone CP13.

Helio-discoaster sublodoensis (Bramlette and Sullivan)
Theodoridis

Discoaster sublodoensis Bramlette and Sullivan, 1961, p. 162, pl. 12, figs. 6a, b; Sullivan, 1965, p. 43, pl. 10, fig. 11; Haq, 1967, p. 63, pl. 8, figs. 1–3; Haq, 1969, pp. 13, 14, pl. 5, fig. 3; Kapellos, 1973, p. 113, pl. 15, fig. 4, pl. 17, figs. 1–4, 8; Perch-Nielsen, 1977, pl. 14, figs. 11, 12.

Discoaster strictus Stradner, 1961, p. 85, text-fig. 80; Black, 1968, pl. 153, fig. 5.

Helio-discoaster sublodoensis (Bramlette and Sullivan) Theodoridis, 1983, p. 20.

Description: The asterolith consists of 5, or more rarely of 6 segments with long and pointed free portions. In inferior view a ridge can be observed on the right side of each segment. In superior view ridges are seen along the median axes of the segments. A knob is present on each side of the asterolith but the one on the inferior face is more pronounced.

Differential diagnosis: *H. sublodoensis* is distinguished from *H. lodoensis* by the smaller size and the more pointed and straight free portions of its segments.

Occurrence: This species ranges from CP12 to CP14.

Helio-discoaster saipanensis (Bramlette and Riedel) Theodoridis
(Pl. 30, figs. 1–3)

Discoaster saipanensis Bramlette and Riedel, 1954, p. 398, pl. 39, fig. 4; Stradner and Papp, 1961, p. 90, pl. 22, figs. 5–7, 9, text-fig. 9/5; Perch-Nielsen, 1971, p. 65, pl. 51, fig. 4, pl. 52, fig. 4; Bukry, 1974, fig. 6; Haq and Lohmann, 1976, pl. 6, fig. 4; Wise and Wind, 1977, pl. 17, figs. 3–5.

Helio-discoaster saipanensis (Bramlette and Riedel) Theodoridis, 1983, p. 20.

Remarks: The asteroliths of this species are similar to those of *H. barbadiensis* but they possess fewer segments (7 to 9) and the free portions of the segments are much more pointed. The two species closely resemble each other and the possibility that *H. saipanensis* might be no more than a variant of *H. barbadiensis* cannot be ruled out.

Occurrence: Bukry (1971) presented a range for *H. saipanensis* from CP12b to CP15b. The first occurrence of this species in subzone CP12b was confirmed in section Aspe.

Helio-discoaster bifax (Bukry) Theodoridis

Discoaster bifax Bukry, 1971, p. 313, pl. 3, figs. 6–11; Perch-Nielsen, 1977, pl. 14, figs. 2, 8, 9.

Helio-discoaster bifax (Bukry) Theodoridis, 1983, p. 19.

Description: The asteroliths of this species are concavo-convex and consist of 13 to 19 segments without free portions. The centre of the convex face is ornamented by a broad funnel-like knob. A small stem is present in the centre of the concave face.

Occurrence: This species is confined to zone CP14.

HELIO-DISCOASTER BINODOSUS GROUP

Diagnosis: Asteroliths of *Helio-discoaster* type with well-developed and usually parallel-sided arms. The arms often bear lateral ornamentation.

Helio-discoaster ornatus (Stradner) Theodoridis (Pl. 31, figs. 1, 2)

Discoaster ornatus Stradner, 1958, p. 188, fig. 38.

Discoaster geometricus Brönnimann and Stradner, 1960, p. 366, figs. 4, 5.

Discoaster binodosus Martini, Kapellos and Schaub, 1973, partim, pl. 9, fig. 9, non: pl. 9, fig. 8.

Helio-discoaster ornatus (Stradner) Theodoridis, 1983, p. 20.

Description: The asteroliths consist of 5 to 9 segments with long and pointed free portions. The free portions are widest at about half their length and are thicker along their median axis. The interray areas are deep and U-shaped. In the superior face the sutures curve in anticlockwise direction. The central area of this face shows a large knob with a diameter which is almost equal to that of the central area.

The suture of the inferior face may be slightly curved. A low central knob with a small diameter may be present.

Differential diagnosis: *Helio-discoaster ornatus* differs from *H. binodosus* by its more robust shape and the lack of knobs along the sides of its free portions.

Occurrence: *H. ornatus* occurs from zone CP9 to zone CP11.

Helio-discoaster binodosus (Martini) Theodoridis, emended

Discoaster binodosus Martini, 1958, pp. 361, 262, pl. 4, figs. 18a, b, 19a, b; Stradner, 1959, p. 1085, figs. 18, 19; Bramlette and Sullivan, 1961, p. 158, pl. 11, figs. 1a, b; Martini, 1961, p. 12, pl. 3, fig. 25; Stradner and Papp, 1961, pp. 66, 67, pl. 4, figs. 1, 7, pl. 5, figs. 1–6, text-fig. 8/4; Sullivan, 1965, p. 41; Levin and Joerger, 1967, p. 172, pl. 3, figs. 18a, 18b; Perch-Nielsen, 1967, p. 30, pl. 7, figs. 1–7, 9; Kapellos, 1973, pl. 6, fig. 12, pl. 7, fig. 9–11, figs. 1, 2, 4; Kapellos and Schaub, 1973, partim, pl. 9, fig. 8, non: pl. 9, fig. 9; Haq and Lohmann, 1976, pl. 6, figs. 1, 2; Romein, 1979, p. 163, pl. 7, fig. 2.

Discoaster tanii Bramlette and Riedel; Deflandre, 1968, partim, pp. 44, 45, pl. 11, fig. 15, non: pl. 11, figs. 13, 14, 16, 17.

Discoaster binodosus binodosus Martini, 1958, p. 362, pl. 4, fig. 18; Perch-Nielsen, 1971, p. 61, pl. 52, fig. 5.

Discoaster binodosus hirundinus Martini, 1958, partim, p. 362, pl. 4, fig. 19a, non: pl. 4, fig. 19b; Perch-Nielsen, 1971, p. 62, pl. 52, fig. 7.

Helio-discoaster binodosus (Martini) Theodoridis, 1983, p. 19.

Description: The asterolith consists of 7 to 9 segments with a wide central area, and relatively short and tapering arms. The interray areas are characteristically round. A shallow notch may or may not be present at the tip of

each arm. Specimens with some of their arms notched and others pointed are common. Each arm bears at least one pair of lateral nodes which are placed opposite each other and away from the tip of the arm. The nodes of the adjacent arms of multisegmented variants often touch each other. The sutures on the superior face are strongly curved in anticlockwise direction; almost the entire central area is covered by a large knob.

The sutures on the inferior face are straight and often subradial. A central knob with small diameter may be present at this side.

Differential diagnosis: Features useful for the differentiation of *H. binodosus* from *H. tanii* and *H. nodifer* are: the large diameter of the central area in relation to the length of the arms, the slender arms and the larger diameter of the central knob of the superior face.

Moreover, *H. tanii* and *H. nodifer* possess lateral blade-like protrusions close to the tips of the arms but not robust nodes far from the arm-tips as in *H. binodosus*.

Helio-discoaster mirus has a comparably large central area but short arms with lateral-blades at their tips.

Emendation: The definition of the species is emended to include astero-liths with or without notches at the tips of the arms.

Remarks: The presence or absence of notches at the tips of the arms of *H. binodosus* is not regarded as a reliable characteristic for specific (*H. binodosus* vs. *H. tanii* and *H. nodifer*) or intraspecific (*H. binodosus binodosus* vs. *H. binodosus hirundinus*) differentiation.

Although the majority of the specimens of *H. tanii* and *H. nodifer* exhibit deeper notches than the individuals of *H. binodosus*, the depth of the notches is variable for all these taxa, and variants without notches at the arm tips are common for each species.

Occurrence: *H. binodosus* ranges from zone CP9 to zone CP15.

Helio-discoaster mirus (Deflandre) Theodoridis, emended (Pl. 31, figs. 3–5)

Discoaster mirus Deflandre in Grassé, 1952, p. 465, fig. 362; Deflandre, 1954, p. 168, fig. 118; Kapellos, 1973, p. 112, pl. 18, figs. 8, 11; Martini, 1961, p. 12, pl. 3, fig. 24; Müller, 1979, pl. 4, figs. 10, 11.

Discoaster monstratus Martini, 1961, p. 12, pl. 3, fig. 26, pl. 5, fig. 53.

Discoaster gemmifer Stradner, 1961, p. 86, fig. 83; Stradner and Papp, 1961, partim, pp. 69–71, pl. 24, fig. 6, table 9, figs. 2–5, text-fig. 8/6, non: pl. 24, figs. 4, 5, table 9, fig. 1; Perch-Nielsen, 1971, pp. 63, 64, pl. 53, figs. 3, 4.

Discoaster nonaradiatus Klumpp, Sullivan, 1965, p. 43, pl. 10, fig. 6; Perch-Nielsen, 1971, pp. 64, 65, pl. 52, fig. 8.

Discoaster deflandrei Bramlette and Riedel; Black, 1968, pl. 153, fig. 6.

Discoaster distinctus Martini; Kapellos, 1973, partim, pl. 14, figs. 7–9, pl. 18, fig. 7, non: pl. 9, fig. 12, pl. 13, fig. 9, pl. 21, fig. 3, pl. 22, fig. 11, pl. 27, fig. 4; Kapellos and Schaub, 1973, partim, pl. 5, figs. 3, 4, non: pl. 2, fig. 5, pl. 8, fig. 5.

Helio-discoaster mirus (Deflandre) Theodoridis, 1983, p. 19.

Description: The number of segments of the asteroliths of this species varies from 5 to 10. The central area is large in relation to the arms. The arms are short, broaden towards their tips and bifurcate because of a shallow notch. The bifurcations are short, pointed and possess lateral blade-like extensions.

The sutures on the superior face are curved or hooked in anticlockwise direction. At the centre of the same face a pronounced knob is present.

Exceptionally well-preserved specimens show superior faces ornamented by nodes. The nodes are arranged in rows that radiate from the centre of the asterolith towards the tips of the arms.

On the inferior face the sutures may be slightly curved and a small central knob may be present occasionally.

Differential diagnosis: The asteroliths of *H. mirus* and *H. binodosus* are comparable in having large central areas and relatively short arms. *H. mirus* differs from *H. binodosus* in having lateral blades close to the tip of the arms. Furthermore, the knob of the superior face of *H. mirus*, if present at all, is smaller than the equivalent structure of *H. binodosus*.

Emendation: We emend the definition of this species to confine it to specimens with curved or hooked sutures.

Remarks: In the original description of *Helio-discoaster mirus* no mention is made about the shape of the sutures. The emendation was prompted in order to avoid confusion of this species with closely similar species of *Eudiscoaster* such as *E. deflandrei* and *E. distinctus*.

Occurrence: *H. mirus* ranges from zone CP10 to zone CP13.

Helio-discoaster colletii (Parejas) Theodoridis (Pl. 30, figs. 7, 8)

Discoaster colleti Parejas, 1939, fide Stradner, 1959, p. 478, figs. 30–32; Stradner and Papp, 1961, p. 78, pl. 13, figs. 1–6, text-figs. 8/15, 24/8.

Helio-discoaster colletii (Parejas) Theodoridis, 1983, p. 19.

Remarks: The taxonomic status of this species is questionable since it might be a preservational artefact. It probably represents heavily overgrown specimens of *H. mirus*.

Occurrence: This species has been recorded in the interval from zone CP11 to zone CP13.

Helio-discoaster tanii (Bramlette and Riedel) Theodoridis,
emended
(Pl. 31, figs. 8–10)

Discoaster tanii Bramlette and Riedel, 1954, p. 397, pl. 39, figs. 19a, b; Martini, 1958, p. 359, table 3, figs. 13a, b; Stradner, 1959, p. 479, text-figs. 43, 44; Martini, 1960, p. 78, table 9, figs. 18, 19; Deflandre, 1968, partim, pp. 44, 45, pl. 11, figs. 16, 17, non: pl. 11, figs. 13–15; Kapellos, 1973, p. 114, pl. 23, fig. 1; Bukry, 1973, pl. 5, figs. 4–6.

Discoaster tanii ornatus Bramlette and Wilcoxon, 1967, p. 112, pl. 7, figs. 7, 8.

Discoaster tanii nodifer Bramlette and Riedel; Stradner and Papp, 1961, p. 83, text-figs. 7/12, 8/19;

Roth, 1970, p. 868, pl. 12, fig. 4; Kapellos, 1973, partim, p. 114, pl. 23, fig. 2, non: pl. 23, fig. 3.

Discoaster aff. *D. tanii nodifer* Bramlette and Riedel; Haq and Lohmann, 1976, pl. 5, fig. 6.

Helio-discoaster tanii (Bramlette and Riedel) Theodoridis, 1983, p. 20.

Description: *H. tanii* consists of 3 to 5 segments that terminate in long and rather robust arms. The central area is small in relation to the length of the arms. The arms may be notched at their tips or they may terminate bluntly. The sides of the arms are ornamented by blade-like protrusions of variable shape. The blades are located at varying distances from the tips of the arms and there is no fixed number per arm. Specimens with small or no protrusions are common.

The sutures of the superior face are curved or hook-shaped in anticlockwise direction. In the central area of this face a large pentagonal knob is present. This knob is orientated with the corners of the pentagon pointing towards the right sides of the arms. On the same face every arm is ornamented with a row of nodes that run along the median axis.

The sutures on the inferior face are straight, and a small knob may ornament the centre of the central area.

Differential diagnosis: *Helio-discoaster tanii* differs from *Helio-discoaster nodifer* in the number of segments. *Helio-discoaster nodifer* has a larger central area, thinner arms and a larger superior knob than of *H. tanii*. In addition, it differs in the position and the shape of the lateral ornamentation of the arms; *H. mirus* bears lateral blades close to the tips of the arms and not at about the middle of the arms as is the case in *H. tanii*.

Emendation: We confine the concept of the species to specimens with up to 5 segments and arms that may or may not bear lateral ornamentation and may or may not be notched at their tips. This was prompted by the need to facilitate the distinction of *H. tanii* from *H. nodifer*.

Occurrence: The range of *H. tanii* falls outside the range of our closely sampled sections. It has been recorded only in individual samples from Egypt (Umbarca) and S. Italy (Calabria). The species has been reported from zone CP14 to CP18.

Helio-discoaster nodifer (Bramlette and Riedel) Theodoridis,
emended
(Pl. 31, figs. 6, 7)

Discoaster tanii nodifer Bramlette and Riedel, 1954, p. 397, pl. 39, fig. 2; Martini, 1960, p. 78, table 9, fig. 19; Levin, 1965, p. 270, pl. 34, fig. 5; Haq, 1968, p. 46, pl. 10, fig. 7; Haq, 1969, p. 14, pl. 5, fig. 5; Bukry, 1974, figs. 6J, 6L.

Discoaster tanii Bramlette and Riedel; Deflandre, 1968, partim, pp. 44, 45, pl. 11, figs. 13, 14, non: pl. 9, figs. 15–17.

Discoaster nodifer (Bramlette and Riedel) Bukry, 1973, p. 678, pl. 4, fig. 24.

Discoaster binodosus hirundinus Martini, 1958, partim, p. 362, pl. 4, fig. 19b, non: pl. 4, fig. 19a.

Discoaster germanicus Martini, 1958, p. 360, pl. 3, figs. 15a, b.

Discoaster stradneri Noël, Bukry, 1971, pl. 1, fig. 10.

Helio-discoaster nodifer (Bramlette and Riedel) Theodoridis, 1983, p. 20.

Description: Asteroliths with 6 segments are assigned to this species. The segments exhibit relatively long, robust and rather parallel-sided arms. The central area is small in relation to the length of the arms. The arms are deeply notched in most specimens of this species, but specimens with blunt terminations are considered to be within the variation of the species. The sides of the arms are ornamented by lateral blades of varying shape and number. The blades are situated close to the middle of the arms and towards their tips. The superior faces of the arms are ornamented by nodes arranged in rows along the right side of each arm. The sutures of the superior face are curved or slightly hooked in anticlockwise direction. At the central area a pronounced hexagonal knob with rather small diameter is present. The points of the hexagon are orientated towards the right side of the corresponding arm.

The inferior face of the asteroliths shows straight but slightly subradial sutures. The arms do not possess any ornamentation at this face.

Differential diagnosis: *Helio-discoaster nodifer* has a relatively smaller central area and a smaller central knob on the superior face than *H. binodosus*.

H. tanii differs from *H. nodifer* in the number of arms.

Emendation: The concept of this species is made to fit specimens with 6 or more segments. This emendation follows from the restriction of *H. tanii* to specimens with 5 or less than 5 segments.

Occurrence: *H. nodifer* was observed in samples belonging to zone CP19 (Calabria). It has been reported to range as low as zone CP13.

Genus Eu-discoaster Tan Sin Hok, 1927, emend. Theodoridis

Synonyms: *Hemi-Discoaster* Tan Sin Hok, 1927. *Discoaster* Tan Sin Hok, 1931, *Agalmatoaster* Klumpp, 1953. *Catinaster* Martini and Bramlette, 1963. *Clavodiscoaster* Prins, 1971.

Diagnosis: Asteroliths with straight sutures on both their proximal and distal faces.

Remarks: The asteroliths are composed of a limited number of segments (3 to 6 segments; exception: *E. nonaradiatus* with up to 8 segments). The segments are wedge-shaped towards the centre of the asterolith and are attached to each other by planar surfaces without imbrication. The majority of species of *Eu-discoaster* possess well-developed arms.

All asteroliths of this genus (except *E. misconceptus* n. sp.) are non-birefringent in plane view, unless they are overgrown or pronouncedly curved. In side view they show extinction parallel to the direction of polarization.

Subdivision: The genus is subdivided into six morphological groups: (a) *E. deflandrei* group, (b) *E. exilis* group, (c) *E. kugleri* group (d), *E. coalitus* group, (e) *E. bellus* group and (f) *E. brouweri* group.

Type species: *Eu-discoaster brouweri* (Tan Sin Hok) Theodoridis. Basionym: *Discoaster brouweri* Tan Sin Hok.

EU-DISCOASTER DEFLANDREI GROUP

Diagnosis: Asteroliths with predominantly 6 segments, parallel-sided arms, broadly bifurcating arm terminations and little or no curvature of the arms. The arms often possess a longitudinal ridge on their distal surface.

Eu-discoaster distinctus (Martini) Theodoridis (Pl. 32, figs. 1, 2)

Discoaster distinctus Martini, 1958, p. 363, pl. 4, figs. 17a, b; Bramlette and Sullivan, 1961, p. 162, pl. 11, figs. 11, 13; Stradner and Papp, 1961, p. 72, pl. 11, fig. 1, text-fig. 8/8; Sullivan, 1965, p. 41, pl. 10, fig. 4; Kappelos and Schaub, 1973, p. 728, partim, p. 8, fig. 5, non: pl. 5, figs. 3, 4; Haq and Lohmann, 1976, pl. 6, fig. 6; Müller, 1979, pl. 4, fig. 12.

Discoaster gemmifer Stradner, 1961, p. 86, fig. 83; Stradner and Papp, 1961, partim, pp. 69–71, pl. 24, figs. 4, 5, table 9, figs. 1a, b, non: pl. 24, fig. 6, table 9, figs. 2–5, text-fig. 8/6.

Eu-discoaster distinctus (Martini) Theodoridis, 1983, p. 17.

Description: The discoasters of this species consist of 6 and rarely of 5 segments. Asteroliths with 7 segments do exist but they are rare and often malformed. The central area is small in relation to the length of the arms. The arms broaden towards their tips. The tips of the arms are incised by deep U-shaped notches producing two prominent and pointed branches. Very characteristic lateral nodes or blades can be seen at the base of the bifurcations.

The distal face of the central area is ornamented by shallow depressions around the centre of the asterolith. The remaining elevated area at the centre (distal knob) has the shape of a hexagon (pentagon or heptagon if the astero-

lith has 5 or 7 segments) with its points orientated towards the interarray areas. The distal faces of the arms are ornamented by ridges.

A star-shaped knob can be observed at the centre of the proximal face. The points of the star are directed to the right sides of the arms. Ridges are present also along the proximal faces of the arms. The ridges are situated to the right of the median axis and may be connected to the points of the proximal knob.

Differential diagnosis: *Eu-discoaster distinctus* possesses very characteristic U-shaped terminal notches and the branches of its bifurcations are parallel to the longitudinal axis of the arms. Furthermore, the lateral blades or nodes at the base of the bifurcations give the branches a triangular shape. The observation of these features facilitates the distinction of this species from *E. deflandrei*.

Occurrence: *E. distinctus* ranges from zone CP10 to zone CP12.

Eu-discoaster deflandrei (Bramlette and Riedel) Theodoridis
emended
(Pl. 32, fig. 5)

Discoaster deflandrei Bramlette and Riedel, 1954, p. 399, pl. 33, fig. 6, text-fig. 1; Martini, 1958, pp. 363, 364, pl. 5, figs. 23a–c; Stradner, 1958, p. 184, figs. 17, 18; Stradner, 1959, p. 1087, fig. 25; Bramlette and Sullivan, 1961, p. 158, pl. 11, figs. 4a–b; Stradner and Papp, 1961, p. 71, pl. 10, figs. 1–6, text-fig. 8/7; Sullivan, 1964, p. 190, pl. 11, figs. 8, 9; Bramlette and Wilcoxon, 1967, p. 109, pl. 7, fig. 4; Black, 1968, p. 153, fig. 6; Bukry, 1971, p. 995, pl. 4, fig. 4; Haq, 1971, p. 90, pl. 12, fig. 10; Ellis, Lohman and Wray, 1972, p. 43, pl. 13, fig. 1; Bukry, 1973, pl. 4, figs. 12–14; Roth, 1973, p. 736, pl. 6, fig. 5, pl. 8, fig. 3; Perch-Nielsen, 1974, pl. 15, figs. 18–20; Proto Decima et al., 1978, pl. 9, figs. 3, 6; Haq and Berggren, 1978, pl. 4, fig. 16; Moshkovitz and Ehrlich, 1980, pl. 2, fig. 12.

Discoaster cf. *D. molengraaffi* Tan; Stradner, 1959, p. 1085, fig. 24.

Discoaster cf. *D. deflandrei* Bramlette and Riedel; Sullivan, 1965, p. 41, pl. 10, fig. 5.

Discoaster sp. (*deflandrei* group) Martini, 1965, p. 406, pl. 35, fig. 10, pl. 37, figs. 3–6.

Discoaster sp. (*tani* group) Martini, 1965, p. 406, pl. 37, figs. 1, 2.

Clavodiscoaster deflandrei (Bramlette and Riedel) Prins, 1971, pl. 5, fig. 43: Invalid combination, ICBN art. 33, 2.

Eu-discoaster deflandrei (Bramlette and Riedel) Theodoridis, 1983, p. 17.

Description: The discoasters of *E. deflandrei* usually consist of 6 and less frequently of 5 segments. Discoasters with 3, 4 and 7 segments are atypical forms that occur rarely and cannot always be assigned to the species with certainty.

The central area of *E. deflandrei* is large, relative to the length of the arms. The arms are parallel-sided, relatively thick and they terminate in broad bifurcations. Very often the bifurcations are primarily filled by calcite. In extreme cases this filling resembles a blade or a membrane connecting the two

branches of the bifurcation and it may bend proximally. The branches of the bifurcation are rounded or truncated at their tips and they may possess lateral nodes or blades.

The distal faces of the asterolith is almost flat. The central area is ornamented by depressions that are arranged around the centre of the asterolith. A polygonal knob is present at the centre of the distal face with its points orientated towards the interray areas.

The distal faces of the arms are ornamented by median ridges. The proximal face of the asterolith is slightly concave and bears no additional features.

Differential diagnosis: *E. deflandrei* differs from *E. distinctus* in the shape of the bifurcations and the ratio between central area and arm.

Emendation: The figures that accompany the original description of the *E. deflandrei* give no indication about the features of the central area. Subsequent descriptions by Stradner (1958, 1959), Stradner and Papp (1961) and Romein (1979) – probably based on observations of *H. mirus* – attributed to the species characteristics of *Helio-discoaster* by ascribing curved sutures to one of the faces.

Here the species concept is confined to discoasters with straight sutural lines on both proximal and distal faces of the central area.

Occurrence: This is the longest-ranging species of *Eu-discoaster*, having its first occurrence in the Eocene zone CP10 and ranging up to the Miocene *M. convallis* Zone.

Eu-discoaster nonaradiatus (Klumpp) Theodoridis (Pl. 32, figs. 3, 4)

Discoaster nonaradiatus var. Klumpp, 1953, p. 383, text-fig. 3/5.

Discoaster heptaradiatus var. Klumpp, 1953, p. 383, text-fig. 3/3.

Agalmatoaster septemradiatus Klumpp, 1953, p. 384, text-fig. 4/1, pl. 6, figs. 8–9; Prins, 1971, pl. 4, fig. 34.

Discoaster nonaradiatus Klumpp, Martini, 1958, p. 364, pl. 4, figs. 21a, b; Bramlette and Sullivan, 1961, p. 162, pl. 12, figs. 13–15.

Discoaster septemradiatus (Klumpp) Martini, 1958, pp. 364, 365, pl. 4, figs. 20a, b; Bramlette and Sullivan, 1961, p. 162, pl. 12, figs. 16, 17.

Eu-discoaster nonaradiatus (Klumpp) Theodoridis, 1983, p. 18.

Remarks: The asteroliths of this species are small and except for the number of arms (7 or 8) they resemble the asteroliths of *E. deflandrei*.

Occurrence: This species is restricted to zones CP10 and CP11.

Eu-discoaster druggii (Bramlette and Wilcoxon) Theodoridis (Pl. 12, fig. 1, pl. 32, figs. 6, 7)

Discoaster extensus Bramlette and Wilcoxon, 1967, p. 110, pl. 8, figs. 2–8.

Discoaster druggi Bramlette and Wilcoxon, 1967, p. 220, nomen subst. pro *Discoaster extensus* Bramlette and Wilcoxon, 1967, non: Hay, 1967.
Eu-discoaster druggii (Bramlette and Wilcoxon) Theodoridis, 1983, p. 17.

Description: Only asteroliths consisting of 5 or 6 segments have been observed. They are flat and are of irregular thickness which given them a mottled appearance in transmitted light.

The arms are parallel-sided or they may be slightly tapering; they are ornamented by lateral nodes or blades. The tips of the arms are incised by a shallow and V-shaped notch.

Both the proximal and the distal face of the asterolith lack any features such as knobs or ridges.

Differential diagnosis: *E. druggii* is distinguished from *E. deflandrei* by the lateral nodes of its arms and the lack of extended bifurcations.

Occurrence: This species ranges from the *E. druggii* Subzone to the *S. belemnos* Subzone.

Eu-discoaster variabilis (Martini and Bramlette) Theodoridis (Pl. 32, fig. 8)

- Discoaster brouweri* var. α Tan Sin Hok, 1927, p. 415, fig. 13. Invalid: ICBN art. 43, 1.
Discoaster brouweri var. α Tan Sin Hok, 1931, p. 93. Valid: ICBN art. 41, 1b.
Discoaster brouweri var. γ Tan Sin Hok, 1927, p. 415, fig. 7. Invalid: ICBN art. 43, 1.
Discoaster brouweri var. γ Tan Sin Hok, 1931, p. 93. Valid: ICBN art. 41, 1b.
Discoaster challengerii Bramlette and Riedel, Stradner in Stradner and Papp, 1961, partim, pp. 83–85, pl. 18, figs. 4–6, non: pl. 17, figs. 1–3, 6, pl. 18, figs. 1, 3, pl. 19, figs. 4–6, text-figs. 8/21, 24/10, 24/11.
Discoaster variabilis Martini and Bramlette, 1963, p. 854, pl. 104, figs. 4–9; Martini, 1969, p. 293, pl. 28, fig. 8; Cati and Borsetti, 1970, p. 630, pl. 82, figs. 1, 2; Hay et al., 1967, pl. 3, fig. 11; Ellis, Lohman and Wray, 1972, p. 54, pl. 16, fig. 1; Perch-Nielsen, 1972, pl. 12, figs. 1–4, 6; Müller, 1974, pl. 8, figs. 11, 12; Fuchs and Stradner, 1977, pp. 34, 35, pl. 1, figs. 21–23, pl. 5, figs. 4–9; Perch-Nielsen, 1977, pl. 15, fig. 14; Proto Decima et al., 1978, pl. 7, figs. 10–14; Haq and Berggren, 1978, pl. 4, fig. 28; Moshkovitz and Ehrlich, 1980, pl. 5, figs. 3, 4; Huang and Okamoto, 1980, pl. 4, fig. 3; Bukry, 1981, pl. 1, figs. 1, 2; Driever, 1981, pl. 1, figs. 4–6.
Discoaster sp. (*variabilis* Group) Martini, 1965, pp. 406, 407, pl. 37, figs. 7, 8.
Discoaster saundersi Hay, in Hay et al., 1967, p. 453, pl. 3, figs. 2–6.
Discoaster divaricatus Hay, in Hay et al., 1967, p. 451, pl. 3, figs. 7–9.
Discoaster extensus Hay, in Hay et al., 1967, p. 451, pl. 3, figs. 10–12, pl. 4, figs. 1–2.
Discoaster dilatus Hay, in Hay et al., 1967, pp. 450, 451, pl. 4, figs. 3, 4.
Discoaster phyllodus Hay, in Hay et al., 1967, p. 453, pl. 4, figs. 5, 6; Cati and Borsetti, 1970, p. 629, pl. 78, figs. 1, 2.
Discoaster aulakos Gartner, 1967, p. 2, pl. 4, figs. 4a, b, 5a, b; Cati and Borsetti, 1970, p. 624, pl. 78, figs. 1–6; Bukry, 1973, pl. 4, fig. 3; Jafar, 1975, pl. 6, fig. 6; Fuchs and Stradner, 1977, p. 33, pl. 7, figs. 27, 35, 36; Hojjatzadeh, 1978, pl. 1, fig. 2.
Clavodiscoaster variabilis (Martini and Bramlette) Prins, 1971, pl. 5, fig. 46. Invalid: ICBN art. 33, 2.
Clavodiscoaster aulakos (Gartner) Prins, 1971, pl. 5, fig. 45. Invalid: ICBN art. 33, 2.
Discoaster moorei Bukry, 1971, p. 46, pl. 2, figs. 11, 12, pl. 3, figs. 1, 2.

Discoaster cf. *D. exilis* Martini and Bramlette, Jafar, 1975, pp. 48, 49, pl. 6, fig. 3.

Discoaster cf. *D. variabilis* Martini and Bramlette, Jafar, 1975, pp. 52, 53, pl. 6, fig. 4; Moshkovitz and Ehrlich, 1980, pl. 5, figs. 5–8.

Discoaster pentaradiatus Tan Sin Hok, Jafar, 1975, partim, p. 50, pl. 7, fig. 5, fig. 7, non: pl. 7, fig. 6.

Discoaster aff. *D. deflandrei* Bramlette and Riedel, Hojjatzadeh, 1978, p. 6, pl. 1, fig. 7.

Eu-discoaster variabilis (Martini and Bramlette) Theodoridis, 1983, p. 19.

Description: The discoasters of this species usually consist of 6 and rarely of 3, 4, or 5 segments. The variants with 5 segments are asymmetrical. The arms are long relative to the diameter of the central area; they are parallel-sided and bifurcate at their tips. The branches of the bifurcations are long and bear lateral blades. The notch between the branches is filled by a primary calcareous membrane.

The distal face of the central area of well-preserved specimens has well-developed depressions around its centre, whereas the centre is elevated and forms a polygonal knob with its points orientated towards the interray areas. The arms show ridges along the median axis of their distal face.

Ridges are present also along the median axis of the proximal faces of the arms. These ridges meet at the centre of the asterolith and form a low stellate knob orientated with its points towards the arms.

Differential diagnosis: *E. variabilis* differs from *E. deflandrei* mainly in the relative proportions of the arms to the diameter of the central area, having longer arms and smaller central area than the latter species.

Occurrence: From the *S. heteromorphus* Zone up to the Pliocene subzone CN12d.

Eu-discoaster pseudovariabilis (Martini and Worsley) Theodoridis (Pl. 32, figs. 12, 13)

Discoaster pseudovariabilis Martini and Worsley, 1971, p. 1500, pl. 3, figs. 2–8; Bukry, 1973, pl. 4, fig. 26; Müller, 1974, pl. 7, figs. 9, 10; Proto Decima et al., 1978, pl. 7, figs. 9a–d, pl. 8, figs. 2a, b; Martini, 1980, pl. 3, figs. 10, 11.

Eu-discoaster pseudovariabilis (Martini and Worsley) Theodoridis, 1983, p. 18.

Description: *E. pseudovariabilis* consists of 6 and rarely 5 segments. The variants with 5 segments are asymmetrical. The asteroliths of this species have a relatively small central area and long arms. The arms are parallel-sided and their tips bifurcate into two, relatively long branches.

A prominent blade-like projection appears between the branches of the bifurcation. The termination of this projection is incised by a V-shaped notch which produces two pointed tips. The distal surface of the projection is depressed.

The distal face of the central area shows well-developed depressions but

no central knob. The arms bear prominent distal ridges along their median axis.

In proximal view the arms exhibit ridges along their entire length. The ridges are in continuity with the tips of a stellate central knob.

Differential diagnosis: *E. pseudovariabilis* differs from *E. variabilis* in the presence of a prominent projection between the branches of its bifurcation.

Occurrence: This species has been observed from the *E. bollii* Subzone to the *C. pelagicus* Zone.

Eu-discoaster surculus (Martini and Bramlette) Theodoridis

Discoaster brouweri Tan Sin Hok sens. emend. Bramlette and Riedel, Stradner, in Stradner and Papp, 1961, partim, pp. 85–87, pl. 20, figs. 2a, b, 3a, b, 6, text-fig. 8/23, non: pl. 20, figs. 1a, b, 4a, b, 5a, b.

Discoaster surculus Martini and Bramlette, 1963, p. 854, pl. 104, figs. 10–12; Bukry, 1969, pl. 7, fig. D; Bukry, 1971, pl. 3, fig. 3; Nishida, 1971, p. 55, pl. 18, fig. 4; Martini, 1971, pl. 4, fig. 13; Perch-Nielsen, 1971, pl. 11, fig. 1; Ellis, Lohman and Wray, 1972, p. 52, pl. 15, figs. 3–5; Akers and Koeppel, 1973, pl. 4, fig. 2; Müller, 1974, pl. 6, fig. 12; Perch-Nielsen, 1977, pl. 15, figs. 1, 2, 5, 6, 10; Dermitzakis and Theodoridis, 1978, pl. 2, figs. 6, 7; Haq and Berggren, 1978, pl. 4, figs. 26, 27; Proto Decima et al., 1978, pl. 8, figs. 1a, b; Conley, 1979, p. 28, pl. 1, fig. 13; Moshkovitz and Ehrlich, 1980, pl. 5, figs. 13–16; Martini, 1980, pl. 2, fig. 5; Driever, 1981, pl. 1, figs. 1–3, pl. 2, figs. 17–19, pl. 3, fig. 1; Varol, 1982, pl. 5, fig. 5, pl. 6, fig. 12.

Clavodiscoaster surculus (Martini and Bramlette) Prins, 1971, pl. 5, fig. 45. Invalid: ICBN art. 33, 2.

Discoaster dilatus Hay, Nishida, 1971, p. 154, pl. 18, fig. 2.

Discoaster toralus Ellis, Lohman and Wray, 1972, p. 53, pl. 16, figs. 2–6.

Eu-discoaster surculus (Martini and Bramlette) Theodoridis, 1983, p. 18.

Description: The discoasters of this species are nearly complanate and consist of 3 to 6 segments. The 5-segment variants are asymmetrical.

The central area is small in relation to the length of the arms and bears a distal and a proximal central knob. Its distal surface, around the knob, is ornamented by shallow depressions.

The arms are parallel-sided and their tips trifurcate exhibiting two lateral branches in the plane of the discoaster while the third one is curved proximally. The distal surface of the trifurcation may be slightly caved. The arms bear median ridges on both their proximal and distal surface.

Differential diagnosis: *E. surculus* differs from *E. variabilis* in exhibiting trifurcating arm tips. It is distinguished from *E. pseudovariabilis* by the relatively more massive and blunt trifurcations instead of the protruding notched blades that are characteristic for the latter species.

Occurrence: The species ranges from the *G. rotula* Subzone of the Miocene to the CN12c Subzone of the Pliocene.

Eu-discoaster pansus (Bukry) Theodoridis
(Pl. 32, figs. 9, 10)

Discoaster variabilis pansus Bukry, 1971, p. 129, pl. 3, figs. 8, 9; Perch-Nielsen, 1977, pl. 15, fig. 17.

Discoaster icarus Stradner, 1973, pp. 1138, 1139, pl. 41, figs. 10, 11, text-fig. 1.

Discoaster pansus (Bukry) Bukry, 1973, pl. 4, fig. 25.

Eu-discoaster pansus (Bukry) Theodoridis, 1983, p. 18.

Remarks: In general morphology *E. pansus* is similar to *E. variabilis*, but it is larger, it has a broader central area and longer bifurcations. Some specimens exhibit large blades that fill the space between the branches of the bifurcations (*D. icarus* morphology).

Occurrence: This species has a consistent occurrence within the interval from the *E. pseudovariabilis* Subzone to the *C. leptoporus* Zone. Rare specimens of *E. pansus*, however, have been recorded in samples as low as the *E. kugleri* Subzone.

Eu-discoaster loeblichii (Bukry) Theodoridis

Discoaster loeblichii Bukry, 1971, pp. 315, 316, pl. 4, figs. 3–5; Bukry, 1973, pl. 4, fig. 18; Proto Decima et al., 1978, pl. 9, figs. 7, 8.

Eu-discoaster loeblichii (Bukry) Theodoridis, 1983, pp. 17, 18.

Description: The asteroliths of this species have 6 and rarely 5 segments. The 5-segment variants are asymmetrical.

The arms are parallel-sided or show slightly curved sides becoming broader towards their tips. The tips bifurcate into two unequal branches. The asymmetric bifurcations may point dextrally or sinistrally but their orientation is uniform for the same specimen. Small blade-like protrusions project between each pair of branches. The arms bear median ridges on their proximal surface.

The central area has a low, rounded or polygonal knob associated with shallow depressions on its distal surface, whereas a stellate central knob can be observed in proximal view. The points of the proximal knob are connected to the proximal median ridges of the arms.

Differential diagnosis: *E. loeblichii* is distinguished from all other discoasters with bifurcating tips by the asymmetric bifurcations.

Occurrence: *E. loeblichii* is restricted to the *E. pentaradius* and the *G. rotula* Subzone.

Eu-discoaster decorus (Bukry) Theodoridis
(Pl. 32, fig. 11)

Discoaster variabilis decorus Bukry, 1971, p. 48, pl. 3, fig. 6; Proto Decima et al., 1978, pl. 7, figs. 15, 16, pl. 9, fig. 10.

Eu-discoaster decorus (Bukry) Theodoridis, 1983, p. 17.

Remarks: *E. decorus* resembles *E. variabilis* in general characteristics but it is larger and its bifurcations show short pointed limbs and no lateral blades.

Occurrence: This species occurs in the Pliocene zone CN12.

EU-DISCOASTER EXILIS GROUP

Diagnosis: Asteroliths with predominantly 6 segments, tapering arms and acute bifurcations.

Eu-discoaster protoexilis n. sp.

(Pl. 33, figs. 1, 2)

Discoaster extensus Hay, Müller, 1974, pl. 7, fig. 4.

Etymology: From protos (= first, Gr.) and exilis.

Description: The asteroliths of this species usually possess 6 and rarely 5 segments. The pentaradial variants are asymmetrical.

The central area is large relative to the length of the arms and bears both a proximal and a distal central knob. The distal knob is surrounded by depressions.

The arms taper outwards but their tips bifurcate into two long branches which form an acute angle. The space between all pairs of branches often has a calcareous filling which gives the bifurcation a fish-tail appearance. The arms exhibit pronounced median ridges or median knobs in distal view.

In proximal view the ridges are confined to the central area, up to the base of the arms.

Differential diagnosis: *E. protoexilis* resembles *E. exilis* from which it differs in having shorter arms and highly pronounced distal ridges (or knobs). Typical forms of *E. protoexilis* are easily distinguished from typical forms of *E. deflandrei*, but intermediate forms between the two are common (compare figs. 3 and 4 in Müller, 1974, pl. 7).

Holotype: Pl. 33, fig. 1, sample: 369A-67, coordinates: 122.8/14.5.

Isotype: Pl. 33, fig. 2, sample, 369A-67.

Type level: *E. druggii* Subzone.

Type locality: D.S.D.P. Site 369A, Sierra Leone Rise, Atlantic Ocean.

Occurrence: *E. protoexilis* has been observed from the interval *E. druggii* Subzone to the *H. ampliapertura* Zone only in the D.S.D.P. Site 369A, Atlantic.

Eu-discoaster exilis (Martini and Bramlette) Theodoridis
(Pl. 12, fig. 2, pl. 33, figs. 3–5)

Discoaster challengeri Bramlette and Riedel, Stradner, 1959, p. 1087, fig. 26; Stradner, in Stradner and Papp, 1961, partim, pp. 83–85, pl. 18, figs. 1a, b, 3a, b, text-figs. 8/21, 24/10, 24/11, non: pl. 17, figs. 1–3, 6, pl. 18, figs. 4–6, pl. 19, figs. 4–6.

Discoaster cf. *D. challengeri* Bramlette and Riedel, Stradner, in Stradner and Papp, 1961, pl. 19, figs. 1–3.

Discoaster exilis Martini and Bramlette, 1963, p. 852, pl. 104, figs. 1–3; Martini, 1965, p. 405, pl. 37, fig. 9; Bramlette and Wilcoxon, 1967, p. 110, pl. 7, fig. 3; Cati and Borsetti, 1970, p. 628, pl. 76, figs. 1–3; Martini, 1971, pl. 3, fig. 22; Ellis, Lohman and Wray, 1972, p. 46, pl. 13, figs. 4, 5; Müller, 1974, pl. 7, fig. 7; Fuchs and Stradner, 1977, pp. 33, 34, pl. 1, figs. 24, 25, pl. 6, fig. 1, pl. 7, figs. 6, 13; Proto Decima et al., 1978, pl. 8, figs. 5a–c.

Discoaster browneri picentinus Cati and Borsetti, 1970, p. 625, pl. 79, figs. 1–4.

Eu-discoaster *exilis* (Martini and Bramlette) Prins, 1971, pl. 5, fig. 52. Invalid: ICBN art. 33, 2; Theodoridis, 1983, p. 17.

Discoaster cf. *D. exilis* Martini and Bramlette, Jafar, 1975, pl. 6, fig. 3.

Description: The discoasters have commonly 6 and rarely 5 segments. The 5-segment variants are asymmetrical.

The arms are slender, roughly cylindrical in cross-section and taper towards the tips. The tips bifurcate producing two slender and pointed branches that form an acute angle in typical forms. The space between the branches (of all sets of bifurcations) contains a thin calcareous filling. Ridges occur rarely on the distal surfaces of the arms and, when present, they are not pronounced. In proximal view, ridges radiate from the centre of the asterolith and continue along the median axis of the arms.

A round central knob is present on the distal surface of the central area. The area around this knob shows deep distal depressions. A stellate central knob is present on the proximal surface of the central area.

Differential diagnosis: *E. exilis* is distinguished from *E. protoexilis* by the longer arms and the absence of pronounced ridges on the distal faces of the arms.

Occurrence: *E. exilis* occurs from the *H. obliqua* Subzone to the *E. pseudovariabilis* Subzone.

Eu-discoaster signus (Bukry) Theodoridis, emended
(Pl. 12, figs. 5–7, pl. 33, figs. 14–17, pl. 34, figs. 1–6)

Discoaster exilis Martini and Bramlette, Hay et al., 1967, pl. 4, figs. 7, 8.

Discoaster signus Bukry, 1971, p. 48, pl. 3, figs. 3, 4.

Discoaster petaliformis Moshkovitz and Ehrlich, 1980, pp. 17, 18, pl. 6, figs. 1–7.

Discoaster signus Bukry, Ellis, Lohman and Wray, 1972, p. 51, fig. 1.

Eu-discoaster *signus* (Bukry) Theodoridis, 1983, p. 18.

Description: Only asteroliths with 6 segments have been observed. The

arms are long, taper outwards and show no curvature. The tips of the arms bifurcate into two relatively long and pointed branches which, as a rule, form an acute angle. The cross-section of the arms is roughly circular.

Ridges can be observed only at the proximal surface of the central area where they form a stellate knob and radiate to the bases of the arms. The majority of the discoasters of this species exhibit a characteristic prominent knob at the centre of the distal face. This knob flares out and forms a mushroom-like structure. There is a continuous variation, however, between specimens with prominent distal knobs and specimens with knobs of smaller dimensions.

Differential diagnosis: The discoasters of *E. signus* are easily distinguished when they exhibit the characteristic distal knob.

Specimens without such a distal knob differ from *E. exilis* in their more slender arms, more acute angle of the bifurcations and in that they lack a calcareous filling between the branches of the bifurcations.

Emendation: The species concept of *E. signus* is emended in order to include variants with prominent distal knobs (i.e. *E. petaliformis* (Moshkovitz and Ehrlich)). The emendation is supplementary to the original diagnosis by Bukry who depicted only the knobless variants of the species, and he referred to the absence of "a central area development".

The knobless variants and the variants with prominent distal knobs have an identical range in our samples and cannot be separated at any interval due to the existence of intermediate morphotypes.

Occurrence: *E. signus* is restricted to the *S. heteromorphus* Zone ranging from the *E. signus* Subzone to the *E. musicus* Subzone.

Eu-discoaster cf. *E. signus*
(Pl. 34, figs. 7–14)

Remarks: Intermediate types between *E. signus* and *E. musicus*, with short arms, have been observed in the *E. signus* Subzone. These asteroliths are indicated in our range charts as *E. cf. E. signus*.

Eu-discoaster musicus (Stradner) Theodoridis
(Pl. 34, figs. 15–18, pl. 35, fig. 5)

Discoaster musicus Stradner, 1959, p. 1088, fig. 28; Stradner, in Stradner and Papp, 1961, partim, p. 85, pl. 17, figs. 7a, b, 8a, b, 9a, b, pl. 18, fig. 2, text-fig. 8/22, non: pl. 18, figs. 4a, b, 5a, b.
Discoaster sanmiguelensis Bukry, 1981, p. 462, pl. 2, figs. 7–10, pl. 3, figs. 1–14.
Eu-discoaster musicus (Stradner) Theodoridis, 1983, p. 18.

Description: Only asteroliths with 6 segments have been observed. The

asteroliths are complanate with relatively short arms and a broad central area. The arms taper towards their tips and at the tips they exhibit only a tiny notch.

The distal face of the central area has very pronounced sutural ridges and a high central knob, which are very characteristic for this species. In some specimens the sutural ridges extend somewhat further from the periphery of the central area creating the impression of a double discoaster (cf. pl. 34, fig. 17).

In proximal view low ridges can be observed only close to the centre where a small stellate knob may be present. The proximal ridges radiate towards the base of the arms.

Differential diagnosis: The species is readily distinguished due to the characteristic sutural ridges. The only other species with prominent sutural ridges is *E. quinqueramus* but that species has longer and pointed arms and is predominantly pentaradial.

Occurrence: This species ranges from the *E. signus* to *E. musicus* Subzones of the *S. heteromorphus* Zone.

Eu-discoaster subsurculus (Gartner) Theodoridis

(Pl. 33, figs. 12, 13)

Discoaster subsurculus Gartner, 1967, p. 3, pl. 5, figs. 1, 2; Cati and Borsetti, 1970, p. 630, pl. 76, figs. 4, 5.

Eu-discoaster subsurculus (Gartner) Theodoridis, 1983, p. 18.

Remarks: All morphological features of this species are comparable to those of *E. exilis* except for the thick nodes that appear between the branches of all sets of bifurcations.

Occurrence: In our sections this species ranges from the *H. walbersdorfen-sis* Subzone to the *E. kugleri* Subzone.

Eu-discoaster bollii (Martini and Bramlette) Theodoridis

(Pl. 33, figs. 8–11)

Discoaster bollii Martini and Bramlette, 1963, p. 851, pl. 105, figs. 1–4, 7; Bramlette and Wilcoxon, 1967, p. 109, pl. 8, fig. 11; Perch-Nielsen, 1971, pl. 9, fig. 4; Ellis, Lohman and Wray, 1972, p. 40, pl. 11, fig. 2, 3; Müller, 1974, pl. 7, figs. 5, 6; Jafar, 1975, pp. 45, 46, pl. 6, fig. 5; Proto Decima et al., 1978, pl. 9, fig. 4.

Eu-discoaster bollii (Martini and Bramlette) Prins, 1971, pl. 5, fig. 51. Invalid: ICBN art. 33, 2.

Eu-discoaster bollii (Martini and Bramlette) Theodoridis, 1983, p. 17.

Description: The discoasters of *E. bollii* consist of 5 or 6 segments. The pentaradial forms are rare and usually they are asymmetrical. The central area is relatively large and the arms are short and slender.

The distal surface of the central area is ornamented by a prominent, stellate knob and depressions. A lower, rounded knob and ridges radiating from it towards the arms can be observed on its proximal surface.

The arms are roughly circular in cross-section, they lack median ridges and they taper prior to the bifurcations. The bifurcations form an acute angle and the branches are long and slender. Well-preserved specimens do not have any calcareous filling between the branches of the bifurcations.

Differential diagnosis: *E. bollii* closely resembles *E. exilis*, from which it is distinguished only by the larger central area and the shorter arms as well as by the more prominent proximal and distal knobs.

It can be distinguished from the knob-bearing variants of *E. signus* (Bukry) emend. by the shorter arms and the larger central area, as well as by the smaller diameter of its distal knob.

E. cf. E. signus has a smaller central area and a larger (in diameter and height) distal knob than *E. bollii*.

Remarks: *E. bollii* occurs sporadically in our sections and it is not easily distinguished from *E. exilis* in all cases.

Occurrence: *E. bollii* occurs from the *E. kugleri* Subzone to the *E. pseudo-variabilis* Subzone.

Eu-discoaster cf. *E. bollii*

(Pl. 33, figs. 6, 7)

Remarks: This taxonomic label is given to specimens of *E. bollii* with subdued knobs and relatively long arms. Such specimens have been observed in the *H. intermedia* and *E. kugleri* Subzones.

Eu-discoaster pentaradiatus (Tan Sin Hok, sens. emend. Bramlette and Riedel) Theodoridis

(Pl. 12, figs. 10, 11, pl. 35, figs. 1–4)

Discoaster pentaradiatus var. γ Tan Sin Hok, 1927, p. 416, fig. 14. Invalid: ICBN art. 43, 1.

Discoaster pentaradiatus var. γ Tan Sin Hok, 1931, p. 93. Valid: ICBN art. 41, 1b.

Discoaster pentaradiatus Tan Sin Hok emend. Bramlette and Riedel, 1954, pp. 401, 402, pl. 39, fig. 11, text-fig. 2a, b.

Discoaster pentaradiatus Tan Sin Hok, Martini, 1958, p. 359, pl. 3, figs. 12a, b; Kamptner, 1967, p. 165, pl. 24, fig. 129; Boudreaux and Hay, 1969, p. 282, pl. 9, figs. 1–3; ? Ellis, Lohman and Wray, 1972, p. 49, pl. 14, figs. 3, 4; Jafar, 1975, p. 50, pl. 7, figs. 6, 7.

Eu-discoaster pentaradiatus (Tan Sin Hok) Prins, 1971, pl. 5, fig. 53. Invalid: ICBN art. 33, 2.

Discoaster extensus Hay, Boudreaux and Hay, 1969, p. 286, pl. 9, figs. 7, 8, ?, fig. 8; Jafar, 1975, p. 49, pl. 6, fig. 10.

Discoaster prepentaradiatus Bukry, 1971, p. 129, pl. 3, figs. 6, 7.

Dicoaster moorei Bukry, Proto Decima et al., 1978, pl. 7, figs. 6, 8 ?, fig. 5.

Eu-discoaster pentaradiatus (Tan Sin Hok) Theodoridis, 1983, p. 18.

Description: *E. pentaradiatus* consists predominantly of 5 and rarely of 6 segments.

The central area is medium-sized and the arms are short and flat. The arms taper prior to a bifurcation with equal branches. The branches of the bifurcations are relatively long, pointed and form an obtuse angle. Ridges are observed only on the proximal face and they are more pronounced on the central area where they meet the tips of a low and stellate central knob. The ridges extend from the points of this knob up to the base of the bifurcations.

The distal face of the central area is ornamented with depressions and a low and rounded central knob.

The asterooliths of *E. pentaradiatus* exhibit no birefringence.

Differential diagnosis: *E. pentaradiatus* is distinguished from *E. exilis* by the obtuse angle of the bifurcations and the lack of calcareous filling between the branches. Moreover, the proximal ridges and the knobs of *E. exilis* are more pronounced than those of *E. pentaradiatus*.

E. misconceptus n. sp. has longer and pronouncedly curved arms, a more acute angle of bifurcation and it is birefringent in cross polarized light.

Remarks: The concept of *E. pentaradiatus* is confined here to forms similar to those originally described by Tan Sin Hok (1927). His concept has undergone subsequent modifications by later authors who attributed to this species morphological and optical characteristics deviating largely from those described by Tan.

Stradner (1959) depicted specimens which differed from the type specimens of Tan (1927) in having pronouncedly curved arms and longer and more acute bifurcations.

Bukry and Bramlette (1969) – in their description of *D. quintatus* – modified even further the concept of the species by implying that *E. pentaradiatus* exhibited birefringence. Asterooliths with such optical properties have been depicted by Moshkovitz and Martinotti (1979), Huang (1980) and Driever (1981).

Bukry (1971) observed the presence of flat pentaradial discoasters (comparable in shape with the drawings of Tan) but he isolated them as a different species with the name *D. prepentaradiatus*.

Our observations on the Bebalain sample 168 (i.e. the topotype of *E. pentaradiatus*) did not reveal any birefringent pentaradial discoasters, a fact we attribute to the lower biostratigraphic position of this sample relative to the first occurrence of such discoasters. This assumption is in agreement with the observations of Jafar (1975) who assigned the Bebalain sample to zone NN9; that is an interval below the level we observed in our sections the first occurrence of birefringent pentaradial discoasters with slender arms and apparent convexity.

The birefringent pentaradial discoasters are assigned here to *E. misconceptus* n. sp.

Occurrence: *E. pentaradiatus* is restricted to the *E. pseudovariabilis* Subzone (Zonule b) and the *E. pentaradiatus* Subzone. The species is absent from our Mediterranean sections. It is common or abundant in the D.S.D.P. Site 231, Indian Ocean.

Eu-discoaster misconceptus n. sp.
(text-figs. A–D, Pl. 37, figs. 19, 20)

Discoaster pentaradiatus Tan Sin Hok, Stradner, 1959, p. 11, figs. 46, 48; Martini and Bramlette, 1963, p. 853, pl. 105, fig. 5; Bukry, 1971, pl. 1, fig. 5; Cati and Borsetti, 1970, pp. 628, 629, pl. 81, figs. 1, 5; Sachs and Skinner, 1973, pl. 6, figs. 6, 7; Perch-Nielsen, 1977, pl. 15, figs. 7, 8; Samtleben, 1978, pl. 5, figs. 3, 5, 6; Proto Decima et al., 1978, pl. 8, figs. 4a–c; Haq and Berggren, 1978, pl. 4, figs. 23, 24; Huang, 1980, pl. 6, figs. 8a, b; Moshkovitz and Ehrlich, 1980, pl. 6, fig. 22; Driever, 1981, pl. 2, figs. 1–16, pl. 3, figs. 12–15; Varol, 1982, pl. 6, fig. 15.

Discoaster pentaradiatus Tan Sin Hok sens. emend. Bramlette and Riedel, Stradner, in Stradner and Papp, 1961, pp. 87–88, pl. 21, figs. 1a, b, 3a, b, 6, text-fig. 8/24, ? figs. 2a, b, 4a, b; ? Nishida, 1971, pp. 154, 155, pl. 18, figs. 3, 6, 13, 14; Martini, 1971, pl. 4, fig. 14; Müller, 1974, pl. 7, figs. 11, 12.

Discoaster challengeri Bramlette and Riedel, Perch-Nielsen, 1971, pl. 11, fig. 3.

Discoaster signus Bukry, Ellis, Lohman and Wray, 1972, p. 51, pl. 15, fig. 1.

Discoaster quadramus Bukry, 1973, p. 307, pl. 1, figs. 5, 6.

Etymology: From the prefix mis- (= wrongly) and concept.

Description: The asteroliths have a small central area and long and slender arms. They consist predominantly of 5 and rarely of 4 or 6 segments. The variants with 4 segments are X-shaped.

The central area possesses low central knobs on its proximal and on its distal surface. The distal surface of the central area is ornamented by shallow depressions.

The arms are roughly circular in cross section and usually they curve proximally. The terminations of the arms have acuteangled bifurcations with long and pointed branches. Electron micrographs of the bifurcations of some specimens revealed branches with a wavy surface. The arms bear median ridges only on their proximal surface. These ridges extend to the proximal knob of the central area.

Optical pattern: All asteroliths of *E. misconceptus* are slightly birefringent with extinction bands along the sutures of the central area. The entire asterolith shows sectors with different brightness that correspond to the different segments.

Differential diagnosis: *E. misconceptus* is distinguished from all other discoasters of *Eu-discoaster* by its birefringence. It differs from *E. pentaradiatus* by the more acutely angled bifurcations, the longer arms, the smaller central

area and the more pronounced curvature.

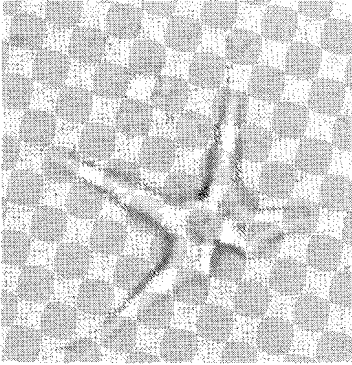
Holotype: Pl. 37, fig. 19, sample: JT1935.

Isotypes: Text-figs. A–D, Pl. 37, fig. 20, sample JT1935.

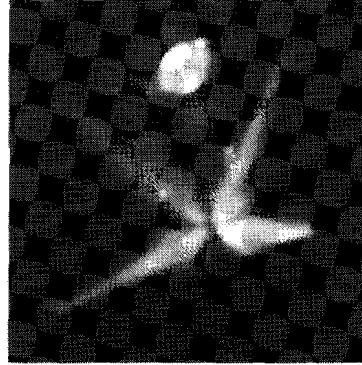
Type level: *C. pelagicus* Zone.

Type locality: Falconara, Sicily.

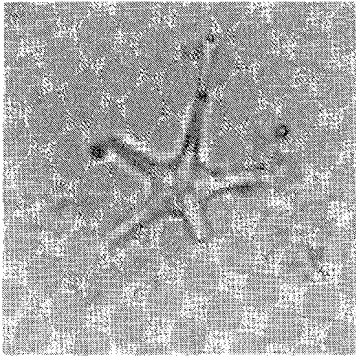
Occurrence: This species ranges from the *G. rotula* Subzone of the Miocene to the Pliocene zone CN12c.



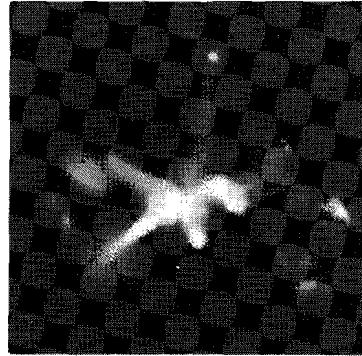
A



B



C



D

Text-figs. A–D. *E. misconceptus* n. sp. Light micrographs, 7500X.

EU-DISCOASTER KUGLERI GROUP

Diagnosis: Asteroliths with faint ornamentation on the distal face of their central area, and notched or bifurcated arm terminations. The asteroliths are predominantly hexaradial. The arms are slightly tapering.

Eu-discoaster kugleri (Martini and Bramlette) Theodoridis
(Pl. 12, figs. 3, 4, 8, pl. 35, figs. 15–18)

Discoaster kugleri Martini and Bramlette, 1963, p. 853, pl. 102, figs. 11–13; Bramlette and Wilcoxon, 1967, p. 110, pl. 7, figs. 1, 2; Ellis, Lohman and Wray, 1972, p. 47, pl. 14, fig. 1; Martini, 1971, pl. 3, fig. 24; Müller, 1974, pl. 7, fig. 2.

Clavodiscoaster kugleri (Martini and Bramlette) Prins, 1971, pl. 5, fig. 40. Invalid: ICBN art. 33, 2.

Discoaster dilatatus Hay, Ellis, Lohman and Wray, 1972, pp. 43, 33, pl. 13, fig. 2.

Eu-discoaster kugleri (Martini and Bramlette) Theodoridis, 1983, p. 17.

Description: The discoasters of *E. kugleri* consist of 5 or 6 segments. The asteroliths are complanate with a characteristically large central area and broad interray areas. The outline of the interray areas corresponds to a circle.

The arms are relatively short and they are thickest at their tips. A sharp notch is present at the tips of the arms, producing two short and pointed limbs. Specimens with equal as well as unequal limbs have been observed. When unequal, the longer of the two limbs points in a clockwise direction (in proximal view). The arms frequently trifurcate with a third limb bent in a proximal direction.

The distal face of the central area is entirely flat and featureless. The central area of the proximal face bears a low and stellate central knob with its points directed towards the arms. Low ridges extend from the points of this proximal knob to the tips of the arms.

The arms of *E. kugleri* appear brighter than the central area in transmitted light.

Differential diagnosis: *E. kugleri* is readily distinguished by the very large and featureless distal surface of its central area. Discoasters with similarly large central areas, such as *E. bollii* and *E. cf. E. bollii* exhibit pronouncedly “sculptured” distal central areas with knobs and depressions.

Occurrence: The species is restricted to the *E. kugleri* Subzone. It is absent from the Mediterranean sections.

Eu-discoaster micros n. sp.
(Pl. 36, figs. 1–3)

Etymology: From micros (= small, Gr.).

Diagnosis: Very small discoasters with short and broadly bifurcating arms that are thickest (and therefore brightest in transmitted light) at the position of the bifurcations.

Description: The asteroliths consist of 6 segments.

The central area is relatively large and the arms are very short and bifur-

cate. The bifurcations have short and pointed limbs that form an obtuse angle. The asteroliths appear dim in transmitted light except for the terminations of the arms that are brighter, indicating their relative thickness. The distal central area is featureless. Some specimens show a very low proximal knob and low proximal ridges that extend from the points of the knob towards the terminations of the arms.

Differential diagnosis: *E. micros* is distinguished from all other discoasters with bifurcating arms by its small size and the very short arms.

Holotype: Pl. 36, figs. 1, 2, sample: 369A-7, coordinates: 130.5/8.3.

Isotype: Pl. 36, fig. 3, sample: 369A-7.

Type level: *E. kugleri* Subzone.

Type locality: D.S.D.P. Site 369A, Sierra Leone rise, Atlantic Ocean.

Occurrence: *E. micros* is restricted to the *E. kugleri* Subzone.

Eu-discoaster calcaris (Gartner) Theodoridis, emended (Pl. 12, fig. 12, pl. 35, figs. 13, 14)

Discoaster calcaris Gartner, 1967, p. 2, pl. 2, figs. 1–3; Martini, 1971, pl. 4, fig. 2; Ellis, Lohman and Wray, 1972, p. 42, pl. 12, figs. 4, 5; Müller, 1974, pl. 7, fig. 8; Proto Decima et al., 1978, pl. 6, figs. 4, 5; Conley, 1979, pl. 1, fig. 15.

Clavodiscoaster calcaris (Gartner) Prins, 1971, pl. 5, fig. 49. Invalid: ICBN art. 33, 2.

Discoaster neohamatus Bukry and Bramlette, Jafar, 1975, partim, p. 50, pl. 6, fig. 2, non: pl. 6, fig. 1.

Discoaster hamatus Martini and Bramlette, Proto Decima et al., 1978, pl. 6, figs. 6a, b.

Eu-discoaster calcaris (Gartner) Theodoridis, 1983, p. 17.

Description: Hexaradial asteroliths with a small central area and long and slender arms. The arms have a roughly circular cross-section, they taper and they may bend slightly in a proximal direction.

The arms terminate in a shallow, V-shaped notch which produces two short, pointed and unequal limbs. The longer limbs point in a clockwise direction (in proximal view). Usually a blade-like protrusion is present on the proximal face of the longer limb.

The central area shows very shallow distal depressions that extend up to its centre, which lacks a distal knob.

The discoasters bear ridges on their proximal face. The ridges are more accentuated on the central area where they bend proximally to form a small proximal knob. The ridges extend along the median axis to the tips of the arms. The arms do not possess a median ridge on their distal face.

Differential diagnosis: *E. calcaris* can be distinguished from *E. kugleri* by the longer and more slender arms and the relatively small central area. It differs from *E. exilis* in the lack of accentuated features on the distal surface of its central area, the unequal bifurcations and the occasional presence of a blade-like trifurcation.

E. loeblichii also bears unequal bifurcations but it is more comparable to *E. variabilis* with parallel-sided arms, distal ridges and blade-like projections that fill the space between the limbs of the bifurcations.

Emendation: The species concept of *E. calcaris* is confined to discoasters with 6 segments. This emendation is intended to permit the distinction of this species from *E. hamatus*.

Remarks: *E. calcaris* and *E. hamatus* are indiscriminable if the number of segments is not taken into consideration. Their retention here as different species facilitates their use in biostratigraphy.

Occurrence: *E. calcaris* ranges from the *E. bellus* Subzone to the *C. pelagicus* Zone.

Eu-discoaster giganteus n. sp.

(Pl. 36, figs. 4–10)

Etymology: From gigas (= giant, Gr.).

Description: The asteroliths have a broad central area and long arms and consist of 6 segments.

The distal surface of the central area is almost flat and without a central knob; in some specimens very shallow depressions can be observed. The depressions extend up to the very centre. No ridges are present on the distal faces of the arms.

The arms show a tiny V-shaped notch at their tips which produces two very short and pointed limbs. No calcareous filling is present between these limbs. A very large third limb is present perpendicular to the proximal surface of the arms. In side view these third limbs are often as large as the free length of the arms. In some specimens the trifurcations are present on only some of the arms.

In proximal view a small stellate central knob can be seen on the central area with its points orientated towards the arms. The points of the proximal knob merge into the ridges which are present on the central area and along the median axes of the arms.

Differential diagnosis: *E. giganteus* is readily distinguished from *E. calcaris* by the large size of its central area, the thicker arms and the larger perpendicular third limbs of the trifurcations. *E. kugleri* has a similarly large central area but the arms are shorter and thinner and the third branches that appear occasionally at the tips of its arms are smaller and oblique.

E. surculus exhibits pronounced features on the distal surface of its central area and ridges on the same surface of its arms. Moreover, the third branch of the trifurcations of *E. surculus* is smaller and extends obliquely relative to the arms and not perpendicular to the arms as in *E. giganteus*.

Holotype: Pl. 36, figs. 5, 6, sample: 231–110, coordinates: 100. 0/6. 6.

Isotypes: Pl. 36, figs. 4, 7, sample: 231–117; Pl. 36, figs. 8–10, sample: 231–113.

Type level: *M. convallis* Subzone.

Type locality: D.S.D.P. Site 231, Indian Ocean.

Occurrence: This species has been observed from the *E. hamatus* Subzone to the *E. pentaradiatus* Subzone.

EU-DISCOASTER COALITUS GROUP

Diagnosis: Asteroliths with predominantly 6 segments and very pronounced sutural ridges on the distal face of the central area.

Eu-discoaster coalitus (Martini and Bramlette) n. comb.

(Pl. 12, fig. 15, pl. 35, figs. 6, 7, 9)

Discoaster musicus Stradner, in Stradner and Papp, 1961, partim, p. 85, pl. 17, figs. 4a, b, non: pl. 17, figs. 5, 7, 8, 10.

Catinaster coalitus Martini and Bramlette, 1963, p. 851, pl. 103, figs. 7–10; Bramlette and Wilcoxon, 1967, p. 108, pl. 8, figs. 9–10; Martini, 1971, pl. 4, fig. 4; Ellis, Lohman and Wray, 1972, pp. 36, 37, pl. 9, fig. 5, 6; Müller, 1974, pl. 10, figs. 1–5; Jafar, 1975, p. 53, pl. 6, fig. 15, 16; Martini, 1980, pl. 3, figs. 1–4.

Description: The asteroliths of this species consist of 5 or 6 segments radially arranged, but they lack arms. The sutures on both sides of the asteroliths are straight, indicating planar attachment surfaces between the segments. They exhibit very deep distal depressions, high distal sutural ridges, a high proximal knob and high ridges.

Occurrence: *E. coalitus* occurs in the interval from the *E. bollii* Subzone to the *E. pentaradiatus* Subzone. The species is absent from our Mediterranean samples.

Eu-discoaster mexicanus (Bukry) n. comb.

(Pl. 35, figs. 10–12)

Catinaster mexicanus Bukry, 1971, p. 50, pl. 3, figs. 7–9; Ellis, Lohman and Wray, 1972, p. 37, pl. 10, fig. 1; Müller, 1974, pl. 10, figs. 6–8; Bukry, 1981, pl. 1, figs. 1–4.

Remarks: The morphology of *E. mexicanus* is comparable to that of *E. coalitus* but it deviates slightly by the blade-like protrusions that form at the terminations of the proximal ridges.

Occurrence: *E. mexicanus* is restricted to the *E. hamatus* Subzone.

Eu-discoaster calyculus (Martini and Bramlette) n. comb.
(Pl. 35, fig. 8)

Catinaster calyculus Martini and Bramlette, 1963, p. 850, pl. 103, figs. 1–6; Bramlette and Wilcoxon, 1967, p. 108, pl. 8, fig. 13; Martini, 1971, pl. 4, fig. 5; Müller, 1974, pl. 10, figs. 9–12; Jafar, 1975, p. 54, pl. 6, figs. 11–12; Martini, 1980, pl. 3, figs. 5–9, pl. 5, figs. 3–6.

Remarks: *E. calyculus* resembles *E. coalitus* but its proximal ridges extend beyond the periphery of the asterolith, forming short pointed free portions.

Occurrence: This species is restricted to the *E. pseudovariabilis* Subzone. The species was not recorded in our Mediterranean sections.

EU-DISCOASTER HAMATUS GROUP

Diagnosis: Asteroliths with predominantly 5 segments.

Eu-discoaster bellus (Bukry) Theodoridis
(Pl. 12, fig. 14, pl. 37, figs. 1–3)

Discoaster quinqueramus Gartner, Ellis, Lohman and Wray, 1972, p. 5, pl. 14, fig. 6; Moshkovitz and Ehrlich, 1980, pl. 6, figs. 1, 23, 24.

Discoaster bellus Bukry, 1971, p. 128, pl. 3, figs. 1, 2; Bukry, 1973, pl. 4, fig. 6; Haq and Berggren, 1978, pl. 4, figs. 3, 8.

Discoaster cf. *D. quinqueramus* Gartner, Moshkovitz and Ehrlich, 1980, pl. 6, figs. 12–15.

Eu-discoaster bellus (Bukry) Theodoridis, 1983, p. 17.

Description: The asteroliths of this species are very small and consist of 5 segments. They are very thin and appear dim in transmitted light except for the tips of their arms which appear brighter. A very small proximal knob is the only feature of the central area visible in the light microscope.

Differential diagnosis: *E. bellus* is distinguished from all other five-rayed species or five rayed variants of species by its very small size and almost featureless proximal and distal surfaces.

Remarks: The specimens figured by Bukry show obvious overgrowth, thus appearing considerably thicker than the specimens observed in our samples.

Occurrence: *E. bellus* is the earliest pentaradial discoaster lacking birefringence and having pointed arm terminations. It ranges from the *E. bellus* Subzone to the *C. leptoporus* Subzone A.

Eu-discoaster hamatus (Martini and Bramlette) Theodoridis,
emended
(Pl. 12, fig. 13, pl. 37, figs. 4–7)

Discoaster hamatus Martini and Bramlette, 1963, pp. 852, 853, pl. 105, figs. 8, 10, 11; Bramlette and Wilcoxon, 1967, p. 110, pl. 7, figs. 9–11; Martini, 1971, pl. 4, fig. 1; Perch-Nielsen, 1972, pl. 9,

fig. 3, pl. 11, figs. 2, 4, 6; Bukry, 1973, pl. 4, fig. 16; Jafar, 1975, p. 49, pl. 5, fig. 15; Haq and Berggren, 1978, pl. 4, fig. 18.

Clavodiscoaster hamatus (Martini and Bramlette) Prins, 1971, pl. 5, fig. 48. Invalid: ICBN art. 33, 2.

Eu-discoaster hamatus (Martini and Bramlette) Theodoridis, 1983, p. 17.

Description: The species includes asteroliths with 3 to 5 segments. The predominant variants are symmetrical with 5 segments. Asymmetrical 5-segmented variants are rare. The variants with 4 segments are cross-shaped.

The asteroliths of *E. hamatus* show a large variation in size. The central area is relatively small. The arms are long and slender and they bend proximally. The cross-section of the arms is roughly circular.

The arms may have a tiny V-shaped notch at their tips which produces two small, pointed and unequal limbs. The arms possess ridges only on their proximal surface. The ridges are situated along the right sides of the arms and they extend towards the centre of the asterolith where they form a low and stellate proximal knob. The proximal knob is slightly rotated and its tips point towards the right sides of the arms (in proximal view).

The proximal ridges extend beyond the bifurcations, and bend proximally and slightly to the right (in proximal view) producing a sense of a clockwise rotation of the arm tips.

The distal face of the central area is ornamented with depressions and a small knob. Some specimens exhibit ridges along the sutural lines of this face of the central area (compare e.g. pl. 11, figs. 2, 4, 6 in Perch-Nielsen, 1972).

Differential diagnosis: *E. hamatus* is distinguished from all other pentaradial discoasters by the clockwise pointing of its arms in proximal view. It differs from *E. calcaris* in the number of arms.

Emendation: From the species concept of *E. hamatus* are excluded variants with 6 segments. This emendation is essential for the differentiation of the species from *E. calcaris* (see also to the description of *E. calcaris*).

Occurrence: This species ranges from the *E. hamatus* Subzone to the *E. pseudovariabilis* Subzone.

Eu-discoaster quinqueramus (Gartner) Theodoridis, emended (Pl. 12, fig. 9, pl. 37, figs. 8–18)

Discoaster quinqueramus Gartner, 1969, p. 598, pl. 1, figs. 1–3; Bukry, 1971, pl. 1, fig. 6; Martini, 1971, pl. 4, fig. 6; Perch-Nielsen, 1971, pl. 9, figs. 1, 2, pl. 10, figs. 2, 4; Bukry, 1973, pl. 4, fig. 27; Müller, 1974, pl. 8, figs. 5–10; Perch-Nielsen, 1977, pl. 15, figs. 12, 15; Proto Decima et al., 1978, pl. 7, fig. 4; Huang, 1980, pl. 6, figs. 4a, b.

Discoaster quintatus Bukry and Bramlette, 1969, p. 133, pl. 1, figs. 6–8.

Discoaster berggrenii Bukry, 1971, p. 45, pl. 2, figs. 4–6; Perch-Nielsen, 1972, pl. 10, figs. 1–3, 5, 7; Bukry, 1973, pl. 4, fig. 7; Proto Decima et al., 1978, pl. 7, figs. 1–3; Haq and Berggren, 1978, pl. 4, fig. 4.

Eu-discoaster quinqueramus (Gartner) Prins, 1971, pl. 5, fig. 54. Invalid: ICBN art. 33, 2.
Eu-discoaster quinqueramus (Gartner) Theodoridis, 1983, p. 18.

Description: The discoasters of *E. quinqueramus* consist of 3 to 6 segments. All variants are symmetrical and the predominant variant has 5 segments.

The proportion of the central area relative to the arms varies greatly and so does the overall size of the asteroliths.

The arms are slender with a roughly circular cross-section; they are tapering and curve proximally. The tips of the arms are pointed. A prominent polygonal knob is present at the centre of the proximal face. The points of the knob are directed to the right side of the arms in proximal view (cf. pl. 12, fig. 9). Relatively low ridges radiate from the points of the knob towards the arms.

In distal view, the central area exhibits very characteristic ridges along the sutural lines. These sutural ridges meet at the centre of the asterolith to form a stellate distal knob with its points orientated towards the interray areas (cf. pl. 37, figs. 8, 10, 11, 12, 14, 17). Distal depressions are present between the sutural ridges.

Differential diagnosis: *E. quinqueramus* is the only discoaster with non-bifurcating tips that exhibits a pronounced proximal knob and distal sutural ridges; as such it is easily distinguished from all other discoasters.

Emendation: The species concept is emended to include specimens with short arms comparable to *E. berggrenii* (Bukry) as well as variants with 3, 4 and 6 segments.

Remarks: Specimens with 3, 4 and extremely rarely 6 segments occur throughout the range of the species. They can easily be assigned to *E. quinqueramus* by the large proximal knobs and the distal sutural ridges on their central areas.

Extremely rich associations of *E. quinqueramus* such as those of D.S.D.P. Sites 231 and 219 revealed all variations between discoasters with short (i.e. *E. berggrenii*) and long arms (i.e. *E. quinqueramus*). Although the number of long-rayed forms increases at the expense of the short-rayed ones in the upper part of the range of the species, both extremes have identical ranges.

Occurrence: From the *G. rotula* Zonule a to the *C. leptoporus* Subzone A. The species is absent from our Mediterranean sections.

EU-DISCOASTER BROUWERI GROUP

Diagnosis: Predominantly hexaradial discoasters with tapering arms and pointed arm terminations. The asteroliths of this group are slightly to strongly bent in a proximal direction.

Eu-discoaster brouweri (Tan Sin Hok emended Bramlette
and Riedel) Theodoridis
(Pl. 36, figs. 11–13)

Remarks: The species is subdivided into two subspecies: *E. brouweri* subsp. *brouweri* n. subsp. and *E. brouweri* subsp. *streptus* n. subsp.

Eu-discoaster brouweri subsp. *brouweri* n. subsp.
(Pl. 36, fig. 13)

- Discoaster brouweri* typ. Tan Sin Hok, 1927, p. 415, figs. 8a, b. Invalid: ICBN art. 43, 1.
- Discoaster brouweri* typ. Tan Sin Hok, 1931, p. 93. Valid: ICBN art. 41, 1b.
- Discoaster brouweri* Tan Sin Hok, sens. emend. Bramlette and Riedel, 1954, p. 402, pl. 39, fig. 12, text-figs. 3a, b; Stradner, in Stradner and Papp, 1961, partim, pp. 85–87, pl. 20, figs. 1, 4, 5, non: pl. 20, figs. 2, 3, 6.
- Discoaster brouweri* Tan Sin Hok, Martini and Bramlette, 1963, p. 851, pl. 102, figs. 9, 10; McIntyre, Bé and Preikstas, 1967, pl. 3, fig. C; Kamptner, 1967, p. 164, pl. 24, fig. 133; Bramlette and Wilcoxon, 1967, p. 109, pl. 8, fig. 12; Black, 1968, pl. 153, fig. 8; Bukry, 1969, pl. 7, fig. C; Cati and Borsetti, 1970, pp. 624, 625, pl. 78, figs. 3–5; Bukry, 1971, pl. 3, fig. 2; Bukry, 1971, pl. 1, figs. 1, 2, 7; Martini, 1971, pl. 4, fig. 15; Nishida, 1971, pl. 18, figs. 7, 8, 9; Perch-Nielsen, 1972, pl. 11, fig. 5; Sachs and Skinner, 1973, pl. 6, fig. 8; Müller, 1974, partim, pl. 8, figs. 2–4, non: pl. 8, fig. 1; Jafar, 1975, p. 46, pl. 7, fig. 12; Perch-Nielsen, 1977, pl. 15, fig. 9; Samtleben, 1978, pl. 5, figs. 1, 2, 3; Proto Decima et al., 1978, pl. 6, fig. 2, pl. 9, figs. 2a, b; Haq and Berggren, 1978, pl. 4, fig. 7; Moshkovitz and Ehrlich, 1980, partim, pl. 6, fig. 17, non: pl. 5, figs. 17, 18, 19; Driever, 1981, pl. 1, figs. 10–13, pl. 3, figs. 6–9; Varol, 1982, pl. 5, figs. 1, 2.
- Discoaster tamalis* Kamptner, 1967, p. 166, pl. 24, fig. 131, text-fig. 28; Perch-Nielsen, 1977, pl. 15, fig. 4; Dermitzakis and Theodoridis, 1978, pl. 2, figs. 1a, 5; Haq and Berggren, 1978, pl. 4, fig. 21; Moshkovitz and Ehrlich, 1980, pl. 6, fig. 21; Driever, 1981, pl. 1, figs. 14, 15, pl. 3, figs. 10, 11.
- Discoaster furus* Kamptner, 1967, p. 164, text-fig. 27.
- Discoaster tarosus* Kamptner, 1967, p. 166, text-fig. 29.
- Discoaster tridenus* Kamptner, 1967, pp. 166, 167, text-fig. 30.
- Discoaster brouweri* Tan Sin Hok *rutellus* Gartner, 1967, p. 2, pl. 1, figs. 1, 2; Nishida, 1971, p. 154, pl. 18, figs. 5, 8; Ellis, Lohman and Wray, 1972, pp. 41, 42, pl. 12, fig. 3.
- Discoaster asymmetricus* Gartner, 1969, p. 598, pl. 1, figs. 1–3; Bukry, 1971, pl. 1, figs. 3–4; Martini, 1971, pl. 4, fig. 12; Ellis, Lohman and Wray, 1972, p. 39, pl. 10, figs. 5, 6; Akers and Koepfel, 1973, pl. 4, fig. 4; Perch-Nielsen, 1977, pl. 15, fig. 3; Dermitzakis and Theodoridis, 1978, pl. 2, fig. 1b; Proto Decima et al., 1978, pl. 6, fig. 2, pl. 9, figs. 2a, b; Haq and Berggren, 1978, pl. 4, fig. 7; Moshkovitz and Ehrlich, 1980, pl. 6, fig. 17; Driever, 1981, pl. 1, figs. 10–13, pl. 3, figs. 6–9; Varol, 1982, pl. 5, figs. 1, 2.
- Discoaster* sp. aff. *D. brouweri* Tan Sin Hok, Bukry, 1969, pl. 6, fig. C.
- Discoaster* sp. Bukry, 1969, pl. 6, figs. A, B.
- Discoaster brouweri recurves* Cati and Borsetti, 1970, p. 626, pl. 80, figs. 1–5.
- Discoaster brouweri tridenus* (Kamptner) Hay, 1970, p. 461.
- Discoaster brouweri tamalis* (Kamptner) Hay, 1970, p. 461.
- Discoaster brouweri triradiatus* (Tan Sin Hok) Hay, 1970, p. 461.
- Discoaster braarudii* Bukry, 1971, pp. 45, 46, pl. 6, fig. C; Bukry, 1973, pl. 4, fig. 10.
- Eu-discoaster *brouweri* (Tan Sin Hok) Prins ssp. *brouweri*, 1971, pl. 5, fig. 55. Invalid: ICBN art. 33, 2 and 43, 1.
- Eu-discoaster *brouweri* (Tan Sin Hok) Prins ssp. 3R 4R, Prins, 1971, pl. 5, fig. 56. Invalid: ICBN art. 33, 2 and 43, 1.

Eu-discoaster asymmetricus (Gartner) Prins, 1971, pl. 5, fig. 56. Invalid: ICBN art. 33, 2.
Discoaster triradiatus Tan Sin Hok, Dermitzakis and Theodoridis, 1978, pl. 2, fig. 4.
Discoaster tridenus Kamptner, sens. emend. Bukry, 1981, p. 462, pl. 3, figs. 15–17.
Eu-discoaster brouweri (Tan Sin Hok) Theodoridis, 1983, p. 17.

Description: The asteroliths consist of 3 to 6 segments. The variants with 4 segments are cross-shaped whereas the variants with 5 segments are asymmetrical. The dominant variants are those with 6 segments.

The central area of the asteroliths is small and the arms are slender, long and tapering. The cross-section of the arms is roughly circular and the terminations are pointed or they may be shaped like a pointed blade.

The distal face of the central area is ornamented by shallow distal depressions and may or may not bear a distal knob. The proximal face of the central area may be featureless or it may show very low ridges that extend from the centre of the asterolith towards the arms. A low and rounded knob may ornament the centre of this face.

The asteroliths of *E. brouweri brouweri* show a continuous variation from flat to pronouncedly bent.

Some specimens show a slight clockwise curvature of their arms (in proximal view).

Differential diagnosis: *E. brouweri brouweri* is distinguished from *E. hamatus* and *E. calcaris* by the pointed arm terminations. It differs from *E. quinquerramus* by the lack of ridges along the sutures of the distal face of the central area and the lack of a pronounced proximal knob.

Occurrence: This subspecies ranges from the *G. rotula* Subzone of the Miocene to the Pliocene zone CN12d.

***Eu-discoaster brouweri* subsp. *streptus* n. subsp.**
(Pl. 36, figs. 11, 12)

Discoaster brouweri Tan Sin Hok, Ellis, Lohman and Wray, 1972, partim, p. 41, pl. 11, fig. 6, pl. 12, fig. 2, non: pl. 11, figs. 4, 5, pl. 12, fig. 1; Akers and Koeppel, 1973, partim, pl. 4, fig. 1, non: pl. 4, fig. 3; Müller, 1974, partim, pl. 8, fig. 1, non: pl. 8, figs. 2–4; Moshkovitz and Ehrlich, 1980, partim, pl. 5, figs. 17, 18, 19, non: pl. 6, fig. 17; Varol, 1982, partim, pl. 5, fig. 4, non: pl. 6, fig. 14.

Discoaster sp. Proto Decima et al., 1978, pl. 6, fig. 1.

Etymology: From *strefo* (= turn, Gr.).

Remarks: This subspecies of *E. brouweri* bears a pronounced stellate proximal knob in addition to all other features characteristic for the other subspecies. The knob is slightly rotated so that its tips are orientated towards the right sides of the arms in proximal view. Ridges radiate from the tips of the knob towards and along the right sides of the arms.

E. brouweri streptus is the dominant subspecies in the Miocene part of the range of *E. brouweri*, but it becomes sporadic in the Pliocene, and it is entirely replaced by *E. brouweri brouweri* prior the last occurrence of the species.

It is distinguished from *E. intercalaris* by the longer arms and from *E. quinqueramus* by the lack of distal sutural ridges.

Holotype: Pl. 36, fig. 12, sample: 231–27, coordinates: 130. 0/5. 4.

Isotype: Pl. 36, fig. 11, sample: 231–90.

Type level: *C. leptoporus* Zone.

Type locality: D.S.D.P. Site 231, Gulf of Aden.

Occurrence: *E. brouweri streptus* occurs from the *E. pseudovariabilis* Subzone of the Miocene to the Pliocene subzone CN12d. In the Upper Pliocene this subspecies has a sporadic occurrence.

Eu-discoaster intercalaris (Bukry) n. comb.
(Pl. 36, figs. 15, 16)

Discoaster intercalaris Bukry, 1971, p. 315, pl. 3, fig. 12, pl. 4, figs. 1, 2.

Description: The asteroliths of this species consist of 6 segments.

The central area and the arms are small. The terminations are blunt. On the proximal face of the central area a prominent stellate knob can be seen. The knob is slightly rotated so that its points are directed towards the right sides of the arms in proximal view. In the same view ridges are observed to radiate from the points of the proximal knob towards and along the right sides of the arms.

A low knob and shallow depressions may be present on the distal face of the central area.

Differential diagnosis: *E. intercalaris* is distinguished from all other discoasters with blunt arms by its short arms.

It differs from *E. altus* (Müller) in the lack of pointed arm tips.

Occurrence: This species has been observed in the *E. pentaradiatus* and the *G. rotula* Subzones.

Eu-discoaster neorectus (Bukry) Theodoridis
(Pl. 36, figs. 14, 17)

Discoaster neorectus Bukry, 1971, pp. 316, 318, pl. 4, figs. 6, 7; Proto Decima et al., 1972, pl. 9, fig. 9; Moshkovitz and Ehrlich, 1980, p. 16, pl. 6, figs. 19, 20.

Eu-discoaster neorectus (Bukry) Theodoridis, 1983, p. 18.

Remarks: *E. neorectus* is comparable to *E. brouweri* but it is larger and complanate.

Occurrence: This species is restricted to the *G. rotula* Subzone. Although present, it is extremely scarce in the Mediterranean sections.

Eu-discoaster altus (Müller) Theodoridis

Discoaster altus Müller, 1974, p. 592, pl. 9, figs. 1–3.

Eu-discoaster altus (Müller) Theodoridis, 1983, p. 17.

Description: This is a species of *Eu-discoaster* with relatively small astero-liths which exhibit a broad central area and six short and pointed arms. A large proximal knob is the main feature of the central area. The knob is stellate and (in proximal view) its tips are orientated towards the right sides of the arms. Short ridges extend from the points of the knob towards and along the right sides of the arms.

Differential diagnosis: *E. altus* is distinguished from *E. intercalaris* by its pointed arms. It differs from *E. brouweri streptus* in having much shorter arms.

Occurrence: Müller (1974) reported this species from the Lower Pliocene (NN14–NN15).

Eu-discoaster tristellifer (Bukry) Theodoridis

Discoaster tristellifer Bukry, 1976, p. 499, pl. 1, figs. 1–17; Bukry, 1981, p. 462, pl. 4, figs. 1–6.

Eu-discoaster tristellifer (Bukry) Theodoridis, 1983, pp. 18, 19.

Remarks: This species has been described by Bukry (1976 and 1981) from Lower Pliocene samples. It has not been observed in our samples.

MORPHOLOGICAL CATEGORIES WITHOUT STATUS OF SEPARATE SPECIES

E. asymmetricus morphotypes

Diagnosis: Asymmetrical astero-liths with five segments, tapering arms and pointed arm terminations.

Remarks: Astero-liths with such characteristics have a biostratigraphically useful acme in the Upper Pliocene (Zone CN12, Subzones CN12a, CN12b) but they occur sporadically from as low as Subzone CN10a (Bukry, 1973a and 1975). In our samples they have been observed from Subzone CN7b (Middle Miocene) upwards.

Gartner (1969) classified these asymmetrical astero-liths as *D. asymmetricus*. Here we reject the species status of this morphological category because asymmetrical, 5-segmented discoasters belong to the variation common for most species of *Eu-discoaster*. The acceptance of asymmetry as a charac-

ter defining species would lead to unnecessary splitting, as asymmetrical forms of all other species then can also be considered as separate species.

Moreover, we wish to avoid classification of such morphotypes within a particular species, because there are more than one species within which the *E. asymmetricus* morphotypes can be included; both *E. brouweri* and *E. bellus* could be considered as potential candidates. Both species have overlapping but not identical ranges which would make the choice of a name impossible.

E. tamalis morphotypes

Diagnosis: Asteroliths with 4 segments, tapering arms and pointed arm terminations. The asteroliths are cross-shaped.

Remarks: Asteroliths with this morphology occur sporadically from zone CN7 up to the lower part of zone CN12. In the interval represented by sub-zones CN12a and CN12b they have a biostratigraphically significant acme. These morphotypes are considered here to belong to different species, such as *E. brouweri*, *E. bellus* and *E. hamatus*.

E. triradiatus morphotypes

Diagnosis: Symmetrical asteroliths with 3 segments. The arms of the asteroliths taper and they are pointed at their terminations.

Remarks: The *E. triradiatus* morphotypes may derive from *E. brouweri*, *E. hamatus*, *E. quinquemus* and *E. bellus*. They occur sporadically throughout the combined ranges of these species (zones CN7 up to CN12).

E. neohamatus morphotypes

Diagnosis: Asteroliths with 6 segments, tapering arms and pointed arm terminations. The arm terminations are curved in clockwise direction when the specimens are observed from their proximal side.

Remarks: The asteroliths depicted by Bukry and Bramlette (1969) as *D. neohamatus* show signs of heavy overgrowth. It is possible that they are preservational artefacts of *E. calcaris* or/and of *E. brouweri streptus* which often also show arm terminations which are curved in a clockwise direction. The *E. neohamatus* morphotypes occur from zone CN7 to zone CN8a.

Despite the preservational origin of such asteroliths we retain their distinction under an informal name as they are useful for the biostratigraphic assignment of samples from that interval in which the asteroliths are largely altered by overgrowth.

E. moorei morphotypes

Diagnosis: Asymmetrical asteroliths with 5 segments and arms with bifurcated terminations.

Remarks: The *E. moorei* morphotypes may be asymmetrical variants of *E. deflandrei*, *E. variabilis* and *E. exilis*.

REFERENCES

- Achuthan, M. V. and Stradner, H. (1969). Calcareous nannoplankton from the Wemmelian stratotype. *In* Brönnimann, P. and Renz, H. H. (ed.), Proc. First Int. Conf. Plankt. Microfos., Geneva, 1967, E. J. Brill, Leiden, 1, pp. 1–13.
- Akers, H. W. and Koepfel, P. E. (1973). Age of some Neogene formations, Atlantic Coast Plains, United States and Mexico. *In* Smith, L. A. and Hardenbol, J. Proc. Symp. Calc. Nannofos., Gulf Coast Section S.E.P.M., Houston 1973, pp. 80–93.
- Backman, J. (1978). Late Miocene-Early Pliocene nannofossil biochronology and biogeography in the Vera basin, SE Spain. *Stockholm Contr. Geol.*, 32, pp. 93–114.
- Backman, J. (1980). Miocene-Pliocene nannofossils and sedimentation rates in the Hatton-Rockall basin, NE Atlantic Ocean. *Stockholm Contr. Geol.*, 36, pp. 1–91.
- Baldi-Beke, M. (1977). Stratigraphical and faciological subdivisions of the Oligocene as based on Nannoplankton. *Bull. Hungarian Geol. Soc.*, 107, pp. 59–69.
- Baldi-Beke, M. (1980). The nannoplankton of the Oligocene-Miocene sediments underlying the Borzsony Mts. (N. Hungary) andesites. *Bull. Hungarian Geol. Soc.*, 110, pp. 159–179.
- Barbieri, F. and Rio, D. (1974). Calcareous nannoplankton from the Upper Miocene (Messinian) of the Crostolo Torrent (W. Emily). *Ateneo Parmense, Acta Nat.*, 10, pp. 15–28.
- Bemmelen van, R. W. (1949). The Geology of Indonesia. Staatsdrukkerij, The Hague, 732 pp.
- Bersier, A. (1939). Discoastéridées et Coccolithophoridées des marnes Oligocènes vaudoises. *Bull. Soc. Vaud. Sc. Nat.*, 60, pp. 229–248.
- Biolzi, M. and Perch-Nielsen, K. (1982). *Helicosphaera truempyi*, a new Early Miocene calcareous nannofossil. *Eclogae Geol. Helv.*, 75, pp. 171–175.
- Biolzi, M., Perch-Nielsen, K. and Ramos, I. (1981). *Triquetrorhabdulus* — an Oligocene/Miocene calcareous nannofossil genus. *INA newsletter*, 3, pp. 89–92.
- Bizon, G. and Müller, C. (1977). Remarks on some biostratigraphic problems in the Mediterranean Neogene. *Int. Symp. on the Structural History of the Mediterranean Basins*, Split, pp. 381–390.
- Bizon, G. and Müller, C. (1979). Remarks on the Oligocene/Miocene boundary based on results obtained from the Pacific and the Indian Oceans. VIIth Int. Congr. Medit. Neogene, Athens 1979, *Ann. Géol. Pays Hellén. Tome hors séries*, 1, pp. 101–111.
- Black, M. (1965). Coccoliths. *Endeavour*, 24, pp. 131–137.
- Black, M. (1968). Taxonomic problems in the study of coccoliths. *Paleont.*, 11, pp. 793–813.
- Black, M. (1971). The systematics of coccoliths in relation to the paleontological record. *In* Funnell, B. M. and Riedel, W. R. (ed). *The Micropaleontology of the Oceans*, pp. 611–621.
- Black, M. and Barnes, B. (1961). Coccoliths and discoasters from the floor of the south Atlantic Ocean. *Journ. Royal Microscopical Soc.*, 80, pp. 137–147.
- Boudreaux, J. E. (1974). Calcareous Nannoplankton Ranges, Deep Sea Drilling Project Leg. 23, Init. Rpts. D.S.D.P., 23, pp. 1073–1090.
- Boudreaux, J. E. and Hay, W. W. (1969). Calcareous nannoplankton and biostratigraphy of the Late Pliocene-Pleistocene-Recent sediments in the Submarex cores. *Rev. Esp. Micropal.*, 1, pp. 249–292.
- Braarud, T., Deflandre, G., Halldal, P. and Kamptner, E. (1955). Terminology, nomenclature, and systematics of the Coccolithophoridae. *Micropaleontology*, 1, pp. 157–159.
- Bramlette, M. N. and Riedel, W. R. (1954). Stratigraphic value of discoasters and some other microfossils related to recent coccolithophores. *Journ. of Paleontology*, 28, pp. 385–403.
- Bramlette, M. N. and Sullivan, F. R. (1961). Coccolithophorids and related nannoplankton of the Early Tertiary in California. *Micropal.*, 7, pp. 129–188.
- Bramlette, M. N. and Wilcoxon, J. A. (1967). Middle Tertiary calcareous nannoplankton of the Cipero section, Trinidad. *W. I. Tulane Studies Geol.*, 5, pp. 93–132.
- Bramlette, M. N. and Wilcoxon, J. A. (1967). *Discoaster druggii* nom. nov. pro *Discoaster extensus* Bramlette and Wilcoxon 1967, non Hay, 1967. *Tulane Studies Geol.*, 5, p. 220.

- Brönnimann, P. and Stradner, H. (1960). Die Foraminiferen- und Discoasteridenzonen von Kuba und ihre interkontinentale Korrelation. *Erdöl Zeitschrift*, 76, pp. 364–369.
- Bukry, D. (1970). Coccolith age determination. *Init. Repts. D.S.D.P.*, 2, pp. 349–355.
- Bukry, D. (1970). Coccolith age determination. *Init. Repts. D.S.D.P.*, 3, pp. 589–611.
- Bukry, D. (1971). *Discoaster* evolutionary trends. *Micropaleontology*, 17, pp. 43–52.
- Bukry, D. (1971). Cenozoic calcareous nannofossils from the Pacific Ocean. *Trans. San Diego Soc. of Nat. Hist.*, 16, pp. 303–327.
- Bukry, D. (1971). Coccolith stratigraphy. *Init. Repts. D.S.D.P.*, 6, pp. 965–1004.
- Bukry, D. (1971). Coccolith stratigraphy. *Init. Repts. D.S.D.P.*, 7, pp. 1513–1528.
- Bukry, D. (1972). Further comments on coccolith stratigraphy. *Init. Repts. D.S.D.P.*, 12, pp. 1071–1083.
- Bukry, D. (1973). Coccolith stratigraphy. *Init. Repts. D.S.D.P.*, 13, pp. 817–822.
- Bukry, D. (1973). Low-latitude coccolith biostratigraphic zonation. *Init. Repts. D.S.D.P.*, 15, pp. 685–703.
- Bukry, D. (1973). Coccolith stratigraphy, Eastern equatorial Pacific, Leg 16, Deep Sea Drilling Project. *Init. Repts. D.S.D.P.*, 16, pp. 65–711.
- Bukry, D. (1973). Phytoplankton stratigraphy, central Pacific Ocean. *Init. Repts. D.S.D.P.*, 17, pp. 871–889.
- Bukry, D. (1974). Coccoliths as paleosalinity indicators – evidence from Black Sea. *The Black Sea, geology, chemistry and biology. Am. Assoc. Petrol. Geol. Memoir*, 20, pp. 353–363.
- Bukry, D. (1975). Coccolith and silicoflagellate stratigraphy, Northwestern Pacific Ocean. *Init. Repts. D.S.D.P.*, 32, pp. 677–692.
- Bukry, D. (1976). Coccolith stratigraphy of Manihiki Plateau, Central Pacific, Deep Sea Drilling Project, Site 317. *Init. Repts. D.S.D.P.*, 33, pp. 493–501.
- Bukry, D. (1978). Cenozoic silicoflagellate and coccolith stratigraphy. SE Atlantic Ocean. *Init. Repts. D.S.D.P.*, 40, pp. 635–649.
- Bukry, D. (1978). Cenozoic coccoliths and silicoflagellate stratigraphy, offshore Northwest Africa. *Init. Repts. D.S.D.P.*, 41, pp. 689–707.
- Bukry, D. (1978). Biostratigraphy of Cenozoic marine sediment by calcareous nannofossils. *Micropaleontology*, 24, pp. 44–60.
- Bukry, D. (1980). Coccolith stratigraphy, tropical Eastern Pacific Ocean. *Init. Repts. D.S.D.P.*, 54, pp. 535–543.
- Bukry, D. (1981). Pacific coast coccolith stratigraphy between Point Conception and Cabo Corrientes, Deep Sea Drilling Project Leg 63 (1). *Init. Repts. D.S.D.P.*, 63, pp. 445–471.
- Bukry, D. (1981). Cenozoic coccoliths from the D.S.D.P. SEPM special publ., 32, pp. 335–353.
- Bukry, D., Brabb, E. E. and Vedder, J. G. (1973). Correlation of Tertiary nannoplankton assemblages from the coast and peninsular ranges of California. *Proc. 2nd Latin American Geol. Congr.*, pp. 1–33.
- Bukry, D. and Bramlette, M. N. (1968). Stratigraphic significance of two genera of Tertiary calcareous nannofossils. *Tulane Studies Geol.*, 6, pp. 149–155.
- Bukry, D. and Bramlette, M. N. (1969). Coccolith age determinations, Leg 1, Deep Sea Drilling Project. *Init. Repts. D.S.D.P.*, 1, pp. 369–387.
- Bukry, D. and Bramlette, M. N. (1969). Some new and stratigraphically useful calcareous nannofossils of the Cenozoic. *Tulane Studies Geol. Pal.*, 7, pp. 131–142.
- Bukry, D. and Bramlette, M. N. (1970). Coccolith age determinations Leg 3, Deep Sea Drilling Project. *Init. Repts. D.S.D.P.*, 3, pp. 589–611.
- Bukry, D., Douglas, R. G., Kling, S. A. and Krasheninnikov, V. (1971). Planktonic microfossil biostratigraphy of the Northwestern Pacific Ocean. *Init. Repts. D.S.D.P.*, 6, pp. 1253–1300.
- Bukry, D. and Percival, S. F. (1971). New Tertiary calcareous nannofossils. *Tulane Studies Geol. Pal.*, 8, pp. 123–146.
- Bystrická, H. (1966). Nouvelles espèces du genre *Discoaster* du Paléogène des Karpates Occidentales. *Geol. Sbor. Slov. Akad. Vied, Bratislava*, 17, pp. 237–240.

- Cati, F. and Borsetti, A. M. (1970). I discoasteridi del miocene delle Marche. *Giornale di Geologia*, 2, pp. 617–652.
- Cita, M. B. (1973). Inventory of biostratigraphical findings and problems. *Init. Repts. D.S.D.P.*, 13, pp. 1045–1073.
- Clocchiatti, M. (1969). Contribution a l'étude de *Helicosphaera carteri* (Wallich) Kamptner (Coccolithophoridae). *Revue de Micropaléontologie*, 12, pp. 75–83.
- Colalongo, M. L. et al. (1979). A proposal for the Tortonian – Messinian boundary. *Proc. VIIth Int. Congr. Medit. Neogene, Ann. Géol. Pays Hellén.*, tome hors série, pp. 285–294.
- Conley, S. M. (1979). Recent coccolithophores from the Great Barrier Reef – Coral Sea region. *Micro-paleontology*, 25, pp. 20–43, pls. 1–6.
- Deflandre, G. (1934). Les Discoasteridés, microfossiles calcaires incertae sedis. *Bull. Soc. Franc. Micr.*, 3, pp. 59–67.
- Deflandre, G. (1952). Classe des Coccolithophoridés (Coccolithophoridae Lohmann, 1902). *In* Grassé, P. P. (1952). *Traité de zoologie*. Masson, Paris, 1, pp. 439–470.
- Deflandre, G. (1953). Hétérogénéité intrinsèque et pluralité des éléments dans les coccolithes actuels et fossiles. *C. R. Acad. Sc., Paris*, 237, pp. 1785–1787.
- Deflandre, G. and Fert, C. (1954). Observations sur les coccolithophoridés actuels et fossiles en microscopie ordinaire et électronique. *Ann. Paléont.*, 40, pp. 1–68.
- Deflandre, G. and Fert, C. (1968). Observations sur les coccolithophoridés actuels et fossiles en microscopie ordinaire et électronique. 2nd edition, *Ann. Paléont.*, 40, pp. 1–68.
- Dermitzakis, M. D. (1978). Stratigraphy and sedimentary history of the Miocene of Zakynthos (Ionian Islands, Greece). *Ann. Géol. Pays Hellén.*, 29, pp. 47–186.
- Dermitzakis, M. D. and Theodoridis, S. (1978). Planktonic foraminifera and calcareous nannoplankton from the Pliocene of Koufonisi Island (E. Crete, Greece). *Ann. Géol. Pays Hellén.*, 29, pp. 630–642.
- Driever, B. W. M. (1981). A quantitative study of Pliocene associations of *Discoaster* from the Mediterranean. *Proc. Kon. Ned. Akad. Wetensch.*, B, 84, pp. 437–455.
- Edwards, A. R. (1968). The calcareous nannoplankton evidence for New Zealand Tertiary marine climate. *Tuatara*, 16, 1, pp. 26–31.
- Ehrenberg, C.G. (1854). *Mikrogeologie. Das Erden und Felsen schaffende Wirken des unsichtbar kleinen selbständigen Lebens auf der Erde*. Leipzig, 374 pp.
- Ellis, H. (1975). Calcareous nannofossil biostratigraphy, Deep Sea Drilling Project Leg 31. *Init. Repts. D.S.D.P.*, 31, pp. 655–676.
- Ellis, H. (1979). Neogene nannoplankton zonation in Eastern Mediterranean. *Ann. Géol. Pays Hellén.*, tome hors série, pp. 391–401.
- Ellis, H. and Lohman, W. H. (1979). Neogene calcareous nannoplankton biostratigraphy in Eastern Mediterranean deep-sea sediments, *D.S.D.P. Leg 42A*, sites 375 and 376. *Mar. Micropal.*, 4, pp. 61–84.
- Ellis, H., Lohman, W. H. and Wray, J. L. (1972). Upper Cenozoic Calcareous nannofossils from the Gulf of Mexico, *D.S.D.P. Leg 1*, site 3. *Quart. Colorado School of Mines*, 67, pp. 1–103.
- Farinacci, A. (1969–1983). *Catalogue of calcareous nannofossils*. *Tecnoscienza* (publ.), Roma, volumes 1–11.
- Farinacci, A. (1971). Round Table on calcareous nannoplankton. *Proc. II Plankt. Conf.*, Rome 1970, 2, pp. 1343–1360.
- Felix, R. (1973). Oligo-Miocene stratigraphy of Malta and Gozo. *Meded. Landbouwhogeschool Wageningen*, 73–20, pp. 1–103.
- Fleisher, R. L. (1974). Cenozoic planktonic foraminifera and Biostratigraphy, Arabian Sea. *Deep Sea Drilling Project Leg. 23. Init. Repts. D.S.D.P.*, 23, pp. 1001–1072.
- Fuchs, R. and Stradner, H. (1977). Ueber Nannofossilien im Badenien (Mittelmiozaen) der Zentralen Paratethys. *Beitr. Palacont. Oesterr.*, 2, pp. 1–58.
- Gaarder, K. R. (1970). Three new taxa of coccolithineae. *Mytt. mag. bot.*, 17, pp. 113–126.

- Gaarder, K. R. and Hasle, G. R. (1971). Coccolithophorids of the Gulf of Mexico. *Mar. Science*, 21, pp. 519--544.
- Gartner, S. (1967). Nannofossil species related to *Cyclococcolithus leptoporus*. *Univ. of Kansas Paleontological Contr.*, 28, pp. 1-3.
- Gartner, S. (1967). Calcareous nannofossils from the Neogene of Trinidad, Jamaica and Gulf of Mexico. *Univ. of Kansas, Paleontological Contr.*, 29, pp. 3-7.
- Gartner, S. (1969). Correlation of Neogene planktonic foraminifera and calcareous nannofossil zones. *Trans. Gulf Coast Assoc. of Geol. Societies*, 19, pp. 585-599.
- Gartner, S. (1969). Two new calcareous nannofossils from the Gulf Coast Eocene. *Micropaleontology*, 15, pp. 31-34.
- Gartner, S. (1973). Absolute Chronology of the Late Neogene calcareous nannofossil succession in the equatorial Pacific. *Geol. Soc. America Bull.*, 84, pp. 2021-2034.
- Gartner, S. (1974). Nannofossil biostratigraphy, Leg 22, Deep Sea Drilling Project. *Init. Repts. D.S.D.P.*, 22, pp. 577-599.
- Gartner, S. (1977). Calcareous nannofossil biostratigraphy and revised zonation of the Pleistocene. *Mar. Micropal.*, 2, pp. 1-25.
- Gartner, S. (1977). Nannofossils and biostratigraphy, an overview. *Earth-Science Reviews*, 13, pp. 227-250.
- Gartner, S. (1977). Nannofossil biostratigraphy of the Monte Narbone Formation at the type locality of the Rossellian Superstage. *Riv. Ital. Paleontol.*, 83, pp. 179-190.
- Gartner, S. and Bukry, D. (1974). *Ceratolithus acutus* Gartner and Bukry n. sp. and *Ceratolithus amplificus* Bukry and Percival-nomenclatural clarification. *Tulane Studies Geol. Pal.*, 11, pp. 115-118.
- Gartner, S. and Bukry, D. (1975). Morphology and phylogeny of the coccolithophyceae family Ceratolithaceae. *Journ. Research U.S. Geol. Survey*, 3, pp. 451-465.
- Gartner, S. and Smith, L. A. (1967). Coccoliths and related calcareous nannofossils from the Yazoo Formation (Jackson, Late Eocene) of Louisiana. *Univ. of Kansas Pal. Contr.*, 20, pp. 1-6.
- Genevraye, P. de and Samuel, L. (1972). Geology of the Kendeng zone (Central and East Java). *Proc. First An. Conv. Indonesian Petr. Assoc.*, pp. 17-30.
- Gorsel, J. T. van and Troelstra, S. R. (1981). Late Neogene planktonic foraminiferal biostratigraphy and climatostratigraphy of the Solo river section (Java, Indonesia). *Mar. Micropal.*, 6, pp. 183-209.
- Grassé, P. P. (1952). *Phylogénie. Protozoaires: généralités. Flagellés. Traité de zoologie. Anatomie, systématique, biologie.*, 1. Masson, Paris (ed.) xii + 1071 pp.
- Hansen, H. J., Schmidt, R. R. and Mikkelsen, N. (1975). Convertible techniques for the study of the same nannoplankton specimen. *Kon. Ned. Akad. Wet. Proc.*, B, 78, pp. 225-230.
- Haq, B. U. (1966). Electron microscope studies on some Upper Eocene calcareous nannoplankton from Syria. *Stockholm Contr. Geol.*, 15, pp. 23-37.
- Haq, B. U. (1967). Calcareous nannoplankton from the Lower Eocene of Zinda Pir, District Dera Ghazi Khan, West Pakistan. *Geol. Bull. Punjab Univ.*, 6, pp. 55-83.
- Haq, B. U. (1968). Studies on Upper Eocene calcareous nannoplankton from NW Germany. *Stockholm Contr. Geol.*, 18, pp. 13-74.
- Haq, B. U. (1969). The structure of Eocene coccoliths and discoasters from a Tertiary deep-sea core in the Central Pacific. *Stockholm Contr. Geol.*, 21, pp. 1-19.
- Haq, B. U. (1971). Paleogene calcareous nannoflora. Part 1: The Paleocene of West-Central Persia and the Upper Paleocene-Eocene of West Pakistan. *Stockholm Contr. Geol.*, 25, pp. 1-56.
- Haq, B. U. (1971). Paleogene calcareous nannoflora. Part 2: Oligocene of Western Germany. *Stockholm Contr. Geol.*, 25, pp. 1-97.
- Haq, B. U. (1971). Paleogene calcareous nannoflora. Part 3: Oligocene of Syria. *Stockholm Contr. Geol.*, 25, pp. 1-127.
- Haq, B. U. (1973). Evolutionary trends in the Cenozoic coccolithophore genus *Helicopontosphaera*. *Micropaleontology*, 19, pp. 32-52.

- Haq, B. U. (1978). Calcareous Nannoplankton. In Haq, B. U. and Boersma, A. (ed.). Introduction to marine micropaleontology, Elsevier, New York, pp. 79–107.
- Haq, B. U. (1984). Jurassic to Recent nannofossil biochronology: an update. In Haq, B. U. (ed.), Nannofossil Biostratigraphy. Benchmark Papers in Geology, 78, pp. 358–378.
- Haq, B. U. and Berggren, W. A. (1978). Late Neogene calcareous plankton biochronology of the Rio Grande Rise (S. Atlantic Ocean). J. Paleont., 52, pp. 1167–1194.
- Haq, B. U. and Lohmann, G. P. (1976). Early Cenozoic calcareous nannoplankton biogeography of the Atlantic Ocean. Mar. Micropal., 1, pp. 119–194.
- Haupt, O. (1906). Eine Kreide ähnlicher, wahrscheinlich jungtertiärer Kalkmergel aus Kaiser-Wilhelmsland (Deutsch-Neu-Guinea). Z. Deutsch. Geol. Ges., 57, pp. 565–569.
- Hay, W. W. (1970). Calcareous nannofossils from cores recovered on Leg 4. Init. Repts. D.S.D.P., 4, pp. 455–501.
- Hay, W. W. (1977). Calcareous nannofossils. In Ramsay, A.T.S. (ed.). Oceanic Micropal., 2, pp. 1055–1200.
- Hay, W. W., Mohler, H. P. and Wade, M. E. (1966). Calcareous nannofossils from Nal'chik (Northwest Caucasus). Eclog. Geol. Helv., 59, pp. 379–399.
- Hay, W. W., Mohler, H. P., Roth, P. H., Schmidt, R. R. and Broudreux, J. E. (1967). Calcareous nannoplankton zonation of the Cenozoic of the Gulf Coast and Caribbean-Antillean area and transoceanic correlation. Trans. Gulf Coast Assoc. of Geol. Soc., 17, pp. 428–480.
- Hay, W. W. and Towe, K. M. (1962). Electron microscopic examination of some coccoliths from Donzacq (France). Eclog. Geol. Helv., 55, pp. 497–517.
- Hojjat-zadeh, M. (1978). Discoasters of the blue clay (Middle Miocene) of Malta and Gozo. Geol. Magazine, 115, pp. 1–80.
- Honjo, S. and Okada, H. (1974). Community structure of coccolithophores in the photic layer of the mid-Pacific. Micropaleontology, 20, pp. 209–230.
- Huang, T. C. (1977). Calcareous nannoplankton Stratigraphy of the Upper Wulai Group (Oligocene) in Northern Taiwan. Petr. Geol. Taiwan, 14, pp. 147–179.
- Huang, T.C. (1980). Oligocene to Pleistocene calcareous nannofossil biostratigraphy of the Hsüehshan Range and Western Foothills in Taiwan. Geol. Pal. Southeast Asia, 21, pp. 191–210.
- Huang, T. C. and Okamoto, K. (1980). Calcareous nannofossils from the Miocene formations in Yuya and Iki, Southwest Japan. Bull. Mizunami Fossil Mus., 7, pp. 69–72.
- INA Newsletter (1979–1983) volumes 1–5.
- Jafar, S. A. (1975). Calcareous nannoplankton from the Miocene of Rotti, Indonesia. Kon. Ned. Akad. Wet. Verh., 28, pp. 1–99.
- Jafar, S. A. and Martini, E. (1975). On the validity of the calcareous nannoplankton genus *Helicosphaera*. Senck. Lethaia, 56, pp. 381–397.
- Jerković, L. (1971). *Syracosphaera beogradiensis* nov. sp. des coccolithophoridés du Sarmatien des environs de Pancevo (Yougoslavie). Bull. Sci., A16, pp. 206–207.
- Jukes-Browne, A.J. and Harrison, J. B. (1892). The geology of Barbados. Part II. The oceanic deposits. Quart. J. Geol. Soc. London, 48, pp. 170–226.
- Kamptner, E. (1941). Die Coccolithineen der Südwestküste von Istrien. Ann. Naturhist. Mus. Wien, 51, pp. 54–148.
- Kamptner, E. (1944). Coccolithineen-Studien im Golf von Neapel. Österr. Bot. Z., 93, pp. 138–147.
- Kamptner, E. (1948). Coccolithen aus dem Torton des Inneralpinen Wiener Beckens. Sitzber. Österr. Akad. Wiss. Math.-Naturw. Kl., 1, pp. 157.
- Kamptner, E. (1954). Untersuchungen über den Feinbau der Coccolithen. Arch. Protistenkunde, 100, pp. 1–9.
- Kamptner, E. (1955). Fossile Coccolithineen-Skelettreste aus Insulinde. Eine Mikropaläontologische Untersuchung. Verh. Kon. Acad. Wet., Afd. Natuurk., ser. 2, 50, pp. 1–105.
- Kamptner, E. (1956). Zur Systematik und Nomenklatur der Coccolithineen. Anz. der Akad. der Wissenschaft. Wien, 1, pp. 4–11.

- Kamptner, E. (1958). Betrachtungen zur Systematik der Kalkflagellaten, nebst Versuch einer neuen Gruppierung der Chrysomonadales. Arch. Protistenk., 103, pp. 54–116.
- Kamptner, E. (1963). Coccolithineen-Skelettreste aus Tiefseeablagerungen des Pazifischen Ozeans. Ann. Naturhist. Mus. Wien, 66, p. 139–204.
- Kamptner, E. (1967). Kalkflagellaten-Skelettreste aus Tiefseeschlamm des Süd-atlantischen Ozeans. Ann. Naturhist. Mus. Wien, 71, pp. 117–198.
- Kapellos, C. (1973). Biostratigraphie des Gurnigelflysches mit besonderer Berücksichtigung der Nummuliten und des Nannoplanktons, unter Einbeziehung des Paläogenen Nannoplanktons der Krim (U.D.S.S.R.). Mém. Suisse Paléont., 96.
- Kapellos, C. and Schaub, H. (1973). Zur Korrelation von Biozonierungen mit Grossforaminiferen und Nannoplankton im Paläogen der Pyrenäen. Eclog. Geol. Helv., 66, pp. 687–737.
- Klumpp, B. (1953). Beitrag zur Kenntnis der Mikrofossilien des Mittleren und Oberen Eozän. Paläontographica, 103A, pp. 377–406.
- Krashennikov, V. A. and Pflaumann, U. (1978). Zonal stratigraphy of Neogene deposits of the Eastern part of the Atlantic Ocean by means of planktonic foraminifers, Leg 41, Deep Sea Drilling Project. Init. Repts. D.S.D.P., 41, pp. 613–657.
- Langereis, C. G., Zachariasse, W. J. and Zijdeveld, J. D. A. (1984). Late Miocene Magnetobiostratigraphy of Crete. Mar. Micropal., 8, pp. 261–281.
- Levin, H. L. and Joerger, A. P. (1967). Calcareous nannoplankton from the Tertiary of Alabama. Micropaleontology, 13, pp. 163–182.
- Lézaud, L. (1968). Espèces nouvelles de nannofossiles calcaires (Coccolithophoridés) d'Aquitaine Sud-Ouest. Rev. Micropal., 11, pp. 22–28.
- Loeblich, A. R. and Tappan, H. (1963). Type fixation and validation of certain calcareous nannofossil genera. Proc. Biol. Soc. Wash., 76, pp. 191–196.
- Loeblich, A. R. and Tappan, H. (1966). Annotated index and bibliography of the calcareous nannoplankton, part I, Phycologia, 5, pp. 81–216.
- Loeblich, A. R. and Tappan, H. (1968). Annotated index and bibliography of the calcareous nannoplankton, part II, Journ. Paleont., 42, pp. 584–598.
- Loeblich, A. R. and Tappan, H. (1969). Annotated index and bibliography of the calcareous nannoplankton, part III, Journ. Paleont., 43, pp. 568–588.
- Loeblich, A. R. and Tappan, H. (1970). Annotated index and bibliography of the calcareous nannoplankton, part IV, Journ. Paleont., 44, pp. 558–574.
- Loeblich, A. R. and Tappan, H. (1970). Annotated index and bibliography of the calcareous nannoplankton, part B, Phycologia, 9, pp. 157–174.
- Loeblich, A. R. and Tappan, H. (1971). Annotated index and bibliography of the calcareous nannoplankton, part VI, Phycologia, 10, pp. 315–339.
- Loeblich, A. R. and Tappan, H. (1973). Annotated index and bibliography of the calcareous nannoplankton, part VII, Journ. Paleont., 47, pp. 715–759.
- Loeblich, A. R. and Tappan, H. (1978). The coccolithophorid genus *Calcidiscus* Kamptner and its synonyms. Journ. Paleont., 52, pp. 1390–1392.
- Lohmann, H. (1902). Die Coccolithophoridae, eine Monographie der Coccolithen bildenden Flagellaten, zugleich ein Beitrag zur Kenntnis des Mittelmearauftriebs. Arch. Protistenk., 1, pp. 89–165.
- Lohmann, H. (1920). Die Bevölkerung des Ozeans mit Plankton nach den Ergebnissen der Zentrifugenfänge während der Ausreise der "Deutschland" 1911, zugleich ein Beitrag zur Biologie des Atlantischen Ozeans. Arch. Biontol., 4, pp. 1–617.
- Lord, A. R. and Taylor, R. J. (1982). In Lord, A. R. (ed.). A stratigraphical index of calcareous nannofossils. Ellis Horwood Ltd. (publ.), Chichester, pp. 1–189.
- Marks, P. (1957). Stratigraphic lexicon of Indonesia. Keilmuan (publ.), 31, pp. 1–130.
- Martini, E. (1958). Discoasteriden und verwandte Formen im NW-deutschen Eozän (Coccolithophorida). 1. Taxonomische Untersuchungen. Senck. Leth., 39, pp. 353–388.

- Martini, E. (1960). Braarudosphaeriden, Discoasteriden und verwandte Formen aus dem Rupelton des Mainzer Beckens. Notizbl. Hess. Landesamt Bodenforsch. Wiesbaden, 88, pp. 65–87.
- Martini, E. (1961). Nannoplankton aus dem Tertiär und der Obersten Kreide von SW. Frankreich. Senck. Leth., 42, pp. 1–32.
- Martini, E. (1965). Mid-Tertiary calcareous nannoplankton from Pacific deep-sea cores. In Whittard, W. F. and Bradshaw, R. B. (ed.). Submarine geology and geophysics. Proc. 17th Symp. Colston Res. Soc., Butterworths (publ.), London, pp. 393–411.
- Martini, E. (1969). Nannoplankton aus dem Latdorf (locus typicus) und weltweite Parallelisierungen im oberen Eozän und Unteren Oligozän. Senck. Leth., 50, pp. 117–159.
- Martini, E. (1970). Standard Paleogene calcareous nannoplankton zonation. Nature, 226, pp. 560–561.
- Martini, E. (1971). Standard Tertiary and Quaternary calcareous nannoplankton zonation. Proc. II Plankt. Conf., Roma 1970, pp. 739–785.
- Martini, E. (1976). Cretaceous to Recent calcareous nannoplankton from the Central Pacific Ocean (D.S.D.P. Leg 33). Init. Repts. D.S.D.P., 33, pp. 383–423.
- Martini, E. (1980). Oligocene to Recent calcareous nannoplankton from the Philippine Sea, Deep Sea Drilling Project Leg 59. Init. Repts. D.S.D.P., 59, pp. 547–565.
- Martini, E. and Bramlette, M.N. (1963). Calcareous nannoplankton from the experimental Mohole drilling. Journ. Paleont., 37, pp. 845–856.
- Martini, E. and Müller, C. (1972). Nannoplankton aus dem nördlichen Arabischen Meer. Meteor. Forsch.-Ergebnisse, 10, pp. 63–74.
- Martini, E. and Worsley, T. (1970). Standard Neogene calcareous nannoplankton zonation. Nature, 225, pp. 289–290.
- Martini, E. and Worsley, T. (1971). Tertiary calcareous nannoplankton from the Western Equatorial Pacific. Init. Repts. D.S.D.P., 7, pp. 1471–1507.
- McIntyre, A. and Bé, A. W. H. (1967). Modern coccolithophoridae of the Atlantic Ocean – I. Placoliths and cyrtoliths. Deep-Sea Research, 14, pp. 561–597.
- McIntyre, A., Bé, A. W. H. and Preikstas, R. (1967). Coccoliths and the Pliocene-Pleistocene boundary. Progress in oceanography, 4, pp. 3–25.
- McIntyre, A., Bé, A. W. H. and Roche, M. B. (1970). Modern Pacific coccolithophorida: a paleontological thermometer. Trans. N.Y. Acad. Sciences, ser. 2, 32, pp. 720–731.
- Miller, P. L. (1981). Tertiary calcareous nannoplankton and benthic foraminifera biostratigraphy of the Point Arena area, California. Micropaleontology, 27, pp. 419–443.
- Milow, E. D. (1970). Tentative nannofossil zones and subzones and their radiometric age Northeast Pacific. Init. Repts. D.S.D.P., 5, pp. 8–10.
- Moshkovitz, S. (1974). A new method for observing the same nannofossil specimens both by light microscope and scanning electron microscope and preservation of types. Isr. Journ. Earth Sciences, 23, pp. 145–147.
- Moshkovitz, S. (1978). New types of cover-slip and mounting-slide with a graticule for examination of the same small object both in light microscope and in scanning electron microscope. Microsc. Acta., 80, pp. 161–166.
- Moshkovitz, S. and Ehrlich, A. (1980). Distribution of the calcareous nannofossils in the Neogene sequence of the Jaffa-1 borehole, Central coastal plain, Israel, GSI, Project no. 29926, pp. 1–25.
- Moshkovitz, S. and Martinotti, G. M. (1979). The biostratigraphy of the Pliocene-Pleistocene sequence of some boreholes in the Caesaria and Netanya Areas (Calcareous Nannofossils, Planctonic Foraminifera and Molluscs). Isr. J. Earth Sciences, 28, pp. 110–127.
- Müller, C. (1970). Nannoplankton-Zonen der Unteren-Meeressmolasse Bayerns. Geol. Bavarica, 63, pp. 107–118.
- Müller, C. (1972). Kalkiges Nannoplankton aus Tiefseekernen des Ionischen Meers. Meteor. Forsch. Erg. ser. C, 10, pp. 75–95.
- Müller, C. (1974). Calcareous nannoplankton, Leg 25 (Western Indian Ocean). Init. Repts. D.S.D.P., 25, pp. 579–633.

- Müller, C. (1974). Nannoplankton aus dem Mittel-Miozen von Walbersdorf (Burgenland). *Senck. Leth.*, 55, pp. 389–405.
- Müller, C. (1978). Neogene calcareous nannofossils from the Mediterranean, Leg 42A, Deep Sea Drilling Project. *Init. Repts. D.S.D.P.*, 42A, pp. 727–751.
- Müller, C. (1979). Nannoplankton. In: Bizon, G. and Müller, C., Report of the Working Group on Micropaleontology, VIIth Int. Congr. Mediterr. Neogene, Athens 1979. *Ann. Géol. Pays Hellén.*, tome hors série, 3, pp. 1344–1347.
- Müller, C. (1979). Calcareous nannofossils from the North Atlantic (Leg 48). *Init. Repts. D.S.D.P.*, 48, pp. 589–639.
- Müller, C. (1981). Beschreibung neuer *Helicosphaera*-Arten aus dem Miozen und Revision biostratigraphischer Reichweiten einiger Neogenen Nannoplankton-Arten. *Senck. Leth.*, 61, pp. 427–435.
- Müller, C. and Brönnimann, P. (1974). Eine neue Art der Gattung *Helicosphaera* Kamptner aus dem Pazifischen Ozean. *Eclog. Geol. Helv.*, 67/3, pp. 661–662.
- Murray, G. and Blackman, V. H. (1898). On the nature of the coccospheres and rhabdospheres. *Phil. Trans. R. Soc. Lond.*, ser. B, 190, pp. 427–441.
- Nishida, S. (1970). Nannoplankton from the deep-sea ooze of the equatorial Pacific. *Trans. Proc. Palaeont. Soc. Japan*, 79, pp. 355–370.
- Nishida, S. (1979). Atlas of Pacific nannoplankton. *News. Osaka Micropal. Spec. Paper*, 3, pp. 1–31.
- Norris, R.E. (1971). Extant calcareous nannoplankton from the Indian Ocean. *Proc. II Plankt. Conf. Roma 1970*, 2, pp. 899–909.
- Okada, H. and Bukry, D. (1980). Supplementary modification and introduction of code numbers to the low-latitude coccolith biostratigraphic zonation. *Mar. Micropal.*, 5, pp. 321–325.
- Okada, H. and Honjo, S. (1973). The distribution of oceanic coccolithophorids in the Pacific. *Deep Sea Res.*, 20, pp. 355–374.
- Okada, H. and Honjo, S. (1975). Distribution of Coccolithophores in Marginal Seas along the Western Pacific Ocean and the Red Sea. *Marine Biol.*, 31, pp. 271–285.
- Okada, H. and McIntyre, A. (1977). Modern coccolithophores of the Pacific and North Atlantic Oceans. *Micropaleontology*, 23, pp. 1–55.
- Okada, H. and McIntyre, A. (1979). Seasonal Distribution of Modern Coccolithophores in the Western North Atlantic Ocean. *Marine Biol.*, 54, pp. 319–328.
- Perch-Nielsen, K. (1968). Der Feinbau und die Klassifikation der Coccolithen aus dem Maastrichtien von Dänemark. *Det Kongelige Danske Videnskabernes Selskab Biologiske Skrifter*, 16, pp. 1–96.
- Perch-Nielsen, K. (1970). Durchsicht Tertiärer Coccolithen. *Proc. II Planktonic Conf., Roma 1970*, 2, pp. 939–979.
- Perch-Nielsen, K. (1971). Elektronenmikroskopische Untersuchungen an Coccolithen und verwandte Formen aus dem Eozän von Dänemark. *Det Kongelige Danske Videnskabernes Selskab Biologiske Skrifter*, 18, pp. 1–75.
- Perch-Nielsen, K. (1972). Remarks on Late Cretaceous to Pleistocene coccoliths from the North Atlantic. *Init. Repts. D.S.D.P.*, 12, pp. 1003–1069.
- Perch-Nielsen, K. (1977). Albian to Pleistocene calcareous nannofossils from the Western South Atlantic, D.S.D.P. Leg 39. *Init. Repts. D.S.D.P.*, 39, pp. 699–823.
- Prins, B. (1971). Speculations on relations, evolution, and stratigraphic distribution of discoasters. *Proc. II Plankt. Conf., Roma*, 2, pp. 1017–1039.
- Proto Decima, F., Medizza, F. and Todesco, L. (1978). Southern Atlantic Leg 40, calcareous nannofossils. *Init. Repts. D.S.D.P.*, 40, pp. 571–634.
- Rade, J. (1977). Tertiary biostratigraphic zonation based on calcareous nannoplankton in Eastern Australian nearshore basins. *Micropaleontology*, 23, pp. 270–296.
- Rio, D., Mazzei, R. and Palmieri, G. (1976). The stratigraphic position of the Mediterranean Upper Miocene evaporites, based on nannofossils. *Mem. Soc. Geol. It.*, 16, pp. 261–276.
- Romein, A. J. T. (1979). Lineages in Early Paleogene calcareous nannoplankton. *Utr. Micropal. Bull.*, 22, pp. 1–231.

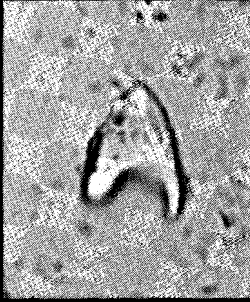
- Roth, P. H. (1968). Calcareous nannoplankton zonation of Oligocene sections in Alabama, on the islands of Trinidad and Barbados, and the Blake Plateau. *Eclog. Geol. Helv.*, 61, pp. 459–465.
- Roth, P. H. (1970). Oligocene calcareous nannoplankton biostratigraphy. *Eclog. Geol. Helv.*, 63, pp. 799–881.
- Roth, P. H. (1973). Calcareous nannofossils — Leg 17, Deep Sea Drilling Project. *Init. Repts. D.S.D.P.*, 17, pp. 695–795.
- Roth, P. H. (1974). Calcareous nannofossils from the Northwestern Indian Ocean. *Init. Repts. D.S.D.P.*, 24, pp. 969–994.
- Roth, P. H., Baumann, P. and Bertolini, V. (1971). Late Eocene-Oligocene calcareous nannoplankton from Central and Northern Italy. *Proc. II Plankt. Conf., Roma 1970*, 2, pp. 1069–1097.
- Roth, P. H. and Thierstein, H. R. (1972). Calcareous nannoplankton, Leg 14 Deep Sea Drilling Project. *Init. Repts. D.S.D.P.*, 14, pp. 421–485.
- Sachs, J. B. and Skinner, C. H. (1973). Late Pliocene-Early Pleistocene nannofossil stratigraphy in the north Central Gulf Coast area. *In* Smith, L. A. and Hardenbol, J. (ed.): *Proc. Symp. Calc. Nann., Gulf Coast Section S.E.P.M., Houston*, pp. 93–125.
- Samtleben, C. (1978). Pliocene-Pleistocene coccolith assemblages from the Sierra Leone Rise. *Init. Repts. D.S.D.P.*, 41, pp. 913–931.
- Schmidt, R. R. (1973). A calcareous nannoplankton zonation for Upper Miocene-Pliocene deposits from the Southern Aegean area, with a comparison to Mediterranean stratotype localities. *Kon. Ned. Akad. Wet., Proc. B*, 76, pp. 287–310.
- Schmidt, R. R., Theodoridis, S. and Driever, B. W. M. (1979). Counting techniques as applied to calcareous nannoplankton for the question of accuracy in correlation. VIIth Int. Congr. Mediterr. Neogene, Athens 1979. *Ann. Géol. Pays Hellén. tome hors série*, 3, pp. 1097–1100.
- Sorby, H. C. (1861). On the organic origin of the so-called “crystalloids” of the Chalk. *Ann. Mag. Nat. Hist.*, ser. 3, 8, pp. 193–200.
- Spaak, P. (1983). Accuracy in correlation and ecological aspects of the planktonic foraminiferal zonation of the Mediterranean Pliocene. *Utr. Micropal. Bull.*, 28, pp. 1–159.
- Sturbaut, E. (1983). The stratigraphic position of the Lower Oligocene Yrieu Sands (Southern France), based on calcareous nannofossils and a new *Helicosphaera* species. *Eclog. Geol. Helv.*, 76, pp. 327–331.
- Stradner, H. (1958). Die fossilen Discoasteriden Österreichs. 1. Teil. Die in den Bohrkernen der Tiefbohrung Korneuburg 1 enthaltenen Discoasteriden. *Erdoel-Z.*, 74, pp. 178–188.
- Stradner, H. (1959). First report on the discoasters of the Tertiary of Austria and their stratigraphic use. 5th world petr. congr., paper 60, pp. 1081–1095.
- Stradner, H. (1959). Die fossilen Discoasteriden Österreichs. II. Teil. *Erdoel-Z.*, 12, pp. 3–19.
- Stradner, H. (1969). The nannofossils of the Eocene Flysch in the Hagenbach Valley (Northern Vienna Woods) Austria. *Rocz. Polsk. Towarz. Geol.*, 39, pp. 403–432.
- Stradner, H. (1970). Catalogue of calcareous nannoplankton from sediments of Neogene Age in the eastern North Atlantic and Mediterranean Sea. *Init. Repts. D.S.D.P.*, 13, pp. 1137–1199.
- Stradner, H. and Allram, F. (1981). The nannofossil assemblages of D.S.D.P. Leg 66, Middle America trench. *Init. Repts. D.S.D.P.*, 66, pp. 589–639.
- Stradner, H. and Edwards, A. R. (1968). Electron Microscopic Studies on Upper Eocene coccoliths from the Oamaru diatomite, New Zealand. *Jb. Geol. B. A.*, 13, pp. 1–66.
- Stradner, H. and Fuchs, R. (1980). Über Nannoplanktonvorkommen im Sarmatien (Obermiozän) der Zentralen Paratethys in Niederösterreich und im Burgenland. *Beitr. Paläont. Österr.*, 7, pp. 251–279.
- Stradner, H. and Papp, A. (1961). Tertiäre Discoasteriden aus Oesterreich und deren stratigraphische Bedeutung. *Jb. Geol. B.A., Sonderband*, 7, pp. 1–160.
- Sullivan, F. R. (1965). Lower Tertiary nannoplankton from the California Coast ranges. II Eocene. *Univ. Calif. Publ. Geol. Sc.*, 53, pp. 1–52.
- Tan Sin Hok (1926). On a Young-Tertiary Limestone of the Isle of Rotti with Coccoliths, Calci- and Manganese-peroxide-Spherulites. *Proc. Ned. Acad. Wet.*, 29, pp. 1095–1105.

- Tan Sin Hok (1927). Discoasteridae incertae sedis. Proc. Ned. Akad. Wet., 30, pp. 1–9.
- Tan Sin Hok (1931). Discoasteridae, Coccolithinae and Radiolaria. Leid. Geol. Med., 5, pp. 92–95.
- Tappan, H. (1980). Haptophyta, coccolithophores and other calcareous nannoplankton. *In*: The paleobiology of plant protists. W. H. Freeman (publ.), San Francisco, pp. 678–803.
- Theodoridis, S. (1983). On the legitimacy of the generic name *Discoaster* Tan, 1927 ex Tan, 1931. INA Newsletter, 5, pp. 15–21.
- Varol, O. (1982). Calcareous nannofossils from the Antalya Basin, Turkey. N. Jb. Geol. Palaeont. Mh., 4, pp. 244–256.
- Vincent, E., Frerichs, W.E. and Heiman, M. (1974). Neogene planktonic foraminifera from the Gulf of Aden and the Western Tropical Indian Ocean, Deep Sea Drilling Project, Leg 24. Init. Repts. D.S.D.P., 24, pp. 827–850.
- Wallich, M. D. (1877). Observations on the coccosphere. Annals and magazine of Nat. Hist., 19, pp. 342–350.
- Watabe, N. (1967). Crystallographic Analysis of the coccolith of *Coccolithus huxleyi*. Calc. Tiss. Res., 1, pp. 114–121.
- Wilcoxon, J. A. (1970). *Cyclococcolithina* Wilcoxon nom. nov. (nom. subst. pro *Cyclococcolithus* Kamptner, 1954). Tulane Stud. Geol. Pal., 8, pp. 82–83.
- Wise, S. W. and Wind, F. H. (1977). Mesozoic and Cenozoic calcareous nannofossils recovered by D.S.D.P. Leg 36 drilling on the Falkland Plateau, Southwest Atlantic sector of the Southern Ocean. Init. Repts. D.S.D.P., 36, pp. 269–503.
- Zachariasse, W. J., Riedel, W. R., et al., (1978). Micropaleontological counting methods and techniques — an exercise on an eight metres section of the Lower Pliocene of Capo Rossello, Sicily. Utr. Micropal. Bull., 17, pp. 1–265.
- Zachariasse, W. J. and Spaak, P. (1983). Middle Miocene to Pliocene paleoenvironmental reconstruction of the Mediterranean and adjacent Atlantic Ocean: planktonic foraminiferal record of Southern Italy. Utr. Micropal. Bull., 30, pp. 91–110.
- Zwaan, G. J. van der (1979). The pre-evaporite Late Miocene environment of the Mediterranean; stable isotopes of planktonic foraminifera from section Falconara, Sicily. Proc. Kon. Ned. Akad. Wet., B, 82, pp. 487–502.
- Zwaan, G. J. van der (1982). Paleocology of Late Miocene Mediterranean Foraminifera. Utr. Micropal. Bull., 25, pp. 1–202.
- Zwaan, G. J. van der (1983). Quantitative analyses and the reconstruction of benthic foraminiferal communities. Utr. Micropal. Bull., 30, pp. 49–69.
- Zwaan, G. J. van der and Hartog Jager, D. den (1983). Paleocology of Late Miocene Sicilian benthic foraminifera. Proc. Kon. Ned. Akad. Wet., B, 86, pp. 211–223.

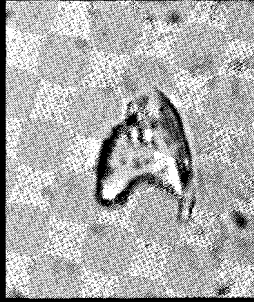
Plate 1

- Figs. 1–8, 10–11: LM micrographs, parallel nicols, 1787.5 X.
- Fig. 12: LM micrograph, crossed nicols, 1787.5 X.
- Fig. 9: SEM micrograph, 3400 X.
- Figs. 1, 2. *Amaurolithus primus* (Bukry and Percival) Gartner and Bukry. Same specimen (fig. 1: low focus, fig. 2: high focus). Sample 219–26.
- Figs. 3–8. *Amaurolithus amplificus* (Bukry and Percival) Gartner and Bukry.
- Figs. 3, 4. Sample 219-43, same specimen (fig. 3: low focus, fig. 4: high focus).
- Figs. 5, 6. Sample 219-21, same specimen (fig. 5: high focus, fig. 6: low focus).
- Figs. 7, 8. Sample 219-30, same specimen (fig. 7: high focus, fig. 8: low focus).
- Figs. 9–11. *Amaurolithus delicatus* Gartner and Bukry.
- Fig. 9. Sample JT1935.
- Fig. 10. Sample JT1935.
- Fig. 11. Sample 219-33.
- Fig. 12. *Ceratolithus acutus* Gartner and Bukry. Sample 219-25, crossed nicols.

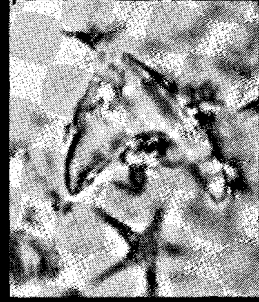
Plate 1



1



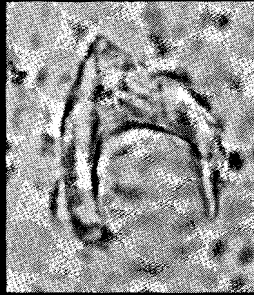
2



3



4



5



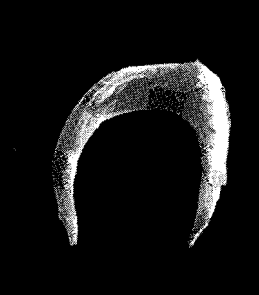
6



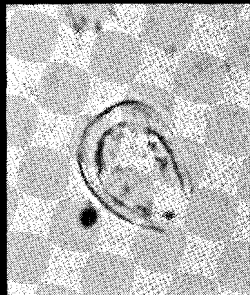
7



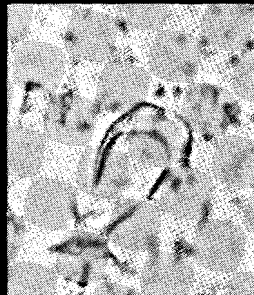
8



9



10



11



12

Plate 2

LM micrographs, crossed nicols, 2447.5 X.

Figs. 1–3.

Calcidiscus premacintyre n. sp.

Fig. 1. Holotype, sample CP3656.

Fig. 2. Sample CP3656.

Fig. 3. Sample MT750.

Figs. 4–6.

Calcidiscus macintyre (Bukry and Bramlette) Loeblich and Tappan.

Fig. 4. Sample 369A-13.

Fig. 5. Sample 369A-16.

Fig. 6. Sample 369A-11.

Plate 2

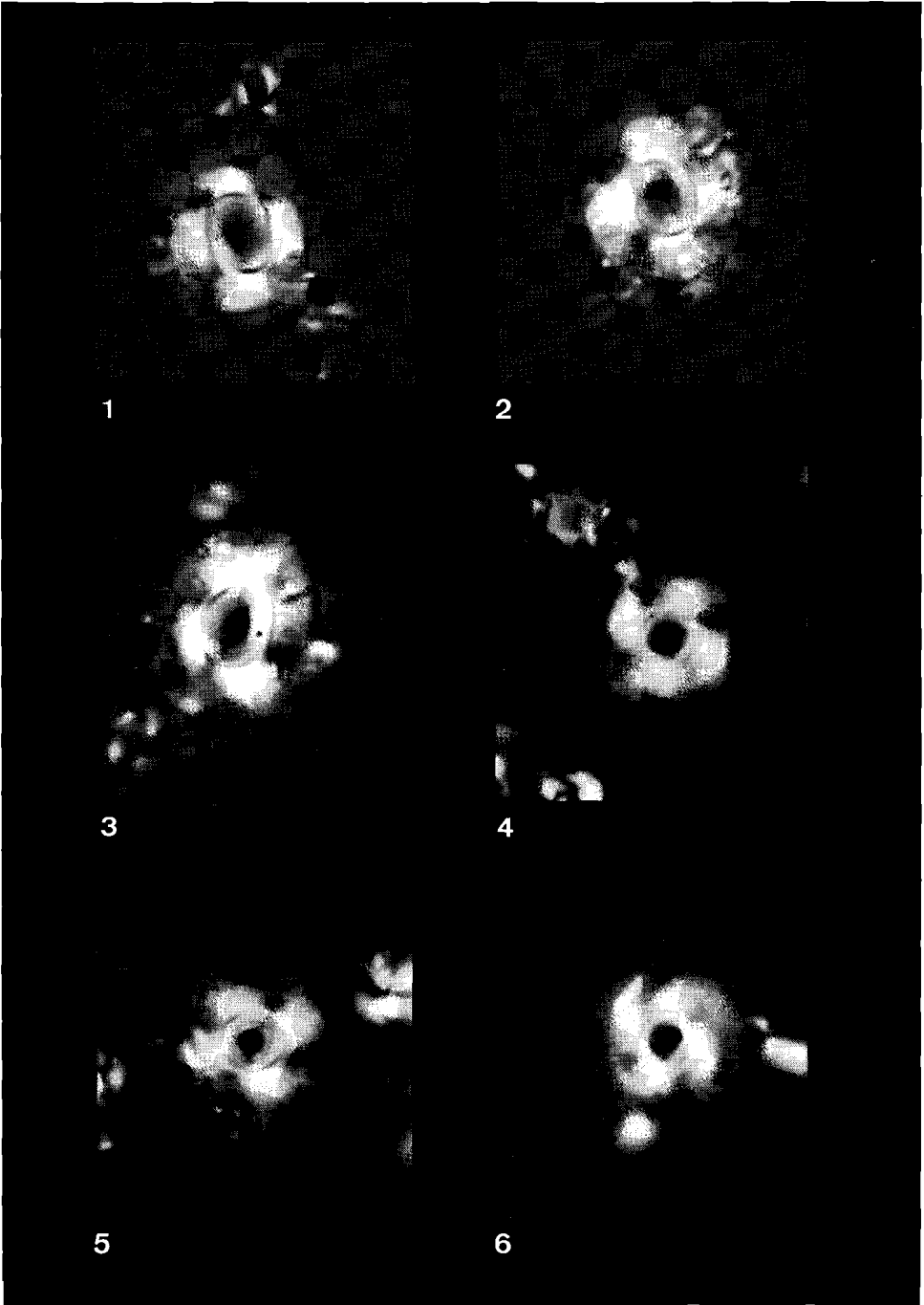


Plate 3

- Figs. 1, 3–8: LM micrographs, crossed nicols, 2447.5 X.
Fig. 2: SEM micrograph, 4500 X.
Figs. 1, 2. *Geminilithella rotula* (Kamptner) Backman. Sample 369A-27.
Figs. 3–8. *Hayella aperta* n. sp.
Fig. 3. Holotype, sample 369A-18.
Fig. 4. Side view, sample 369A-27.
Fig. 5. Sample 369A-18.
Fig. 6. Sample 369A-21.
Fig. 7. Sample 369A-22.
Fig. 8. Sample 369A-22.

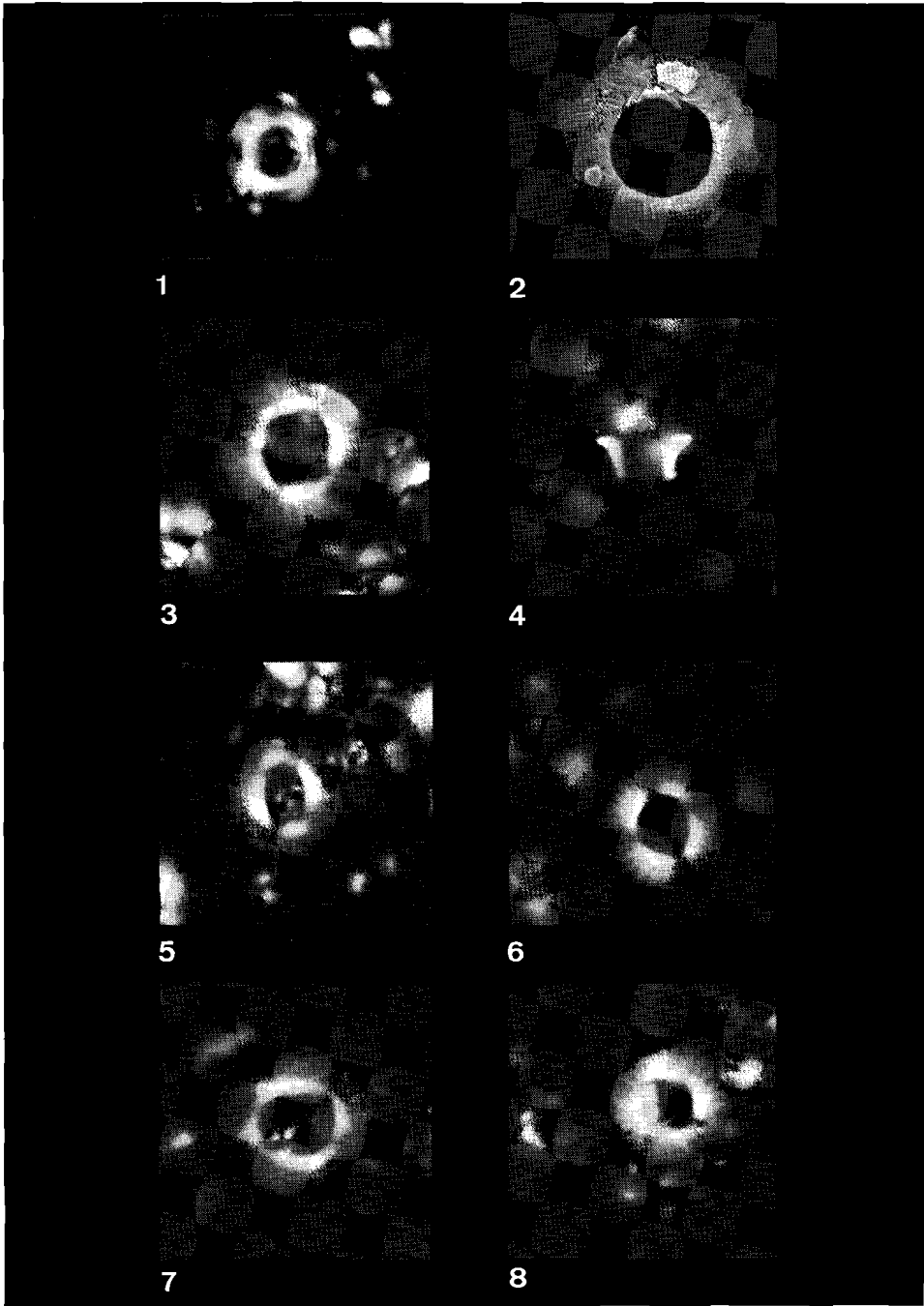
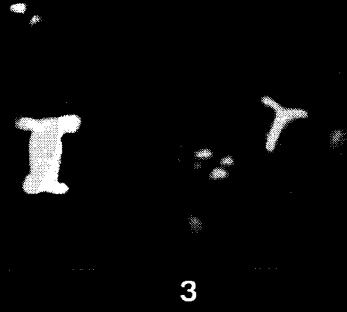


Plate 4

- Fig. 1: SEM micrograph, 8900 X.
- Figs. 2–7: LM micrographs, 2447.5 X.
- Figs. 1–7. *Minylitha convallis* Bukry, emended.
- Fig. 1. Apical view, sample CP3019.
- Fig. 2. Basal view, crossed nicols, sample CP4305.
- Fig. 3. Basal view, crossed nicols, sample 231-111.
- Fig. 4. Side view, crossed nicols, sample 369A-2.
- Figs. 5–7. Side view, parallel nicols, same specimen, sample 231-94 (fig. 5: high focus, fig. 6: middle focus, fig. 7: low focus).

Plate 4



3

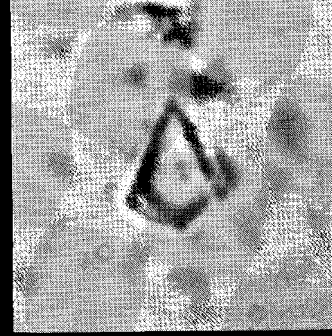
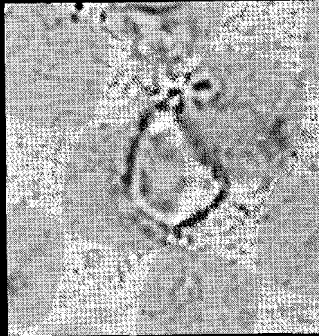
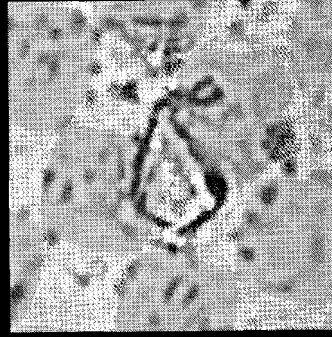


Plate 5

LM micrographs, 2447.5 X.

- Figs. 1–4. *Reticulofenestra rotaria* n. sp.
Fig. 1. Holotype, sample 219-12.
Fig. 2. Sample 219-30.
Fig. 3. Sample JT1910.
Fig. 4. Sample 219-25.
- Figs. 5–7. *Reticulofenestra ampliumbilicus* n. sp.
Fig. 5. Holotype, sample CP4579.
Fig. 6. Sample CP4580.
Fig. 7. Sample CP4579.
- Fig. 8. *Reticulofenestra floridana* (Roth and Hay) n. comb. Sample 369A-58.

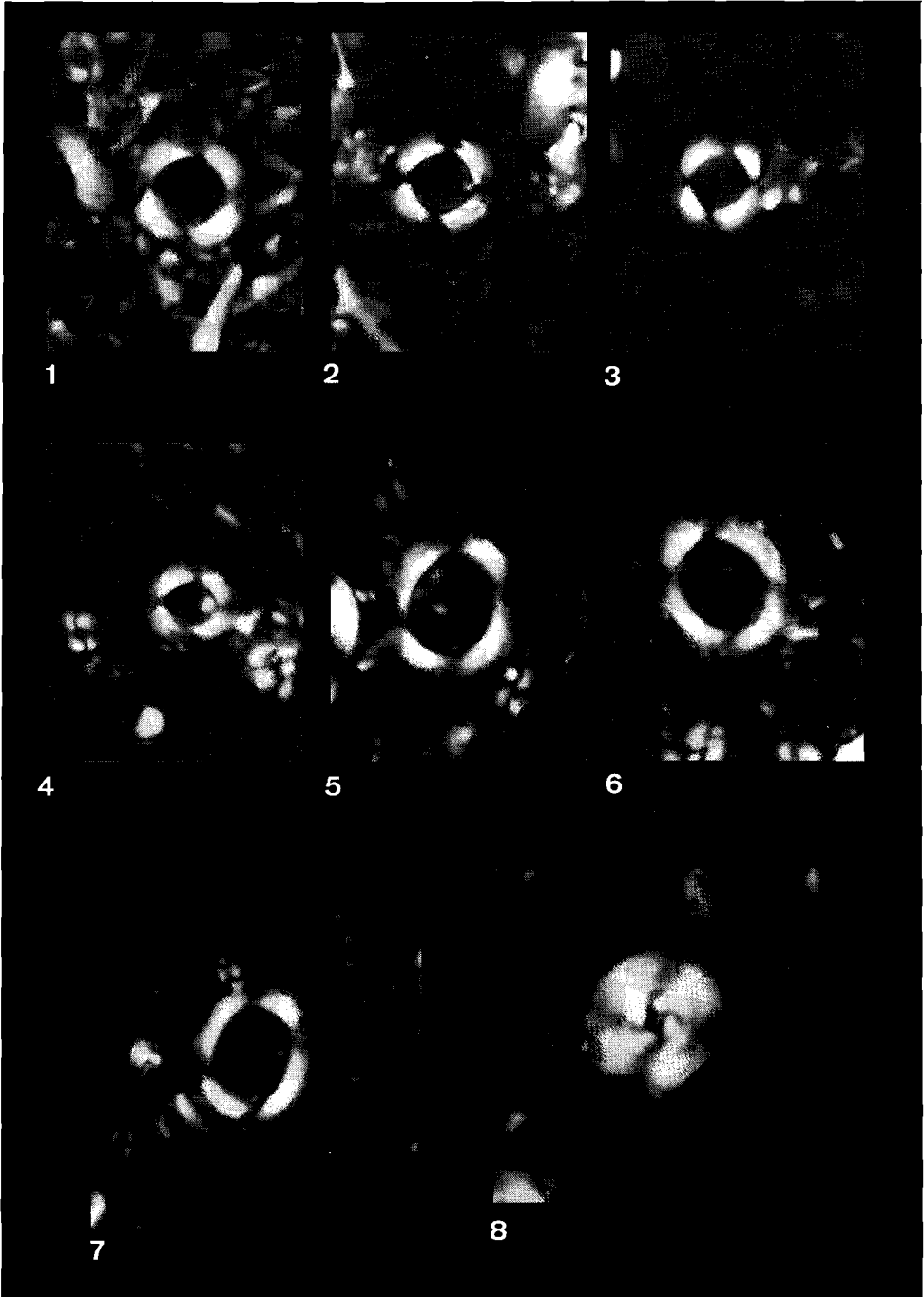


Plate 6

LM micrographs, crossed nicols, 2447.5 X.

- Figs. 1–7. *Solidopons petrae* n. gen., n. sp.
Fig. 1. Holotype, sample 219-39.
Fig. 2. Sample CP4566.
Fig. 3. Sample 369A-17.
Fig. 4. Sample 369A-57.
Fig. 5. Sample 219-39.
Fig. 6. Side view, sample 369A-59.
Fig. 7. Side view, sample 369A-12.

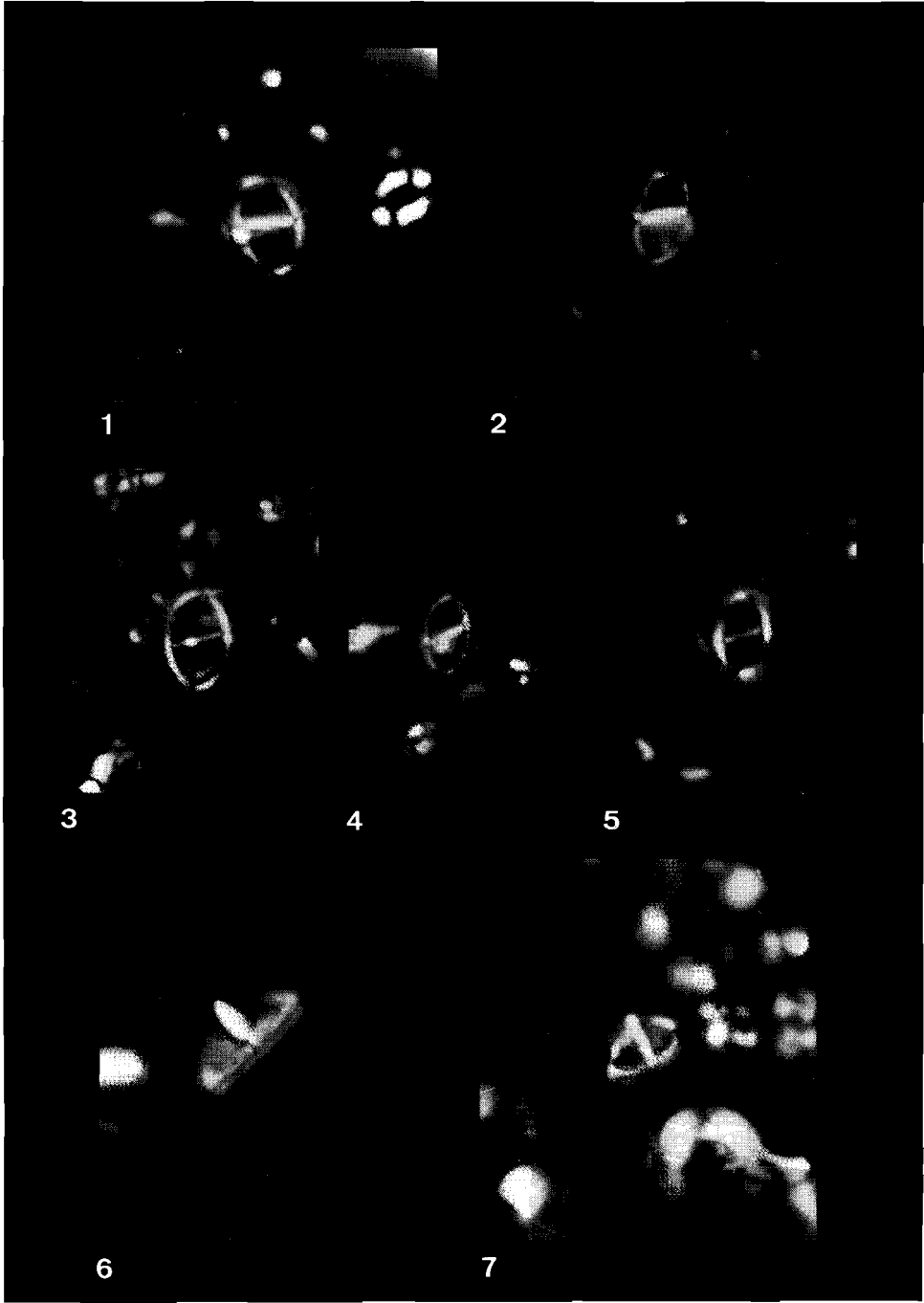


Plate 7

LM micrographs, crossed nicols, magnification: 2447.5 X. All specimens are presented in their original orientation.

- Figs. 1–4. *Sphenolithus belemnos* Bramlette and Wilcoxon.
Fig. 1. Sample 372-114.
Figs. 2, 3. Same specimen, sample 372-113.
Fig. 4. Sample 372-113.
- Figs. 5–12. *Sphenolithus heteromorphus* Deflandre.
Fig. 5. Sample 369A-25.
Fig. 6. Sample 372-94.
Fig. 7. Sample CP3614.
Fig. 8. Sample MT735.
Fig. 9. Sample 372-110.
Figs. 10–12. Sample CP3615.

Plate 7

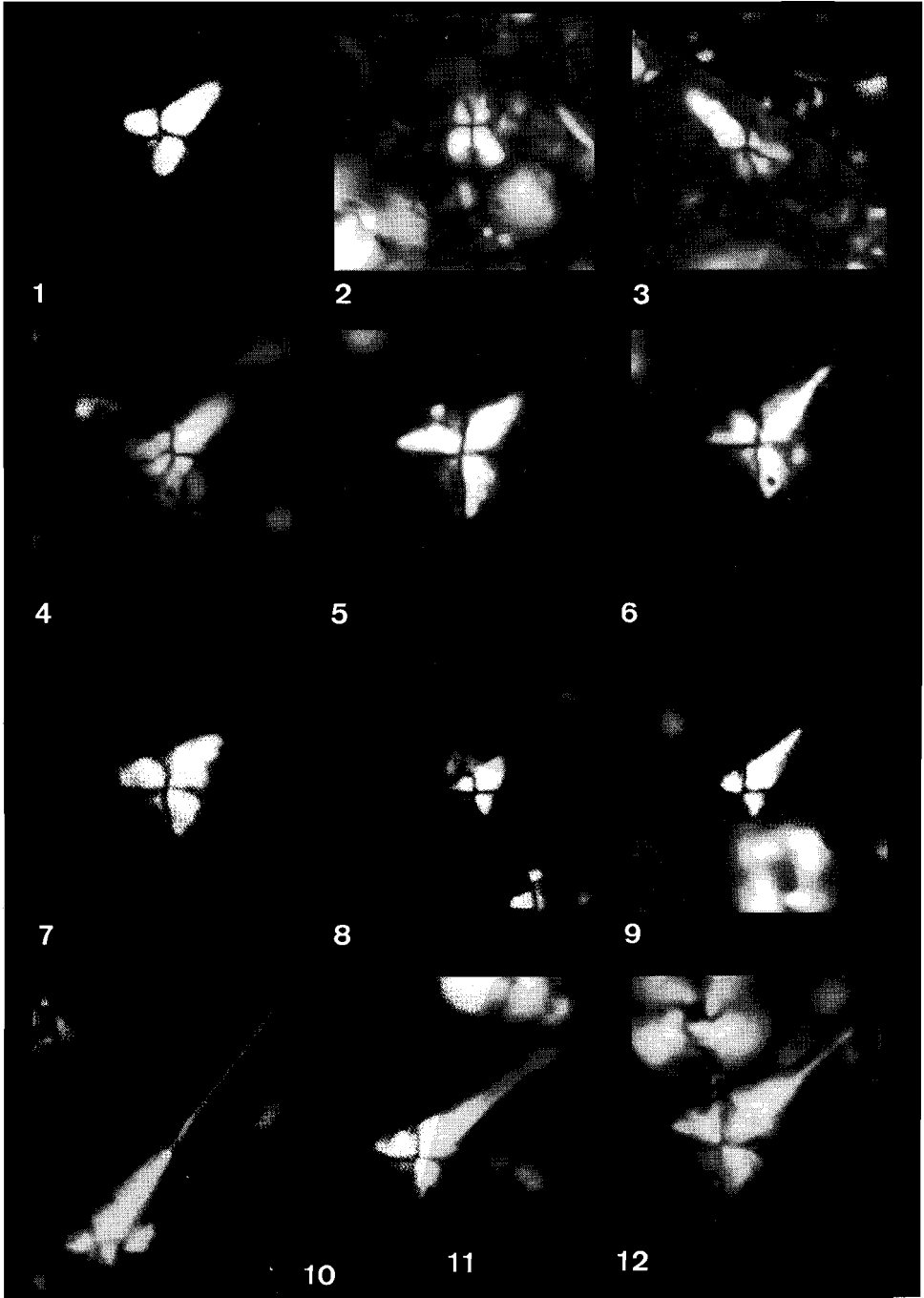


Plate 8

- Figs. 1–7, 9: LM micrographs, crossed nicols, 2447.5 X. All specimens presented in their original orientation.
- Fig. 8: SEM micrograph, 8000 X.
- Figs. 1–3. *Sphenolithus moriformis* (Brönnimann and Stradner) Bramlette and Wilcoxon.
Figs. 1, 2. Same specimen, sample 369A-40.
Fig. 3. Sample 369A-40.
- Figs. 4–7. *Sphenolithus capricornutus* Bukry and Percival.
Figs. 4, 5. Same specimen, sample 369A-75.
Figs. 6, 7. Same specimen, sample 369A-70.
- Figs. 8, 9. *Sphenolithus abies* Deflandre.
Fig. 8. Sample JT1935.
Fig. 9. Sample JT1935.

Plate 8

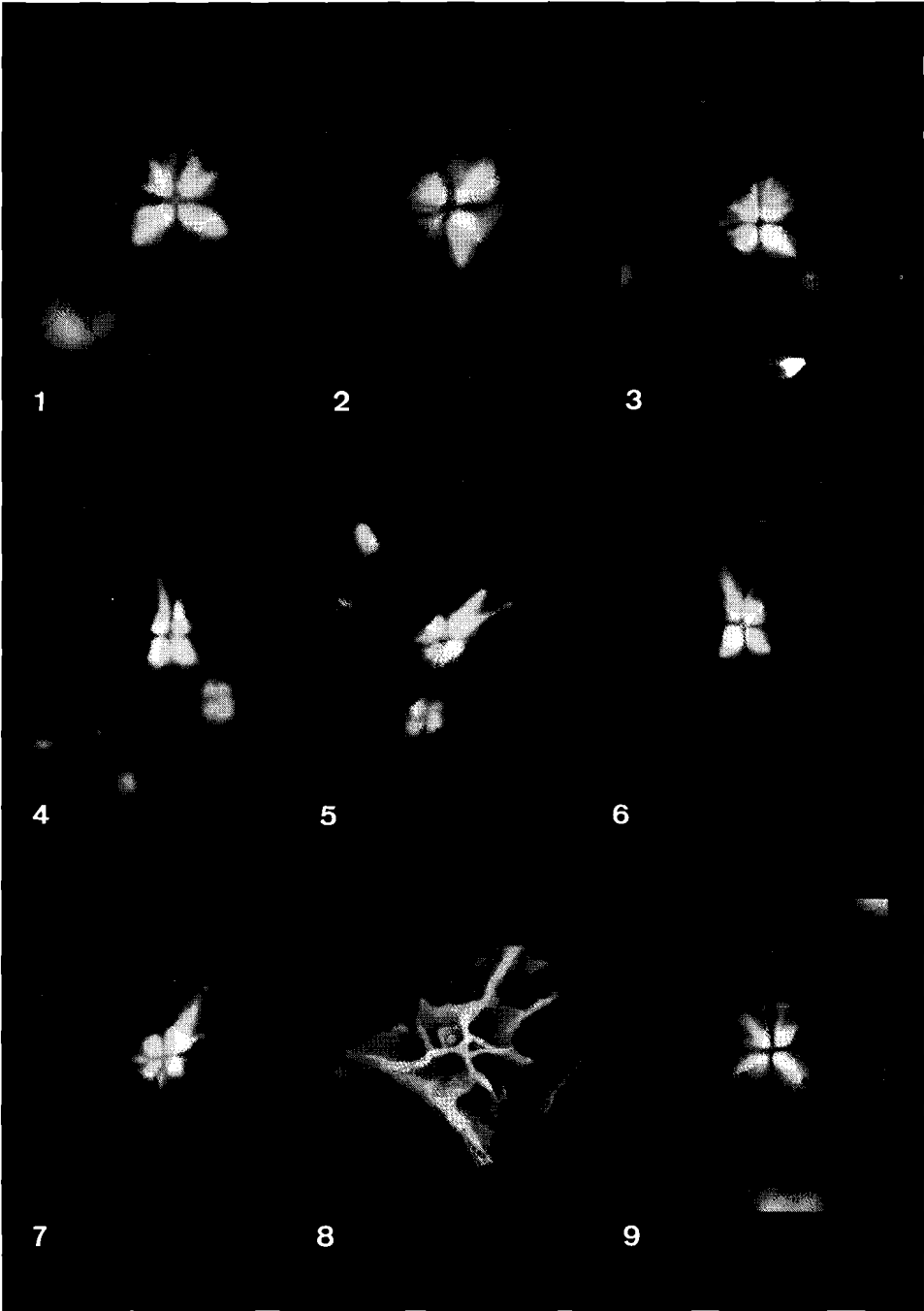


Plate 9

LM micrographs, crossed nicols, magnification: 2447.5 ×. All specimens are presented in their original orientation.

- Figs. 1–4. *Syracosphaera? fragilis* n. sp.
Fig. 1. Holotype, sample CP4581.
Fig. 2. Sample AU163.
Fig. 3. Sample CP4581.
Fig. 4. Sample CP4561.
- Figs. 5–12. *Tetralithoides symeonidesii* n. gen., n. sp.
Fig. 5. Holotype, sample 372-101.
Fig. 6. Sample 369A-13.
Figs. 7, 9. Sample 369A-63.
Fig. 8. Sample 369A-15.
Fig. 10. Sample 369A-64.
Figs. 11, 12. Sample 369A-25.

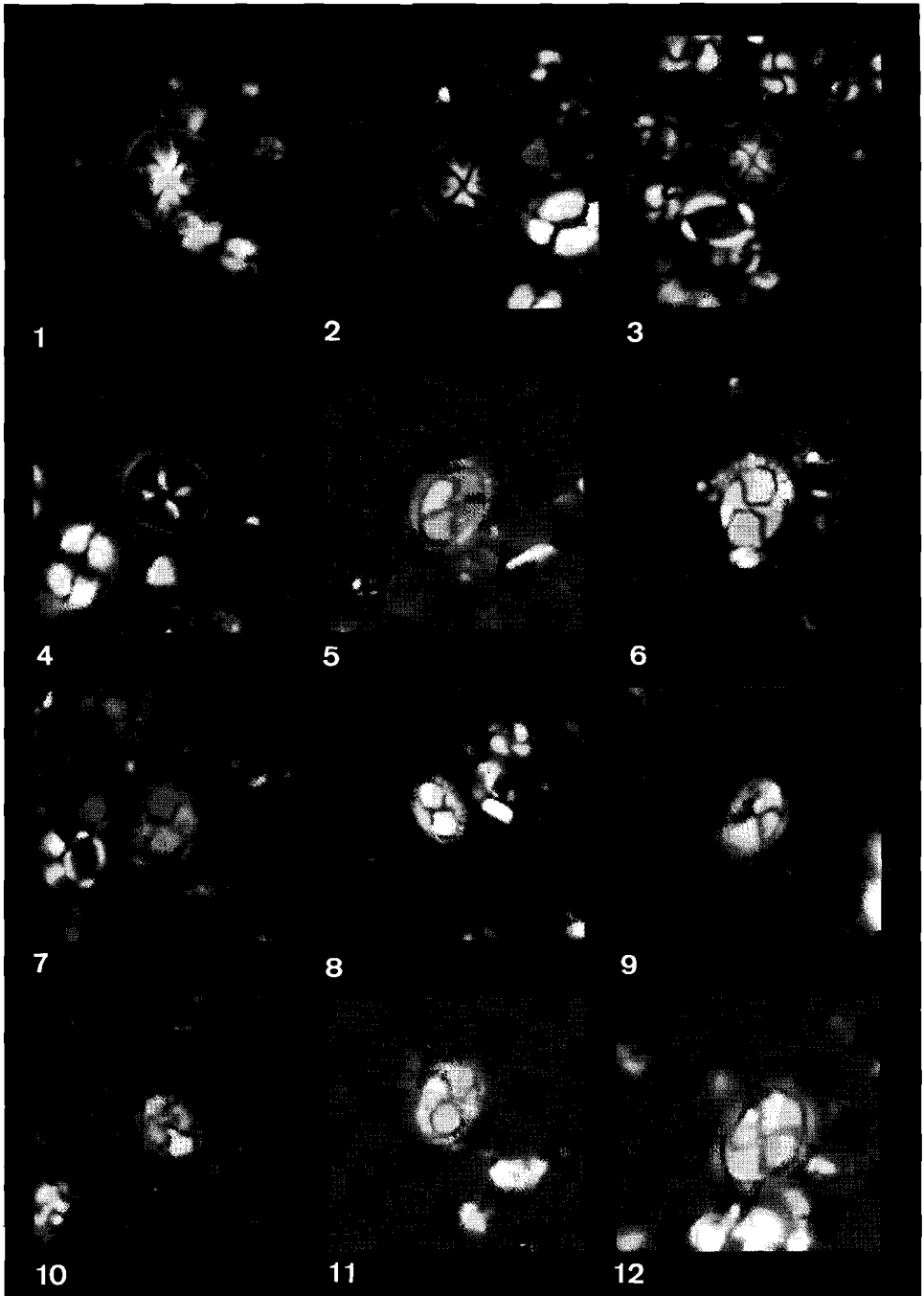


Plate 10

Figs. 1–4, 9–13: LM micrographs, crossed nicols.

Figs. 5–8, 14–16: LM micrographs, parallel nicols.

All specimens are presented in their original orientation. 1760 X.

Figs. 1, 2, 5, 6.

Triquetrorhabdulus carinatus Martini.

Figs. 1, 5. Same specimen, sample 369A-69.

Figs. 2, 6. Same specimen, sample 369A-67.

Figs. 3, 7, 4, 8.

Triquetrorhabdulus milowii Bukry.

Figs. 3, 7. Same specimen, sample 369A-60.

Figs. 4, 8. Same specimen, sample 369A-51.

Figs. 9, 10.

Triquetrorhabdulus challengerii Perch-Nielsen.

Fig. 9. Sample 369A-74.

Fig. 10. Sample 369A-76.

Figs. 11–16.

Triquetrorhabdulus martinii Gartner.

Fig. 11. Side view, sample 369A-30.

Fig. 12. Side view, sample 369A-52.

Figs. 13, 14. Same specimen, side view, sample 369A-32.

Figs. 15, 16. Same specimen, dorsal view (fig. 15: high focus, fig. 16: low focus), sample 369A-43.

Plate 10

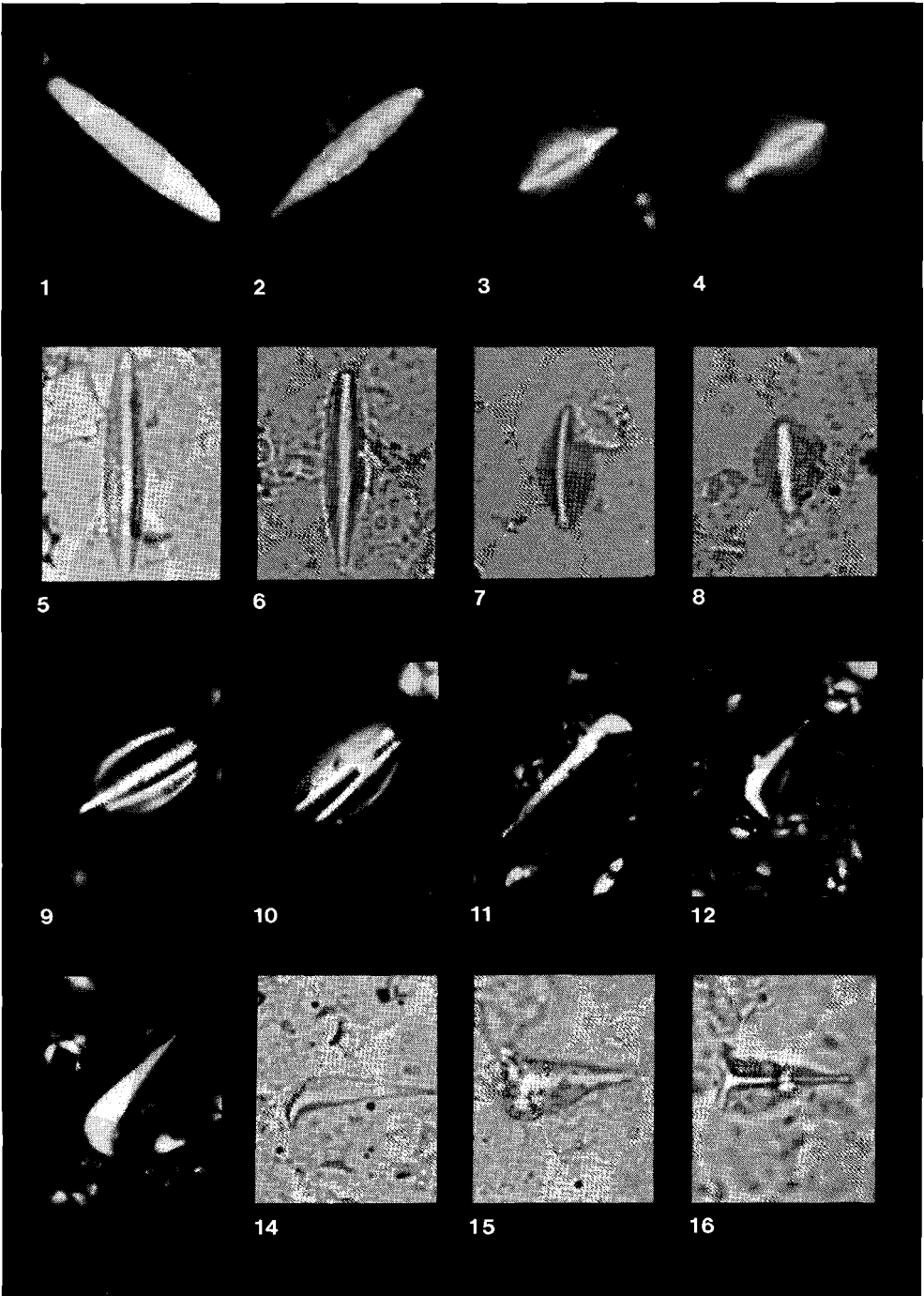
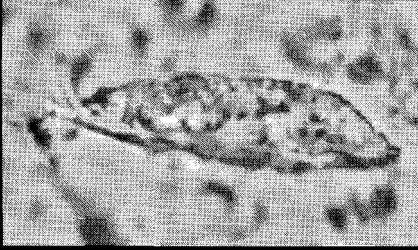


Plate 11

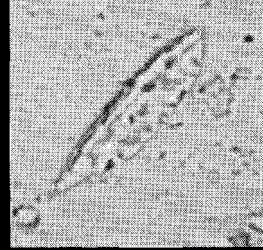
LM micrographs, parallel nicols, 1760 X. All specimens are presented in their original orientation.

- Figs. 1–3. *Triquetrorhabdulus rugosus* Bramlette and Wilcoxon.
Fig. 1. Sample CP3710.
Figs. 2, 3. Sample CP3135.
- Figs. 4–6. *Triquetrorhabdulus extensus* n. sp. Holotype, high (fig. 4), middle (fig. 5) and
low focus (fig. 6). Sample 219-3.
- Figs. 7–10. *Triquetrorhabdulus finifer* n. sp.
Figs. 7, 8. Holotype, low (fig. 7) and high focus (fig. 8), sample 219-1.
Figs. 9, 10. Sample 219-1.

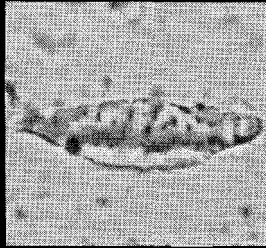
Plate 11



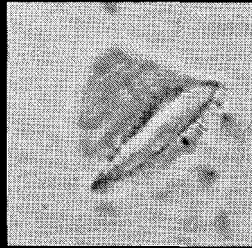
1



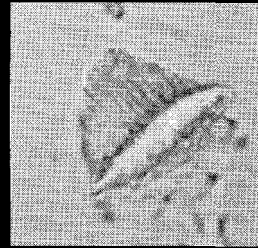
2



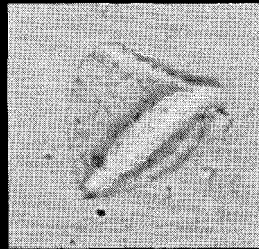
3



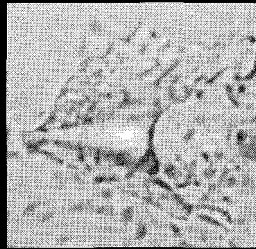
4



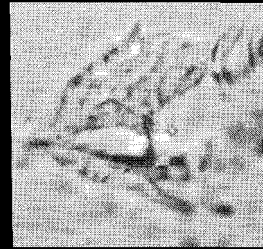
5



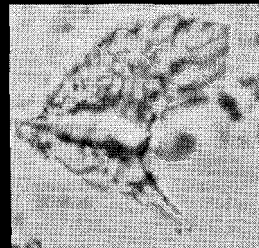
6



7



8



9



10

Plate 12

Eu-discoaster index species

LM micrographs, parallel nicols. 1485 X.

- Fig. 1. *Eu-discoaster druggii* (Bramlette and Wilcoxon) Theodoridis. Distal view, high focus, sample 369A-73.
- Fig. 2. *Eu-discoaster exilis* (Bramlette and Martini) Theodoridis. Distal view, high focus, sample 369A-64.
- Figs. 3, 4, 8. *Eu-discoaster kugleri* (Martini and Bramlette) Theodoridis.
Figs. 3, 4. Same specimen, proximal view, fig. 3: high focus, fig. 4: low focus. Sample 369A-9.
Fig. 8. Distal view, high focus, sample 369A-9.
- Figs. 5–7. *Eu-discoaster signus* (Bukry) Theodoridis. Same specimen, distal view, fig. 5: low focus, fig. 6: middle focus, fig. 7: high focus. Sample 369A-24.
- Fig. 9. *Eu-discoaster quinqueramus* (Gartner) Theodoridis. Proximal view, high focus, sample 231-73.
- Figs. 10, 11. *Eu-discoaster pentaradiatus* (Tan Sin Hok) Theodoridis. Same specimen, distal view, fig. 10: high focus, fig. 11: low focus. Sample 231-113.
- Fig. 12. *Eu-discoaster calcaris* (Gartner) Theodoridis. Proximal view, high focus. Sample 231-110.
- Fig. 13. *Eu-discoaster hamatus* (Martini and Bramlette) Theodoridis. Proximal view, high focus. Sample 231-120.
- Fig. 14. *Eu-discoaster bellus* (Bukry) Theodoridis. Proximal view, high focus. Sample 231-97.
- Fig. 15. *Eu-discoaster coalitus* (Martini and Bramlette) n. comb. Distal view, high focus. Sample 219-23.

Plate 12

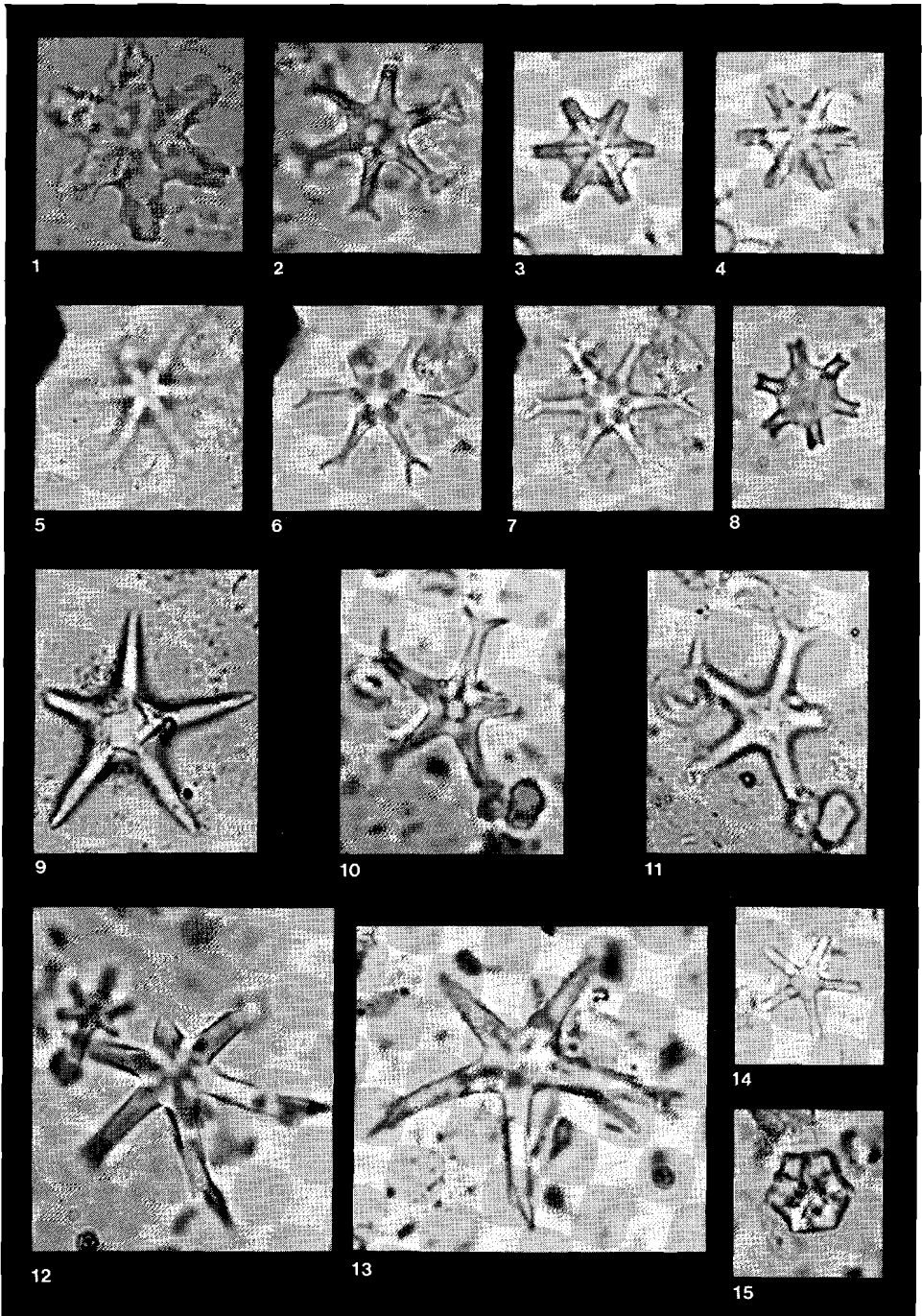


Plate 13

Helicosphaera index species

LM micrographs, crossed nicols. 2447.5 X. All specimens are presented in their original orientation.

- Fig. 1. *Helicosphaera ampliaperta* Bramlette and Wilcoxon. Sample 369A-63.
Fig. 2. *Helicosphaera waltrans* n. sp. Sample 369A-35.
Fig. 3. *Helicosphaera perch-nielseniae* (Haq) Jafar and Martini. Sample 369A-53.
Fig. 4. *Helicosphaera orientalis* Black. Sample 369A-12.
Fig. 5. *Helicosphaera walbersdorfensis* Müller, emended.
Fig. 6. *Helicosphaera stalis* n. sp. Sample CP3118.

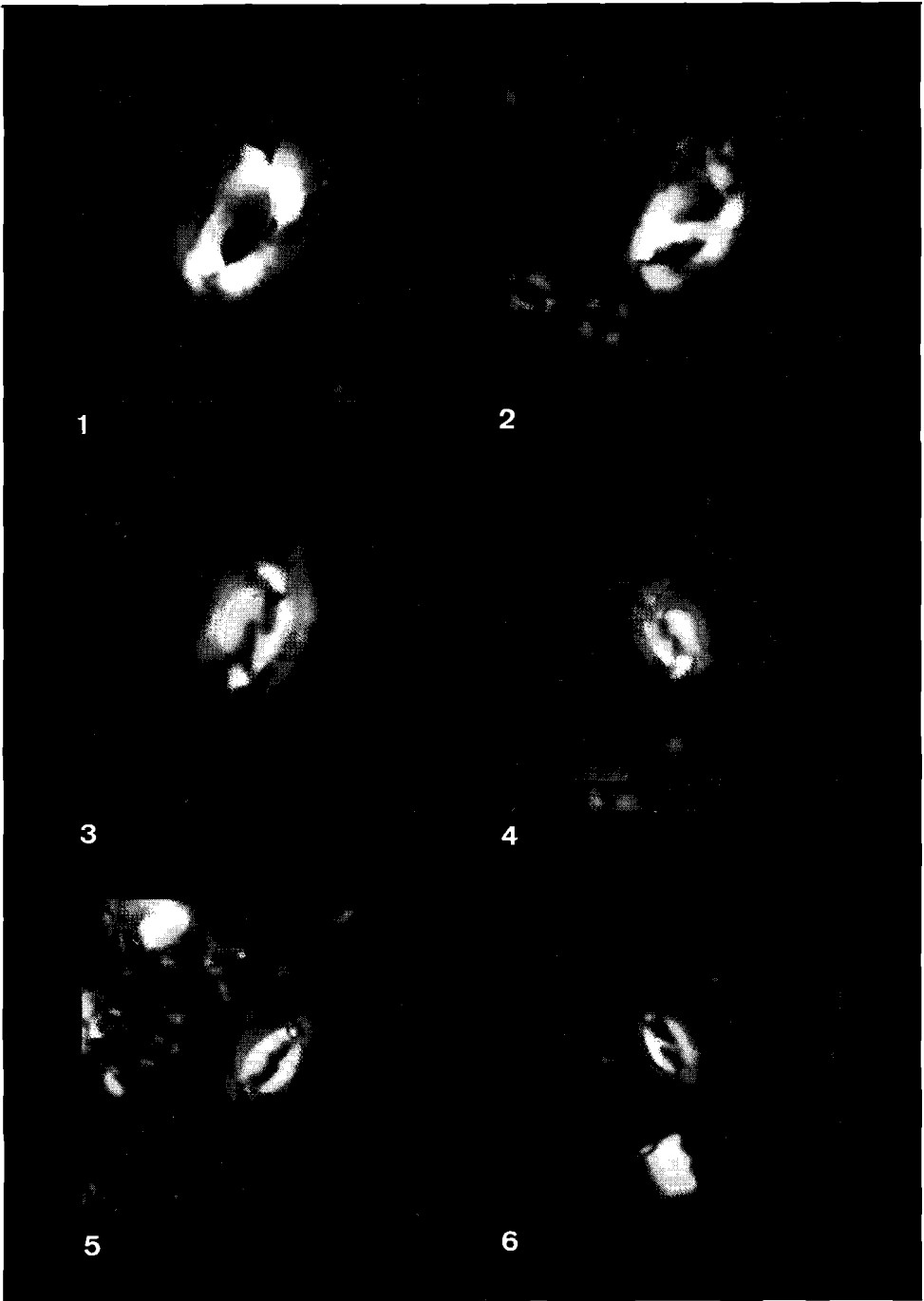


Plate 14

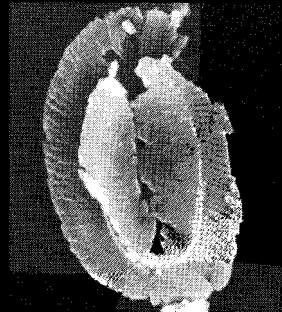
Structural details of the helicoliths

SEM micrographs. Fig. 1: 5400 X; Fig. 2: 5400 X; Fig. 3: 7500 X; Fig. 4: 25000 X; Fig. 5: 35000 X. Fig. 6: 50000 X.

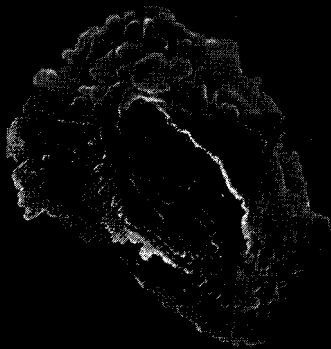
- Fig. 1. Distal view of a helicolith showing characteristics of the blanket. A narrow band of the distal surface of the flange can be observed along the periphery of the specimen.
- Fig. 2. Proximal view of a helicolith showing the proximal plate and part of the flange. The proximal plate is slightly broken (lower left side) exposing part of the proximal portions of the curved elements of the flange.
- Fig. 3. Distal view of a helicolith with partly dissolved centre exposing a cross section of the blanket.
- Figs. 4, 6. Details of figure 3 showing the multiple layers of the blanket and the characteristic bricklaying arrangement of the lamellar elements.
- Fig. 5. Side view of the "wing termination" of the specimen of fig. 3 showing the continuity of the distal and proximal portions of the "curved elements" of the flange.



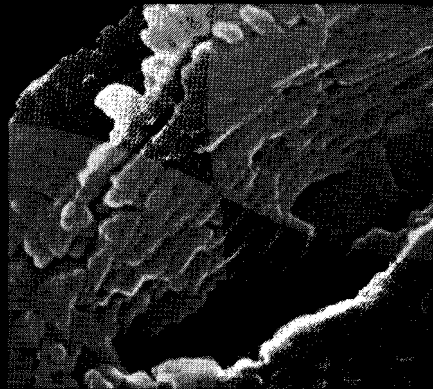
1



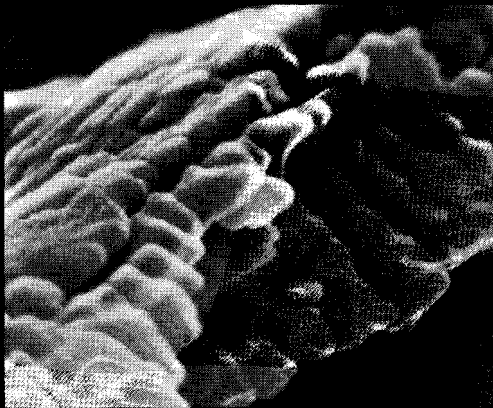
2



3



4



5



6

Plate 15

LM micrographs, crossed nicols. 2447.5 X. All specimens are presented in their original orientation.

Fig. 1. *Helicosphaera seminulum* Bramlette and Sullivan. Sample SP149.

Figs. 2–7. *Helicosphaera bramlettei* (Müller) Jafar and Martini.

Fig. 2. Sample AEB 3920-30.

Figs. 3–7. Sample WEPCO 2500-2530.

Figs. 8–12. *Helicosphaera gartneri* n. sp.

Fig. 8. Holotype. Sample WEPCO 2500–2530.

Figs. 9–12. Sample WEPCO 2500–2530.

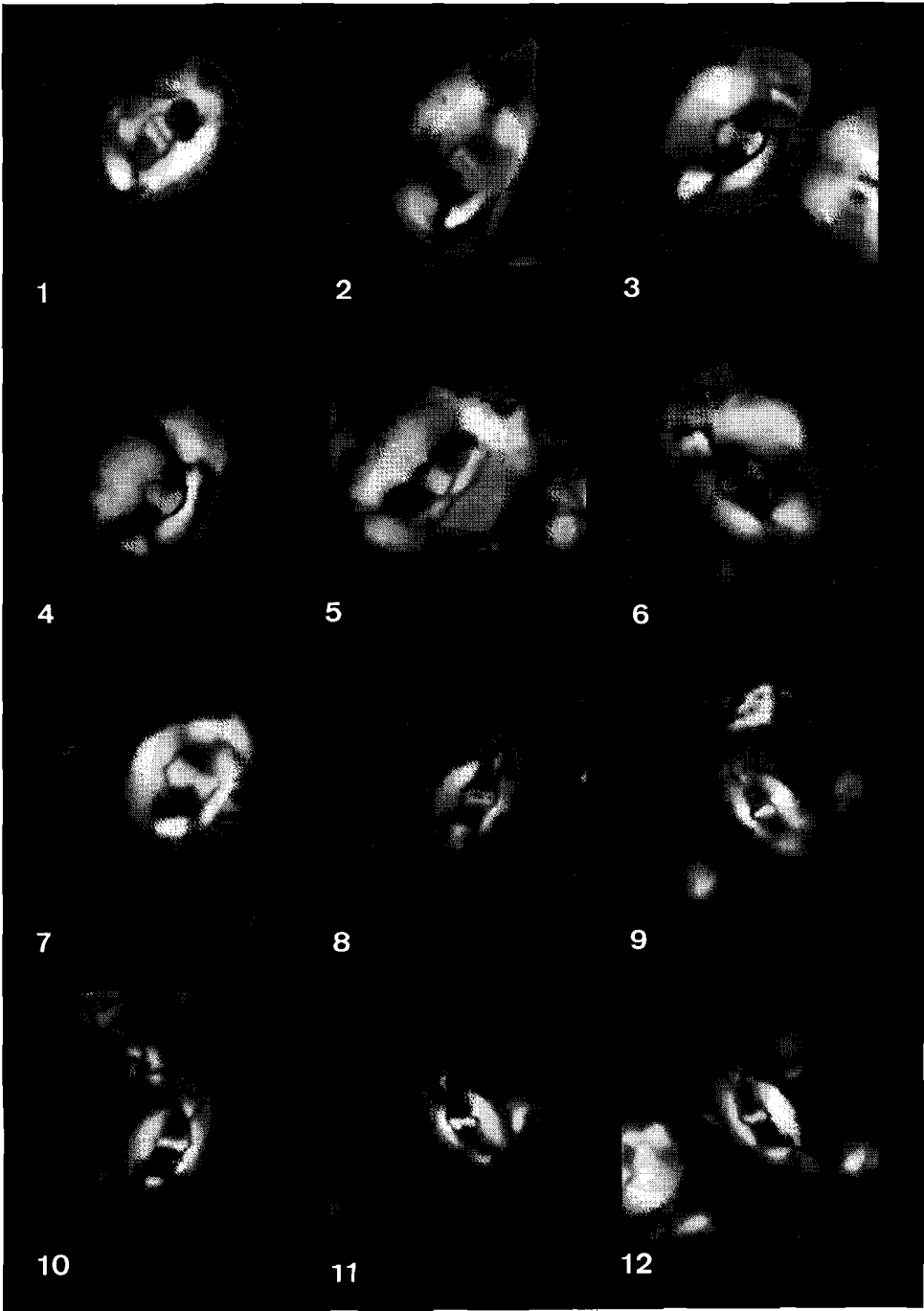


Plate 16

LM micrographs. Figs. 1–6, 8: crossed nicols; Fig. 7: parallel nicols. 2447,5 ×. All specimens are presented in their original orientation.

- Fig. 1. *Helicosphaera heezenii* (Bukry) Jafar and Martini. Sample UM 2990–3000.
Fig. 2. *Helicosphaera papillata* (Bukry and Bramlette) Jafar and Martini. Sample UM 3070–3100.
Figs. 3–5. *Helicosphaera reticulata* Bramlette and Wilcoxon. Sample UM 3070–3100.
Figs. 6–8. *Helicosphaera compacta* Bramlette and Wilcoxon. Sample PL 25.

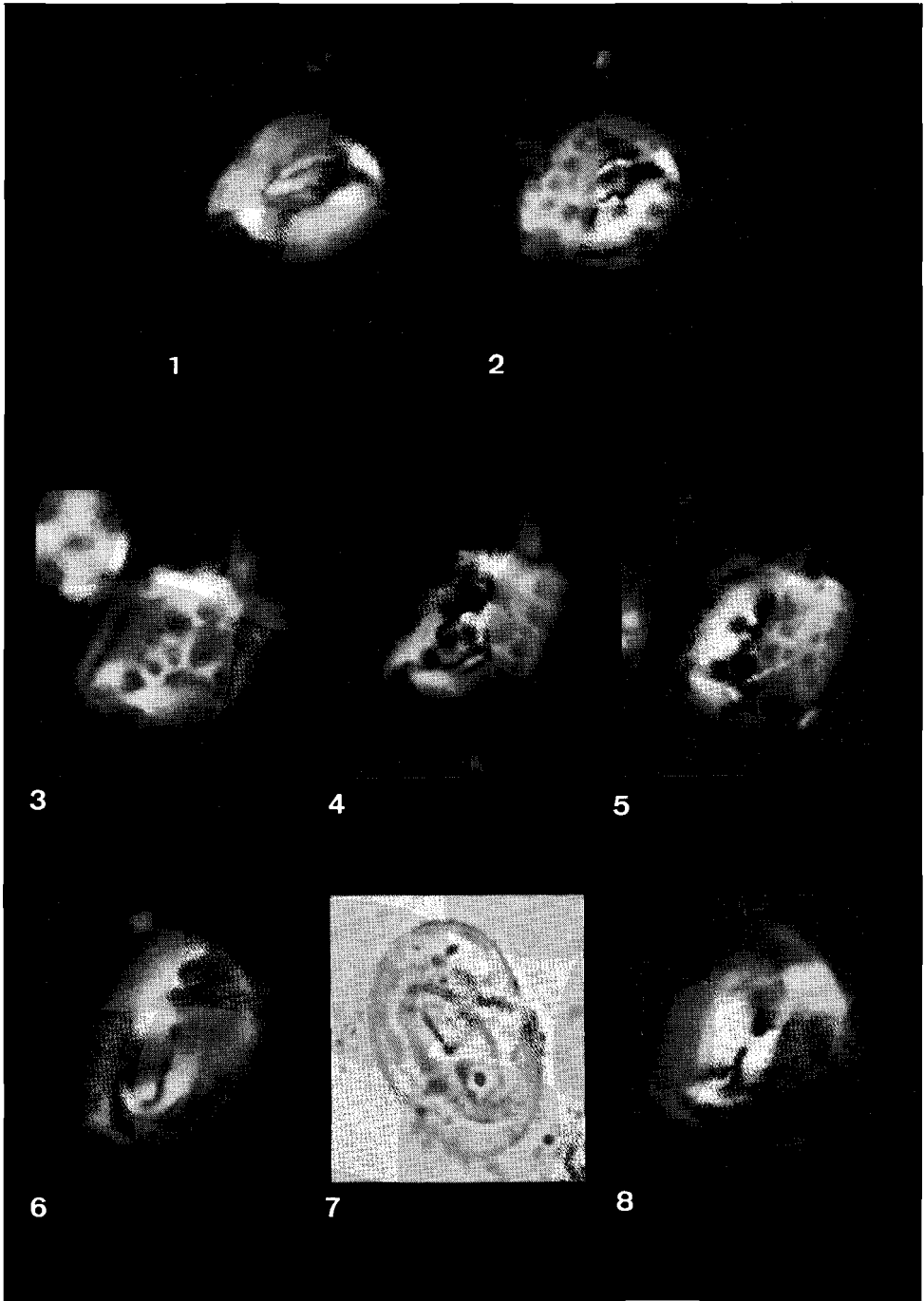


Plate 17

LM micrographs, crossed nicols. Magnification 2447.5 X. All specimens are presented in their original orientation.

- Figs. 1, 2. *Helicosphaera recta* (Haq) Jafar and Martini. Sample 372-147.
- Figs. 3, 4. *Helicosphaera perch-nielseniae* (Haq) Jafar and Martini.
Fig. 3. Sample 372-94.
Fig. 4. Sample MT728.
- Fig. 5. *Helicosphaera obliqua* Bramlette and Wilcoxon. Sample 372-80.
- Figs. 6–9. *Helicosphaera elongata* n. sp.
Fig. 6. Holotype. Sample 369A-10.
Fig. 7. Sample 369A-10.
Fig. 8. Sample 369A-41.
Fig. 9. Sample 369A-49.
- Fig. 10. *Helicosphaera* cf. *H. orientalis* Black. Sample 369A-35.
- Fig. 11. *Helicosphaera orientalis* Black. Sample CP4540.

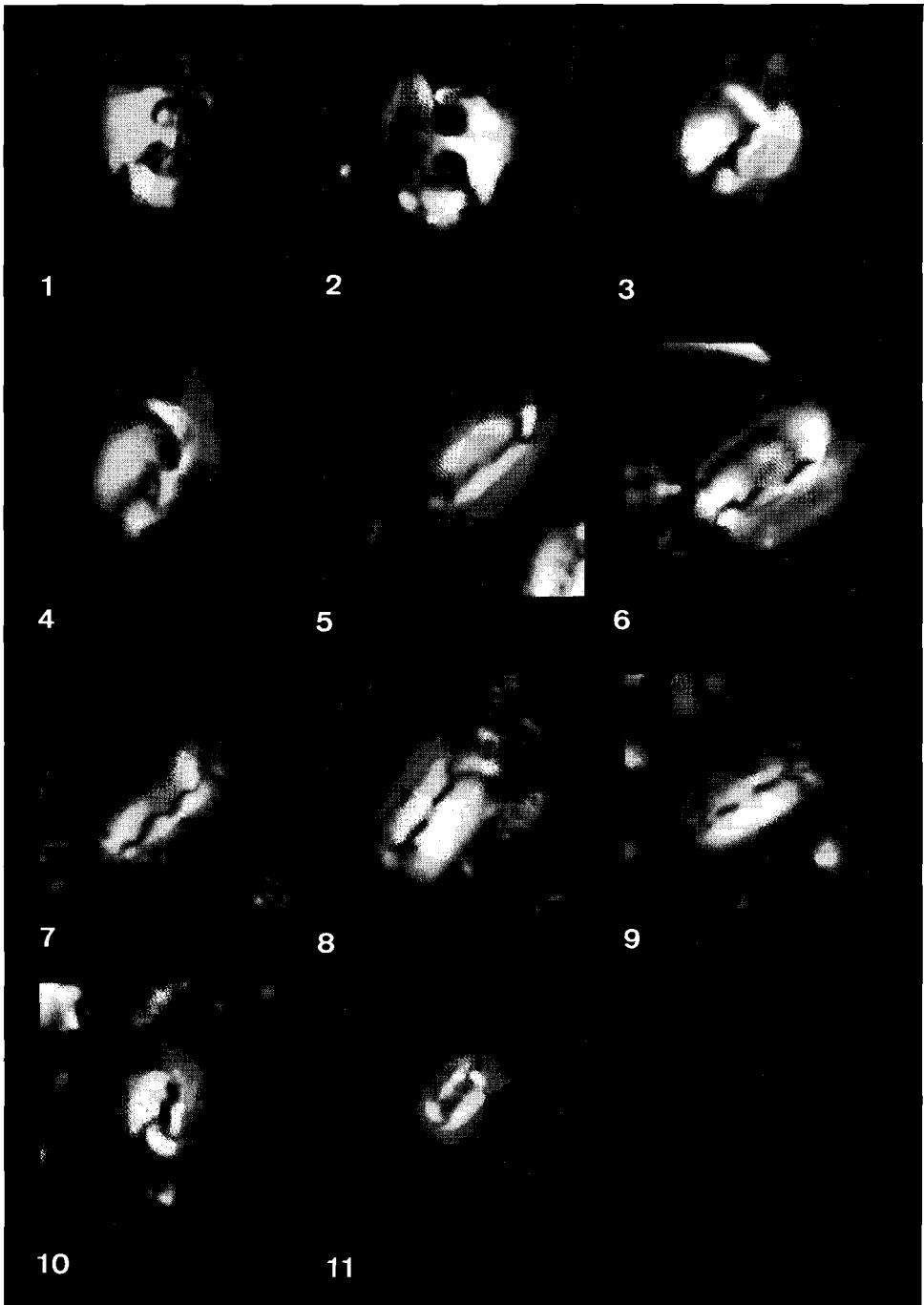


Plate 18

LM micrographs, crossed nicols. Magnification 2447.5 X. All specimens are presented in their original orientation.

- Fig. 1. *Helicosphaera* cf. *H. orientalis* Black. Sample 369A-33.
- Figs. 2–5. *Helicosphaera orientalis* Black.
- Fig. 2. Sample 369A-14.
- Fig. 3. Sample 372-5.
- Fig. 4. Sample CP3730.
- Fig. 5. Sample CP3140.
- Figs. 6–8. *Helicosphaera pacifica* Müller and Brönnimann. Sample CP3149.
- Figs. 9–11. *Helicosphaera acuta* n. sp.
- Fig. 10. Holotype. Sample 397-15-3.
- Figs. 9, 11. Sample 397-15-3.

Plate 18

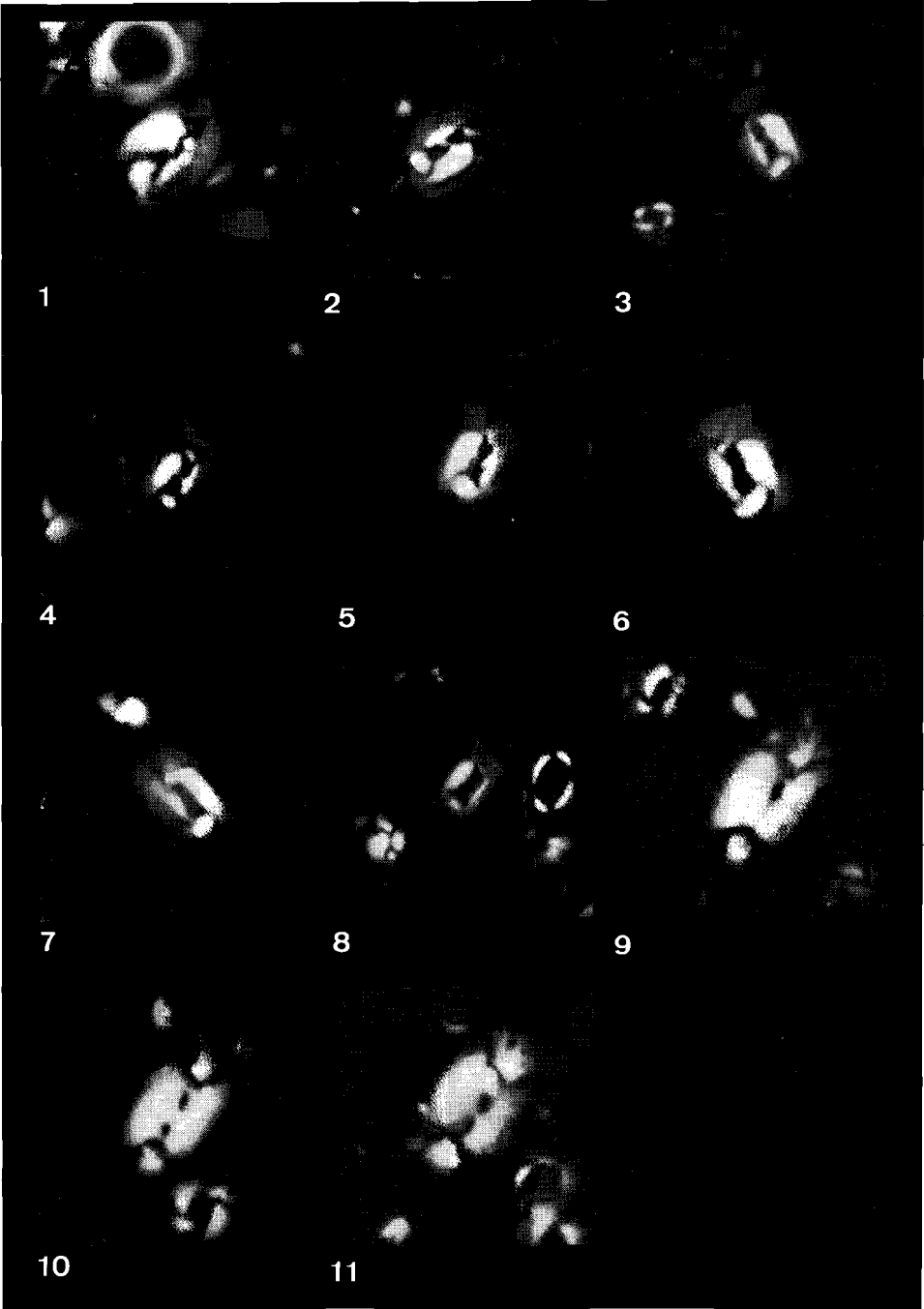


Plate 19

- Figs. 1–10. LM micrographs, crossed nicols. Magnification 2447.5 X. All specimens are presented in their original orientation.
- Fig. 11. SEM micrograph, 8900 X.
- Figs. 1–4. *Helicosphaera ampliaperta* Bramlette and Wilcoxon.
Fig. 1. Sample CP3610.
Fig. 2. Sample 372-110.
Figs. 3, 4. Sample MT732.
- Figs. 5–8. *Helicosphaera scissura* Miller.
Figs. 5, 6. Sample 372-96.
Fig. 7. Sample MT731.
Fig. 8. Sample CP3615.
- Figs. 9–11. *Helicosphaera walbersdorfensis* Müller.
Figs. 9, 11. Sample JT3071.
Fig. 10. Sample CP3690.

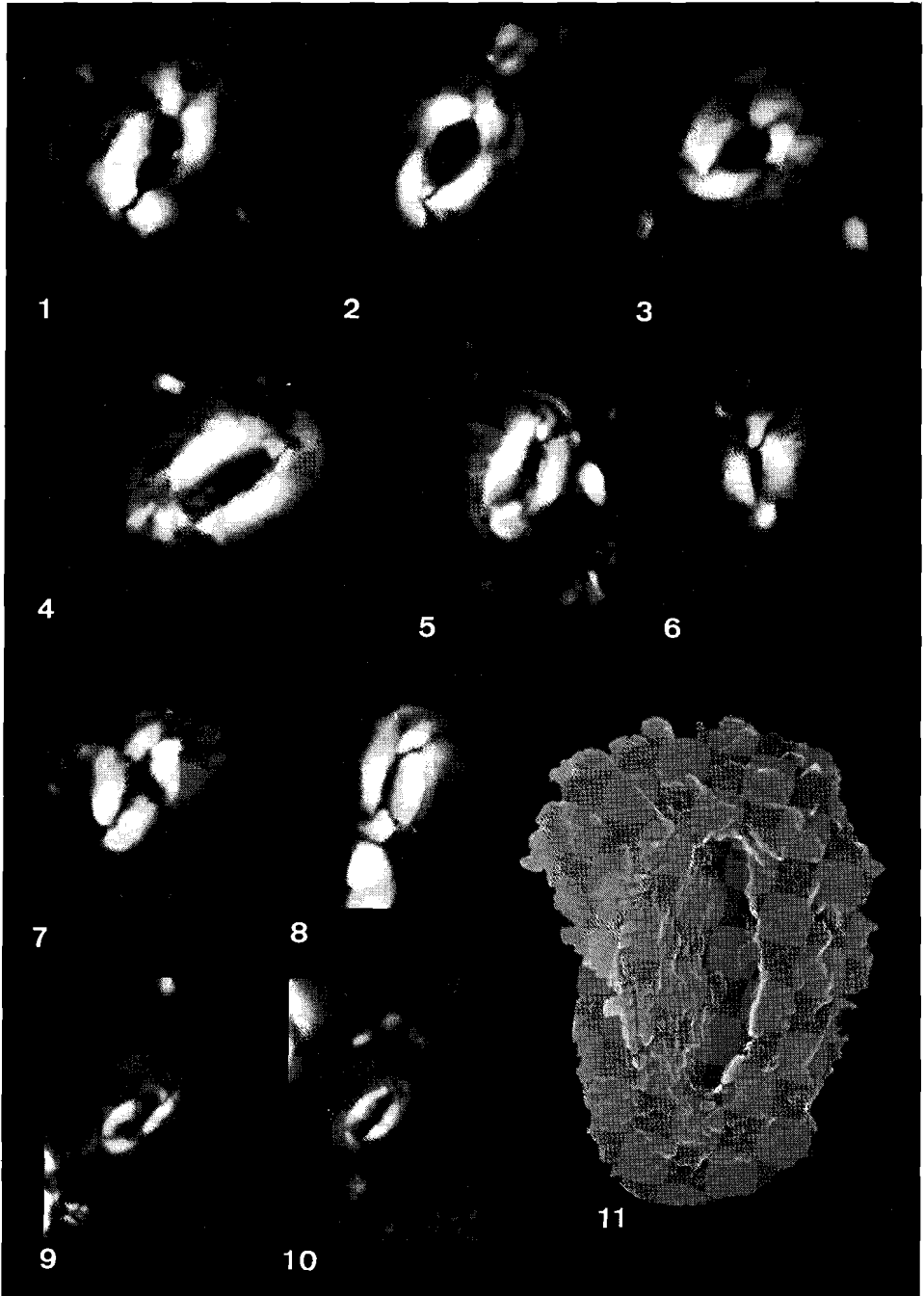


Plate 20

LM micrographs, crossed nicols. Magnification 2447.5 X. All specimens are presented in their original orientation.

- Figs. 1-4. *Helicosphaera vedderi* Bukry.
Fig. 1. Sample CP3616.
Figs. 2, 3. Sample MT729.
Fig. 4. Sample 372-112.
- Figs. 5-9. *Helicosphaera waltrans* n. sp.
Fig. 5. Holotype. Sample MT740.
Fig. 6. Sample MT740.
Fig. 7. Sample MT739.
Fig. 8. Sample MT741.
Fig. 9. Sample MT737.
- Figs. 10-12. *Helicosphaera stalis ovata* n. sp., n. subsp. Sample CP3122.

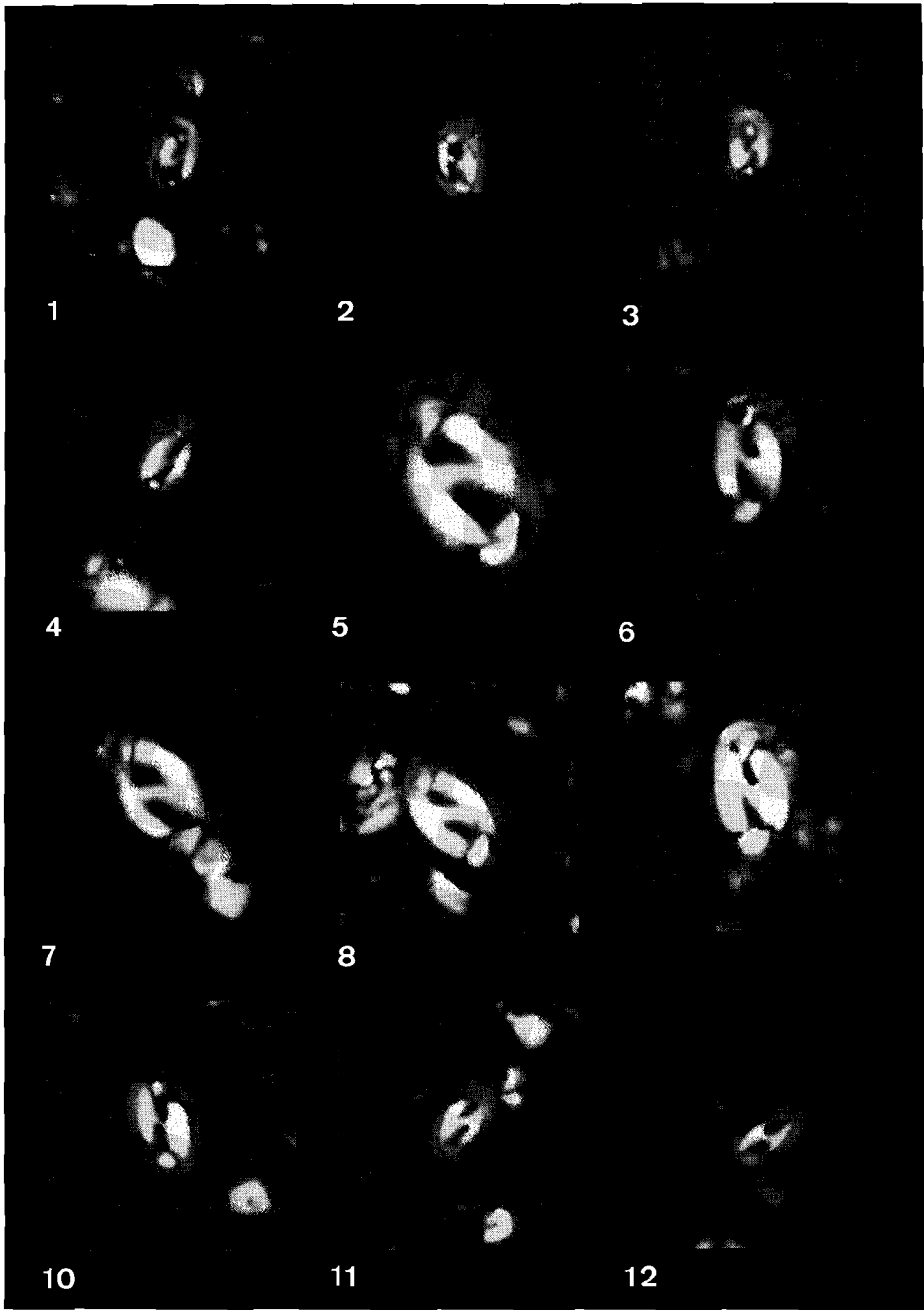


Plate 21

LM micrographs, crossed nicols. Magnification 2447.5 X. All specimens are presented in their original orientation.

- Figs. 1–7. *Helicosphaera stalis ovata* n. sp., n. subsp.
Fig. 1. Holotype of subspecies. Sample CP4609.
Figs. 3, 4. Sample CP3118.
Figs. 5–7. Sample CP3059.
- Figs. 8–12. *Helicosphaera stalis stalis* n. sp., n. subsp.
Fig. 9. Holotype of species and subspecies. Sample CP3018.
Figs. 8, 10, 11. Sample 369A-15.
Fig. 12. Sample CP3020.

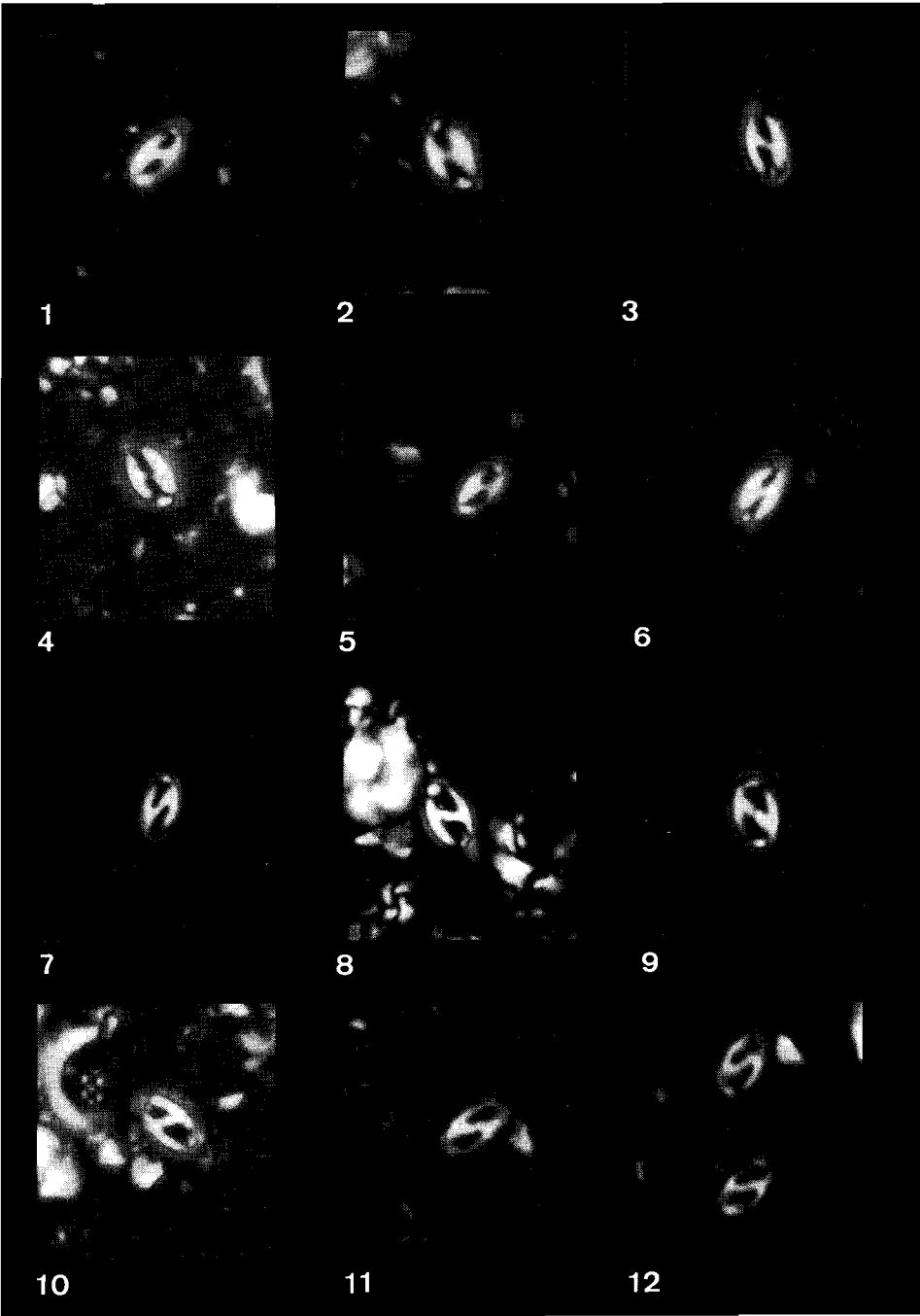


Plate 22

LM micrographs, crossed nicols. Magnification 2447.5 X. All specimens are presented in their original orientation.

- Figs. 1, 2. *Helicosphaera euphratis* Haq.
Fig. 1. Sample 369A-75.
Fig. 2. Sample MT713.
- Fig. 3. *Helicosphaera intermedia* Martini. Sample M110-D.
- Figs. 4–9. *Helicosphaera mediterranea* Müller.
Figs. 4, 5. Sample CP3618.
Fig. 6. Sample 369A-36.
Figs. 7–9. Sample MT736.

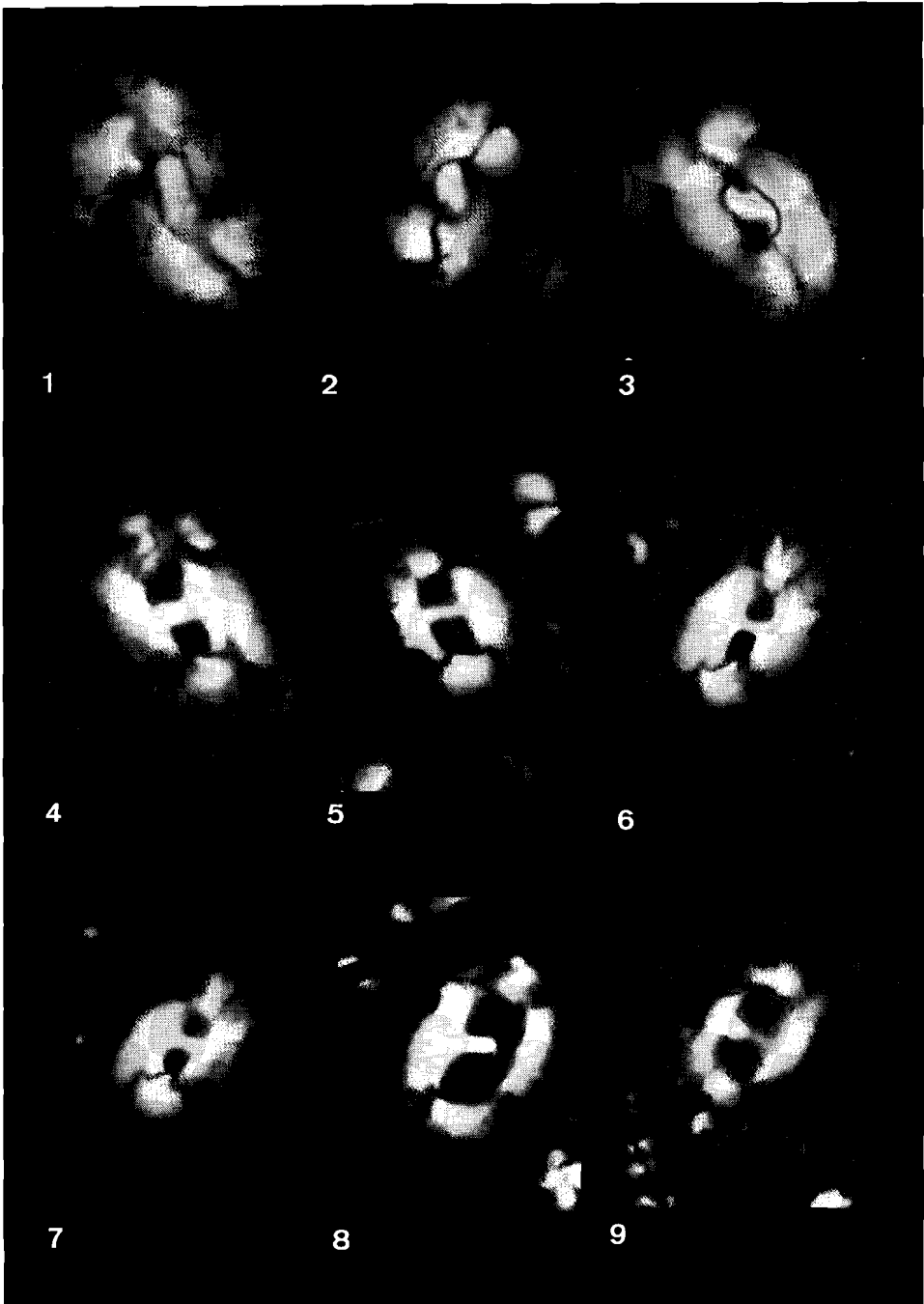


Plate 23

LM micrographs, crossed nicols. Magnification 2447.5 X. All specimens are presented in their original orientation.

- Figs. 1–4. *Helicosphaera paleocarteri* n. sp.
Fig. 1. Holotype. Sample CP3682.
Figs. 2–4. Sample CP3670.
- Fig. 5. *Helicosphaera carteri* var. *carteri* n. var.
 Sample 369A-25.
- Figs. 6, 7. *Helicosphaera carteri* var. *burkei* n. var.
Fig. 6. Sample 369A-5.
Fig. 7. Sample 231-95.
- Figs. 8, 9. *Helicosphaera carteri* var. *wallichii* n. var.
 Sample SI20.

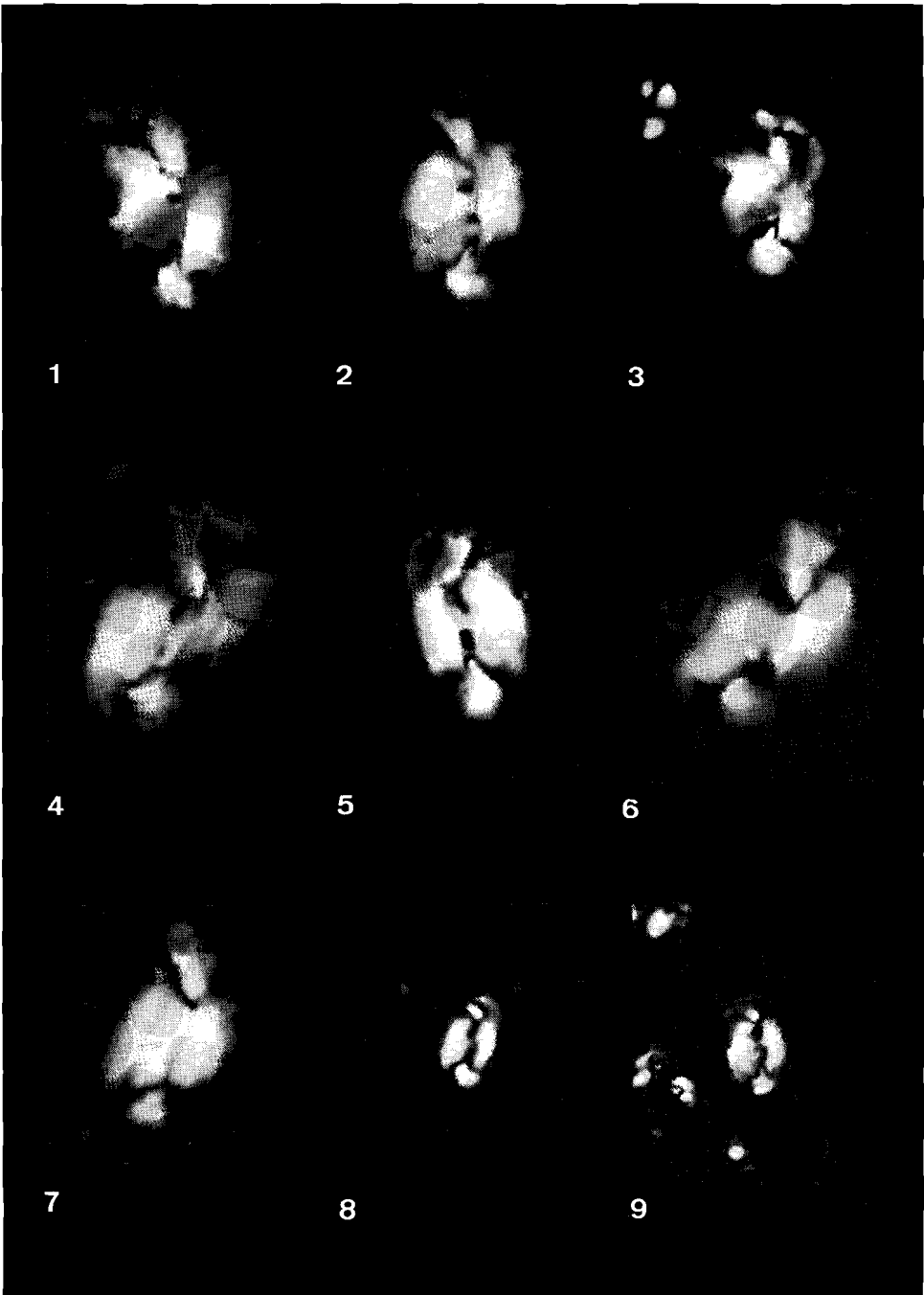
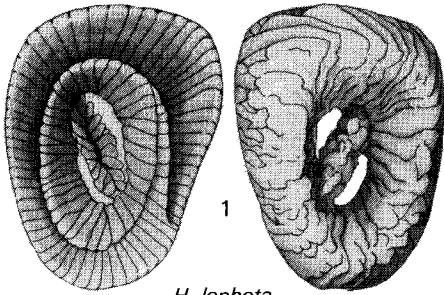


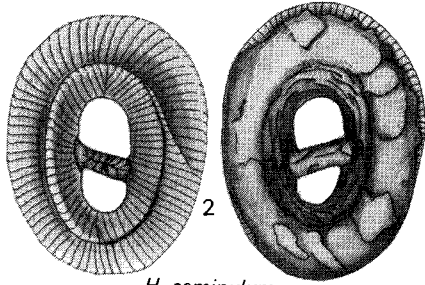
Plate 24

Helicoliths depicted in proximal (left) and distal view (right). 3300 X.

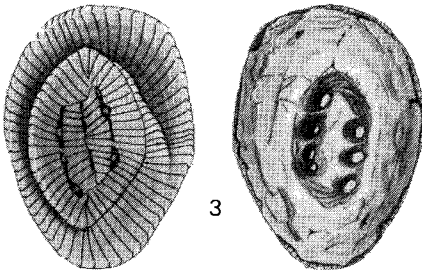
Plate 24



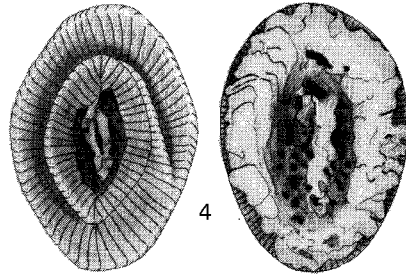
H. lophota



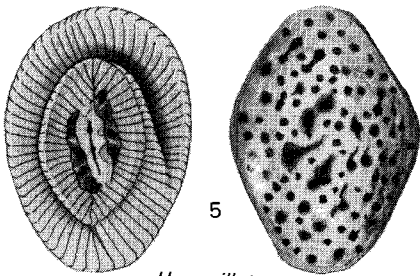
H. seminulum



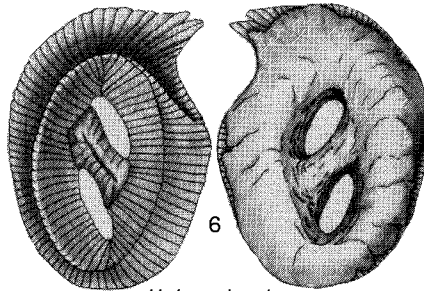
H. heezenii



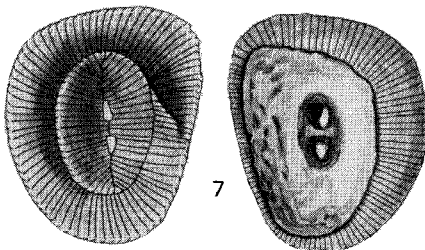
H. dinesenii



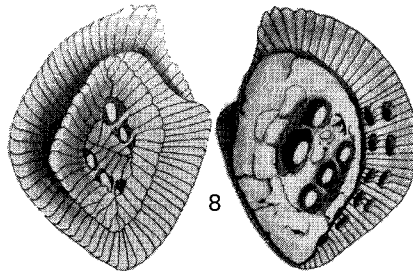
H. papillata



H. bramlettei



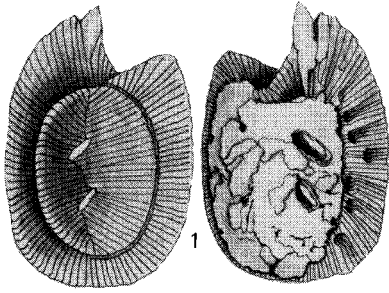
H. compacta



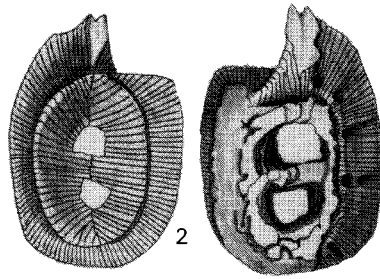
H. reticulata

Plate 25

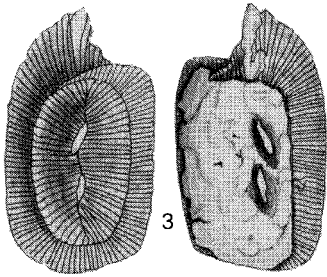
Helicoliths depicted in proximal (left) and distal view (right). 3300 X.



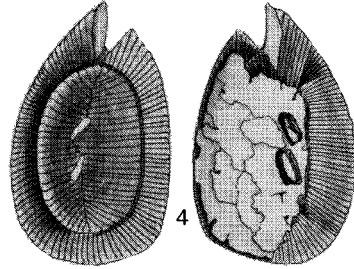
H. perch-nielsenae



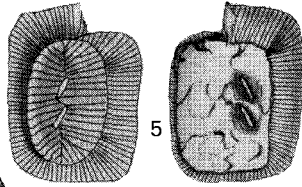
H. recta



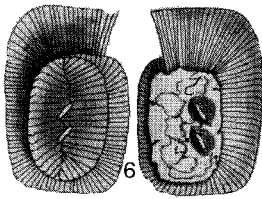
H. elongata



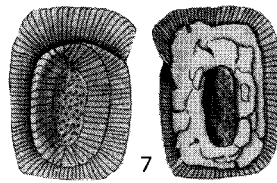
H. obliqua



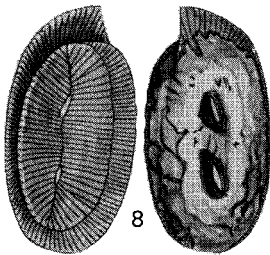
H. cf. H. orientalis



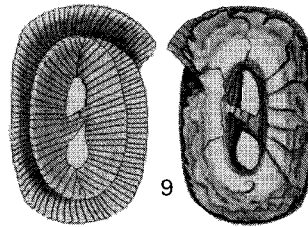
H. orientalis



H. pacifica



H. acuta

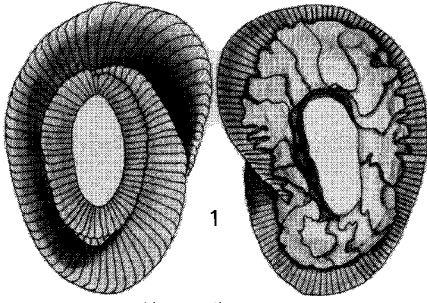


H. inversa

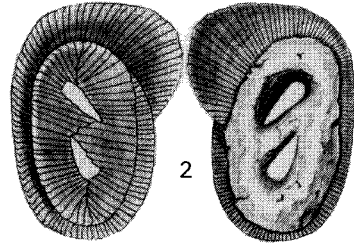
Plate 26

Helicoliths depicted in proximal (left) and distal view (right). 3300 X.

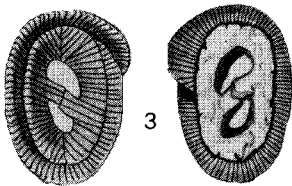
Plate 26



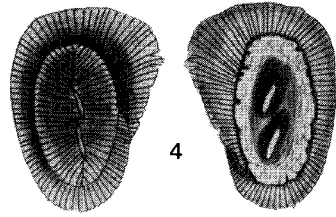
H. ampliaperta



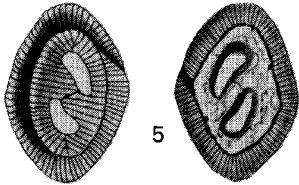
H. waltrans



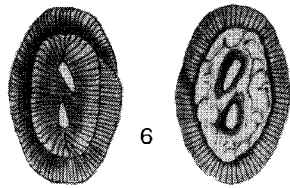
H. vedderi



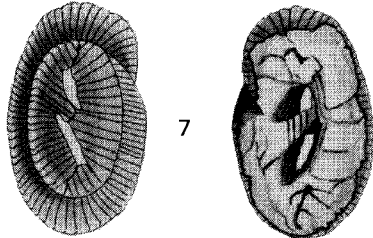
H. walbersdorfensis



H. stalis stalis



H. stalis ovata

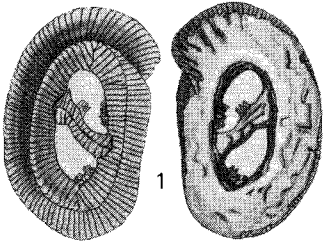


H. sellii

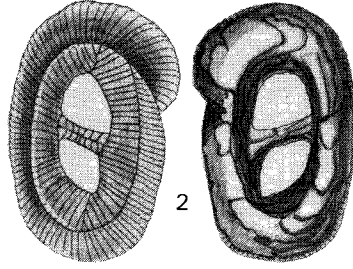
Plate 27

Helicoliths depicted in proximal (left) and distal view (right). 3300 X.

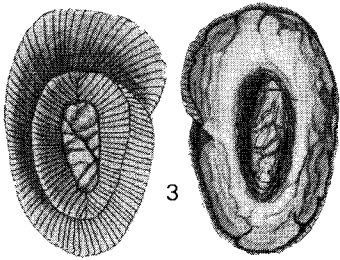
Plate 27



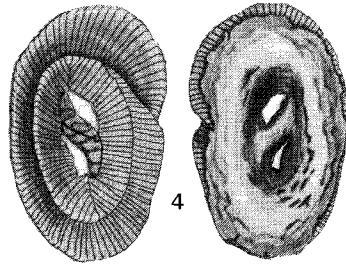
H. gartneri



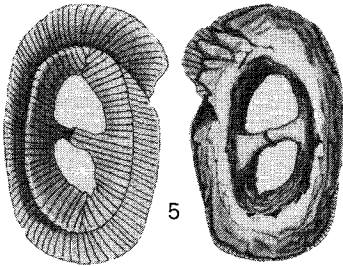
H. truempyi



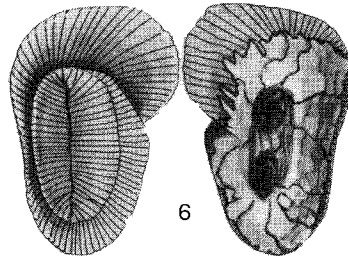
H. euphratis



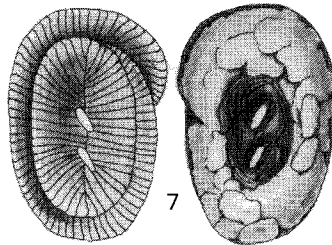
H. intermedia



H. mediterranea



H. paleocarteri



H. carteri

Plate 28

LM micrographs, parallel nicols, 1485 X.

- Figs. 1, 2. *Helio-discoaster mohleri* (Bukry and Percival) Theodoridis. Same specimen, sample IR115, (fig. 1: low focus, fig. 2: high focus).
- Fig. 3. *Helio-discoaster multiradiatus* (Bramlette and Riedel) Theodoridis. Sample SP630.
- Fig. 4. *Helio-discoaster gemmeus* (Stradner) Theodoridis. Sample IR129.
- Figs. 5, 6. *Helio-discoaster nobilis* (Martini) Theodoridis. Same specimen, sample SP630, (fig. 5: low focus, fig. 6: high focus).
- Figs. 7–9. *Helio-discoaster mediosus* (Bramlette and Sullivan) Theodoridis.
Figs. 7, 8. Same specimen, sample IR117, (fig. 7: high focus, fig. 8: low focus).
Fig. 9. Sample IR119.
- Figs. 10–12. *Helio-discoaster elegans* (Bramlette and Sullivan) Theodoridis. Same specimen, sample IR119, (fig. 10: high focus, fig. 11: middle focus, fig. 12: low focus).

Plate 28

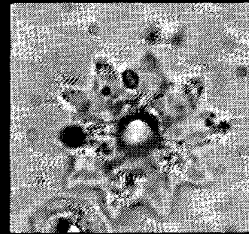
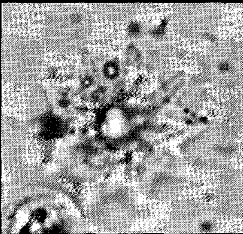
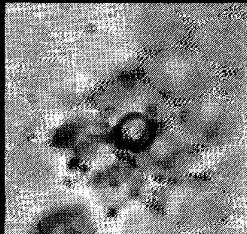
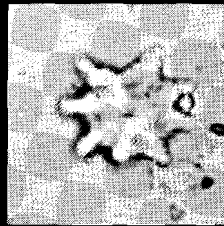
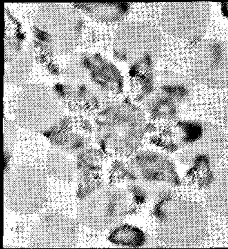
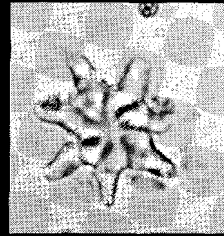
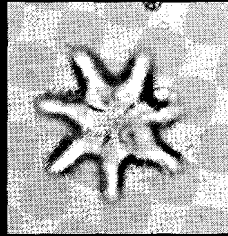
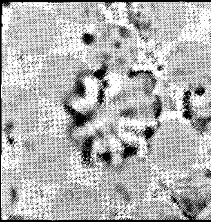
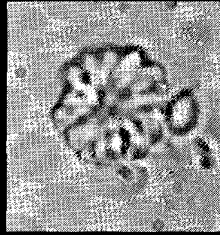
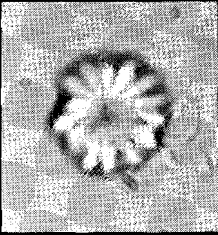
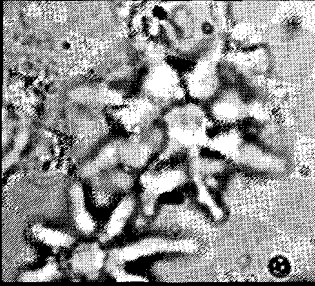


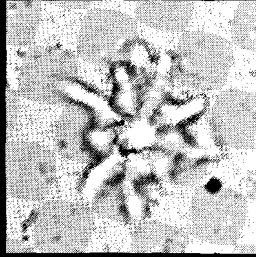
Plate 29

LM micrographs, parallel nicols, 1485 X.

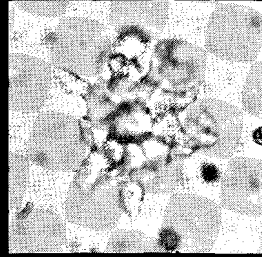
- Figs. 1–3. *Helio-discoaster diastypus* (Bramlette and Sullivan) Theodoridis.
Fig. 1. Sample SP641.
Figs. 2, 3. Same specimen, sample SP641, (fig. 2: high focus, fig. 3: low focus).
- Figs. 4–8. *Helio-discoaster barbadiensis* (Tan) Theodoridis.
Figs. 4–6. Same specimen, sample IR150, (fig. 4: high focus, fig. 5: middle focus, fig. 6: low focus).
Figs. 7, 8. Same specimen, sample IR150, (fig. 7: high focus, fig. 8: low focus).
- Figs. 9–13. *Helio-discoaster kuepperi* (Stradner) Theodoridis.
Figs. 9, 10. Same specimen, sample IR141, (fig. 9: high focus, fig. 10: low focus).
Figs. 11–13. Same specimen, sample IR141, (fig. 11: low focus, fig. 12: middle focus, fig. 13: high focus).



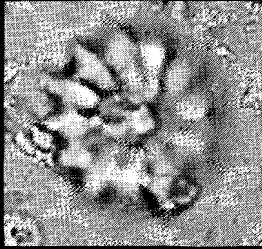
1



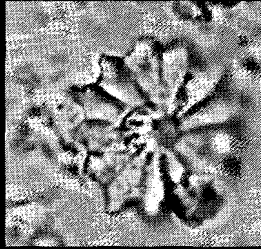
2



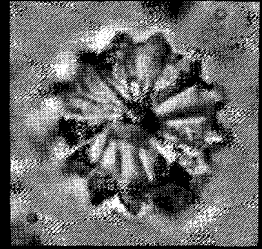
3



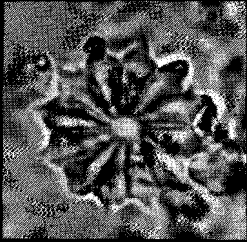
4



5



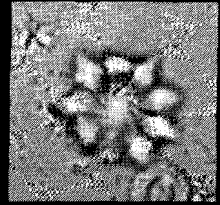
6



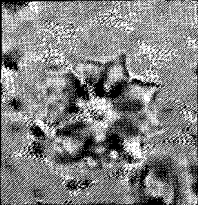
7



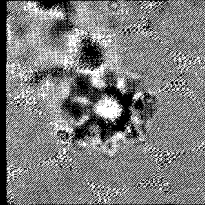
8



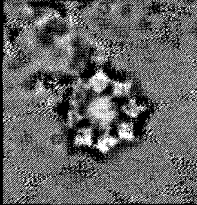
9



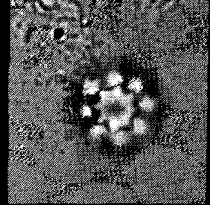
10



11



12



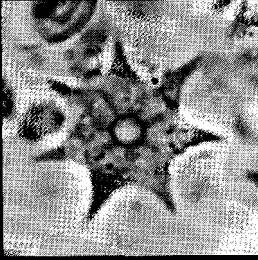
13

Plate 30

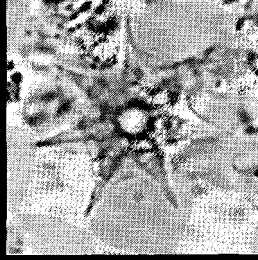
LM micrographs, parallel nicols, 1485 X.

- Figs. 1–3. *Helio-discoaster saipanensis* (Bramlette and Riedel) Theodoridis. Same specimen, sample SP690, (fig. 1: high focus, fig. 2: middle focus, fig. 3: low focus).
- Figs. 4–6. *Helio-discoaster lodoensis* (Bramlette and Riedel) Theodoridis.
Figs. 4, 5. Same specimen, sample SP643 (fig. 4: high focus, fig. 5: low focus).
Fig. 6. Sample SP643.
- Figs. 7, 8. *Helio-discoaster colletii* (Parejas) Theodoridis. Same specimen, sample IR144, (fig. 7: low focus, fig. 8: high focus).

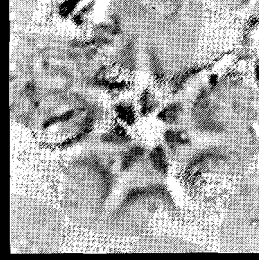
Plate 30



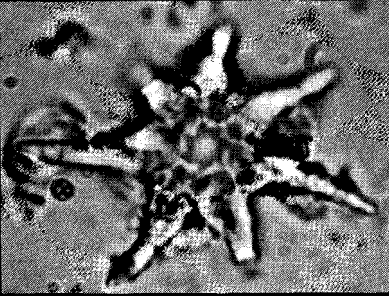
1



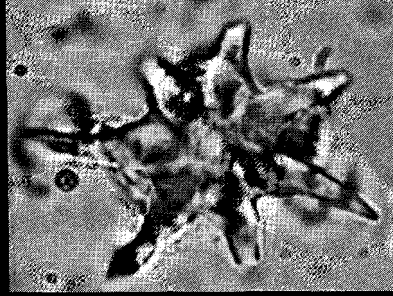
2



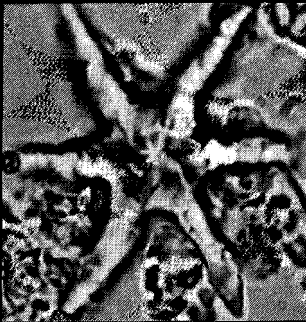
3



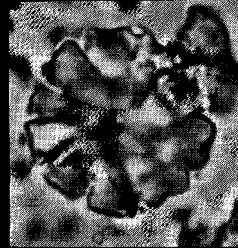
4



5



6



7

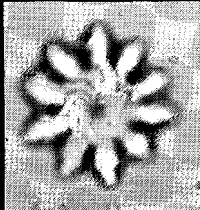


8

Plate 31

LM micrographs, parallel nicols, 1485 X.

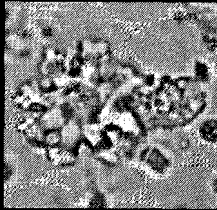
- Figs. 1, 2. *Helio-discoaster ornatus* (Stradner) Theodoridis. Same specimen, sample SP640, (fig. 1: high focus, fig. 2: low focus).
- Figs. 3–5. *Helio-discoaster mirus* (Deflandre) Theodoridis. Same specimen, sample IR134, (fig. 3: high focus, fig. 4: middle focus, fig. 5: low focus).
- Figs. 6, 7. *Helio-discoaster nodifer* (Bramlette and Riedel) Theodoridis. Same specimen, sample UM 2990–3000, (fig. 6: high focus, fig. 7: low focus).
- Figs. 8–10. *Helio-discoaster tanii* (Bramlette and Riedel) Theodoridis.
Fig. 8. Sample UM 2990–3000, high focus.
Figs. 9, 10. Same specimen, sample UM 2990–3000 (fig. 9: low focus, fig. 10: high focus).



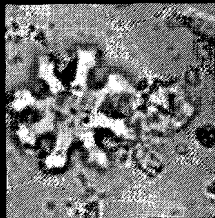
1



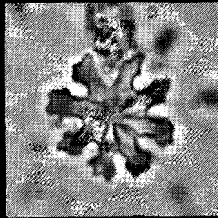
2



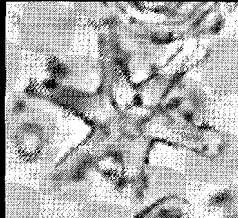
3



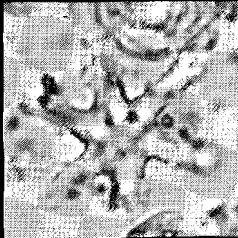
4



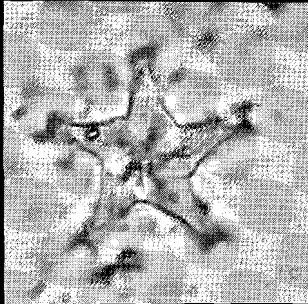
5



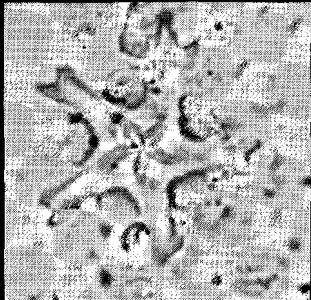
6



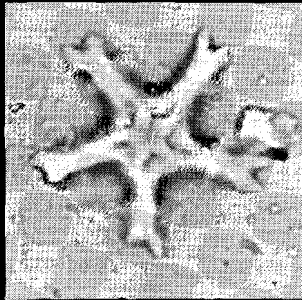
7



8



9



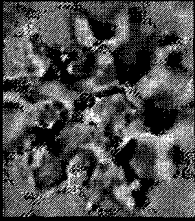
10

Plate 32

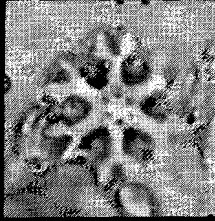
LM micrographs, parallel nicols, 1485 X.

- Figs. 1, 2. *Eu-discoaster distinctus* (Martini) Theodoridis. Sample UM 2990–3000.
- Figs. 3, 4. *Eu-discoaster nonradiatus* (Klumpp) Theodoridis. Sample UM 2990–3000, focus on the distal side.
- Fig. 5. *Eu-discoaster deflandrei* (Bramlette and Riedel) Theodoridis. Sample 372-139.
- Figs. 6, 7. *Eu-discoaster druggii* (Bramlette and Wilcoxon) Theodoridis.
Fig. 6. Sample 372-142, focus on the distal side.
Fig. 7. Sample 369A-73, focus on the distal side.
- Fig. 8. *Eu-discoaster variabilis* (Martini and Bramlette) Theodoridis. Sample 219-1, focus on the proximal side.
- Figs. 9, 10. *Eu-discoaster pansus* (Bukry) Theodoridis. Same specimen, sample 231-93 (fig. 9: focus on the proximal side, fig. 10: focus on the distal side).
- Fig. 11. *Eu-discoaster decorus* (Bukry) Theodoridis. Focus on the distal side.
- Figs. 12, 13. *Eu-discoaster pseudovariabilis* (Martini and Worsley) Theodoridis. Same specimen, sample 231-130 (fig. 12: focus on the distal side, fig. 13: focus on the proximal side).

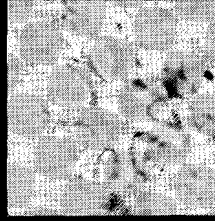
Plate 32



1



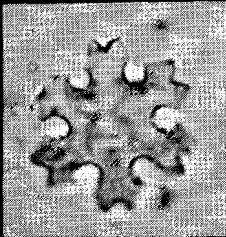
2



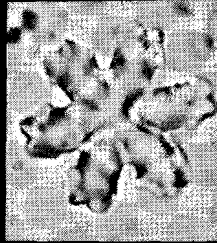
3



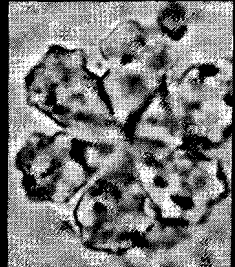
4



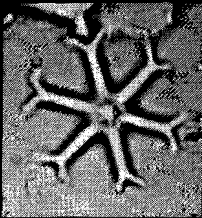
5



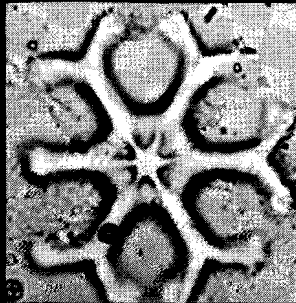
6



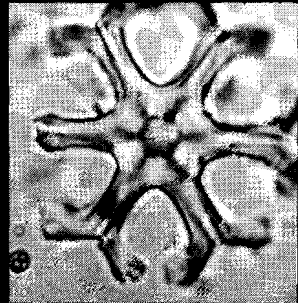
7



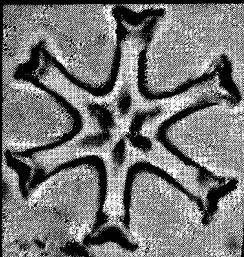
8



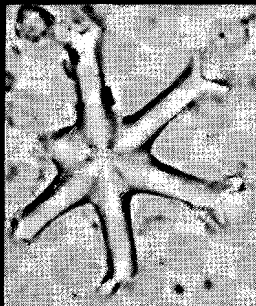
9



10



11



12



13

Plate 33

LM micrographs, parallel nicols, 1485 X.

- Figs. 1, 2. *Eu-discoaster protoexilis* n. sp.
Fig. 1. Holotype. Sample 369A-67, focus on the distal side.
Fig. 2. Sample 369A-67, focus on the distal side.
- Figs. 3–5. *Eu-discoaster exilis* (Martini and Bramlette) Theodoridis.
Fig. 3. Sample 372-44, focus on the outline.
Fig. 4. Sample 372-44, focus on the distal side.
Fig. 5. Sample CP3721 focus on the proximal side.
- Figs. 6, 7. *Eu-discoaster* cf. *E. bollii* (Martini and Bramlette) Theodoridis. Same specimen, sample CP3118, (fig. 6: focus on the distal side, fig. 7: focus on the proximal side).
- Figs. 8–11. *Eu-discoaster bollii* (Martini and Bramlette) Theodoridis.
Figs. 8, 9. Sample 231-116.
Figs. 10, 11. Sample 231-115.
- Figs. 12, 13. *Eu-discoaster subsurculus* (Gartner) Theodoridis. Sample 369A-6.
- Figs. 14–17. *Eu-discoaster signus* (Bukry) Theodoridis. Same specimen, sample 369A-41. The figures are arranged in order from low to high focus.

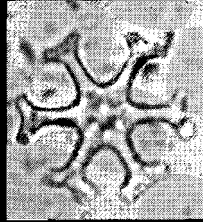
Plate 33



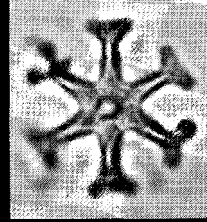
1



2



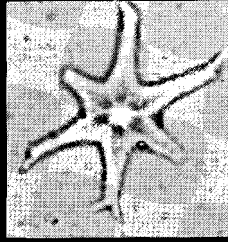
3



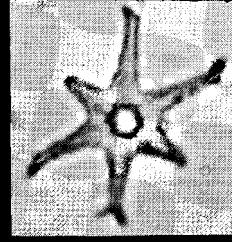
4



5



6



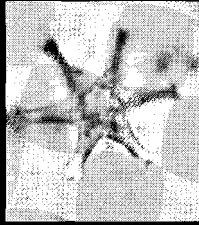
7



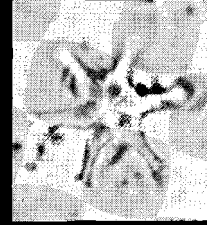
8



9



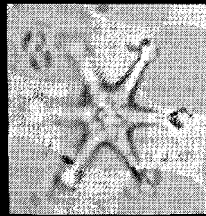
10



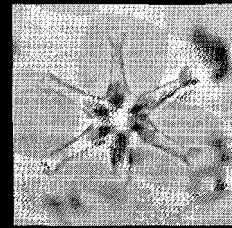
11



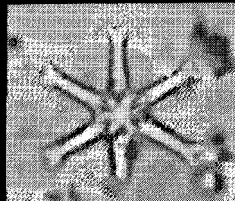
12



13



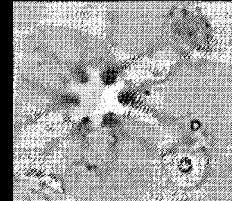
14



15



16



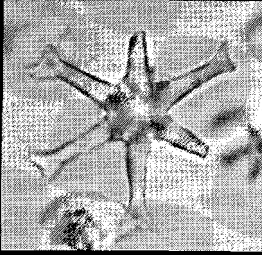
17

Plate 34

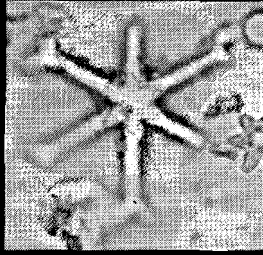
LM micrographs, parallel nicols, 1485 X.

- Figs. 1–6. *Eu-discoaster signus* (Bukry) Theodoridis.
Figs. 1–3. Same specimen, sample 369A-50 (fig. 1: low focus, fig. 2: middle focus, fig. 3: high focus).
Figs. 4, 5. Same specimen, sample 369A-47 (fig. 4: low focus, fig. 5: high focus).
Fig. 6. Sample 369A-39.
- Figs. 7–14. *Eu-discoaster* cf. *E. signus* (Bukry) Theodoridis.
Figs. 7, 8. Same specimen, sample 369A-59 (fig. 7: low focus, fig. 8: high focus).
Figs. 9, 10. Same specimen, sample 369A-59 (fig. 9: low focus, fig. 10: high focus).
Figs. 11, 12. Sample 369-54.
Figs. 13, 14. Same specimen, sample 369A-59 (fig. 13: low focus, fig. 14: high focus).
- Figs. 15–18. *Eu-discoaster musicus* (Stradner) Theodoridis.
Figs. 15–17. Same specimen, sample 369A-52 (fig. 15: low focus, fig. 16: middle focus, fig. 17: high focus).
Fig. 18. Sample 369A-36.

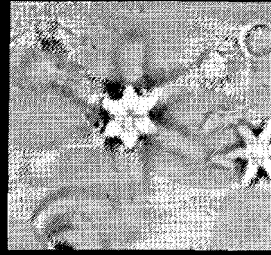
Plate 34



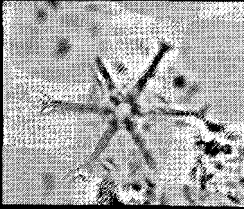
1



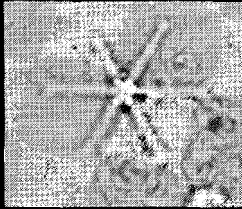
2



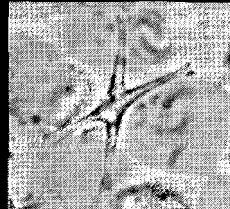
3



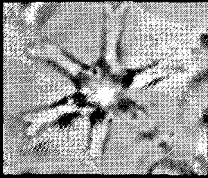
4



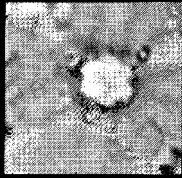
5



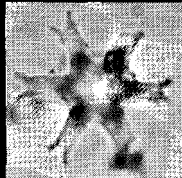
6



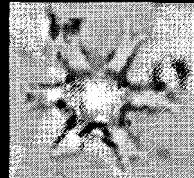
7



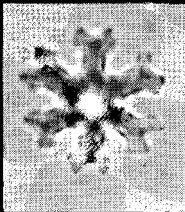
8



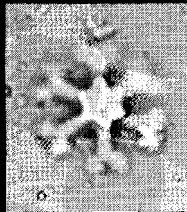
9



10



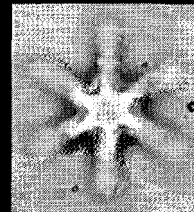
11



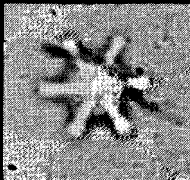
12



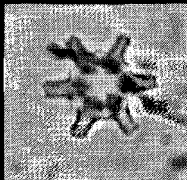
13



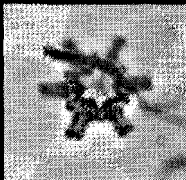
14



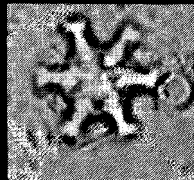
15



16



17



18

Plate 35

LM micrographs, parallel nicols, 1485 X.

- Figs. 1–4. *Eu-discoaster pentaradiatus* (Tan) Theodoridis.
Figs. 1–3. Sample 231-106.
Fig. 4. Sample 101.
- Fig. 5. *Eu-discoaster musicus* (Stradner) Theodoridis. Sample 369A-36.
- Figs. 6, 7, 9. *Eu-discoaster coalitus* (Martini and Bramlette) n. comb. Sample 231-125.
- Fig. 8. *Eu-discoaster calyculus* (Martini and Bramlette) n. comb.
- Figs. 10–12. *Eu-discoaster mexicanus* (Bukry) n. comb.
Fig. 10. Sample 231-117.
Figs. 11, 12. Sample 231-121.
- Figs. 13, 14. *Eu-discoaster calcaris* (Gartner) Theodoridis.
Fig. 13. Sample 231-124.
Fig. 14. Sample CP3131.
- Figs. 15–18. *Eu-discoaster kugleri* (Martini and Bramlette) Theodoridis.
Fig. 15. Sample 369A-6.
Fig. 16. Sample 369A-8.
Figs. 17, 18. Sample 369A-5.

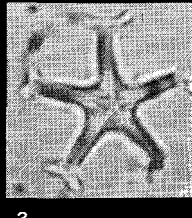
Plate 35



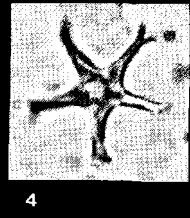
1



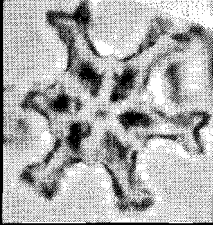
2



3



4



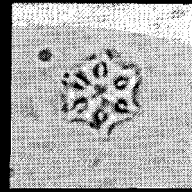
5



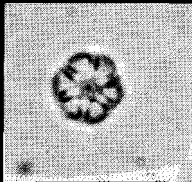
6



7



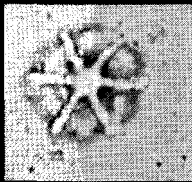
8



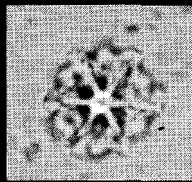
9



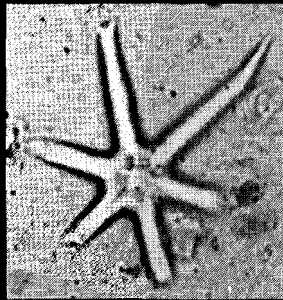
10



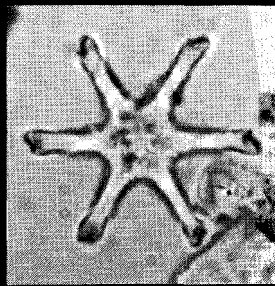
11



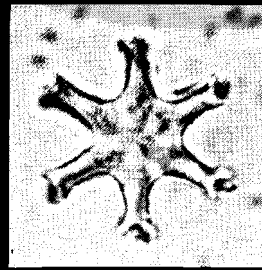
12



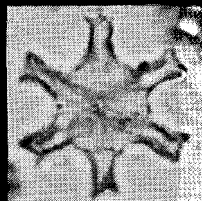
13



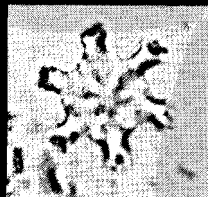
14



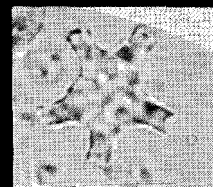
15



16



17

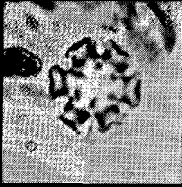


18

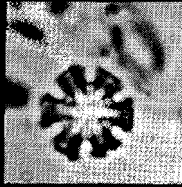
Plate 36

LM micrographs. Figs. 1–7, 9–17 parallel nicols. Fig. 8 crossed nicols, 1485 X.

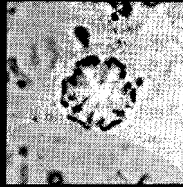
- Figs. 1–3. *Eu-discoaster micros* n. sp.
Figs. 1, 2. Holotype. Same specimen (fig. 1: high focus, fig. 2: low focus), sample 369A-7.
Fig. 3. Sample 369A-7.
- Figs. 4–10. *Eu-discoaster giganteus* n. sp.
Figs. 5, 6. Holotype. Same specimen (fig. 5: high focus, fig. 6: low focus), sample 231-110.
Fig. 4. Sample 231-117.
Fig. 7. Side view of a single segment, sample 231-117.
Fig. 8. Side view of a single segment, sample 231-113.
Figs. 9, 10. Same specimen (fig. 9: high focus, fig. 10: low focus), sample 231-113.
- Figs. 11, 12. *Eu-discoaster brouweri* subsp. *streptus* n. subsp.
Fig. 11. Holotype. Sample 231-27.
Fig. 12. Sample 231-90.
- Fig. 13. *Eu-discoaster brouweri* subsp. *brouweri*. Sample 231-10.
- Figs. 14, 17. *Eu-discoaster neorectus* (Bukry) Theodoridis, Sample 231-92.
- Figs. 15, 16. *Eu-discoaster intercalaris* (Bukry) n. comb. Sample 231-104.



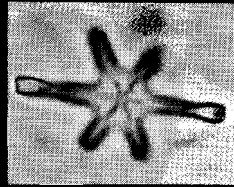
1



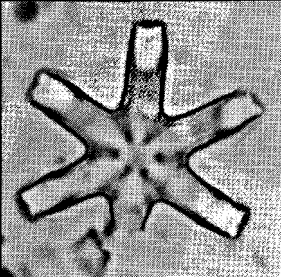
2



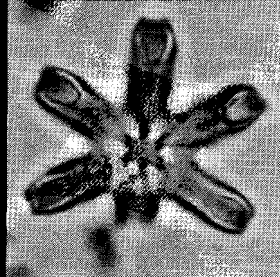
3



4



5



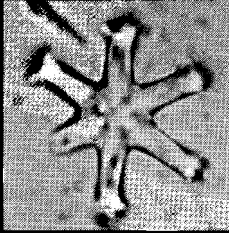
6



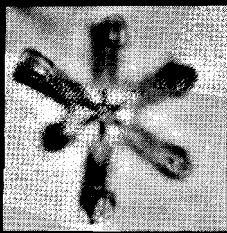
7



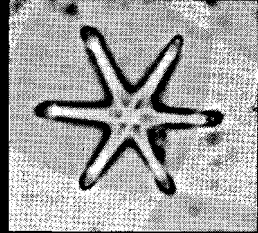
8



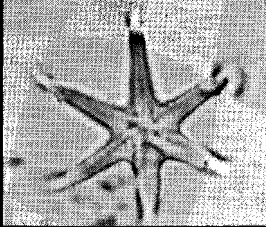
9



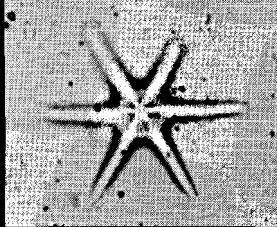
10



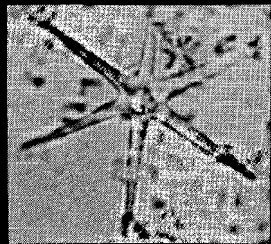
11



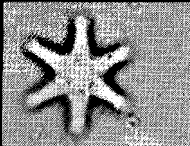
12



13



14



15



16

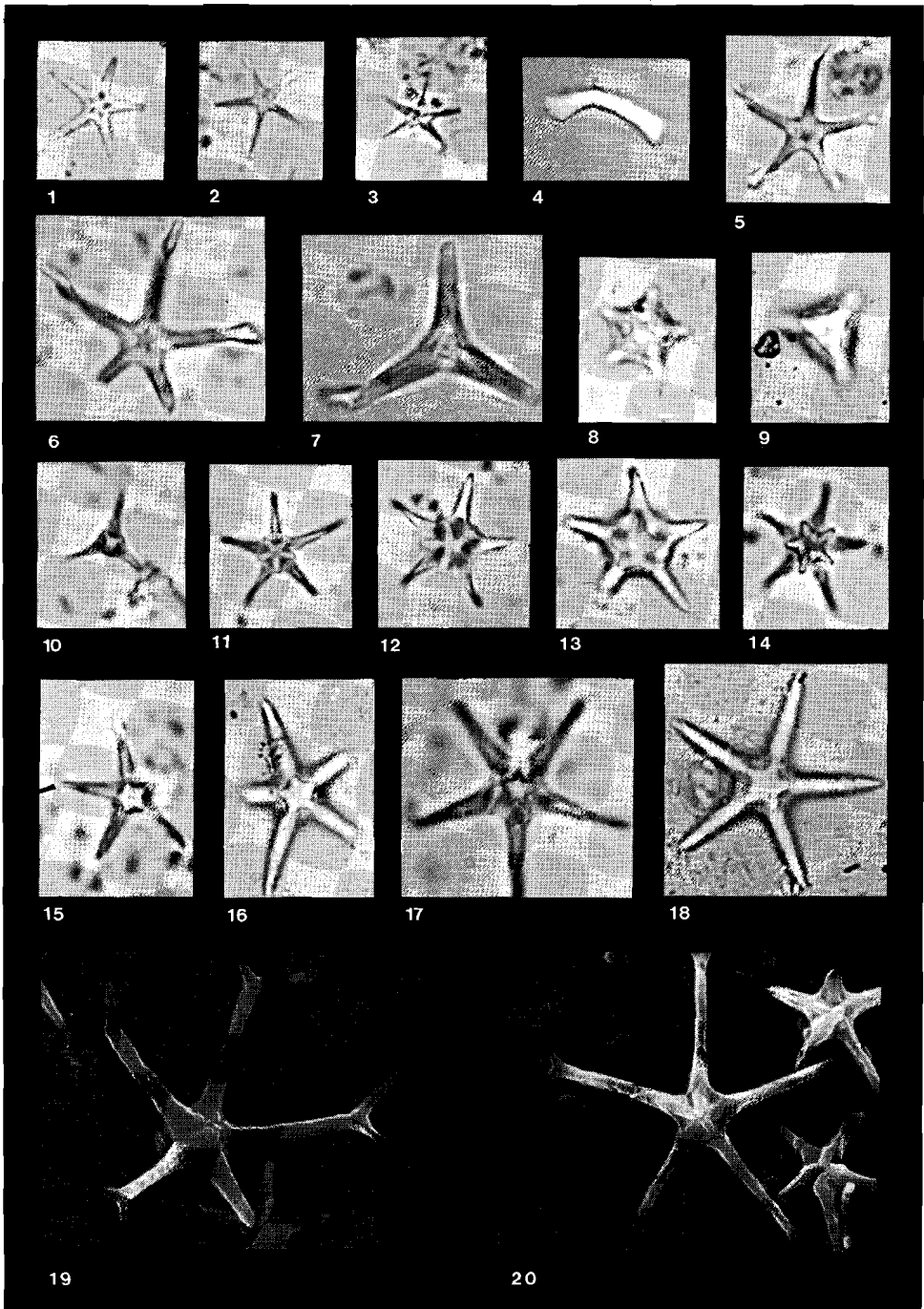


17

Plate 37

- Figs. 1–18. LM micrographs, parallel nicols, 1485 X.
- Figs. 19, 20. SEM micrographs, 2500 X.
- Figs. 1–3. *Eu-discoaster bellus* (Bukry) Theodoridis Sample CP3133.
- Figs. 4–7. *Eu-discoaster hamatus* (Martini and Bramlette) Theodoridis.
- Fig. 5. Sample CP3130.
- Fig. 6. Sample 231-124.
- Fig. 7. Sample 231-120.
- Figs. 8–18. *Eu-discoaster quinquerramus* (Gartner) Theodoridis.
- Fig. 8. Sample 219-31, focus on the distal side.
- Fig. 9. Sample 231-56, focus on the proximal side.
- Fig. 10. Sample 231-32, focus on the distal side.
- Fig. 11. Sample 231-30, focus on the distal side.
- Fig. 12. Sample 219-10, focus on the distal side.
- Fig. 13. Sample 219-22, focus on the proximal side.
- Fig. 14. Sample SR39, focus on the distal side.
- Fig. 15. Sample 231-30, focus on the proximal side.
- Fig. 16. Sample SR40, focus on the proximal side.
- Fig. 17. Sample SR32, focus on the distal side.
- Fig. 18. Sample SR32, focus on the proximal side.
- Figs. 19, 20. *Eu-discoaster misconceptus* n. sp.
- Fig. 19. Holotype, sample JT1935.
- Fig. 20. Sample JT1935.

Plate 37



INDEX

Species listed in alphabetical order

<i>Sphenolithus abies</i>	87
<i>Helicosphaera acuta</i> n. sp.	119
<i>Ceratolithus acutus</i>	82
<i>Eu-discoaster altus</i>	180
<i>Helicosphaera ampliapertura</i>	124
<i>Amaurolithus amplificus</i>	80
<i>Reticulofenestra ampliumbolicus</i> n. sp.	84
<i>Hayella aperta</i> n. sp.	82
<i>E. asymmetricus</i> morphotypes	180
<i>Helio-discoaster barbadiensis</i>	146
<i>Sphenolithus belemnos</i>	87
<i>Eu-discoaster bellus</i>	174
<i>Helio-discoaster bifax</i>	149
<i>Helio-discoaster binodosus</i>	150
<i>Eu-discoaster bollii</i>	165
<i>Eu-discoaster</i> cf. <i>E. bollii</i>	166
<i>Helicosphaera bramlettei</i>	108
<i>Eu-discoaster brouweri</i>	177
<i>Eu-discoaster brouweri</i> subsp. <i>brouweri</i>	177
<i>Eu-discoaster brouweri</i> subsp. <i>streptus</i> n. subsp.	178
<i>Eu-discoaster calcaris</i>	171
<i>Eu-discoaster calyculus</i>	174
<i>Triquetrorhabdulus carinatus</i>	88
<i>Helicosphaera carteri</i>	131
<i>Helicosphaera carteri</i> var. <i>burkei</i>	133
<i>Helicosphaera carteri</i> var. <i>carteri</i>	132
<i>Helicosphaera carteri</i> var. <i>wallichii</i>	133
<i>Triquetrorhabdulus challengerii</i>	89
<i>Hayella challengerii</i>	83
<i>Helio-discoaster collettii</i>	152
<i>Eu-discoaster coalitus</i>	173
<i>Helicosphaera compacta</i>	112
<i>Minylitha convallis</i>	84
<i>Eu-discoaster decorus</i>	161
<i>Eu-discoaster deflandrei</i>	156

<i>Amaurolithus delicatus</i>	80
<i>Helio-discoaster diastypus</i>	145
<i>Helicosphaera dinesenii</i>	111
<i>Eu-discoaster distinctus</i>	155
<i>Eu-discoaster druggii</i>	157
<i>Helio-discoaster elegans</i>	143
<i>Helicosphaera elongata</i> n. sp.	117
<i>Helicosphaera euphratis</i>	121
<i>Eu-discoaster exilis</i>	163
<i>Triquetrorhabdulus extensus</i> n. sp.	89
<i>Triquetrorhabdulus finifer</i> n. sp.	89
<i>Reticulofenestra floridana</i>	85
<i>Syracosphaera ? fragilis</i> n. sp.	87
<i>Helicosphaera gartneri</i> n. sp.	129
<i>Helio-discoaster gemmeus</i>	147
<i>Helicosphaera gertae</i>	112
<i>Eu-discoaster giganteus</i> n. sp.	172
<i>Helicosphaera granulata</i>	134
<i>Eu-discoaster hamatus</i>	174
<i>Helicosphaera heezenii</i>	111
<i>Sphenolithus heteromorphus</i>	87
<i>Helicosphaera hyalina</i>	134
<i>Eu-discoaster intercalaris</i> n. comb.	179
<i>Helicosphaera intermedia</i>	121
<i>Helicosphaera inversa</i>	120
<i>Geminolithella jafari</i>	83
<i>Eu-discoaster kugleri</i>	170
<i>Helio-discoaster kuepperi</i>	147
<i>Helio-discoaster lenticularis</i>	144
<i>Calcidiscus leptoporus</i>	81
<i>Helio-discoaster lodoensis</i>	148
<i>Eu-discoaster loeblichii</i>	161
<i>Helicosphaera lophota</i>	109
<i>Calcidiscus macintyreii</i>	81
<i>Triquetrorhabdulus martinii</i>	90
<i>Helio-discoaster mediosus</i>	142
<i>Helicosphaera mediterranea</i>	122
<i>Eu-discoaster mexicanus</i>	173
<i>Eu-discoaster micros</i> n. sp.	170
<i>Triquetrorhabdulus milowii</i>	90

<i>Helio-discoaster mirus</i>	151
<i>Eu-discoaster misconceptus</i> n. sp.	168
<i>Helio-discoaster mohleri</i>	141
<i>E. moorei</i> morphotypes	182
<i>Sphenolithus moriformis</i>	87
<i>Helio-discoaster multiradiatus</i>	144
<i>Eu-discoaster musicus</i>	164
<i>E. neohamatus</i> morphotypes	181
<i>Eu-discoaster neorectus</i>	179
<i>Helio-discoaster nobilis</i>	141
<i>Helio-discoaster nodifer</i>	154
<i>Eu-discoaster nonaradiatus</i>	157
<i>Helicosphaera obliqua</i>	116
<i>Helicosphaera orientalis</i>	118
<i>Helicosphaera</i> cf. <i>H. orientalis</i>	118
<i>Helio-discoaster ornatus</i>	150
<i>Helicosphaera pacifica</i>	119
<i>Helio-discoaster pacificus</i>	146
<i>Helicosphaera paleocarteri</i> n. sp.	131
<i>Eu-discoaster pansus</i>	161
<i>Helicosphaera papillata</i>	110
<i>Eu-discoaster pentaradiatus</i>	166
<i>Helicosphaera perch-nielseniae</i>	115
<i>Helio-discoaster perpolitus</i>	144
<i>Solidopons petrae</i> n. sp.	86
<i>Calcidiscus premacintyreii</i> n. sp.	81
<i>Amaurolithus primus</i>	80
<i>Eu-discoaster protoexilis</i> n. sp.	162
<i>Eu-discoaster pseudovariabilis</i>	159
<i>Eu-discoaster quinqueramus</i>	175
<i>Helicosphaera recta</i>	114
<i>Helicosphaera reticulata</i>	113
<i>Reticulofenestra rotaria</i> n. sp.	85
<i>Geminilithella rotula</i>	83
<i>Ceratolithus rugosus</i>	82
<i>Triquetrorhabdulus rugosus</i>	90
<i>Helio-discoaster saipanensis</i>	149
<i>Helicosphaera scissura</i>	125
<i>Helicosphaera sellii</i>	128
<i>Helicosphaera seminulum</i>	107

<i>Eu-discoaster signus</i>	163
<i>Eu-discoaster</i> cf. <i>E. signus</i>	164
<i>Helio-discoaster splendidus</i>	143
<i>Helicosphaera stalis</i> n. sp.	127
<i>Helicosphaera stalis stalis</i> n. subsp.	127
<i>Helicosphaera stalis ovata</i> n. subsp.	128
<i>Helio-discoaster sublodoensis</i>	149
<i>Eu-discoaster subsurculus</i>	165
<i>Eu-discoaster surculus</i>	160
<i>Tetralithoides symeonidesii</i> n. sp.	88
<i>E. tamalis</i> morphotypes	181
<i>Helio-discoaster tanii</i>	153
<i>Amaurolithus tricorniculatus</i>	81
<i>E. triradiatus</i> morphotypes	181
<i>Eu-discoaster tristellifer</i>	180
<i>Helicosphaera truempyi</i>	130
<i>Eu-discoaster variabilis</i>	158
<i>Helicosphaera vedderi</i>	123
<i>Helicosphaera walbersdorfensis</i>	126
<i>Helicosphaera waltrans</i> n. sp.	124
<i>Helio-discoaster wemmelensis</i>	145

-
- Spec. Publ. 1. A. A. BOSMA – Rodent biostratigraphy of the Eocene-Oligocene transitional strata of the Isle of Wight. 128 p., 7 pl., 38 figs. (1974) f 43,—
- Spec. Publ. 2. A. VAN DE WEERD – Rodent faunas of the Mio-Pliocene continental sediments of the Teruel – Alfabra region, Spain. 217 p., 16 pl., 30 figs. (1976) f 63,—
- Spec. Publ. 3. R. DAAMS – The dental pattern of the dormice *Dryomys*, *Myomimus*, *Microdryomys* and *Peridyromys*. 115 p., 5 pl., 42 figs. (1981) f 41,—

Sales office U.M.B.: Singel 105, 3984 NX Odijk, Netherlands
Postal account: 3028890, T. van Schaik, Odijk
Bank account: 55 89 19 855, Alg. Bank Nederland, T. van Schaik, Odijk

After *prepayment* to the sales office on one of the above accounts, the books will be sent by surface mail without further charges. Orders for these books not directly from the purchaser to the sales office may cause much higher costs to the purchaser.

- Bull. 15. Z. REISS, S. LEUTENEGGER, L. HOTTINGER, W. J. J. FERMONT, J. E. MEULENKAMP, E. THOMAS, H. J. HANSEN, B. BUCHARDT, A. R. LARSEN and C. W. DROOGER – Depth-relations of Recent larger foraminifera in the Gulf of Aqaba-Elat. 244 p., 3 pl., 117 figs. (1977) f 53,–
- Bull. 16. J. W. VERBEEK – Calcareous nannoplankton biostratigraphy of Middle and Upper Cretaceous deposits in Tunisia, Southern Spain and France. 157 p., 12 pl., 22 figs. (1977) f 51,–
- Bull. 17. W. J. ZACHARIASSE, W. R. RIEDEL, A. SANFILIPPO, R. R. SCHMIDT, M. J. BROLSMA, H. J. SCHRADER, R. GERSONDE, M. M. DROOGER and J. A. BROEKMAN – Micropaleontological counting methods and techniques – an exercise on an eight metres section of the Lower Pliocene of Capo Rossello, Sicily. 265 p., 23 pl., 95 figs. (1978) f 59,–
- Bull. 18. M. J. BROLSMA – Quantitative foraminiferal analysis and environmental interpretation of the Pliocene and topmost Miocene on the south coast of Sicily. 159 p., 8 pl., 50 figs. (1978) f 49,–
- Bull. 19. E. J. VAN VESSEM – Study of Lepidocyclinidae from South-East Asia, particularly from Java and Borneo. 163 p., 10 pl., 84 figs. (1978) f 53,–
- Bull. 20. J. HAGEMAN – Benthic foraminiferal assemblages from the Plio-Pleistocene open bay to lagoonal sediments of the Western Peloponnesus (Greece). 171 p., 10 pl., 28 figs. (1979) f 54,–
- Bull. 21. C. W. DROOGER, J. E. MEULENKAMP, C. G. LANGEREIS, A. A. H. WONDERS, G. J. VAN DER ZWAAN, M. M. DROOGER, D. S. N. RAJU, P. H. DOEVEN, W. J. ZACHARIASSE, R. R. SCHMIDT and J. D. A. ZIJDERVELD – Problems of detailed biostratigraphic and magnetostratigraphic correlations in the Potamidha and Apostoli sections of the Cretan Miocene. 222 p., 7 pl., 74 figs. (1979) f 57,–
- Bull. 22. A. J. T. ROMEIN – Evolutionary lineages in Early Paleogene calcareous nannoplankton. 231 p., 10 pl., 50 figs. (1979) f 64,–
- Bull. 23. E. THOMAS – Details of *Uvigerina* development in the Cretan Mio-Pliocene. 168 p., 5 pl., 65 figs. (1980) f 50,–
- Bull. 24. A. A. H. WONDERS – Planktonic foraminifera of the Middle and Late Cretaceous of the Western Mediterranean area. 158 p., 10 pl., 44 figs. (1980) f 52,–
- Bull. 25. G. J. VAN DER ZWAAN – Paleocology of Late Miocene Mediterranean foraminifera. 202 p., 15 pl., 65 figs. (1982) f 57,–
- Bull. 26. M. M. DROOGER – Quantitative range chart analyses. 227 p., 3 pl., 32 figs. (1982) f 59,–
- Bull. 27. W. J. FERMONT – Discocyclinidae from Ein Avedat (Israel). 173 p., 11 pl., 58 figs. (1982) f 51,–
- Bull. 28. P. SPAAK – Accuracy in correlation and ecological aspects of the Planktonic foraminiferal zonation of the Mediterranean Pliocene. 160 p., 10 pl., 51 figs. (1983) f 52,–
- Bull. 29. J. R. SETIAWAN – Foraminifera and microfacies of the type Priabonian. 173 p., 18 pl., 35 figs. (1983) f 55,–
- Bull. 30. J. E. MEULENKAMP (ed.) – Reconstruction of marine paleoenvironments. 298 p., 5 pl., 112 figs. (1983) f 69,–
- Bull. 31. H. A. JONKERS – Pliocene benthonic foraminifera from homogeneous and laminated marls on Crete. 179 p., 12 pl., 46 figs. (1984) f 56,–
- Bull. 32. S. THEODORIDIS – Calcareous nannofossil biozonation of the Miocene and revision of the Helicoliths and Discoasters. 272 p., 37 pl., 67 figs. (1984) f 68,–